THE INFLUENCE OF NANOMATERIAL UPTAKE ON SMALL ARTERIAL FUNCTION

A SHUKUR

PhD 2015

THE INFLUENCE OF NANOMATERIAL UPTAKE ON SMALL ARTERIAL FUNCTION

ALI SHUKUR

A thesis submitted in partial fulfilment of the requirements of the Manchester Metropolitan University for the degree of Doctor of Philosophy

School of Healthcare Science

Faculty of Science and Engineering

the Manchester Metropolitan University

2015

Abstract

Background

The emergence of nanomedicine, involving the intravenous injection of tracking agents (such as dyes and nanoparticles) and drug-loaded nanoparticles (NPs) for diagnostic and therapeutic purposes may display a biosafety concern specifically to the circulating blood and the vascular system. Dye-encapsulated silica nanoparticles (SiNPs) are one of the most popular NPs recently being explored for medical intervention. However, there are limited studies investigating their biocompatibility and biosafety with regards to blood vessels. Our group's previous findings suggest that SiNPs of 100 and 200 nm in size have no detrimental effect on conduit arterial function. However, their direct effect on small size arteries, which play an important role in controlling blood flow into tissues, has not been investigated previously.

Aim

To investigate the direct influence of SiNPs on small arterial function and contractility.

Methodology

Mono-dispersed dye-encapsulated SiNPs of defined diameters (98 nm) were fabricated using a modified Stöber method and characterised using the Malvern Zetasizer and transmission electron microscopy (TEM). NP characteristics (size and charge) were monitored over a 15-month period in various media. Small mesenteric arteries (MAs) (150-300 µm in diameter) from male Wistar rats were isolated, mounted between two glass cannulae and superfused in gassed physiological salt solution (PSS) at 37℃. Vasoconstrictor (high potassium [KPSS], Phenylephrine [Phe]) and vasodilator (Acetylcholine [ACh], Sodium nitroprusside [SNP] and papaverine [PAPA]) responses were assessed using pressure myography before and 30 minutes after the intravascular infusion of SiNPs under static conditions at intravascular pressure of 60 mmHg. SiNPs were also injected intravenously and mesenteric vessels isolated after a 2-hour period, for assessment of vascular reactivity.

Results and Conclusion

Our findings show that SiNPs are rapidly taken up into ECs lining small mesenteric arteries and were freely localised in the cytoplasm, with no evidence of uptake into the nucleus or the smooth muscle cell layer. SiNPs (calculated at 5.32 x 10^{11} NP/mL) attenuated Phe contractile responses, but did not alter the responses to KPSS *ex vivo*, suggesting that the contractile machinery is unaffected by SiNP uptake. There was an attenuated endothelium dependent (ACh) dilator response following the incubation with SiNPs *ex vivo*. In contrast, the lower dose of SiNPs (at 1.01 x 10^{11} NP/mL) had no overall effect on ACh responses. The endothelium-independent (SNP) vasodilator responses were unaffected by the incubation in SiNPs. When injected intravenously *in vivo*, SiNPs only had a detrimental effect on constrictor (Phe) and endothelial dependent (ACh) dilator responses, at the lower agonist concentrations. At high agonist concentrations, however, the injected SiNPs did not seem to alter the constriction or dilation response, suggesting that possible corona formation may have been protective *in vivo*. SiNPs injected *in vivo*, significantly reduced SNP-induced dilator responses at a lower dosage. This may have clinical implications on the use of SNP drugs for patients with heart disease. A small fraction of the SiNPs administered *in vivo* (6%) were localised within various tissues including; lungs, heart, aorta, mesentery, liver, spleen and kidney, with the MA accounting for the majority of uptake (approximately 5% of total injected SiNPs). Inhibition studies (using L-NNA and potassium channel blockers), demonstrated that both nitric oxide (NO) and endothelial-derived hyperpolarising factors (EDHFs) contribute to the vasodilator component in MAs. The co-incubation of SiNPs in the presence of L-NNA completely abolished the dilator responses to ACh, suggesting the direct effect of SiNPs on the EDHF pathway. The co-incubation in SOD did not reverse the actions of the SiNPs, indicating that a reactive oxygen species (ROS)-independent mechanism may mediate SiNPs actions in small arteries. The reduction of ERK and Akt phosphorylation *ex vivo* may underpin the mechanisms of SiNPs effects on rat mesenteric arteries. Depending on their dosage, we demonstrate that SiNPs uptake and accumulation in ECs have detrimental effects on the function of small arteries.

Table of Contents

Acknowledgement

I am privileged to express my tremendous and deepest gratitude to my supervisor, Dr. May Azzawi for her exceptional supervision, innovative ideas, continuous support, guidance and constructive criticism throughout the research work and academic writing. Her intensive comments helped me systematically throughout this study. She helped me to drive my optimal capabilities and has the experience in allowing me to express myself in research and in networking with other academics within the field of nanomedicine and vascular physiology. She also kept me motivated and excited about the subject area as well as the experimental work with the high demands of preventative and interventional medicine and rewards to patients' care.

Many thanks and deep gratitude goes to Dr. Debra Whitehead for her help in chemistry whether in discussions or on the analysis of data related to nanomaterial synthesis and characterisation. Her expertise in the area of physical chemistry and nanoparticle chemistry was essential in guiding the chemistry work to completion. She is dedicated individual and exceptionally creative, her thoughts and ideas inspired me to understand and carryout the chemistry work related to nanoparticle synthesis, characterisation and manipulation.

Special thanks to Dr. Nasser Al-Shanti and Prof. Claire Stewart (JMU) for their help and expertise in cell and molecular biology work, discussions respectively and their valuable comments and support throughout the study. This study was conducted in collaboration with Professor Alexander M. Seifalian, a director of Centre for Nanotechnology & Regenerative Medicine at the Division of Surgery and Interventional Sciences, University College London (UCL), Royal Free Hampstead NHS Trust Hospital, London, UK. I would like to express my sincere thanks to Prof. Alexander Seifalian from UCL for the supply of the functionalised carbon nanotubes through his student; Mr. Seyed Yazdan Madani and for his assistance in the *in vivo* work carried out at Hampstead Royal Free hospital in London, as well as his valuable contributions to the scientific discussions.

I would like to thank Prof. Yvonne Alexander and her group specially; Dr. Fiona Wilkinson for her support the cellular and molecular aspects of the work and her valuable experience in guiding me through different techniques and tactics used in the proteomics experiments and blot analysis. I would like to thanks Dr. Ria Weston for her guidance and support during the gel electrophoresis and Western blotting. I would also like to thank Dr. Ayman Moawad Mahmoud (an academic visitor from Egypt) for his help and sharing ideas regarding the cellular and molecular work in general and his expertise in the field of vascular biology.

I would like to thank Mr. David Maskew, Miss Caroline Chomiak and Mr. Glenn Ferris for their support and technical expertise during all aspects of laboratory work in physiology and cell biology. I would also like to thank Mr. Lee Harman for his help in aspects related to the chemistry work. Many thanks to Mr. Paul Warren and Mr. David McKendry for their assistance on ICP analysis and results interpretation. Many thanks to Mr. Gary Miller and Mr. Saeed Gulzar and for their training on the use of SEM. I would like to express my thanks to Miss Hayley Andrews (Technical Officer in Analytical Sciences) for her immense help in analysing the scanning electron microscopy samples for the silica nanoparticles. Special thanks to Dr. Aleksandr Mironov at the Electron Microscopy-core Facility (FLS) at The University of Manchester for his help in obtaining and analysing the TEM images of this study.

I would specially want to thank Dr. Asima Farooq for her technical and academic support and expertise during the research work and to being a backup and real friend in need. I would also like to thank Dr. Teba Mohamed for her help and support in the initial stages of the research process and being a friend in difficult times.

I would like to thank my wife (Mrs Sally Merzha), parents (Mrs Sondos Latif and Dr. Majid Shukur), sister (Mrs Mace Al-Nakeeb) and in-laws (Dr. Isam Al Charchafchi and Dr. Said Merzha) for their love, extreme patience, understanding, encouragement, and being supportive and caring at all stages during my research and write-up periods. I particularly like to thanks my brother-in-law Dr. Majid Al-Nakeeb for his help with the chemical drawing of the silica nanoparticle structure and reaction mechanisms and his ideas of which some were adapted in the chemistry discussion. I would particularly like to pay gratitude and high

appreciation for my wife, Sally for her support throughout my study journey and her inspiration, motivation and help in conducting the drawing for some of the figures and schematic representations included in this thesis. I wish that my daughter (Miss Judy Shukur), which I dedicate her with my love and infinite care would follow the path of experimental science and evidence-based learning to read life at all levels. Because knowledge is a human instinct (curiosity-derived) and education is the key to human rights (existence and dignity), morals, integrity and contribution to serve other human beings to the cause of wellbeing and contentment. My definition for an instinct remains as a dependent response provoked by an input due to the availability (presence and existence) of an input-encountering system that can respond to inputs depending upon the output gained from such communication as opposed to a static situation.

Finally yet importantly, I would like to devote my immense respect, tribute, admiration, love and submission to the great, ultimate, unlimited, independent, self-sufficient and most Beautiful One existing entity. I believe he had created, maintained, reasoned life and continues to provide his mercy, peace, love and adoration to Mankind, the entire Universe and beyond. Life is an open book and we read it through our investigate capabilities and organisational skills, which together can achieve perfection.

I dedicate this thesis to my mother (Mrs Sondos Latif) and father (Dr. Majid Shukur), who have been the inspiration of my life. I admire them and love them forever I live.

I would like to express my deepest tribute to my mother for her patience and moral support as well as her hard work in keeping my abilities to their optimum levels. She always listens to my thoughts and beliefs and build constructive arguments with me to achieve better conclusions about all aspects of life. She worked exceptionally hard though my childhood to adulthood to provide care and love I would not get from any other human being.

I would also like to express my deepest gratitude and honour as well as greatly thank my father who displays an icon for me for patience, care, wisdom and intelligence. I consider him as the inspiration to my thoughts, the light I can see through my eyes and the soul that brings kindness as strength to my heart and mind. As well as being well educated from a doctorate in a hospital management background from the former University of Manchester Institute of Science and Technology (UMIST; now known as The University of Manchester (UoM)), my father have a great experience in life at all levels. I learned many things from him. He was brave and always believed in right doing regardless of the corruption that was implemented as a way of life in some societies. I would also like to thank my father for his generous financial support with my tuition fees and living costs throughout the journey of my post-graduate studies here at MMU. He was the main provider for me, without him it would not be possible to complete my masters and doctorate studies and obtain the success I aim to achieve by the end of the course of my studies.

Thus, I would like to dedicate this thesis to my mother and father who have been the inspiration and drive to my studies here at MMU and to obtaining the highest qualification in Science.

Declaration

'With the exception of any statements to the contrary, all the data presented in this report are the results of my own efforts and have not previously been submitted in candidature for any other degree or diploma. In addition, no parts of this report have been copied from other sources. I understand that any evidence of plagiarism and/or the use of unacknowledged third party data will be dealt with as a very serious matter.'

Signature: *Ali Shukur* Date: 5th May 2015

Ethical Consideration for Experimental Animals

The physiological function experiments in this study were performed using animal tissue excised from dead animals (Male Wistar rats, 200-300 g in weight, aged 7-13 weeks), obtained from the BSU, University of Manchester. The Wistar rats were housed under standardised conditions (12 hour light/dark cycles at 24℃). The animals were humanely euthanised by stunning and cervical dislocation. All procedures are conducted in accordance with institutional guidelines of the MMU and the University of Manchester and the United Kingdom Animals (Scientific Procedures) Act of 1986 (schedule 1). A risk assessment for the use and handling of animal tissue was conducted.

Abbreviation List

3MST	3-Mercaptopyruvate sulphuresterase
AA	Arachidonic acid
ACh	Acetylcholine
BK_{Ca}	Large-conductance calcium-activated potassium channels
cAMP	Cyclic AMP
Ca^{2+}	Calcium ion
CaM	Calmodulin
CaMK	Ca^{2+}/CaM-dependent protein kinase
CaMKKβ	CaMK kinase β
CBS	Cystathionine β-synthase
CNT	Carbon nanotubes
CoA-SH	Acyl coenzyme A synthase
COX-2	Cyclooxygenase-2
CREB	Response element-binding protein
CSE	Cystathionine γ-lyase
dH_2O	De-ionised or distilled water
DHET	Dihydroxyeicosatrienoic acids
DLS	Dynamic light scattering
EC	Endothelial cell
ECM	Extracellular matrix
EET	Epoxyeicosatrienoic acid
eNOS	Endothelial-derived nitric oxide synthase
ERK	Extracellular-signal-regulated kinase
FABP	Fatty acid binding protein
GLMM	Generalised linear mixed model
H_2S	Hydrogen Sulphide
H_2O_2	Hydrogen peroxide
HUVECs	Human umbilical vein ECs

IK_{Ca}	Intermediate-conductance calcium-activated potassium channels
IL	Interleukin
K^+	Potassium ion
$K_{Ca}{}^+$	Ca^{+2}-dependent potassium channels
K_{IR}	Inwardly rectifying potassium channels
KPSS	High potassium physiological salt solution
MA	Mesenteric Artery
NF-κB	Nuclear factor κB
NO	Nitric oxide
$O_2^{\bullet-}$	Superoxide
PAPA	Papaverine
PCR	Polymerase chain reaction
PEG	Polyethylene glycol
Phe	Phenylephrine
PI3K	Phosphatidylinositol 3 kinase
PKA	Protein kinase A
PKC	Protein kinase G
PM	Plasma membrane
PPAR	Peroxisome proliferator-activated receptors
REST	Repressor element-1-silencing transcription factor
ROS	Reactive oxygen species
SE	Standard error of mean
SEM	Scanning electron microscopy
SiNP	Silica nanoparticle
SK_{Ca}	Small-conductance calcium-activated potassium channels
SMC	Smooth muscle cell
SNP	Sodium nitroprusside
SOD	Superoxide dismutase
SWCNTs	Single-walled CNTs
TEM	Transmission electron microscopy
TEOS	Tetraethylorthosilicate

TiO_2	Titanium dioxide
TJ	Tight junction
TRP	Transient receptor potential
VSMC	Vascular smooth muscle cell

List of Figures

List of Tables

Chapter 1.

Introduction

1.1 Background

The vascular system permits the transport and controls the flow of circulating blood enriched with oxygen and nutrients or waste to and from organs and tissues (Whittemore, 1999). The preservation of vascular integrity and function is thus essential to ensure that blood flow is matched to demand. The emergence of nanomedicine, involving the intravenous (iv) injection of tracking agents (such as dyes and nanoparticles (NPs)) and drug loaded NPs for diagnostic and therapeutic purposes may potentially cause injury and compromise the function of blood vessels. Preventative and protective measures are thus essential to maintain vascular integrity and function through targeted NPs uptake into living systems, bypass their negative acute (short-term) and chronic (long-term) effects and ensure the safe administration and/or targeting of these agents *in vivo*.

In the present report, the structure and function of the vascular system will initially be described, followed by an introduction to nanotechnology and the use of nanomaterials for diagnostic and therapeutic intervention. The influence that nanomaterials may have on vascular function will be highlighted, leading to the aims and objectives of the study.

1.2 Vascular Anatomy and Physiology

1.2.1 Blood Vessel Architecture

In blood vessels, the arterial wall is composed of three layers, the tunica interna, tunica media and tunica externa (Figure 1). The innermost tunica interna contains a lining of simple endothelium, a basement membrane and a layer of elastic tissue. The tunica media however is the thickest layer of elastic fibre and smooth muscle cells (especially in small arteries), while the tunica externa only contains elastic and collagen fibres. Veins have thinner tunica interna and tunica media (with little smooth muscle and elastic fibres) with a bigger lumen and more intense tunica externa, consisting mainly of collagen and elastic fibres. Arterioles have tunica interna consisting of endothelium elastic and collagen fibres and tunica media composed of smooth muscle and few elastic fibres (Figure 2). Capillaries

in turn are composed of a single layer of endothelial cells (ECs) with a basement membrane and when several capillaries unite, they form small veins called venules. These consist of tunica interna of endothelium and tunica media with scattered smooth muscle fibres and fibroblasts (Tortora, 2003).

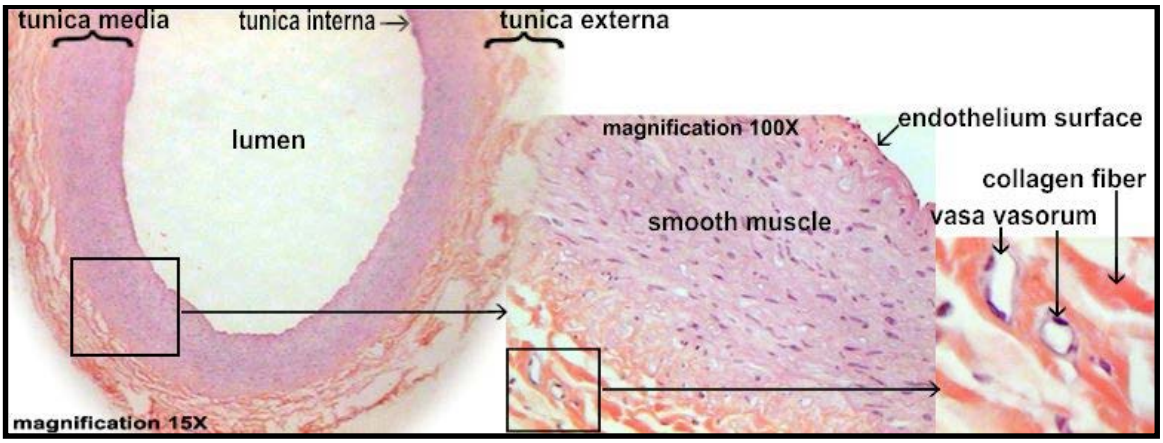

Figure 1. Anatomy of an artery. Adapted from http://science.nhmccd.edu/biol/cardio/artery.htm, access date: 2006.

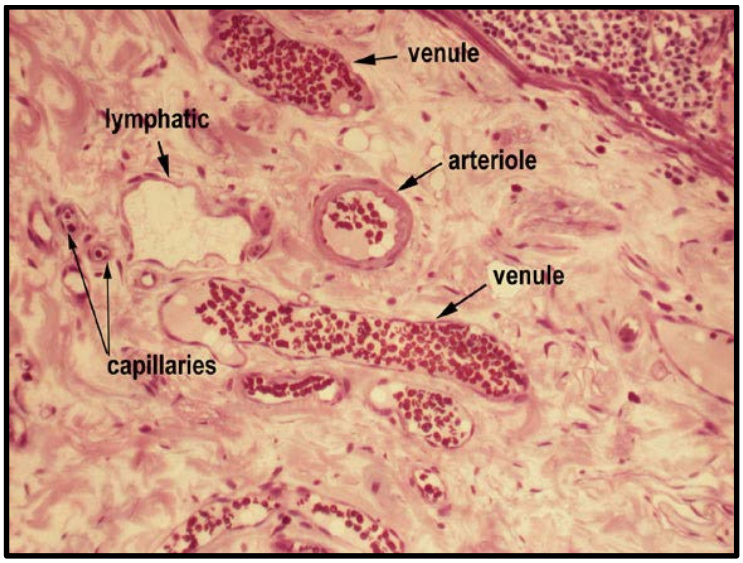

Figure 2. Anatomy of arterioles, capillaries and venules. Adapted from http://apocketmerlin.tumblr.com/post/18660545870/the-hitchhikers-guide-to-the-circulatory-system-basics, access date: 2013.

1.2.1.1 The Vascular Endothelium and Smooth Muscle Layers

The vascular endothelial tissue acts as a secretory tissue and has critical roles in lining blood vessels, forming a barrier to blood flow into the vascular tissue, acting as a selective permeability barrier and maintaining tissue haemodynamics and homoeostasis. ECs are involved in coagulation and fibrinolysis, regulation of vascular tone, growth regulation of other cell types and blood cell activation and migration during physiological and pathological processes (Dora, 2001; Risau, 1995; Shireman and Pearce, 1996). Smooth muscle cells within vascular tissues form along, with elastin, collagen and other extracellular matrix (ECM), components of the vascular media. As vascular smooth muscle cells (VSMCs) grow they attach to ECM and become elongated (pulled or flattened) and spindle-shaped and become known as "differentiated contractile" (medial) cells (Schwartz, 1997; Myit et al., 2003). These contractile VSMCs control blood flow through the maintenance of vascular tone (Fok et al., 2012). The contraction of VSMCs is calcium ion (Ca^{2+})-dependent and triggered by the activation of plasma membrane (PM) receptors (Somlyo and Somlyo, 1994). Thus, VSMCs provide the integrity of the vascular wall structure and have a major impact on the functional characteristics of blood vessels.

ECs are in close proximity to VSMCs, where they communicate directly (Powell et al., 1997) via gap junctions and signalling molecules (Davies, 1986; Lyubimov and Gotlieb, 2004). There is a cross talk and continuous interaction between the endothelium and smooth muscle cell layer which influences blood vessel development and function (Bernanke and Velkey, 2002). These interactions are translated into the regulation of VSMC proliferation and EC migration (Shum-Tim et al., 1999), preventing excessive SMC proliferation into the lumen (Campbell and Campbell, 1986; Casscells, 1992)

1.2.2 The Maintenance of Vascular Tone

Vascular tone is defined as the degree of constriction experienced by a blood vessel relative to its maximally dilated state. All arterial and venous vessels under basal conditions exhibit some degree of smooth muscle contraction that determines the diameter and hence tone, of the vessel (Shimoda et al., 2000). However, the endothelium plays an important role in the modulation of vascular tone (Busse et al., 1985) through the release of vasoconstrictor and vasodilator regulatory factors (Imig and Roman, 1992; Cines et al., 1998). The factors that descend from the endothelium ensure a low level of phosphorylation of the muscular cell kinases to maintain the VSMCs tone in the absence of external stimulation. Vascular tone is also determined by extrinsic factors (neurohumoral) that originate from outside of the organ or tissue in which the blood vessel is located such as sympathetic nerves and circulating hormones (Yamamoto et al., 1994) and intrinsic factors that originate from the vessel itself or the surrounding tissue e.g. metabolites. The primary function of extrinsic factors is to regulate arterial blood pressure by altering systemic vascular resistance, whereas intrinsic mechanisms are important for local blood flow regulation within an organ (Vicent et al., 2003). Vasodilator autacoids include endothelial-derived hyperpolarising factor (EDHF) (Cheung et al., 1999), nitric oxide (NO) (Okamura and Toda, 1992; Yamashita et al., 2001) and prostacyclin (PGI-2), but a substantial component of the vasodilator response observed is in response to receptor-dependent agonists or changes in the flow of blood. Generally, the factors that increase vascular tone cause vasoconstriction; however, those that decrease vascular tone cause vasodilation. Some intrinsic factors may initiate myogenic mechanisms (Davis et al., 2001), originating from vascular smooth muscle to increase tone. While other endothelial factors, such as NO (Van Camp et al., 1994) and endothelin (Gellai et al., 1997), can either decrease or increase tone, respectively.

Myogenic mechanisms of diameter control are intrinsic to the smooth muscle of blood vessels, particularly in small arteries and arterioles. If the pressure within a vessel is suddenly increased, the vessel responds by constricting. In contrast, if the pressure is diminished within the vessel, it causes relaxation and vasodilation. This response is known as myogenic reactivity and is observed *in vivo* and in isolated, pressurised blood vessels (Azzawi and Austin, 2006). The myogenic behaviour may play a role in local autoregulation

of blood flow and in reactive hyperaemia, especially in small-resistant size arteries (<100 µm diameter) that are able to regulate their own diameter, thus protecting dependent capillary beds from large increases in hydrostatic pressure (Davis and Hill, 1999). Electrophysiological studies have shown that VSMC depolarise when stretched, leading to contraction. Stretching also increases the rate of VSMCs that spontaneously undergo depolarisation and repolarisation (Hill and Davis, 2007). The mechanisms by which the above influences either constrict or relax blood vessels involve a variety of signal transduction mechanisms that ultimately influence the interaction between actin and myosin in the smooth muscle (Figure 3). Several signal transduction mechanisms modulate intracellular calcium concentration and therefore the state of vascular tone (Blatter and Wier, 1994).

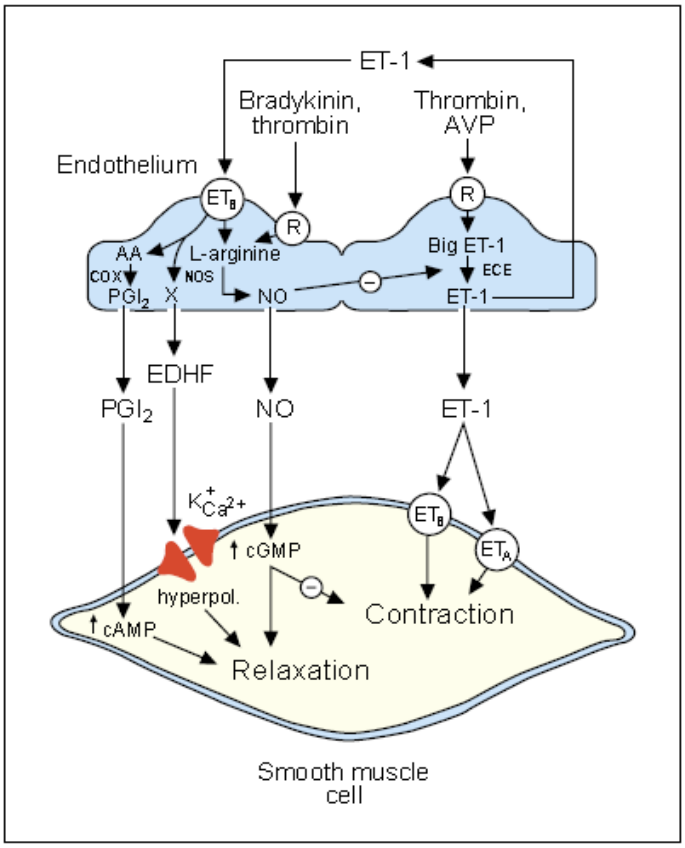

Figure 3. The different signal transduction pathways within vascular cells, which are involved in mediating the action of vascular cell contraction and relaxation. EDHF; endothelial-derived hyperpolarising factor (EDHF), ET-1; endothelin-1, NO; nitric oxide, NOS; NO synthase. Adapted from Channick, R. N. and Rubin, L. J. (2002) 'Endothelin Receptor Antagonism: A New Era in the Treatment of Pulmonary Arterial Hypertension.' *Advances in Pulmonary Hypertension*, 1(1) pp. 13-17.

The role of the different mechanisms alone or in combination in mediating, modulating and controlling the vascular tone is dependent on the type of the blood vessel, its territory and its corresponding size (luminal diameter). Some evidence suggest the contribution of endothelium-dependent hyperpolarisation in the control of endothelial vasomotor function in the majority of human blood vessels (Bellien et al., 2008). Although the role of EDHF becomes prominent in the presence of NO-synthase inhibitors, EDHF has also been suggested to play a key role in dilation under physiological conditions assessed in presence of NO in both resistance and conduit arteries (Honing et al., 2000; Bellien et al., 2006). NO may display a major part in some dilator-pathways, where EDHF has a minor backup role (Bauersachs et al., 1996) and vice versa and/or in combination. For instance, it is well

established that conduit vessels such as the aorta rely on NO more than EDHF-related pathway in mediating vascular dilation; in contrast to coronary arteries that mainly depend on EDHF-related pathways or a combination of both NO and EDHF. In the current study, we have used mesenteric arteries, which have been shown to depend mostly on EDHF-related pathway, similar to that found in many vascular beds within the human body. These microvascular beds, including cerebral arteries (McNeish et al., 2005), coronary arterioles, peripheral muscular arterioles, skin arterioles, gastroepiploic arteries, omental arteries, mesenteric arteries (White and Hiley, 1997), renal arteries and venous vessels, were suggested to have a characteristic EDHF activity (Bellien et al., 2008). However, the type of the vascular bed as well as accompanying position of an artery within the vascular tree, may determine the related contractile and dilatory pathway present. Table 1 summarises the main studies that related specific endothelial-dependent dilatory pathways as assigned to different vascular types and territories.

It was previously shown that nanomolar concentrations of endogenously released NO initiate and maintain the ACh-induced relaxation of the rat superior mesenteric artery (Simonsen et al., 1999), with these being independent of EDHF-related hyperpolarisation to ACh (Crane et al., 2003). This indicates the importance of NO as a vasodilator in the latter arteries. The contribution of NO is found most prominent in large-sized conduit vessels such as the aorta, carotid, femoral arteries and superior MAs (with an unstretched luminal (internal) diameter of 650 µm) (Hwa et al., 1994) whereas that of EDHF is most prominent in small- and microvessels (such as arterioles, meta-arterioles and capillaries.) (Hinton and Langton, 2003). The latter vessels distribute and control the blood perfusion into tissues and are involved in microcirculation of microvascular beds such as distal MAs (Shimokawa et al., 1996) and capillaries. In the review by Mulvany and Aalkjaer, they regarded small arteries as prearteriolar vessels with lumen diameter less than 500 µm in diameter (Mulvany and Aalkjaer, 1990). It was suggested that these small arteries, contribute to regulation of the peripheral resistance, with this being more evident in vessel sized between 10-200 µm in diameter (Mulvany and Aalkjaer, 1990). This idea was further supported through the presence of a deeper resting membrane potential and greater ACh-induced hyperpolarisation in the distal MAs compared to those in the aorta (with the

expression of eNOS in the aorta being higher than that in the distal MAs) (Shimokawa et al., 1996). The EDHF was found to account for 50% or more of dilation experienced in medium-sized (<500 μm in diameter) arteries (e.g. first-order MAs of the superior MA) (Garland and McPherson, 1992), while EDHF on the other hand, is the main dilator in small (~200-300 μm diameter; e.g. second and third-order MAs) and resistance-sized arteries and arterioles (e.g. fourth- and higher-order MAs running along the gut) (Burnham et al., 2006; Leo et al., 2011; Shimokawa et al., 1996; Koeppen et al., 2004). Arterioles are located in the transparent part of the mesentery and stem from first- or second-order branches of the superior mesenteric artery, and they give rise to small capillary networks that supply the mesentery. Thus, the contribution of EDHF to small arterial dilation is thought to increase as the vessel size decreases; with the latter phenomenon being more established in resistance arteries with a diameter <100 μm in diameter (Zhao et al., 2013) and mesenteric terminal arterioles (40 μm in diameter) (Hald et al., 2012). Due to their size (145-300 μm), the dilation of second and third order MAs employed in this current study is likely to be mediated mainly by EDHF (Hwa et al., 1994).

Table 1. Endothelial-dependent dilatory pathways as related to different vascular beds.

Vascular Bed	Model Studied	Stimulus	Pathway(s) Identity	Reference
Carotid artery	Guinea pig	ACh	EDHF	(Quignard et al., 2002)
Forearm microvasculature	Human	Bradykinin	EDHF	(Halcox et al., 2001)
Femoral arteries	Rabbit	ACh and and the calcium ionophore of bradykinin (A23187)	NO and EDHF	(Plane et al., 1995)
Aorta	Rat	ACh	NO	(Yan et al., 2007)
Coronary arterioles	Human	Hydrogen peroxide (H_2O_2)	EDHF	(Zhang et al., 2012)
Superior mesenteric arteries (650 µm diameter)	Rat	ACh	NO	(Hwa et al., 1994)
Mesenteric arteries (250 – 300 µm diameter)	Human	H_2O_2	EDHF	(Matoba et al., 2002)
Mesenteric resistance arteries (200 µm diameter)	Rat	ACh	EDHF	(Hwa et al., 1994)
Subcutaneous resistance arteries	Human	ACh	EDHF	(Coats et al., 2001)

1.2.2.1 The Contractile Mechanisms in Small Arteries

The mechanism of VSMC contraction is initiated in response to changes in the external environment including exogenous physical (mechanical), electrical and chemical stimuli. Blood flow can induce intravascular pressure that may lead to a passive stretching of VSMCs causing VSMC-dependent contraction. Such phenomenon is referred to as myogenic response (Scotland et al., 2001; Kol'tsova et al., 2010). Vasoconstriction is also mediated in response to various vasoconstrictor agonists acting on receptors located on the VSMC membranes. The common vasoconstrictors include; norepinephrine acting through α1-adrenoceptors and prejunctional α2-adrenoceptors (released from the sympathetic nerves that innervate blood vessels), angiotensin II (Ang II) (De Mello, 2013) acting through AT1 receptors (Griendling et al., 2000), arginine vasopressin (AVP) acting through V1a receptors (Yamamoto et al., 1997), endothelin-1 (ET-1) (Loesch et al., 1997) acting through ETA receptors, thromboxane A2, platelet-activating factor and phenylephrine (Phe) acting through α1-adrenergic receptor subtypes (Minneman, 1988). These receptors are coupled to G proteins, which upon conformational change provoked by vasoconstrictor-agonist receptors stimulate phospholipase C (PLC) activity via the activation of adenylyl cyclase, which catalyses the formation of cAMP (Figure 4). PLC acts on the membrane-bound lipid phosphatidy inositol 4-5 bisphosphate (PIP2) to catalyse the formation of diacyl glycerol (DG) and inositol 1,4,5 triphosphate (IP3). DG and IP3 act as second messengers, where IP3 binds to IP3 receptors on the sarcoplasmic reticulum (SR) (Zhou et al., 2008) to allow the opening of voltage-gated calcium ion (Ca^{2+}) channels (Vaca and Kunze, 1995) to allow the mobilisation and release of intracellular Ca^{2+} $[Ca^{2+}]i$ to initiate smooth muscle contraction. DAG and Ca^{2+} activate protein kinase C (PKC) (Geng et al., 1994), which phosphorylates specific regulatory target proteins contributing to vascular smooth muscle contraction. Free $[Ca^{2+}]i$ can also combine with an acid protein called calmodulin (CaM). The Ca^{2+}/CaM complex activates myosin light chain kinase (MLC Kinase) (Sato et al., 1995) which phosphorylates the 20 kDa light chain of myosin found on the myosin heads in the presence of ATP. The phosphorylation of myosin light chains leads to the molecular cross-bridge formation between the myosin heads and the actin filaments. Phosphorylation enables the molecular interaction of myosin with actin fibres. Hence, the sliding effect results in vascular smooth muscle contraction. Ca^{2+} can trigger Ca^{2+}-sensitive chloride (Cl^-) channels

allowing Cl^- efflux and membrane depolarisation to take place. The depolarisation of the membrane leads to the opening of L-type Ca^{2+} channels and extracellular Ca^{2+} influx eliciting VSMC contraction. The activation of Ca^{2+}-sensitive potassium ion (K^+) channels via the high Ca^{2+} concentration leads to the hyperpolarisation of cellular membranes. Hence the electromechanical coupling, resulting from the membrane potential, to determine $[Ca^{2+}]i$ concentration as well as the positive- and negative-feedback loops, both regulate $[Ca^{2+}]i$ storage and mobilisation (Carl et al., 1996). $[Ca^{2+}]i$ concentration thus displays a key factor in the regulation of the vascular tone and vascular smooth muscle contractility, not only through electromechanical coupling, but also through modulating the open probabilities of ion channels within VSMC membranes (Carl et al., 1996). The channels activated by $[Ca^{2+}]i$ include; large-conductance potassium channels, chloride ion channels, and nonselective cation channels has been described, as well as block of delayed rectifier potassium channels and $[Ca^{2+}]i$-induced inactivation of Ca^{2+} channels (Carl et al., 1996). Hence the concentration of $[Ca^{2+}]i$ depends upon the balance between the cellular calcium entry, the calcium release by the intracellular storage sites and either the re-sequestering of calcium by the SR back into storage sites or its removal out of the cell (via an ATP-dependent calcium pump or by the sodium-calcium exchanger) or both (Paltauf-Doburzynska et al., 1999).

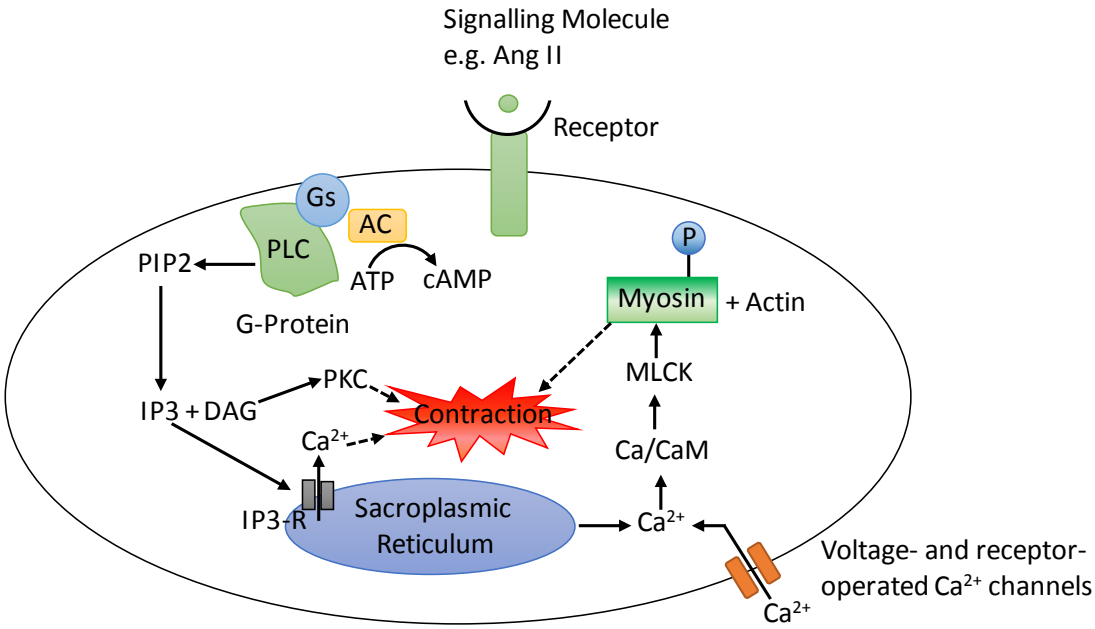

Figure 4. The Phosphoinositide Cascade: An illustration of the VSMC-dependent contraction in response to vasoconstrictors. Upon stimulation by e.g. angiotensin II (Ang II), the AT1 receptor that is coupled to G proteins, causes its conformational change to stimulate phospholipase C (PLC) activity via the activation of adenylyl cyclase (AC). AC catalyses the formation of cAMP. PLC acts on the membrane-bound lipid phosphatidy inositol 4-5 bisphosphate (PIP2) to catalyse the formation of diacyl glycerol (DG) and inositol 1,4,5 triphosphate (IP3). IP3 binds to the IP3 receptor (IP3-R) on the sarcoplasmic reticulum (SR) to allow the mobilisation and release of intracellular Ca^{2+} $[Ca^{2+}]i$ to initiate vascular smooth muscle contraction. DAG and Ca^{2+} activate protein kinase C (PKC), which phosphorylates specific regulatory target proteins contributing to smooth muscle contraction. Free $[Ca^{2+}]i$ can also combine with an acid protein called calmodulin (CaM). The Ca^{2+}/CaM complex activates myosin light chain kinase (MLC Kinase) which phosphorylates the light chain of myosin. Phosphorylation enables the molecular interaction of myosin with actin fibres leading to smooth muscle contraction. The depolarisation of the membrane leads to the opening of L-type Ca^{2+} channels and extracellular Ca^{2+} influx eliciting VSMC contraction. Author originated.

Another pathway to VSMC contraction involves the 20-hydroxyeicosatetraenoic acid (20-HETE) pathway (Fleming, 2001) (Figure 5). Following VSMC stimulation, phospholipase A2

(PLA2) activation leads to the liberation of arachidonic acid (AA) from membrane phospholipids (Fleming, 2001). AA may act as a substrate for the generation of 20-HETE, a reaction catalysed by cytochrome P450 (CYP) 4A through ω-hydroxylation (Fleming, 2001). 20-HETE is an essential component of the signal transduction cascade activated by several hormonal systems; including ET-1 and Ang II that have roles in regulating the blood pressure (Imig, 2000; McGiff and Quilley, 1999; Harder et al., 2000). The action of 20-HETE is mediated via the decreases in the open probability of calcium-dependent K^+ channels (K^+_{Ca}) and inhibits the Na-K-ATPase, which leads to depolarisation of the VSMCs, the activation of L-type Ca^{2+} channels and subsequent contraction (Fleming, 2001). 20-HETE and epoxyeicosatrienoic acids (EETs) (in particular 11,12- and 14,15-EET) activate several intracellular protein kinases including tyrosine kinases, the p38 mitogen activated protein kinase (MAPK), and extracellular-signal-regulated kinases 1 and 2 (Erk1/2) and increase the proliferation of various cell types, including vascular smooth muscle cells and ECs respectively (Uddin et al., 1998; Fleming, Fisslthaler, Michaelis, et al., 2001).

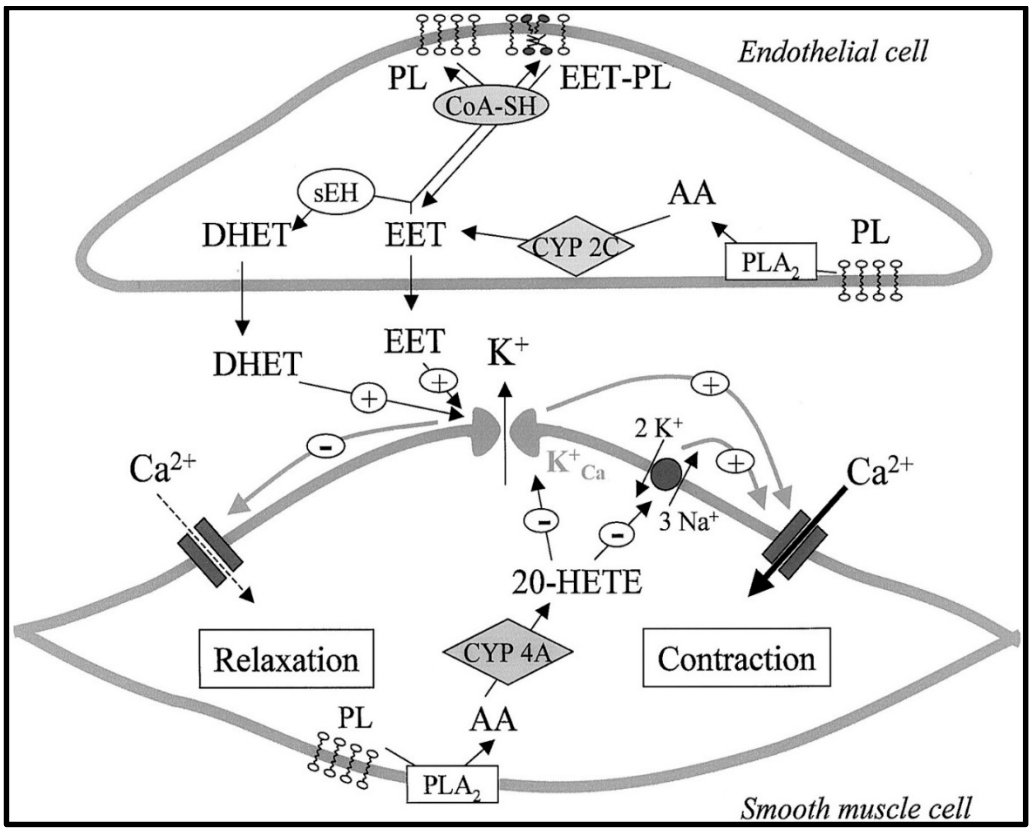

Figure 5. A schematic representation of mechanisms of vascular contraction and relaxation in relation to the epoxyeicosatrienoic acid (EET) and 20-hydroxyeicosatetraenoic acid (20-HETE) pathways. AA; arachidonic acid, CoA-SH; acyl coenzyme A synthase, CYP 4A; cytochrome P450 2A, K^+Ca; calcium-dependent K^+ channels, PL; membrane phospholipids, PLA_2; phospholipase, sEH; soluble epoxide hydrolase. Adapted from Fleming, I. (2001) 'Cytochrome p450 and vascular homeostasis.' *Circ Res*, 89(9), Oct 26, pp. 753-762. Copyright © American Heart Association.

1.2.2.2 The Vasodilatory Mechanisms in Small Arteries

The vasodilatory mechanisms in small arteries are initiated in response to mechanical stimuli (e.g. shear stress) and various vasorelaxing or vasodilator factors and agonists. These include; epinephrine acting through beta (β)2-adrenoceptors; cytokines, bradykinin, acetylcholine (ACh; released from the cholinergic autonomic nerve terminals and acting on muscarinic receptors on the vascular endothelium, e.g. muscarinic M3 receptors (Hsu et al., 2009)); prostacyclin (PGI2; acting through IP receptors), histamine (Adeagbo and Henzel, 1998) and substance P (Mathison and Davison, 1993). The presence of (activating)

agonist provokes a number of pathways depending on the agonist used and the bioavailability of a particular pathway's constituents (Figure 6), which includes the basal levels of mediators as well as their relative gene expression. A number of pathways are involved in mediating vasodilation including the EDHF- (Mehrke and Daut, 1990; Marchenko and Sage, 1993; Welsh and Segal, 2000; Hoepfl et al., 2002), NO- and prostacyclin (PGI)-dependent pathways (Bachschmid et al., 2005). Both EDHF and NO pathways play pivotal role in mediating endothelial-dependent dilation in small arteries. These will be explained in greater detail below.

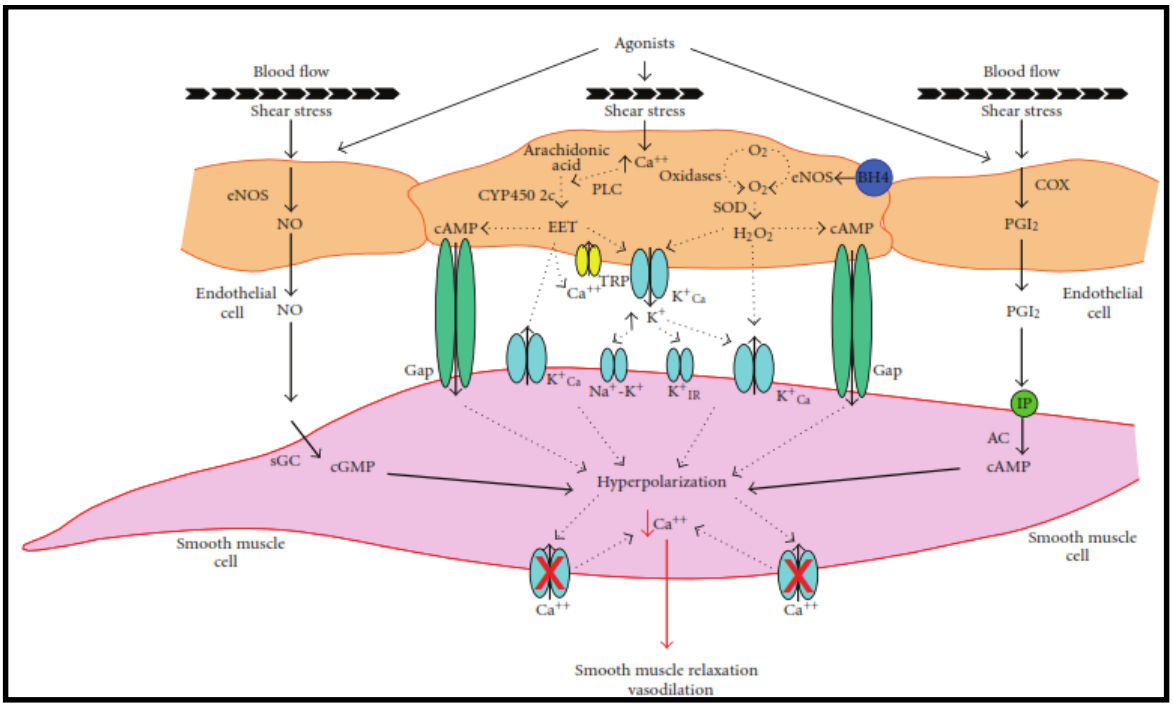

Figure 6. Schematic representation of EC-VSMC interactions to control vascular relaxation. CYP450 2c; cytochrome P450 2C, EETs; epoxyeicosatrienoic acids, K^+_{Ca}; calcium-dependent K^+ channels, PLC; phospholipase C. Adapted from Ozkor, M. A. and Quyyumi, A. A. (2011) 'Endothelium-derived hyperpolarizing factor and vascular function.' *Cardiol Res Pract*, 2011 p. 156146.

1.2.2.2.1 The Nitric Oxide and Prostacyclin-related Pathways

Endothelium-derived NO is an important component of vascular homeostasis through its ability to regulate vascular tone (Lefroy et al., 1993). In the endothelium, NO is synthesised by the oxidation of L-arginine (forming L-citruline and NO) using a NO synthase (NOS), of

which three isoforms exist (endothelial-derived NO synthase (eNOS), neuronal NOS (nNOS) and inducible NOS (iNOS)). eNOS is the main NO synthase associated with the endothelium (Kvasnicka, 2003). The regulation of the activity of eNOS and its constitutive expression helps to maintain a basal production of NO, to keep vessels in a relaxed state (Cardillo et al., 1997; Dawes et al., 1997; Brodde, 1994).

eNOS is subject to various forms of regulation including availability of cofactors and substrates, subcellular localisation, protein-protein interactions and phosphorylation (Govers and Rabelink, 2001). Exogenous stimuli such as shear stress as well as various agonists stimulate ECs within vascular beds and increase the activity of eNOS (Kagota et al., 1999) and cyclooxygenase (COX) (Scotland et al., 2005), providing H_2O_2, NO and prostacyclin (PGI) (Pearson et al., 1983)-mediated dilation respectively (Figure 3). The increase in the intracellular concentration of Ca^{2+} can generate the Ca^{2+}/CaM complex (Wang et al., 1995), which can either directly (Presta et al., 1997) or indirectly through CaMKII (Kida et al., 2012) activate eNOS. The phosphorylation of the Ser-1177 residue-bearing reductase domain of eNOS by CaMKII and the subsequent transfer of electrons from the reductase domain to the oxidase domain (Stuehr et al., 2001) favours the generation of NO. The reductase domain of eNOS converts molecular oxygen (O_2) and nicotinamide adenine dinucleotide phosphate (NADPH) to superoxide ($O_2^{\bullet -}$) and $NADP^+$ respectively (Stuehr et al., 2001). The electron transfer from the reductase domain to the haem group in the oxidase domain of eNOS is mediated by the Ca^{2+}/CaM complex (Ghosh et al., 1998). The Ca^{2+}/CaM complex binds to a consensus site in the eNOS reductase (Abu-Soud and Stuehr, 1993; Presta et al., 1997), which is linked to the oxidase domain via a Thr-495 residue (Fleming, 2010). Agonists which activate the phosphatidylinositol 3 kinase (PI3K)/Akt signalling pathway (Fulton et al., 1999; Michell et al., 1999) result in promotion of eNOS activity by increased Ser-1177 phosphorylation and/or Thr-495 dephosphorylation (Harris et al., 2001; Michell et al., 2001; Fleming, Fisslthaler, Dimmeler, et al., 2001; Hisamoto et al., 2001; Dimmeler et al., 1999; Gallis et al., 1999). Upon the generation of NO by eNOS, the latter diffuses from the EC vicinity into the VSMC where it binds to soluble guanylate cyclase leading to activation of cGMP (Cardillo et al., 1997). cGMP in turn activates cGMP-dependent protein kinase G (PKG) leading to Ca^{2+} resequestration to the

SR, enhanced Ca^{2+} pumping through the indirect stimulation of the Ca^{2+}-dependent ATPase pump and the inhibition of Ca^{2+} influx via channel phosphorylation. The elaborations of these mechanisms lead to a reduction in $[Ca^{2+}]i$ causing muscle relaxation. PKG also acts as a phosphatase to dephosphorylate myosin light chains also resulting in the relaxation of the smooth muscle cell, and hence the vessels.

1.2.2.2.2 The Endothelial-Derived Hyperpolarising Factor-related Pathways

A number of EDHFs have been identified which function by inducing hyperpolarisations of VSMCs leading to dilation. There are multiple potential EDHF-dependent pathways (Quilley and McGiff, 2000; Griffith, 2004) contributing to the regulation vascular tone (Feletou and Vanhoutte, 1988) in various vascular beds (Bellien et al., 2008). These include; the epoxyeicosatrienoic acid (EET), hydrogen sulphide (H_2S) and hydrogen peroxide (H_2O_2) pathways, which will be described in more detail.

1.2.2.2.2.1 The Epoxyeicosatrienoic Acid Pathway

The main EDHF-related pathway that has been identified is that involving the production of EET. This pathway is initiated via the action of various stimuli, which activate PLA2 on EC membranes. The activation of PLA2 may cause a conformational change that leads to the liberation of AA from the membrane phospholipids of ECs (Ozkor and Quyyumi, 2011) (Figure 6). Its metabolism by cyclooxygenases such as CYP epoxygenases (Fleming, 2001; Node et al., 1999; Michaelis and Fleming, 2006) and CYP monooxygenase (Miura and Gutterman, 1998) generate stereo-specific AA epoxides regioisomers or AA-derived EETs (e.g. 5,6-, 8,9-, 11,12-, and 14,15-EETs) (Rosolowsky and Campbell, 1996). There are different isoforms of CYP enzymes including; CYP 2C gene family (CYP 1A1 (Wu et al., 1997), CYP 2B, CYP 2B6 (Wu et al., 1997), 2C (Fisslthaler et al., 1999), 2C8, 2C9 (Potente et al., 2003), 2C10 and 2J2 in humans). EET is considered as an essential component for the EDHF-mediated responses in small vessels (Campbell et al., 1996; Fisslthaler et al., 1999; Fleming, 2004). Here, EET can transfer across the extracellular space to modulate smooth muscle membrane potential (Chen et al., 1991; Mombouli et al., 1996; Popp et al., 1996; Gebremedhin et al., 1998) via direct EC-VSMC vicinity coupling and the activation of membrane-bound channels on ECs and/or gap junctions (Griffith, 2004; Fleming and Busse,

2006). Previous reports suggested that EETs may act in an autocrine manner on ECs by activating voltage-gated Ca^{2+} channels (Luckhoff and Busse, 1990; Kamouchi et al., 1999) and/or transient receptor potential (TRP)V4 channels. These channels promote Ca^{2+} influx, further increasing Ca^{2+} concentration and stimulating various potassium channels on the EC and VSMCs membranes to cause hyperpolarisation and the release of potassium ions into the subendothelial space (Figure 6). The gap junctional communication between the ECs and VSMCs displays a critical phenomenon for the rapid spread of the electrical current from the EC to the smooth muscle cell layers (Griffith et al., 2004). The resulting vascular relaxation can therefore be secondary to the closing of voltage-operated Ca^{2+} channels and associated reductions in the influx of extracellular Ca^{2+} that sustain contraction in VSMCs (Griffith, 2004). There is some evidence to suggest that the metabolism of EETs into their diol products, the dihydroxyeicosatrienoic acids (DHETs) (VanRollins et al., 1996) is catalysed by the epoxide hydrolases. DHETs along with other esterified lipids may form an intracellular storage of EETs, from which EETs can be liberated upon cell activation independently of CYP activity (Weintraub et al., 1997). DHETs (such as 11,12-DHETs (Fang et al., 1996) and 14,15-DHETs (Fang et al., 1997) in particular) may participate in the relaxation of small arteries in an endothelial-dependent manner (Figure 5). In summary EETs and in some cases DHETs may both induce smooth muscle cell hyperpolarisation and vascular relaxation through the activation of Ca^{+2}-dependent potassium channels (K_{Ca}^{+}) and inhibiting L-type Ca^{2+} channels (Fleming, 2011).

Once formed, EETs are either metabolised to DHETs, incorporated into membrane phospholipids by acyl coenzyme A synthase (CoA-SH), or leave the endothelial cell without modification. EETs have an effect in modulating the role of endothelium in relaxation. Previous studies suggested an action of EETs via putative EET receptors to upregulate the expression of cyclooxygenase-2 (COX-2) via a heterotrimeric G protein/adenylyl cyclise/cyclic AMP (cAMP)/protein kinase A (PKA)/cAMP response element-binding protein (CREB)-dependent signalling pathway (Michaelis and Fleming, 2006), thus leading to the modulation of EC vasodilation at the transcriptional level. Other nuclear receptors and transcription factors (TFs) that mediate the actions of EETs involve; nuclear factor κB (NF-κB) (Node et al., 1999), peroxisome proliferator-activated receptors (PPAR)-α (Cowart et

al., 2002), PPAR-γ (Liu et al., 2005) and fatty acid binding proteins (FABPs) such as H-FABP (Widstrom et al., 2001). EETs were also shown to induce EC proliferation (Michaelis and Fleming, 2006) via the phosphorylation and activation of Akt (Potente et al., 2003), PI3K, MAPK (Pozzi et al., 2005) and K_{Ca}^{+} channels.

The basis of EETs' action involve the passive transmission and spread of electrical signals from the vascular endothelium to the SMC layer via gap junctions to precede the rapid hyperpolarisation event of the ECs (Griffith, 2004). The spread of current through gap junctions along the vessel wall (Segal and Duling, 1989) is followed by a subsequent current decay. The current decay depends on the initial hyperpolarisation event (Emerson et al., 2002), the length constant of the vessels receiving the current and the regenerative mechanisms involved in conducting the hyperpolarisation (Goto et al., 2004). The distal spread of the current through the regenerative mechanism of increased K^{+} in the interstitial or extracellular K^{+} (Mehrke and Daut, 1990; Hurjui et al., 2011) are mediated by the activation of various potassium channels located on both ECs and VSMCs membranes (Gordon and Martin, 1983; Mehrke and Daut, 1990; Wiecha et al., 1998; Miura et al., 1999; Faehling et al., 2001; Miura et al., 2001; Wolfram Kuhlmann et al., 2004; Ozkor et al., 2011). These channels include; ATP-sensitive potassium channels (K_{ATP}) (Rivers et al., 2001; Horiuchi et al., 2002; Crane et al., 2004), inwardly rectifying potassium channels (K_{IR}) of three types; small-conductance calcium-activated potassium channels (SK_{Ca}), intermediate-conductance calcium-activated potassium channels (IK_{Ca}) (Edwards et al., 2000; Bychkov et al., 2002) and large-conductance calcium-activated potassium channels (BK_{Ca}) (Edwards et al., 1998; Frieden et al., 1999), and sodium-potassium ATPase (Na^{+}/K^{+}-ATPase) pumps (Ashcroft, 1988; Noma, 1983; Seino, 1999). K_{ATP} channels consist of a pore-forming K_{IR}-6.x tetramer and a regulatory sulphonylurea receptor (SUR) tetramer (Cao et al., 2002), which confers sulphonylurea sensitivity (Standen et al., 1989; Cook and Hales, 1984; Inagaki et al., 1996). K_{ATP} channels are found in different isoforms (Fujita and Kurachi, 2000; Gopalakrishnan et al., 1999; Koh et al., 1998; Chutkow et al., 1996; Suzuki et al., 2001) and combinations yielding tissue-specific K^{+} channels with subtly different properties (Inagaki et al., 1996; Inagaki et al., 1997; Isomoto et al., 1996; Yamada et al., 1997). For instance; in the rat mesenteric artery the combination of four K_{ATP} channel subunit genes

were identified, namely rat-specific vascular tissue (rv)-K_{IR}6.1, rvK_{IR}6.2, rvK_{IR}SUR1 and rvSUR2B (Cao et al., 2002), displaying over 99.6% amino acid sequence identity with previously reported isoforms. Hence, hyperpolarisation of the smooth muscle layer is achieved by the combined effects of the closure of voltage-gated channels leading to a fall in [Ca^{2+}]i concentration as well as the increase in K^+ inside VSMCs and the subsequent vasodilation.

1.2.2.2.2.2 The Hydrogen Sulphide Pathway

H_2S is a gasotransmitter synthesised by several different enzymes from cysteine by 3-mercaptopyruvate sulphuresterase (3MST), cystathionine β-synthase (CBS) and/or cystathionine γ-lyase (CSE) (Osmond, 2012) in ECs (Wang, 2009; Skovgaard et al., 2011; Pan et al., 2012). It has recently been thought to contribute to microvascular dilation though a calcium-dependent activation of eNOS within ECs (Kida et al., 2012) (Figure 7).

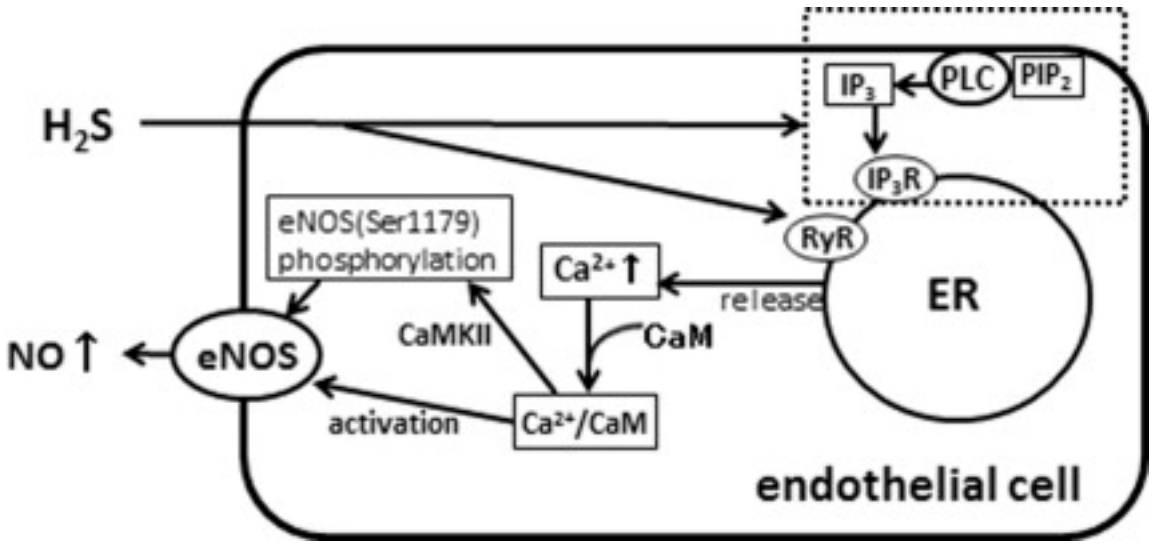

Figure 7. Schematic representation of the H_2S-related pathway. Adapted from Kida, M., Sugiyama, T., Yoshimoto, T. and Ogawa, Y. (2012) 'Hydrogen Sulfide Increases Nitric Oxide Production with Calcium-dependent Activation of Endothelial Nitric Oxide Synthase in Endothelial Cells.' *Eur J Pharm Sci*, Nov 10.

1.2.2.2.2.3 The Hydrogen Peroxide Pathway

H_2O_2 is generated from the spontaneous dismutation from superoxide anion radical ($O_2^{\bullet-}$) or dismutation of superoxide by superoxide dismutase (SOD) (Stuehr et al., 2001), of which three isoforms exist (Faraci and Didion, 2004), localised to different cellular compartments. The Cu,Zn-SOD (SOD1) isoform (Okado-Matsumoto and Fridovich, 2001) is the most abundant isoform found associated with the vascular wall (Didion et al., 2002). It was previously found to dismutate superoxide ($O_2^{\bullet-}$) generated by eNOS and suggested to have a protective role in prolonging the half-life of NO (Mugge et al., 1991). A study by Fujiki, regarded eNOS as one of the major contributor for the synthesis of H_2O_2 (Fujiki et al., 2005). Another isoform of SOD was identified as the extracellular-SOD (ecSOD, SOD3) and was found to dismutate extracellular superoxide to protect the diffusion of NO (Fukai et al., 2002). However the latter was excluded as a source of EDHF (Morikawa et al., 2003). The protective role of SOD in ECs as a scavenger for superoxide radicals generated by eNOS and the production of H_2O_2 was suggested to restore and improve the myoendothelial communication as a result of a reduction in reactive oxygen species (ROS) generation (Griffith et al., 2005).

In a study by Lui et al., the presence of H_2O_2 in human isolated coronary arterioles, derived from mitochondria, was associated in flow-mediated dilation (Liu et al., 2003). There are different signal transduction pathways that have been suggested to mediate the action of H_2O_2 leading to the hyperpolarising effect of the latter in certain blood vessels, such as human mesenteric arteries (Morikawa et al., 2004) (Table 1). In a study by Barlow et al., H_2O_2 action was suggested to be mediated through BK_{Ca} channels and the EET-related signalling cascade in coronary arteries (Barlow et al., 2000). Similarly H_2O_2 was found to dilate human coronary arterioles through the opening of BK_{Ca} channels via a mechanism involving protein dimerisation and activation of protein kinase G (PKG)-Iα in human coronary artery smooth muscle cells (Zhang et al., 2012). In the mesenteric artery, H_2O_2 was suggested to act via the disulphide dimer activation of PKG1α to activate BK_{Ca} channels and lead to an enhancement of EDHF-mediated actions in mice (Ohashi et al., 2012). A recent study by Choi et al., suggested a role of H_2O_2 in increasing the expression of K_{Ca}^+ channels through the upregulation of phosphorylated ERK expression and the

downregulation of repressor element-1-silencing transcription factor (REST) expression using a primary cultured human umbilical vein ECs (HUVECs) as a model (Choi et al., 2013).

A model for the generation of H_2O_2 was suggested via the increase in the intracellular concentration of Ca^{2+} along with caveolin-1 (Ohashi et al., 2012) acting through an alternative fashion to generate H_2O_2 by the activation of the reductase domain of eNOS. This pathway involves the dual action of both Ca^{2+}/CaM-dependent protein kinase (CaMK) kinase β (CaMKKβ), which phosphorylates the eNOS at the Ser-1179 residue and caveolin-1, which antagonises CaMK binding via its interaction with the reductase domain and oxidase domain of eNOS (Ohashi et al., 2012). The binding of caveolin-1 to eNOS shifts the electrons from the oxidase domain to the reductase domain and assists in the generation of H_2O_2 via $O_2^{\bullet-}$ (Ohashi et al., 2012). The compromise in the electron transfer, as a result of the action of caveolin-1 on eNOS, inhibits NO synthesis (Ghosh et al., 1998) and favours the EDHF-related pathway.

In summary EDHFs cause hyperpolarisation through multiple pathways involving the epoxyeicosatrienoic acid, H_2S and H_2O_2 pathways. EDHF action can be blocked experimentally, using potassium channel inhibitors. These inhibitor peptides including; charybdotoxin, apamin and TRAM-34 (1-[(2-chlorophenyl)diphenylmethyl]-1H-pyrazole) can be used to study the pharmacological effects of various potassium channels involved in mediating the EDHF actions. Charybdotoxin was shown to be a selective blockers for BK_{Ca} (Archer et al., 1994; Franca-Silva et al., 2012), whereas apamin and TRAM-34 were shown to block SK_{Ca} (van der Staay et al., 1999) and IK_{Ca} (Wulff et al., 2000) respectively with high affinity. Because charybdotoxin is mainly involved in blocking channels mostly presented by the VSMCs (Miller et al., 1985), apamin and TRAM-34 are used specifically to block potassium channels associated with ECs.

1.2.3 Pathophysiological Considerations to Vascular Function

Vascular injury can impair vascular integrity and/or cause a compromise, disruption, impairment, blockage and/or depletion of the EDHF release and/or action and/or NO bioavailability (Alonso and Radomski, 2003; Pacher et al., 2007), generation and/or their associated mechanisms (mediators and/or facilitators). This may lead to an imbalance in vasoconstrictor and vasodilator mediator release from ECs (termed endothelial dysfunction), upregulation of adhesion molecules and ultimately vascular disease (Marchesi et al., 2009; Sakellariou et al., 2011). The ability of the vascular endothelium to generate NO is critical in small vessels when the EDHF-mediated response is affected and vice versa. Thus NO may act as a backup system to EDHF in instances when the latter is compromised (Gaubert et al., 2007). In disease states, the EDHF-mediated responses become resistant to vascular diseases such as atherosclerosis, thus a potential vascular injury may eliminate the NO-back-up system offered by EDHF and thus lead to the progression and/or worsening of the condition (Urakami-Harasawa et al., 1997; Shimokawa and Matoba, 2004; Shimokawa, 2010). Diseased or injured blood vessels may produce increased levels of ROS, in particular $O_2^{\bullet -}$ (Griendling et al., 2000), a marker of oxidative stress, where superoxide is subject to dismutation by SOD into H_2O_2 (Griendling et al., 2000). Reduced bioavailability of NO may be a result of decreased synthesis of NO and/or increased superoxide generation, which is suggested to react with NO, producing peroxinitrite ($ONOO^-$) (Beckman et al., 1990; Sotnikova et al., 2011). This phenomenon can lead to a low [NO]/[$ONOO^-$] ratio, which can act as an indicator of nitroxidative/oxidative stress (Kalinowski et al., 2004; Villa et al., 1994; Heeba et al., 2007) and ultimately lead to the upregulation of genes (Tumur et al., 2010) involved in inflammation and coagulation of the vasculature (Pober and Sessa, 2007; Pahl, 1999). Hence, it is essential that the endothelial function is preserved for the maintenance of vessel diameter and hence optimal blood transport around major organs and tissues.

1.3 NPs and their Potential in Medical Interventions

The requirement for an accurate delineation, sensitive visualisation, specific targeting and monitoring in medical diagnostic and prognostic procedures has promoted the application of nanotechnology as an alternative strategy to conventional histological, imaging and drug delivery systems (Patricio et al., 2011). Nanobiotechnology and the use of nanomaterials have displayed a platform for intervention in medicine in aiding new pathways to diagnostic and therapeutic options (Hrkach et al., 1997; Pires et al., 2012). According to the publicly available specifications standards driven by the British Standards Institution (BSI), nanotechnology is defined as "the application of scientific knowledge to manipulate and control matter in the nanoscale in order to make use of size- and structure-dependent properties and phenomena distinct from those associated with individual atoms or molecules or with bulk materials". Nanobiotechnology, however, is an interdisciplinary science that bridges areas in physics, chemistry and biology to understand and apply concepts in nanomaterials and their properties. Both concepts are used in manufacturing small nanoscale materials (Jain, 2005). According to BSI, a nanomaterial is described as "material with any external dimension in the nanoscale or having internal structure or surface structure in the nanoscale". According to BSI, NPs are defined as "nano-objects with all three external dimensions in the nanoscale (size range from approximately 1 nm to 100 nm)". NPs display the basis for this nanotechnology and behave as whole units in terms of their transport and properties (Prabhu et al., 2011). Due to their small size, NPs exhibit various properties including; large surface area, high surface reactivity and strong adsorbing ability (Xu et al., 2004). The different physical, chemical and biological properties of NPs depend on their chemical synthesis, composition (coating and polymerisation) and reactivity (Wiesenthal et al., 2011).

The biomedical application of nanomaterials (Skrabalak et al., 2007) depend on their material composition (Yacobi et al., 2007), shape (Gong et al., 2010), size (Sun and Chow, 2008), concentration (Davda and Labhasetwar, 2002), cellular permeability, biodegradability, bioactivity (Suh et al., 2009) and toxicity (Warheit et al., 2004; Mortensen et al., 2008). Nanomaterials of different types such as quantum dots (QDs), silica NPs

(SiNPs) and carbon nanotubes (CNTs) have displayed potential tools for use in medical applications; including; imaging diagnostics (bio-imaging or sensing) (Roy et al., 2012) and medical therapeutics (Cherukuri et al., 2004; Borm and Müller-Schulte, 2006).

Despite the potential clinical uses of NPs, previous studies have suggested a toxic behaviour of selected NPs (Akhtar et al., 2010; Aillon et al., 2009). NPs are very small and in addition to their high penetrability into tissues, cells and organelles they display a large surface area of exposure for non-specific interactivity with different biological molecules (Klein, 2007; Cedervall et al., 2007). This includes the interaction and/or adsorption of biomolecules such as proteins and lipids onto NP surfaces in biological environments (Ehrenberg et al., 2009), leading to the formation of a 'Corona' (Monopoli et al., 2011). This phenomenon may lead to the re-organisation of the NP surface, altered surface chemistry and conformation leading to varied interaction (Monopoli et al., 2011). Thus, there is a concern regarding the application of nanomaterials in biomedicine due to the limited information on their biocompatibility such as stability, porosity, solubility (Kingsley et al., 2006), biodistribution and fate (interaction and clearance) in living systems. Thus, a better understanding and appreciation of the behaviour and monitoring of these nanomaterials *in vitro* as well as *in vivo* is necessary to meet such demands and appreciate the benefits and potentially associated health risks (Ferrante et al., 2012) in the long-term. Among the different NPs present, SiNPs and CNT have displayed a greater potential for use in biomedical research due to their unique properties enabling their use for imaging diagnostics and targeted drug delivery.

1.3.1 SiNPs – Properties and Applications

There is a growing interest in the fabrication of silica NPs (SiNPs) for applications in cell tracking, imaging diagnostics (Choi and Chen, 2003; Giri et al., 2005; Hsiao et al., 2008; Sokolov and Naik, 2008; Tsai et al., 2008; Barshan-Tashnizi et al., 2009; Motwani et al., 2011), drug delivery (Christofidou-Solomidou et al., 2002; Slowing et al., 2009) and medical therapeutics (Zhou et al., 2011; Lu et al., 2007) due to their tuneable size and stability under flow conditions. Colloidal SiNPs can be synthesised using the Stöber sol-gel method described in 1968 (Stöber et al., 1968) and the water-in-oil (W/O) reverse microemulsion method as carried out by Chen et al. (Chen et al., 2013). Stöber sol-gel method uses tetraethyl orthosilicate (TEOS), aqueous ammonia solution ($NH_3 \cdot H_2O$) and water in absolute ethanol in order to generate the SiNPs, hence the silica matrix can be produced by the controlled hydrolysis of TEOS in water nanodroplets with the initiation of ammonia (Chen et al., 2013). SiNPs can also be fabricated to form ordered pore structures (mesoporous SiNPs; MSiNPs) with a greater surface area in contrast to non-porous (amorphous) SiNPs, hence the capability to accommodate various molecular species for potential system drug delivery (Vivero-Escoto et al., 2010). SiNPs have been shown to be highly reactive and can interact efficiently with biological material due to their large surface area to volume ratio (Mortensen et al., 2008). SiNPs can be incorporated into various nanomaterials and nanocomposites for use in biomedical research; including tissue engineering scaffolds (Wang et al., 2012; de Matos et al., 2013). SiNPs are thus of special interest as they can be tagged by thousands of luminescent molecules making them attractive tools in clinical applications.

1.3.1.1 The Synthesis of SiNPs

Silicon dioxide represents the basic molecular structure of silica-based materials. It has a characteristic crystalline structure, where the atoms or molecules are arranged in an ordered array in a liquid or solid phase (Figure 8). The sol-gel method is used to synthesise SiNPs with non-porous amorphous (non-ordered) or crystalline (regular lattice) structure. The term sol-gel refers to the fabrication of particles in the form of a gel or monodispersed solution and was first described by Stöber et al. in 1968 (Stöber et al., 1968). It uses the principle of precipitation and encompasses the use of inorganic precursors such as metal halides, metal salts and alkoxides ($M(OR)_X$), all mixed in solution to form the initial particles in a single synthetic step. The initial synthesis of SiNPs involves the hydrolysis of the inorganic precursor followed by condensation to synthesise the silicon oxide. The colloidal silica generated as a result of the sol-gel method facilitates the production of siloxane polymer from organosilica compounds.

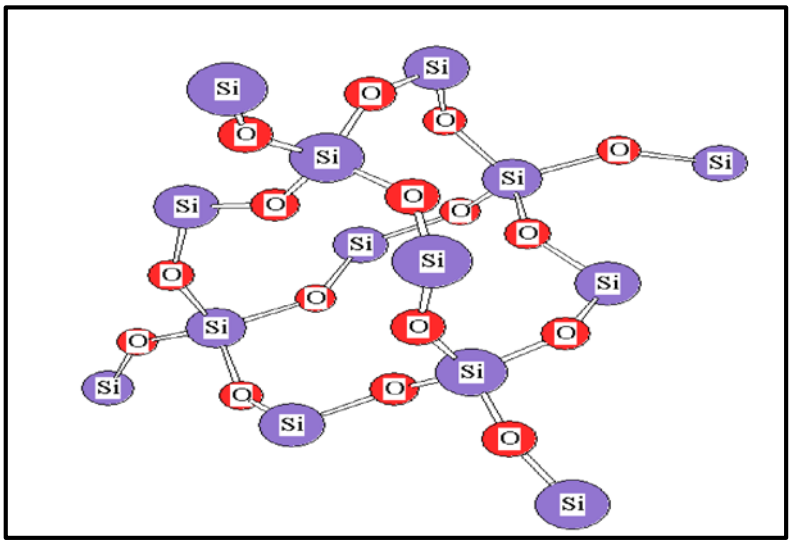

Figure 8. A three-dimensional schematic representation of the crystalline structure of silicon dioxide in a quartz structure. Author originated.

The sol-gel synthetic route for SiNPs allows particle size control by altering the temperature, *pH*, dispersants and precursor concentrations (Giesche, 1994a). Hence, the reaction rate and growth rate of SiNPs can be manipulated by the use of for example acids or bases to affect the hydrolysis or condensation rate. Using low *pH* results in fast hydrolysis and in turn slow condensation favouring the formation of a gel. This phenomenon is reversed with high *pH* conditions leading into slow hydrolysis and fast condensation favouring a monodispersed solution (Oye et al., 2006). The change in the silica precursor and solvent concentrations can also affect the size and monodispersity of SiNPs. Stöber et al. were able to fabricate SiNPs at different size ranges (50 nm to 2 µm) using the latter phenomenon (Stöber et al., 1968). Furthermore, the change in temperature conditions was shown to affect the nucleation of SiNPs generated from hydrolysis of a silica precursor, known as tetraethyl orthosilicate (TEOS), in an alcohol solution and catalysed by ammonia (Figures 9 and 10) (Chang and Fogler, 1997). The hydrolysis reaction was followed by a condensation of the alkoxide silica ($Si(OR)_4$) occurring by alcohol or water molecules to fabricate monodispersed silica spheres (Figure 10) (Chang and Fogler, 1997).

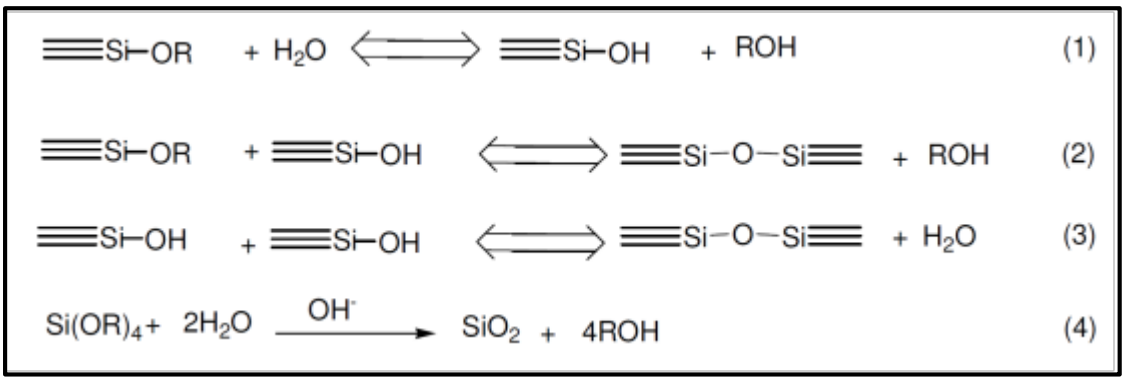

Figure 9. The reaction scheme for the fabrication of silica nanoparticle; where (1) is the initial hydrolysis reaction step, (2) is the alcohol condensation reaction step and (3) is the water condensation reaction step. The overall reaction is given in step (4), where R denotes C_2H_5. Author originated.

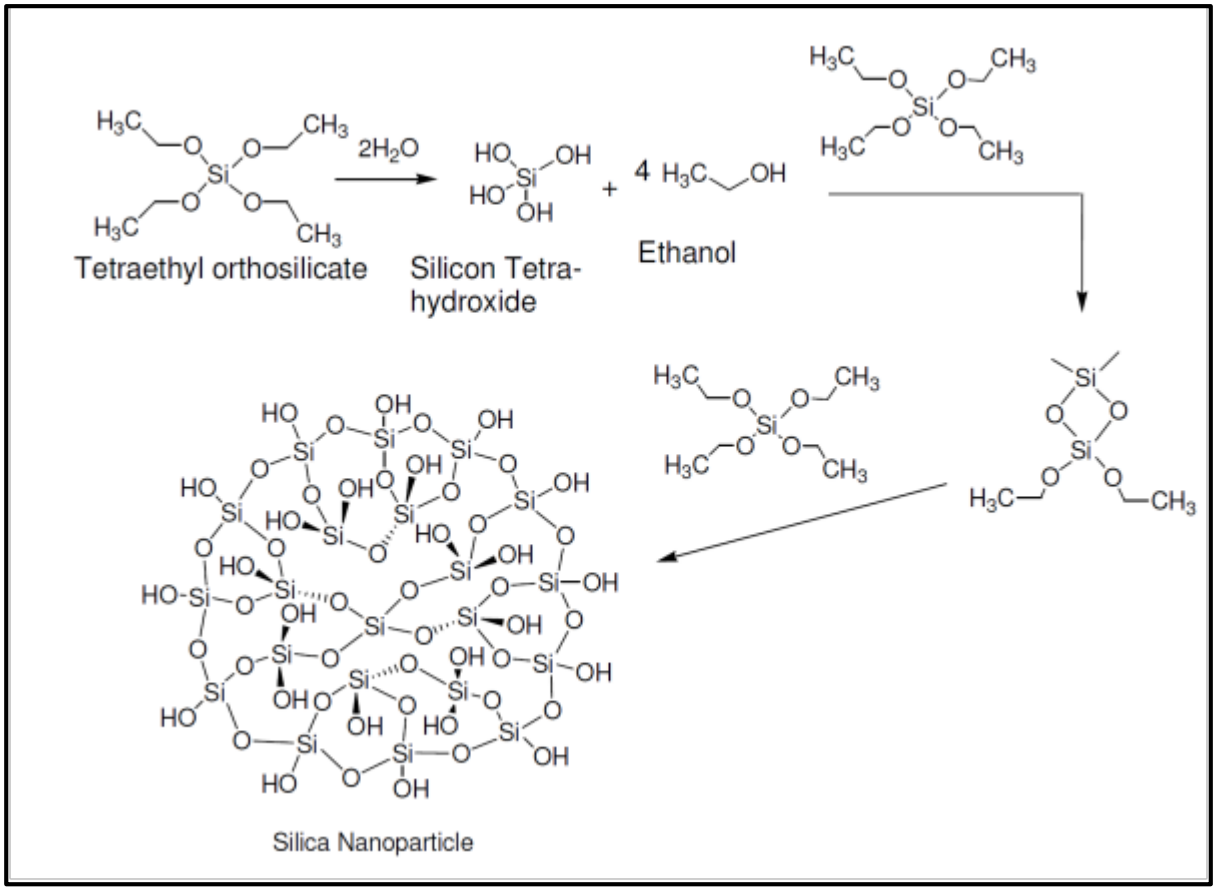

Figure 10. Schematic illustration of the Stöber sol-gel reaction for the production of silica spheres. Author originated.

A number of attempts have been carried out to produce smaller sizes of monodispersive SiNPs (below 100 nm) with smooth surface since Stöber et al. method was accomplished (Bogush et al., 1988; Giesche, 1994b). The demand for such NPs is of huge interest for biomedical applications. These attempts combined different factors that affect the reaction conditions such as changing the temperature as well as altering reagent concentrations (such as TEOS, NH_3 and ethanol) to fabricate SiNPs at the desired sizes. Stöber et al. used the phenomenon of reactant concentration (such as tetraethyl silicate concentration at 0.28 mol dm^{-3}) and certain physical conditions (the occurrence of the reaction at room temperature) as the determinant factor in fabricating monodispersed SiNPs (Stöber et al., 1968). Stöber et al. represented the relationship between particle diameter and reactant (water and ammonia) concentration graphically (Stöber et al., 1968). However, using the Stöber at al. method to obtain larger particles (1-2 µm) tends to yield a poor size distribution, while very small particles (approx. 30 nm) tend to lack a smooth surface.

Bogush et al. had generated a model (growth-only) for synthesising silica in an effort to enhance the monodispersity of SiNPs (Bogush et al., 1988). The “growth-only” model relies initially on SiNPs nucleation where the starting materials fully react to form small core SiNPs known as “seeds”, followed by a diffusion-limited growth where TEOS is added in a molar ratio of 1:2 to water to coat the small SiNPs seeds (Bogush and Zukoski, 1991; Byers et al., 1987). This latter model causes the gradual increase in particle size or seeding growth, preventing the aggregation between particles of the same size as experienced with the “aggregation-only” model (Bogush and Zukoski, 1991). The relationship between reactant concentration and particle size was expressed through an equation, which was derived through the fabrication of over 100 samples at 25℃ (Bogush et al., 1988). The particle diameter size generated depends on the total volume of TEOS added during the seeded growth (Bogush et al., 1988) and derived as follows;

$$d = A[H_2O]^2 exp\ (-B\ [H_2O]^{1/2})$$

Where, *d* is the average particle diameter in (nm) and the reactant concentrations with the units of mol dm^{-3}. The term *A* is specified in the above equation, was corrected by Razink et al. (Razink and Schlotter, 2007) as follows;.

$$A = [\mathrm{TEOS}]^{1/2}\,(82 + 151[\mathrm{NH_3}] + 1200[\mathrm{NH_3}]^2\ - 366[\mathrm{NH_3}]^3)$$

Furthermore, the *B* within the former equation was expressed as follows;

$$B = 1.05 +\ \ 0.523[\mathrm{NH_3}] - 0.128[\mathrm{NH_3}]^2$$

Achieving smooth monodispersive SiNPs at a small size (10-100 nm) is difficult, as the particles tend to be granular in appearance due to the presence of ultra-fine particles surrounding the surface of SiNPs.

1.3.1.2 Stability of SiNPs

Particles in the size range between 1-1000 nm are referred to as being colloidal, where they have a characteristic lyophobic or solvent hating behaviour when dispersed in a continuous medium (Baalousha et al., 2006). This minimises the interaction between the particles and continuous dispersed phase (Baalousha et al., 2006). The laws of free Gibbs energy and entropy change accompany random "Brownian" motion of NPs within a solution according to their kinetic energy and particle collision (Atkins, 2005). The stability of SiNPs is characterised by their ability to remain dispersed in suspension and have a reduced tendency to aggregate. Small size SiNPs disperse in a better fashion than larger ones, which have a tendency to settle quickly (Koohestanian et al., 2004) in a colloidal suspension according to gravity and viscous drag force laws. The increased ratio of electrostatic repulsive forces over the attractive forces (Van der Waals forces) that exist between the NPs (Pashley and Karaman, 2005) helps to prevent the particles from aggregating. There are different types of aggregation including; conservation, gelation, coagulation and flocculation (Figure 11). In addition, the *pH* and ionic strength of the solution containing the NPs can affect the stability of the latter NPs (Birdi, 2009). There is a demand for stable SiNPs in biological media in order to fulfil their role (Akbar et al., 2011). Particles can be linked into branches forming a three-dimensional network leading to increased viscosity followed by gelation, which is characterised by the formation of a solidified network that retains the liquid. Particles can also form bridges together that link them leading into flocculation, or become as closely packed clumps with each other leading into coagulation (Koohestanian et al., 2004; Akitoshi, 2005). The absorption of materials onto the particle surface leads to reduced hydrophilicity and more concentrated liquid phase, which is immiscible in the aqueous phase termed "Conservation".

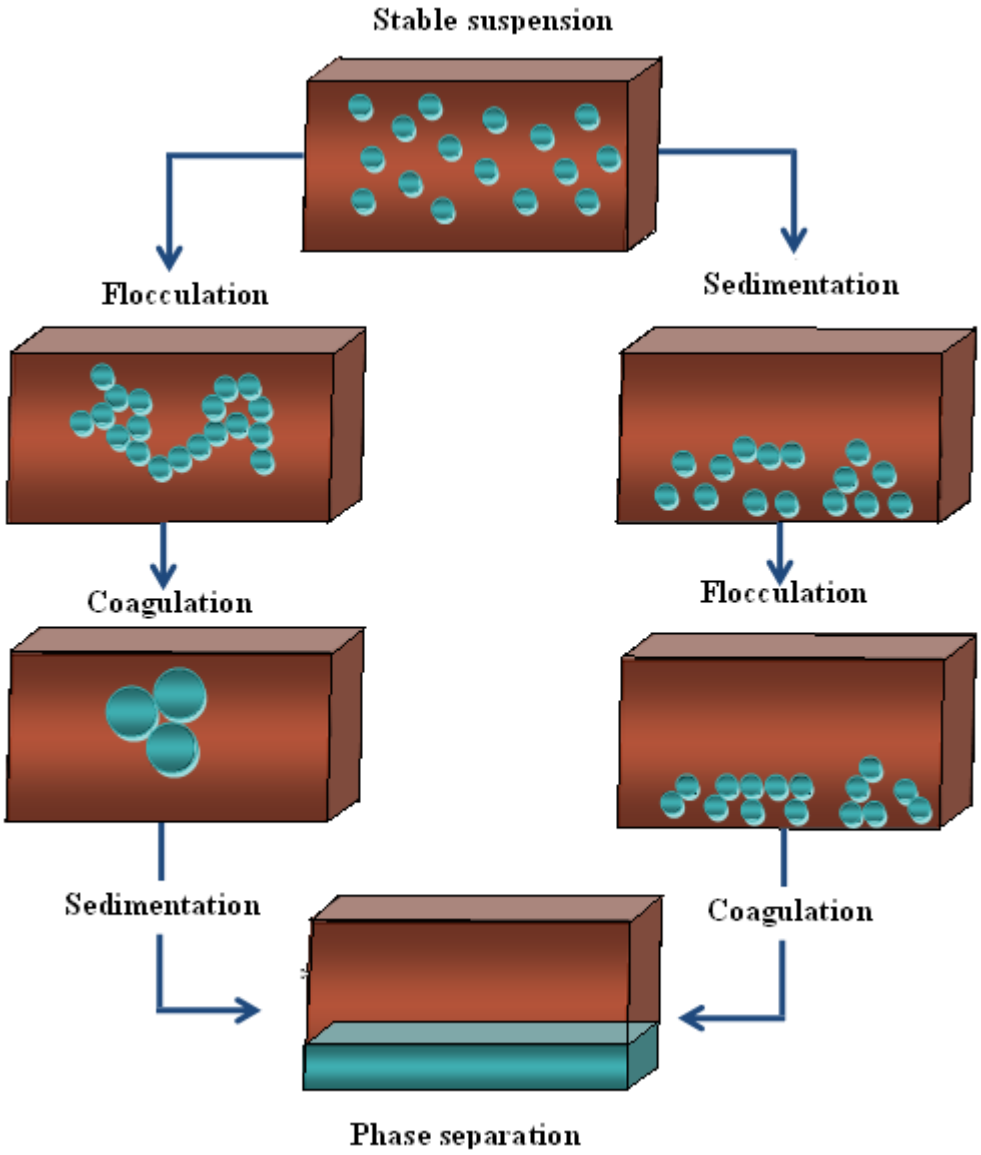

Figure 11. Stable colloidal nanoparticles undergoing the flocculation and coagulation process of aggregation. Author originated.

The stabilisation of NPs can lead to more monodispersed NPs and can be achieved sterically, by creating a surface charge on the NP surfaces or the use of capping agents. Capping agents have the limitation of changing the properties of the intact NPs surfaces.

1.3.1.3 Surface Charge of SiNPs

The overall surface charge of the SiNP is related to the carboxylic groups surrounding the surface. This charge determines NPs reactivity and interaction with other NPs and the surrounding tissue, cells and/or molecules. Hence, SiNP interaction with the surrounding tissue, cells and/or molecules is responsible for minimising aggregation (Ju-Nam and Lead, 2008), dispersive stability, the viscosity, flocculation and film forming abilities of NPs.

NPs are prone to coating with ions and/or molecules when left in an electrolyte solution leading to changes in their surface charge, stability and hence properties. The coating leads to the formation of what is termed "the electrochemical double layer (EDL)", which is described as the interface between two phases, whether it is solid/liquid, liquid/liquid or liquid/gas, which possesses properties in the bulk phase. The EDL is regarded as a phase boundary having different distribution of electrical charges, therefore producing an electrical double layer, which has a potential that is different to both phases. The Stern model provided a graphical model for the charge distribution of particles in the EDL (Figure 12). When NPs are placed in solution that contains electrolytes of anion or cation origin, a monolayer of the electrolyte is adsorbed onto the particle surface in a non-specific and/or specific manner forming an inner Helmholtz plane (IHP). This causes the NPs to become positively charged with a higher tendency to interact with other NP surface(s), whereas the counter-ions become dehydrated in the inner layer. The extent of the overall potential (ψ_i) of the NP surface depends on the strength of interaction between NPs and ions with the possibility of formation of a second layer of hydrated rigidly bound counter-ions referred to as the outer Helmholtz plane (OHP). Together, both the IHP and OHP with a particular thickness (δ) form the Stern layer. The control of the kinetics of the crystal growth of SiNPs and NPs aggregation using the sol-gel precipitation method with some alterations, can lead to the generation of an organised array of small and monodispersed SiNPs with surface stability (Giesche, 1994b). The latter can be achieved by incorporating dye molecules (Marchisio et al., 2006) and coating NPs with inorganic groups to overcome the poly-distribution (Iler, 1979; Andersson et al., 2004) and surface instability.

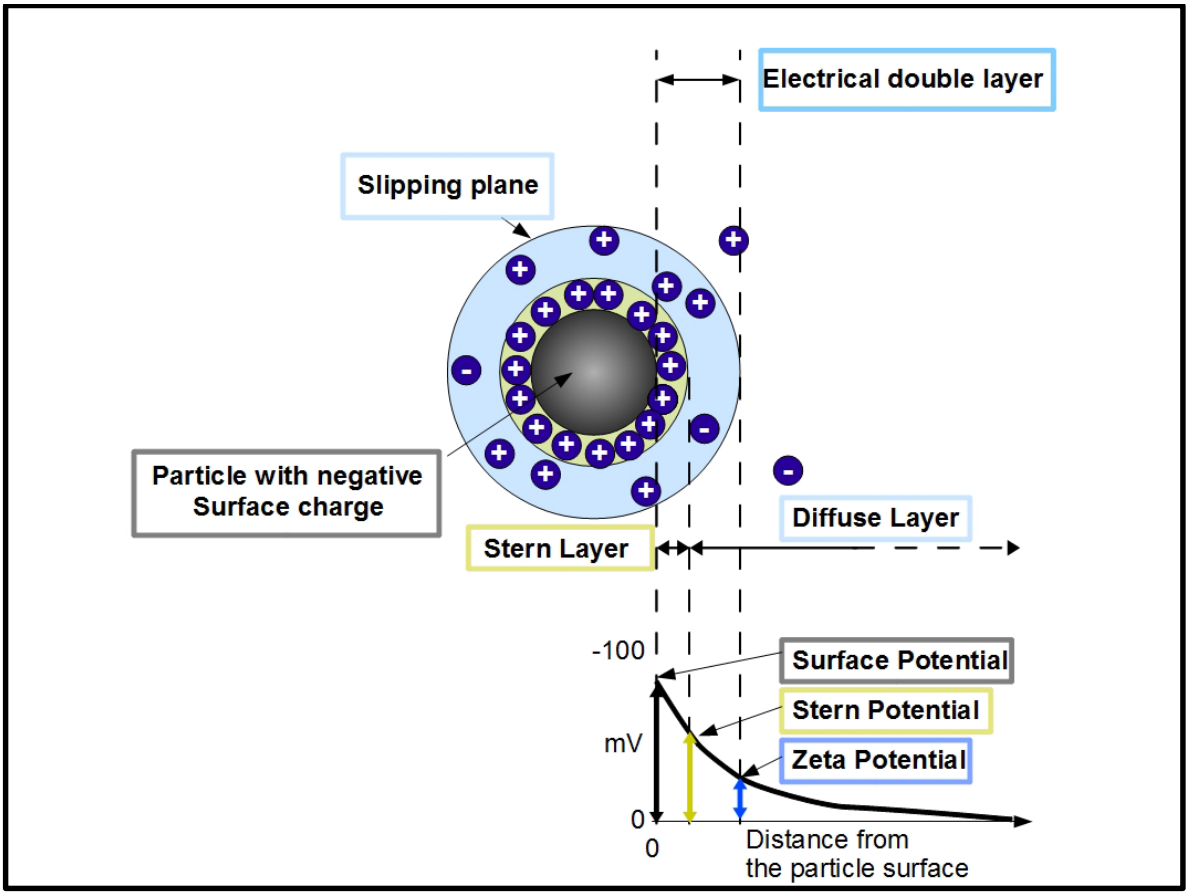

Figure 12. Scheme of the electrical double layer surrounding a nanoparticle in solution. The negatively charged particle is surrounded by firmly attached positively charged ions forming the Stern layer. Zeta potential gives an indication of the colloidal systems stability. This figure was adapted from Malvern. (2013) Zetasizer nano user manual. (Apr) Vol. 3: Malvern Instruments Ltd.

The Debye Landau Verwey Overbeek (DLVO) theory is one theory that is used to describe the stability of lyophobic colloids, such as the SiNPs. Other, non-DVLO theories are also proposed. These will be described in the section below.

1.3.1.3.1 The DLVO Theory

The DLVO was developed by Derjaguin and Landau in 1941 to describe the stability of colloidal solutions, which was dependent on Van der Waals attraction and electrostatic repulsion. The DVLO, which contributes to interface science, was further confirmed by Verwey and Overbeek to determine the interaction between charged surfaces in solution. The nano-scale provides a higher surface area per unit mass compared to bulk materials. When NP size is reduced, the high surface area generated possesses high surface energy, which can cause the NPs to react with each other resulting in aggregation (Ju-Nam and Lead, 2008). The DVLO theory is translated as the sum of attractive and repulsive forces because of double layer of counterions. This is where the attractive forces (V_{Total}) are the Van der Waals attraction (V_A) and the repulsive forces are original electrostatic forces (V_R) (Burns et al., 2006; Churaev, 1999). Particles with their charged surfaces in suspension are considered as electro-neutral entities due to their ability to form a surrounding diffuse layer of oppositely charged ions. When particles come into close contact, a diffuse layer overlap is created forming an osmotic pressure between the particle surfaces. Hence, particle separation in suspension is achieved through the presence of the electrostatic repulsive forces that results from such overlap. The degree of dispersion within the lyophobic colloidal solution depends on the maximum repulsive energy that can be created between particle surfaces (The total potential energy curves for a lyophobic colloid V (1) and for a colloid with a maximal repulsive energy V_R (1) respectively; Figure 13).

The addition of electrolytes into the colloidal solution (The total potential energy curve V (2); Figure 13) favours Van der Waals attraction between particle surfaces as opposed to the repulsive energy that exists (V_R (2); Figure 13). There is a correlation between particle surface potential and the electrolyte concentration within a colloidal suspension. When the electrolyte concentration is increased, particle surface potential is decreased leading to the compression of the diffused layer and the reduction in the repulsive forces. The latter helps the particles to overcome the electrostatic energy barrier thus leading to aggregation (Figure 13). The minimal amount of reduction in repulsive force required to remove the energy barrier is referred to as the critical coagulation concentration of electrolytes. Higher

concentrations of electrolytes lead to the further reduction in the energy barrier and thus rapid aggregation of NPs (The total potential energy curve *V* (3); Figure 13) (Shaw, 1992).

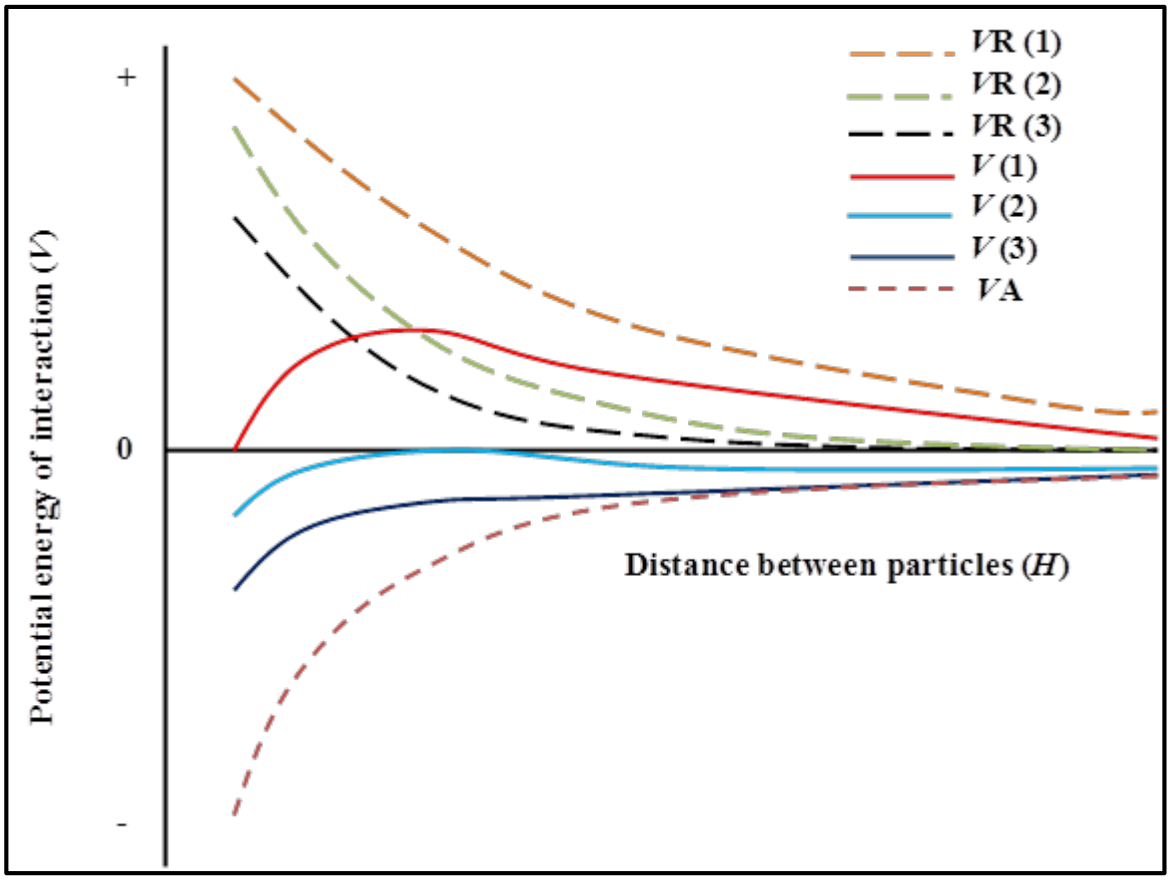

Figure 13. The total energy of interaction (V(1), V(2) and V(3)) between two particles, acquired from the sum of attraction curve (V_A) and repulsion curves ($V_R(1)$, $V_R(2)$ and $V_R(3)$). Author originated.

1.3.1.3.2 Non-DLVO Interactions

The DLVO theory used to describe the stability of particles within numerous colloidal systems (Ninham, 1999; Norrish and Rausell-Colom, 1961; Donners et al., 1977; Israelachvili and Adams, 1978; Pashley et al., 1986) does not account for the additional interactions within silica solutions (Hartley et al., 1997; Pashley, 1981). These include NP surface interactions with the other surfaces, the solvents as well as ionic species. Due to the dielectric-continuum nature of the solvent, additional repulsion (V_{Solv}) may be produced by the interaction between the highly structured hydration layer surrounding the particle surface-to-solvent and solvent-to-solvent. The existence of steric repulsion (V_{Ster}) between surfaces containing grafted polymers can also cause them to come close to each other. The DLVO theory differs from the non-DVLO theory in that it considers point charges, defined as the dimensions of the charge or charged ions to be infinitely interacting with particle surfaces at equal concentrations and different electrolyte types in an ion-specific manner. The degree of point charges depends on the distance between an ion and a NP surface, solvent or another ion but does not provide accurate estimation of any interaction between the ions to NP surface, solvent or another ion. According to the DVLO theory large SiNPs in an alkali solution (*pH* 2) will have no charge and be in the least stable region in contrast to previous studies, which suggest NP steric stabilisation due to the hydrogen bonding between the water molecules and the hydroxyl groups attached to the particle surface forming an interactive monolayer (Koohestanian et al., 2004; Michael and Zhuravlev, 2005; Kobayashi et al., 2005). The stability and dispersion of NPs therefore depends on the surface properties, surface interactions and the surrounding environment.

1.3.1.3.3 Ion specificity

Ion specific adsorption influences the stability of the dispersion of colloidal NPs. The dispersion of NPs is affected by the ions surrounding its surface. When ions are in close contact with the particle surface, they are able to indiscriminately interact with the surface with a great screening efficiency leading to NPs dispersion destabilising even when lower concentrations of electrolyte are present (Lyklema, 2003). According to the Stern model, the absorbability of ions to the SiNPs surfaces is dependent on ion charge and size. Thus, highly charged ions and small ions have greater absorbability; whereas large-sized ions and less

charged ions have lower absorbability (Grahame, 1951; Gierst and Herman, 1966).

Ions can be categorised depending on how they interact with the solvent (Marcus, 1994; Marcus, 2009). The presence of structure-maker water forming ions such as Li^+ and Na^+ ions can cause the solvent to become structured on the particle surface. In contrast, the presence of structure-breaker ions can cause the solvent to become less structured on the particle surface compared to the bulk phase. Hence, the ions can promote or destroy water structures on the particle surface (Dumont et al., 1990; Gierst et al., 1966). The adsorption due to numerous oxides can be described as like seeks like. Oxides with a high isoelectric point (IEP), such as aluminium, are referred to as structure-maker surfaces and thus the structure-maker ions will adsorb on their surface, while structure-breaker surfaces such as Silica have low IEP (Dumont et al., 1990; Franks, 2002). Depending on the charge fluctuations and strength of the ion-to-ion correlation, ion-to-ion interactions within the double layer may lead to the build-up of an attractive electrostatic pressure between two NP surfaces (Kjellander, 1996; Lyklema, 2003). The latter interactions are thought to be stronger than the Van der Waals attractive forces (Kjellander, 1996; Labbez et al., 2009). The double layer is generated when two approaching surfaces containing high ion density interact causing repulsion to occur. However, depending on the ionic density of either surface when the ions are adsorbed close to one surface, lower ion density is generated at the mid-plane and causing the attractive force to predominate.

1.3.1.4 Surface Stabilisation

Surfactant agents such as polymers, biological or organic molecules that encapsulate or surround (dope, coat or cap) NPs can add surface stability and prevent NP aggregation and sedimentation while maintaining dispersed NPs. Kobayashi et al. confirmed that larger SiNPs follow the DLVO theory (Kobayashi et al., 2005). At high *pH* where there is a low ionic strength, the rate constant decreases and there is a slow tendency for the large SiNPs to aggregate, whereas at low *pH* where there is a high ionic strength, the aggregation becomes fast. In contrast, small SiNPs below 80 nm in size become well dispersed at a low and high *pH* values with less tendency to aggregate. Hence, Kobayashi et al. proposed the hairy model theory considering small SiNPs as stable NPs due to the presence of additional repulsive forces as postulating hairy layers with poly (silicilic acid) chains surrounding the particle surface (Kobayashi et al., 2005).

1.3.1.4.1 SiNPs as Fluorescent Nanoprobes – mechanisms for SiNPs probe loading

Core SiNPs can be doped with fluorescent and luminescent dyes such as tris (2,2'-bipyridyl)ruthenium (II) chloride hexahydrate (Rubpy) (Wu et al., 2008), fluorescein isothiocyanate (FITC) or rhodamine B isothiocyanate (RBITC) as fluorescent signal elements either by steric hindrance or by covalent bonding (Chen et al., 2013). This promotes their use as agents for bioimaging (Canton et al., 2011) and biosensing (Barshan-Tashnizi et al., 2009) due to their fluorescent capabilities. The fluorescent signal detected from dye-doped SiNPs may vary in intensity depending on the type of dye used, its bonding to other conjugates and its corresponding stability; hence SiNPs can be used in the targeted recognition (labelling and tracking) of cellular organelles and biological markers in a targeted and/or untargeted manner (Shi et al., 2010). The dye-doped fluorescent SiNPs can be further stabilised using photostable linker compounds and used to recognise for example cancer cells *in vitro* (Chen et al., 2013). The study by Chen et al. doped SiNPs of 60 ± 5 nm in size with FITC or RBITC conjugated with dextran (RBITC-Dextran) (Chen et al., 2013). These NPs were further conjugated (with a secondary antibody (goat anti-rabbit IgG)) or functionalised (with rabbit anti-epithelial cell adhesion molecule (EpCAM) antibody on the surface of the polyethylene glycol (PEG)-terminated modified FITC-doped or RBITC-Dextran-doped SiNPs) by covalent binding to the PEG linkers using the cyanogen bromide

method (Chen et al., 2013). The functionalised rabbit anti- EpCAM NPs, used for the targeting of the human breast cancer SK-Br-3 cell surface tumour marker, as compared with fluorescent dye labelled IgG SiNPs, displayed better stability of fluorescence as well as photostability under continuous irradiation (Chen et al., 2013). Another study by Wu et al. suggested the use of Rubpy dye-encapsulated SiNPs for the sensitive detection of interleukin (IL)-6 (IL-6), on a microarray format, thus promoting the latter use as labels with high fluorescent intensity, photostability and biocompatibility for the clinical detection of IL-6 related diseases *in vivo* (Wu et al., 2008). The 50 nm Rubpy-doped SiNPs were fabricated using a simple one-step microemulsion synthesis and the non-ionic surfactant system entailing Igepal CA520 ((C_8H_{17})-C_6H_4-O-$(CH_2$-CH_2-$O)_5H$) and n-heptane (Wu et al., 2008). The CA520 and heptane system was suggested to have a good solubility for both the surfactant and water, and has a large, stable single phase microemulsion region in the phase diagram (Wu et al., 2008). Hence, the encapsulation of dye molecules within a silica matrix or the doping of SiNPs with dyes may add stability to SiNPs, enhance their optical properties and thus display a platform for the specific targeting of cytokines or proteins to aid the clinical diagnosis of biomarkers.

1.3.1.5 SiNPs Applications in Medical Diagnostics

Previous studies have suggested the use of nanomaterials for the visualisation and targeting of tumours and for drug-delivery (Sá et al., 2012). SiNPs of 20-200 nm size have been employed in the targeting of vessels in ischaemia for diagnostic and therapeutic purposes (J. Kim et al., 2011). SiNPs-based ultrasmall inorganic hybrid nanoparticles, "C dots" (Cornell dots) were used for the first time in patients with metastatic melanoma as part of a clinical study assessing (the safety, pharmacokinetics, clearance properties and radiation dosimetry of) iodine-labelled and cRGDY peptide-modified positron emission tomography (PET) C dots (^{124}I-cRGDY-PEG-C dots) after iv administration (Phillips et al., 2014). These hybrid PET-optical imaging agents were suggested to be biocompatible and well-tolerated as they exhibited *in vivo* stability and were capable of being preferentially taken up and localised within disease sites and were excreted over a 2-week period (Phillips et al., 2014). Such studies may form a platform for the clinical translation or safe use of silica-based NPs as a delivery system for imaging probes possibly replacing the invasive surgical procedures in human cancer lesion detection, staging, diagnosis and management (Phillips et al., 2014).

Dysregulation of MicroRNAs is associated with a number of diseases including cancer and may display a marker for a particular disease and/or its progression. A recent study by Li et al. had developed fluorescent dye-doped SiNPs (fabricated by the reverse microemulsion method) for target-cell-specific delivery and intracellular microRNA imaging (Li et al., 2015). Surfactant molecules were co-immobilised on the surface of SiNPs to aid the guided delivery of the latter agents specifically to human breast cancer cells *in vitro* by adhering to cell surface molecules with high affinity (Li et al., 2015). Thus, the highly sensitive luminescent non-viral vector transfection nano-agents may display a platform for nano-based diagnostic research in a clinical setting.

1.3.1.6 SiNPs Applications in Medical Therapeutics

SiNPs may have a potential in cancer treatment. A study by Badr et al. showed that SiNPs loaded with snake venom (Walterinnesia aegyptia venom; WEV) were able to enhance and robustly sensitise the human breast cancer cells isolated from cancer biopsies to cellular growth arrest and death over WEV alone *ex vivo* (Badr et al., 2014). The route of cancer cell apoptosis was suggested via the increase in the levels of free radicals (including ROS, hydroperoxide and nitric oxide) and caspases activities (including caspase-3, caspase-8 and caspase-9) (Badr et al., 2014). The phenomenon of drug-loading and slow drug-release via the aid of SiNPs loaded with chemical therapeutics may have a pivotal role in effects observed on enhanced toxin and/or drug action *in vivo*. This can be explained in part by the ability of NPs to be endocytosed and/or phagocytosed by cells, resulting in the internalisation of the encapsulated drug (Barratt, 2003).

Due to the therapeutic effects of small interfering RNA (siRNAs) and the obstacles accompanying their specific targeting, studies have developed methods using SiNPs as candidates for siRNA delivery *in vivo*. A study by Chen et al. used magnetic mesoporous SiNPs for lung cancer treatment (Chen et al., 2014). The siRNA designed by the Chen et al. group was loaded into the mesopores of SiNPs, followed by polyethylenimine (PEI) capping, PEGylation and fusogenic peptide KALA modification. The resultant SiNPs exhibited a prolonged half-life in the bloodstream, enhanced cell membrane translocation, were capable of escaping endosomes and possessed favourable tissue biocompatibility and biosafety (Chen et al., 2014). Together, the latter properties of SiNPs enabled the *in vivo* imaging of target tissues and the specific suppression of tumour growth and metastasis in subdermal and orthotopic lung cancer models when loaded with vascular endothelial growth factor (VEGF) siRNA (Chen et al., 2014). It has also been shown that polycationic SiNPs decorated with PEI were capable of delivering siRNA for the purposes of gene silencing and hence disease prevention (Kapilov-Buchman et al., 2015). PEI is a positively charged branched polymer of 25 kDa in size of biocompatible nature (Kapilov-Buchman et al., 2015). PEI was attached to the SiNPs via a non-covalent inorganic linker cerium (III) cations (Ce^{3+}) between both polyNH_2-SiO_2 NP surface and the polycationic PEI polymer (Kapilov-Buchman et al., 2015). Thus, the use of PEI-modified SiNPs for siRNA delivery may

have a therapeutic potential overcoming the obstacles of inefficient delivery and/or the off-target effect of sole siRNA.

Various studies have shown that SiNPs can be utilised in aiding guided stem cell delivery and/or implantation to injured sites that require stem cell therapy thereby overcoming cells death and the consequences of ischemia, inflammation, immune response, mis-injection and/or implantation into fibrotic tissue (Jokerst et al., 2013). In the study by Jokerst et al. multimodal, fluorescent silica-based NPs (300 nm) were used for cell sorting, real-time ultrasound-guided cell delivery and implantation at high-resolution and long-term monitoring by magnetic resonance imaging (MRI) (Jokerst et al., 2013). The study demonstrated that SiNPs increased the ultrasound and MRI contrast of labelled human mesenchymal stem cells (hMSCs) 700 and 200% versus unlabelled cells respectively, and allowed cell imaging to be performed in animal models for 13 days after implantation (Jokerst et al., 2013). The SiNPs used were biocompatible with no effects observed on hMSC cell metabolic activity, proliferation, or pluripotency (Jokerst et al., 2013). This may be in part due to the *in vivo* aggregation of SiNPs into larger silica frameworks that amplify the ultrasound backscatter. This guided cell-delivery and multimodal optical/ultrasound/MRI intracardiac cell-tracking may act as a platform for improved cell therapy in the clinic by minimising misdelivery or implantation into fibrotic tissues (Jokerst et al., 2013). SiNPs, whether used as a delivery system and or guiding routes for therapeutic strategies, may therefore display a platform for future therapy for a wide-range of diseases. However, the drawbacks to such potential of SiNPs may due to the unknown fate and/or the indiscriminate interference of SiNPs with other tissues or biological processing leading to injury and disease.

1.4 Methods used for NP Characterisation

NPs can be characterised by their morphology, size and surface charge. In the following section, the techniques used to determine the morphology, size and surface charge of NPs are presented. NPs sizes have been determined by electron microscopy. The hydrodynamic size and stability of NPs however can be examined in suspension based on their Brownian motion. The application of NPs and the understanding of their biological reactivity requires accurate determination of their characteristics.

1.4.1 Scanning Electron Microscopy

The Scanning Electron Microscopy (SEM) is an analytical instrument that can be used to characterise the physical properties of nanomaterials, such as morphology, shape and size as well as the distribution of nanomaterials within cells and tissues (Kim et al., 2015). The objective lens design in scanning electron microscopes can combine the electrostatic and magnetic fields to maximise optical performance while reducing field influences at the sample. The Gemini-SEM relies on in-lens detection for efficient signal detection by detecting secondary (SE) and backscattered (BSE) electrons in parallel (Figure 14). The detectors are arranged on the optical axis, which reduce the need for realigning the imaging time. This high power resolution technology allows the imaging of nano-sized materials at high signal-to-noise ratios, with the introduction of high voltages from the beam throughout the column for efficient sample detection (Figure 15). The resolution of the images obtained depend on optimising the geometry and electrostatic and magnetic field distributions by the lenses utilised.

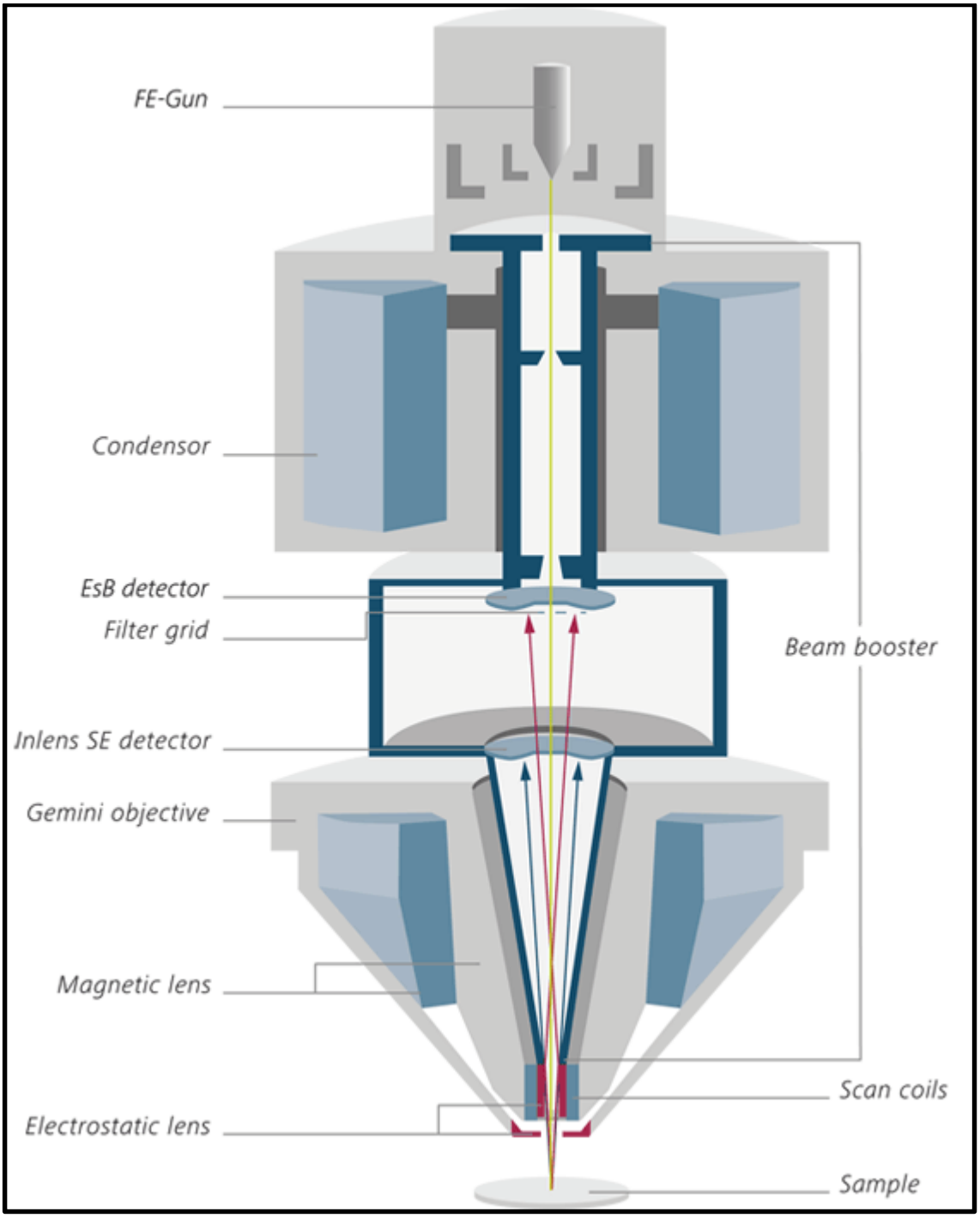

Figure 14. Schematic cross section of Gemini optical column. Adapted from http://www.zeiss.co.uk/microscopy/en_gb/products/scanning-electron-microscopes/geminisem.html#gemini--optics, access date: 2015.

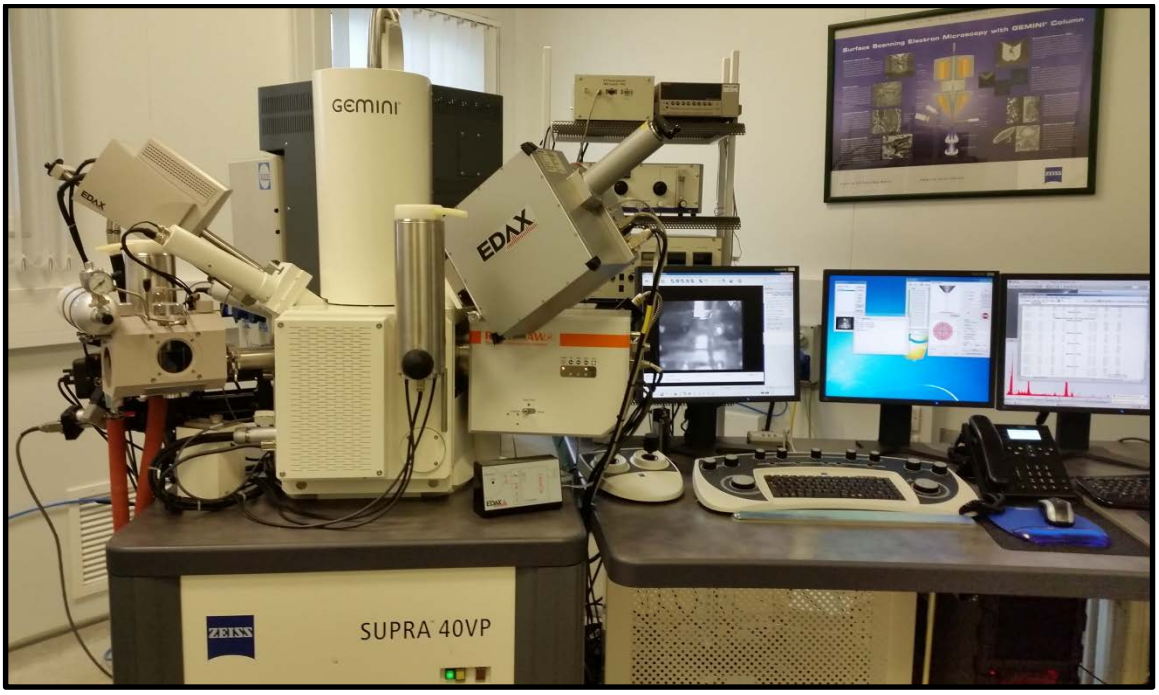

Figure 15. An image of a scanning electron microscope (GeminiSEM 500 by Carl Zeiss) based at Manchester Metropolitan University; operated previously by Dr. Vladimir Vishnyakov.

1.4.2 Transmission Electron Microscopy

NP characterisation in terms of morphology and diameter size can be examined using the transmission electron microscope (Figure 16). Transmission electron microscopy (TEM) can also be used to visualise NPs uptake by cells and tissues from *in vitro*, *ex vivo* and *in vivo* studies. The specimen is secured in standard sized grid within an airlock chamber, which holds the specimen in a channel leading into the vacuum in order to prevent the build-up of pressure in other areas of the microscope. The electron emission source, located on the top column of the TEM, contains the tungsten filament, which generates a stream of electrons (electron beam) (Tanaka, 2014). The electron beam is transmitted through the vacuum pipe into the specimen and subsequently detected by TEM, producing an image for the specimen. The electron beam is controlled by electromagnetic lenses (Pennycook and Nellist, 2002).

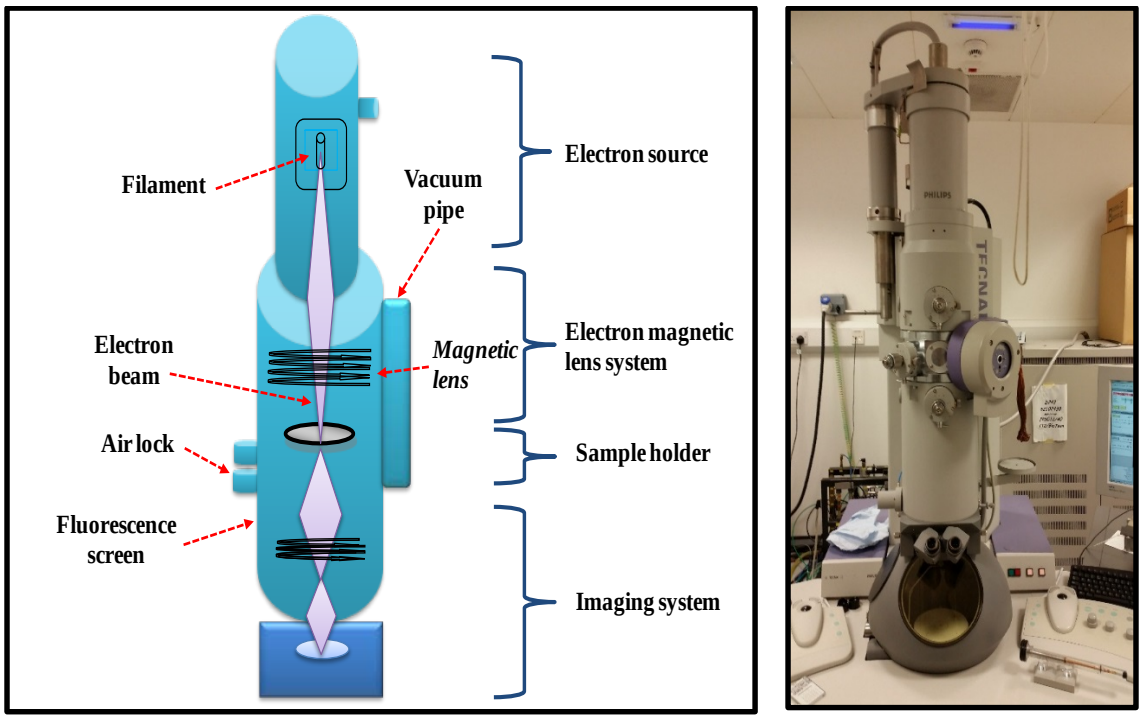

Figure 16. A schematic representation for the components of a TEM (top); containing an electron source, electromagnetic lens, sample holder, airlock chamber and imaging system.

Image adapted from http://www.hk-phy.org/atomic_world/tem/tem02_e.html, access date: 2015). Image of the transmission electron microscope (Technai 12 Biotwin by Philips) based at the University of Manchester; operated by Dr. Aleksandr Mironov (bottom).

1.4.3 Dynamic light scattering

Dynamic light scattering (DLS) is a non-invasive technique capable of characterising particles in suspension using the Malvern Zetasizer Nano ZS (Figure 17). The term light scattering refers to the passage of a monochromatic light from a beam source through the samples, such that the intensity of light scattered by the particles is detected. The intensity of the scattered light is time dependent and relies on the Brownian motion of the particles. This latter phenomenon is used to determine the translational diffusion coefficient D which is converted into the hydrodynamic diameter (R_H) using the Stokes-Einstein equation (Kaszuba and Connah, 2006), as follows;

$$R_H = \frac{KT}{6\pi\eta D}$$

Where η represents the viscosity of the solvent, k is the Boltzmann constant and T the temperature of the medium (Medebach et al., 2007). Since only the hydrodynamic diameter of a particle is determined by DLS, SEM and TEM are used to measure the size of the particle without the solvation shell, thus providing a more accurate measurement of NP surface diameter.

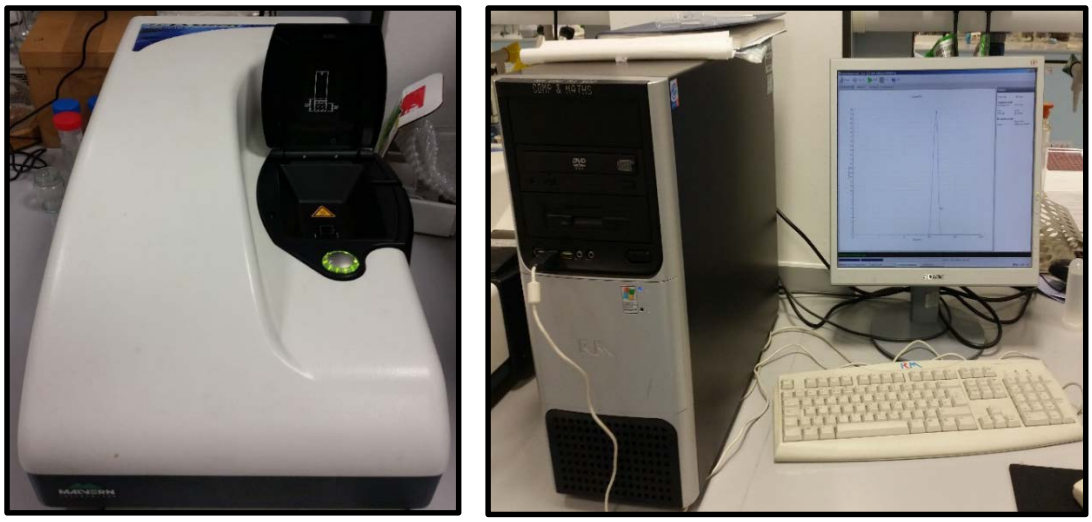

Figure 17. An image of Malvern Zetasizer Nano ZS used for DLS and Zeta potential measurements (left) with the data acquisition system (PC) (right).

1.4.4 Zeta Potential

NP interactivity with biological systems and cells may depend on NP surface charge as well as other factors such as size and dosage. Negatively charged NPs can be repelled by negatively charged species (such as some proteins and cellular surfaces) whereas positively charged ones can be attracted to cellular surfaces and some proteins (E. C. Cho et al., 2009; Villanueva et al., 2009). The surface charge of NPs is determined by their Zeta potential, which is defined as electric potential of the solid-liquid interface (the slipping plane (Delgado et al., 2005)) between the particle surface and the surrounding fluid (Kirby and Hasselbrink, 2004). Ions that surround the particle form an electrical double layer (Figure 12). The inner part of this double layer is called the Stern layer where ions are firmly attached to the particles, whereas the outer part belongs to the diffuse layer where ions are loosely attached (Figure 42). Within the latter outer region an additional boundary, the slipping plane, is defined. The movement of ions between the Stern layer and the slipping plane coincide with particle's movement whereas ions on the other side of the slipping plane do not follow a particle's movement (Malvern, 2013). Hence the electric potential at the Stern layer is called "Stern Potential", whereas that of the slipping plane is called the Zeta potential (Kaszuba and Connah, 2006) (Figure 12). NPs in suspension or electrolyte solution move towards the oppositely charged electrode within an electric field *E*. The linear relation between the steady state-electronic velocity of the particles v_e and the applied uniform and weak electric field are used to calculate the electrophoretic mobility U_e of the particles, as illustrated in the equation below (Delgado et al., 2005).

$$Ve = UeE$$

The Zeta potential *z* can then be calculated applying the Henry equation (Malvern, 2013), as follows;

$$Ue = \frac{2\,\boldsymbol{\varepsilon}\,z\,f(ka)}{3\eta}$$

The Henry's function *f(ka)* is equal to 1.5 for Zeta potential measurements performed in aqueous solutions with moderate electrolyte concentrations. The electrophoretic mobility is dependent on the dielectric constant $\boldsymbol{\varepsilon}$ and the viscosity η of the medium as well as on the Zeta potential (Malvern, 2013). The latter is dependent on the charge present on NP

surface, the *pH* of the system, the electrolyte concentration of the solution, the type of electrolyte and the type of solvent (Delgado et al., 2005).

Hence, the magnitude of forces between particles measured by Zeta potential can be calculated from the electrophoretic mobility of the samples solution (Figure 18). The samples are placed into a micro-electrophoresis cell attachment that contains electrodes on both sides. When a potential is applied, it causes the particles to undergo electrophoresis, which is to move to the electrode with the opposing charge. The laser Doppler velocimetry (LDV) method is used to measure the velocity, in order to quantify the unit field strength mobility. The relevant amount of repulsive forces that exist between NPs renders them dispersed in suspension whereas attractive forces lead to NP aggregation (Shaw, 1992).

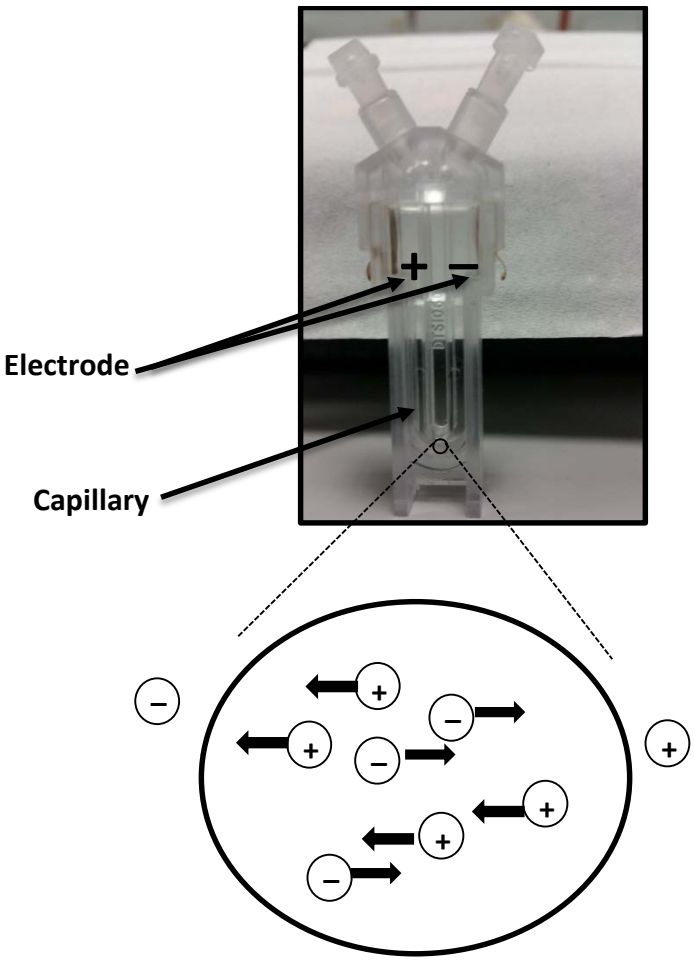

Figure 18. Micro-electrophoresis cell attachment used to measure the samples velocity by a laser Doppler velocimetry within the Malvern Zetasizer Nano series machine.

1.4.5 Fluorescence Spectroscopy

Fluorescence spectroscopy enables the visualisation of NPs. This can be conducted using the Hitachi fluorescence (or similar) spectrophotometer F-2500 (Figure 19). When a fluorescent sample is excited at a particular wavelength, it may lead to the loss of energy by heat or fluorescence emittance. The emission wavelength is longer than excitation because vibrational energy is lost as heat. The basic components of fluorescence spectrophotometer consists of a light source that produces high-energy radiation. This radiation passes through a monochromator and then a beam divider, where the excitation wavelength is selected. The beam then passes through the sample contained within the cuvette. The excited molecules within the sample cause the fluorescence radiation to transpire in all directions. This radiation will pass through a second monochromator

positioned at a right angle to the cuvette, in order for the emitted fluorescence to enter the detector and measured as a fluorescent signal (Kealey and Haines, 2002; Glencross et al., 2011).

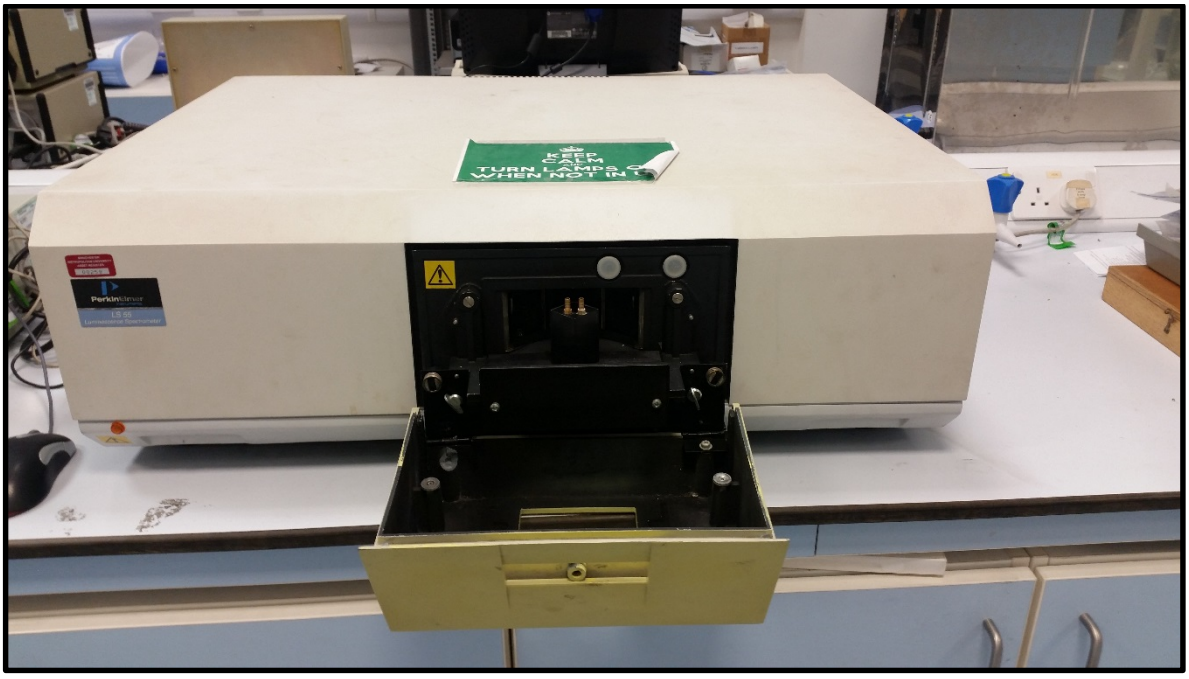

Figure 19. An image of the Hitachi fluorescence spectrophotometer F-2500.

1.5 The Influence of SiNPs on Biological Systems

Despite their numerous applications and high demand, SiNPs role(s), their effects and their biocompatibility in living systems have been poorly studied. Various attempts have been carried out to investigate the role and effects of SiNPs on whole animals and cell models in order to investigate their role in biological systems, and assess their biosafety to justify their administration *in vivo* for diagnostic purposes and therapeutic interventions. *In vivo* studies have shown the ability of SiNPs to enter the blood stream, leading to their systemic uptake where they can be detected within organs that are distal to the exposure site (M. Cho et al., 2009; So et al., 2008). It was suggested that the biodistribution of SiNPs was dependent on their surface functionalisation (Yu, Hubbard, et al., 2012). SiNPs may exhibit cytotoxic behaviour depending on their shape, aspect ratio, the surface area per unit mass and interactions with target molecules (Akhtar et al., 2010).

1.5.1 The Influence of SiNPs on Cells *in vitro*

A study carried out by Thomassen et al. (2010) using SiNPs of 2-335 nm in size, showed that their toxicity on a human endothelial cell line was related to the degree of NP contact with the cell surface (Thomassen et al., 2010). SiNPs incubation with human lung epithelial cells (Akhtar et al., 2010) and myocardial cells (Ye at al., 2010), resulted in their uptake. SiNPs uptake was accompanied by the generation of ROS (Park and Park, 2009) and the subsequent oxidative stress damage to the different cells. A previous study by Kasper et al., suggested the harmful effects of small sized SiNPs (30 and 70 nm) on reducing lung epithelial cell viability, triggering NP-induced inflammatory responses (Kasper et al., 2013) and illustrated the dependence of SiNP size on mediating the cellular effects. Incubating cultured human lung epithelial cells with a concentration up to 0.5 mg/mL of luminescent SiNPs (equivalent to 5×10^{11} NP/mL) (50 ± 3 nm in diameter) caused a drastic reduction in cell survival in contrast to a concentration of 0.1 mg/mL, which did not show a significant reduction in cell survival rates (Jin et al., 2007).

In a recent study; 50 nm but not 500 nm amorphous SiNPs were shown to induce human umbilical vein endothelial cells' (HUVECs) cytotoxicity in a size-dependent fashion following

24 hours of incubation (Nemmar et al., 2014). The latter model indicates the importance of higher-surface-area-to-volume ratio in favouring biochemical interactions. The influence of SiNPs was also tested under flow conditions *in vitro* (Freese et al., 2014). A particular study by Freese et al. indicated that HUVECs under physiological cyclic stretch culture conditions did not enhance the uptake and/or the cytotoxicity of amorphous SiNPs when compared to those internalised by the static culture conditions (Freese et al., 2014).

1.5.1.1 Modes of NP Cellular-Uptake and Behaviour Path in vitro

The route of uptake of NPs into cells may be dependent on several factors including; nanomaterial composition and cell type, NP surface functionalisation, cellular metabolism (Rejman et al., 2004) and cell surface markers (glycoproteins, cell surface integrins, receptors, ion channels and adapter proteins). The uptake pathway that may mediate NP-cellular entry is critical to determining the NP fate and intracellular distribution including the attachment of different sets of proteins or enzymes and the formation of a "protein corona". NPs can be exposed to proteins and/or changing pH values which might lead to changes in the protein corona (Nel et al., 2009), ion release or particle decomposition (Stark, 2011) all of which may contribute to altering the fate of NPs. A number of mechanisms of NP uptake exist, these include; endocytosis, pinocytosis and cytoskeleton rearrangement. Examples of endocytosis mediated uptake are described below.

1.5.1.1.1 Clathrin-mediated Endocytosis

Previous studies have indicated the internalisation of 500 nm sized SiNPs via clathrin-dependent endocytosis and macropinocytosis in dermal fibroblasts (Zhang et al., 2010), 200 nm fluorescent microspheres via clathrin-dependent endocytosis by B16-F10 cells (Rejman et al., 2004), and 150 nm and 200 nm sized monodisperse hydrogel particles via the clathrin-mediated pathway in HeLa cells (Gratton et al., 2008). Changing the cell type can also influence the pathway of NPs uptake. For instance, when B16-F10 cells were used the internalisation of the 500 nm sized of SiNPs fluorescent microspheres was mediated via a clathrin-independent pathway (Rejman et al., 2004).

1.5.1.1.2 Cytoskeleton Rearrangement-mediated Endocytosis

NPs uptake may also be dependent on the actin and tubulin networks, where actin filaments or microtubules may play a role in facilitating the uptake of NPs. Actin filaments act to provide a framework supporting the PM and hence determine the shape of the cell (Lodish, 2000). They may have an influence on phagocytosis, macropinocytosis and clathrin- dependent and independent processes. The microtubule network serves as track for the motor protein mediated transport of membrane vesicles as it spans the cell from the nucleus to the cell membrane (Lodish, 2000) and is thus responsible for the active transport of endosomes. When disrupted by cytochalasin D (at 5 µg/mL (Dausend et al., 2008)) or nocodazole (at 10 µg/mL (Rejman et al., 2004; Dausend et al., 2008)) actin filaments but not microtubules showed the internalisation of silicon NPs (1600 nm and 3200 nm) in HeLa cells and the process is thought to be actin-dependent (Dausend et al., 2008). In contract, microtubule disruption did not affect the uptake of negatively charged polystyrene particles (113 nm) (Dausend et al., 2008) but reduced the uptake of 50 and 100 nm SiNPs by more than 50% whereas 200 nm particles uptake was only reduced by 25% (Rejman et al., 2004). This indicates that actin cytoskeleton is actively involved in clathrin-dependent uptake of NPs (Merrifield et al., 2002) whereas microtubules contribute to the further distribution of cargo inside the cell.

1.5.2 The Influence of SiNPs on the Vasculature *ex vivo* and *in vivo*

The lining EC layer displays the first initial contact surface for NPs when intravenously injected for diagnostic and/or therapeutic purposes. In light of the limited awareness regarding nanomaterial fate in biological systems, the blood vessels may be a victim to such innovative technology. Hence, an appreciation of the role and fate of NPs in blood vessels is essential to draw conclusions and set up decisions on the applicability and possible incorporation of such technology in the clinic. The fate of NPs may be determined by their deposition, biodistribution, bioaccumulation and/or incomplete breakdown in the vasculature, as well as to being prone to immunological attack and/or clearance due to prolonged exposure. These foreign materials may thus lead to chronic macrophage activation and in turn to chronic inflammation (Donaldson and Tran, 2004). For instance; a study conducted by Corbalan et al. suggested the capability of amorphous SiNPs of causing endothelial dysfunction in human umbilical vein ECs (Corbalan et al., 2011) thus promoting disruption of vascular homeostasis (Corbalan et al., 2012). These effects were mediated via a NO/peroxynitrite imbalance associated with an increased peroxynitrite ($ONOO^-$) production leading to a low [NO]/[$ONOO^-$] ratio (Corbalan et al., 2012) and platelet aggregation within the blood stream via adenosine diphosphate and matrix metalloproteinase 2-dependent mechanisms (Corbalan et al., 2012) respectively. Du et al. suggested that intratracheal-instilled SiNPs could pass through the alveolar-capillary barrier into systemic circulation with their concentration in the heart and serum being dependant on the particles size and dosage (Du et al., 2013). It may be speculated that the effects of NPs on blood vessels may vary in large and small blood vessels, based on the elaboration of endothelial derived mediators and hence NPs may have different consequences on each type of vascular bed as well as segments within the vascular tree. Studies investigating the long-term biodistribution of SiNPs *in vivo*, suggested their clearance from the brain, muscle, liver, spleen and adipose tissue and the distribution and accumulation within the reticuloendothelial system including the lungs and kidneys for at least 8 weeks (Malfatti et al., 2012).

1.5.2.1 Routes of Vascular Exposure to NPs

There are different routes of exposure of blood vessels to NPs or NP delivery depending on the way in which NPs are administered, using experimental and real-time approaches. NPs can be inhaled, orally administered and intravenously (Arap et al., 2013; Wang et al., 2013) or intra-arterially injected. This exposes the vasculature via two modes of NP-vascular penetration and/or uptake; namely intravascular (also termed intraluminal) and extravascular. The vasculature can be intravascularly exposed to NPs via iv and intra-arterial injection *in vivo* (Seliger et al., 2007) or infusion and perfusion *ex vivo*. The intra-coronary arterial infusion of NPs was demonstrated to reach the myocardium, liver and lung as well as vascular media and adventitia (Labhasetwar et al., 1998). Infusion catheters, which are inserted into the lumen of blood vessels, can be used to infuse NPs into the target tissues or organs. It is also possible to deliver drug-loaded NPs coating drug-eluting stents via inserting the latter into the lumen of large and medium size arteries for localised, implant-based drug delivery or through perfusion holes through the vessel walls, preventing restenosis. Utilising either approach, NPs can come in direct contact with the EC layer lining the vessel wall where they can be taken up either actively or passively. To promote the active uptake of NPs, they can be specifically tagged with specific ligands to target ECs and become actively internalised (Margolis et al., 2007).

The vasculature can also be extravascularly exposed to NPs via inhalation or oral administration *in vivo* or superfusion *ex vivo*. The latter enables NPs to translocate and infiltrate through extracellular tissues and interstitial spaces and come in contact with the outer adventitial layer of blood vessels. The effects of NP uptake may be in part related to the way in which they are administered and NP dosage and biodistribution may undergo redundancy if for example administered via inhalation as opposed to direct injection into the blood stream. This phenomenon was confirmed by Oberdorster, who suggested the decrease in the amounts of NPs biodistributed following intravenously administration versus those inhaled through the respiratory track (Oberdorster, 2010). This may be due to slow translocation of inhaled NPs into the circulatory system as well as the small amounts compared to the dose that was originally administered (Oberdorster, 2010). NP translocation across alveolar epithelial cells and capillary endothelial cells into the blood

may have taken place through different forms of caveolae, involving capillary endothelial small and large fenestrae and intercellular gaps. It is critical to note however that in disease states NPs may move across widened tight junctions (TJs) (Oberdorster et al., 2005). Furthermore, the extravascular exposure to NPs through other routes (e.g. the gastrointestinal (GI) track and the dermis), may not prevent the latter from reaching and localising in the blood (Jani et al., 1990) and in nearby lymph nodes, where they can penetrate through vessel walls via the adventitial layer and reach into the EC layer (Manolova et al., 2007; Manolova et al., 2008). NPs absorbed through the mucosa via inhalation, GI tract ingestion or via skin absorption may originate from pollutants and components of chemical, cosmetic and food reagents (Jani et al., 1990; Nemmar et al., 2004). Whether through their properties (ability to translocate) and/or high concentrations, NPs from intravenous, intradermal and intraperitoneal routes may deposit in the extracellular spaces and integrate into the surrounding blood and lymph vessels with blood being the ultimate target of exposure. In this way, NPs may bypass the vasculature, if specifically targeted or may deposit in blood vessels following exposure regardless of the initial exposure site.

1.5.2.2 The Effects of SiNPs on Large Vessels

Previous findings from our group suggest that the acute (30 minute) exposure of rat aortic vessels to SiNPs [100 and 200 nm nonmodified and positively charged NPs at 1.1×10^{11} NP/mL] resulted in their uptake by the lining ECs with no detrimental effect on conduit arterial function (Akbar et al., 2011). The 100 nm and positively charged SiNPs had a greater degree of attenuation on the dilator responses of the aortic vessels in contrast to the unmodified 200 nm particles, suggesting the detrimental effect of surface charge rather than NP size on vascular function (Akbar et al., 2011). Another study by Farooq et al. demonstrated the attenuation of endothelial-dependent vasodilator responses by 30 and 70 nm SiNPs and dye-encapsulated SiNPs (1.96×10^{12} NP/mL) in aortic vessels whereby the degree of attenuation was related to NP surface area rather than size (Farooq et al., 2013). A study conducted by Courtois et al. on isolated pulmonary arteries, has also shown that titanium dioxide (TiO_2) NPs can lead to an attenuated vasodilator function in these vessels through ROS-dependent mechanisms (Courtois et al., 2008).

1.5.2.3 The Effects of NPs on Small Vessels

Limited information is available regarding the effect of SiNPs on the vasculature, specifically on small sized vessels. However, animal inhalation studies have provided some insight. For example, Nurkiewicz et al. previously reported the impairment of murine systemic (skeletal muscle) microvascular (arteriolar) endothelium-dependent dilation following pulmonary (extravascular) exposure of rats to particulate matter encompassing TiO_2 (0.1-2.5 μm in size) (Nurkiewicz et al., 2004). The attenuated dilation was related to a local inflammatory event evidenced by significantly higher polymorphonuclear leukocyte (PMNL) cell counts and venular leukocyte adhesion and rolling provoked by the NPs (Nurkiewicz et al., 2004). The Nurkiewicz's group further characterised the effect of pulmonary particulate matter exposure on systemic microvascular function in rats intratracheally instilled with TiO_2 (at 0.1 or 0.25 mg for 24 hours per rat) (Nurkiewicz et al., 2006). They identified changes in some bronchoalveolar lavage markers of inflammation (e.g. focal alveolitis and increased PMNL rolling and adhesion in paired venules), impairment of endothelium-dependent arteriolar dilation and a local oxidative stress in the microvascular wall from the lungs of rats at sites of particle deposition exposed to 0.1 mg TiO_2 (Nurkiewicz et al., 2006). The inhalation exposure of rats to smaller TiO_2 NPs (20 nm in size) produced more detrimental microvascular dysfunction characterised by blunted arteriolar dilations and induced arteriolar constrictions with the presence of particle-containing macrophages seen in intimate contact with the alveolar wall (Nurkiewicz et al., 2008). The endothelium-dependent vasodilation in subepicardial arterioles from the coronary microvascular bed in rats was also significantly impaired by the inhalation exposure to TiO_2 NPs (21 nm in size) (LeBlanc et al., 2009) and multi-walled carbon nanotubes (MWCNTs) from aerosols (Stapleton et al., 2012). The observations with TiO_2 NPs were suggested to be mediated via a reactive oxygen species (ROS)-dependent mechanism (LeBlanc et al., 2010), inflammatory-dependent mechanism (Nurkiewicz et al., 2011) and the reduction in NO bioavailability (Knuckles et al., 2012).

A very recent study by Nemmar et al., demonstrated a significant reduction in the endothelium-dependent relaxation (at ACh concentration of 0.1 μM) of rat small MAs (third-branches) following the exposure to amorphous SiNPs (of 50 and 500 nm size

respectively, at 50 µg/mL) *in vitro* using the wire myography system (Nemmar et al., 2014). Another type of NPs such as cerium dioxide (CeO_2) (4-6 nm size) that is used as a fuel catalyst was found to significantly impair endothelium-dependent and endothelium-independent dilation of mesenteric and coronary arterioles in a dose-dependent manner following 24 hours of pulmonary exposure (Minarchick et al., 2013).

1.5.2.4 Preliminary Study Leading to this Project

1.5.2.4.1 QDs

Our previous study demonstrated that the acute intravascular exposure to quantum dots (QDs) resulted in their uptake into the ECs of small MAs (Figure 20) (Shukur et al., 2013). Their uptake was accompanied by an attenuated endothelial-dependent (acetylcholine; ACh) and independent (sodium nitroprusside; SNP) vasodilation dependent on their surface coatings and concentration *ex vivo* and *in vivo* (Figure 21) (Shukur et al., 2013). The dilator response of the QDs-injected rat to the endothelial-independent agonist (SNP) *in vivo* was lower than that after incubation in PSS and *ex vivo* (Shukur et al., 2013). These findings have implications in the use of QDs for imaging diagnostics and therapeutic intervention, particularly in disease states where SNP based drugs are utilised (Shukur et al., 2013). This study was the first study to be conducted on small vessels using QDs, which prompted the present study to investigate the influence of dye-encapsulated SiNPs on small arterial function and contractility.

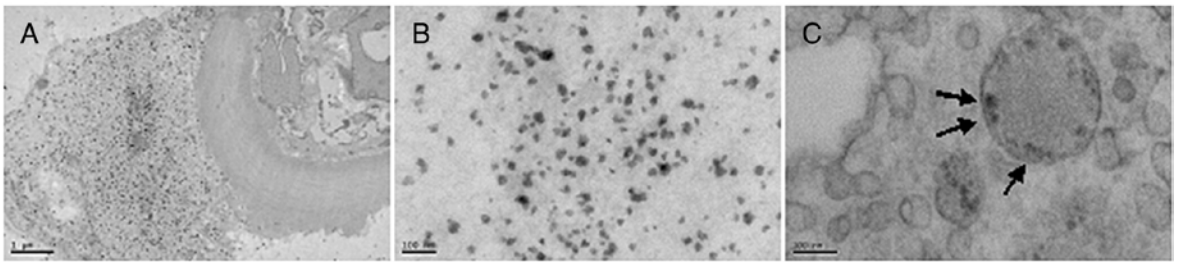

Figure 20. Representative TEM micrographs showing uptake of POSS-PCU coated QDs by ECs lining a mesenteric vessel (A: at 2,900 mag; B: inset at 23,000 mag). C: uptake of POSS-PCU coated QDs by endosomal structures within an endothelial cell (arrows; 30,000 mag). Adapted from Shukur, A., Rizvi, S. B., Whitehead, D., Seifalian, A. and Azzawi, M. (2013) 'Altered sensitivity to nitric oxide donors, induced by intravascular infusion of quantum dots, in murine mesenteric arteries.' *Nanomedicine*, 9(4), May, pp. 532-539.

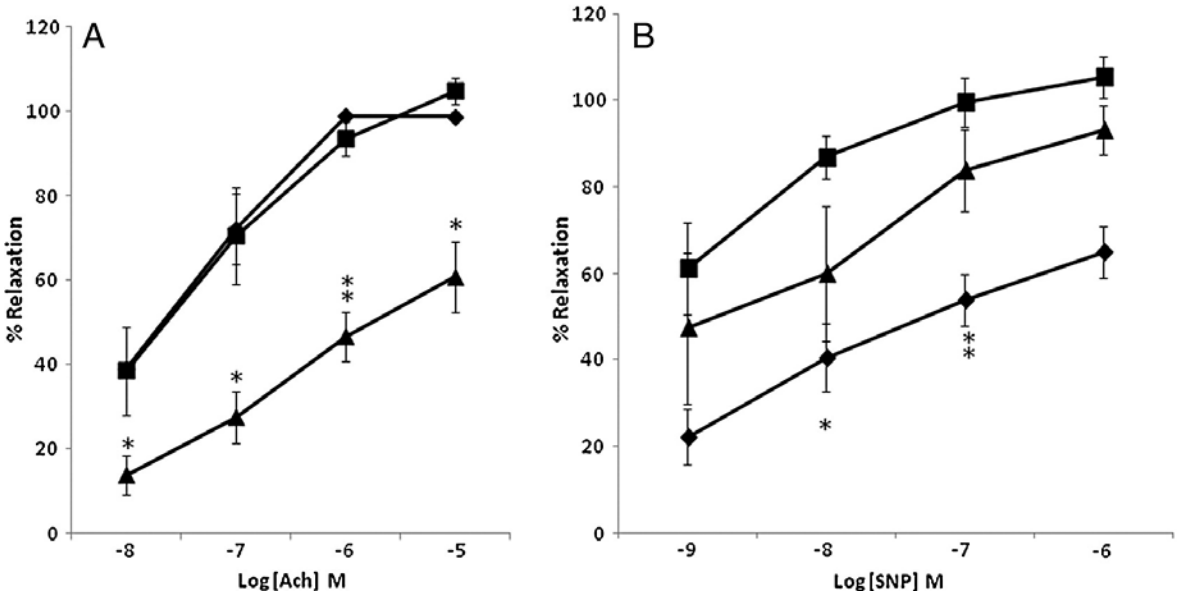

Figure 21. The influence of QD incubation on vasodilator responses. ACh (A) and SNP (B) responses after incubation in PSS (control; squares; n = 4) are compared to responses after incubation in MUA coated QDs (diamonds; n = 5); and after incubation in POSS-PCU coated QDs (triangles; n = 5). 'n' is number of vessels. * p<0.05 and **p<0.01, error bars = SE. Adapted from Shukur, A., Rizvi, S. B., Whitehead, D., Seifalian, A. and Azzawi, M. (2013) 'Altered sensitivity to nitric oxide donors, induced by intravascular infusion of quantum dots, in murine mesenteric arteries.' *Nanomedicine*, 9(4), May, pp. 532-539.

1.5.2.4.2 Carbon Nanotubes

Carbon nanotubes (CNTs) are one of the most popular nanomaterials. There has been increasing interest in the development and applications of carbon nanotubes due to their potential in industrial and medical applications (Tosun and McFetridge, 2010). Recent applications of CNTs include the development of scaffolds and drug delivery systems (Bottini et al., 2006). Despite rapidly emerging applications of CNTs, little is known about the biocompatibility of these nanomaterials and/or their influence on blood vessels. Previous studies reported an increase in the expression of inflammatory mediators such as IL-8 in response to CNTs in both human alveolar epithelial cells (Baktur et al., 2011) and human epidermal keratinocytes (Monteiro-Riviere et al., 2005) using two types of CNTs; the single-walled and the multi-walled CNTs, respectively. Overall, these studies suggest that oxidative stress is one possible mechanism of toxicity related to the CNTs uptake into cells (Shvedova et al., 2003). A study by Cui et al. reported the effects of single-walled CNTs on the inhibition of human HEK293 cell proliferation, induced cell apoptosis and decreased cellular adhesive ability (Cui et al., 2005). *In vitro* studies involving CNTs suggested no inflammatory response from macrophage cells (Allen et al., 2001; Allen et al., 1994; Linder et al., 2002) or cytotoxic effects on fibroblasts or osteoblast cells (Allen et al., 1994; Allen et al., 2001).

1.5.2.4.2.1 CNTs uptake by MAs

Single-walled CNTs originally purchased from Sigma (Poole, UK), were provided and functionalised by Seyed Yazdan Madani under the supervision of Prof. Alexander M Seifalian (UCL). Following the luminal infusion of the CNTs (of 20-40 nm in length and 2.7 nm in width) into MAs, they were observed to be clustered in aggregated clumps inside the vascular lumen with no evidence of uptake (Figure 22).

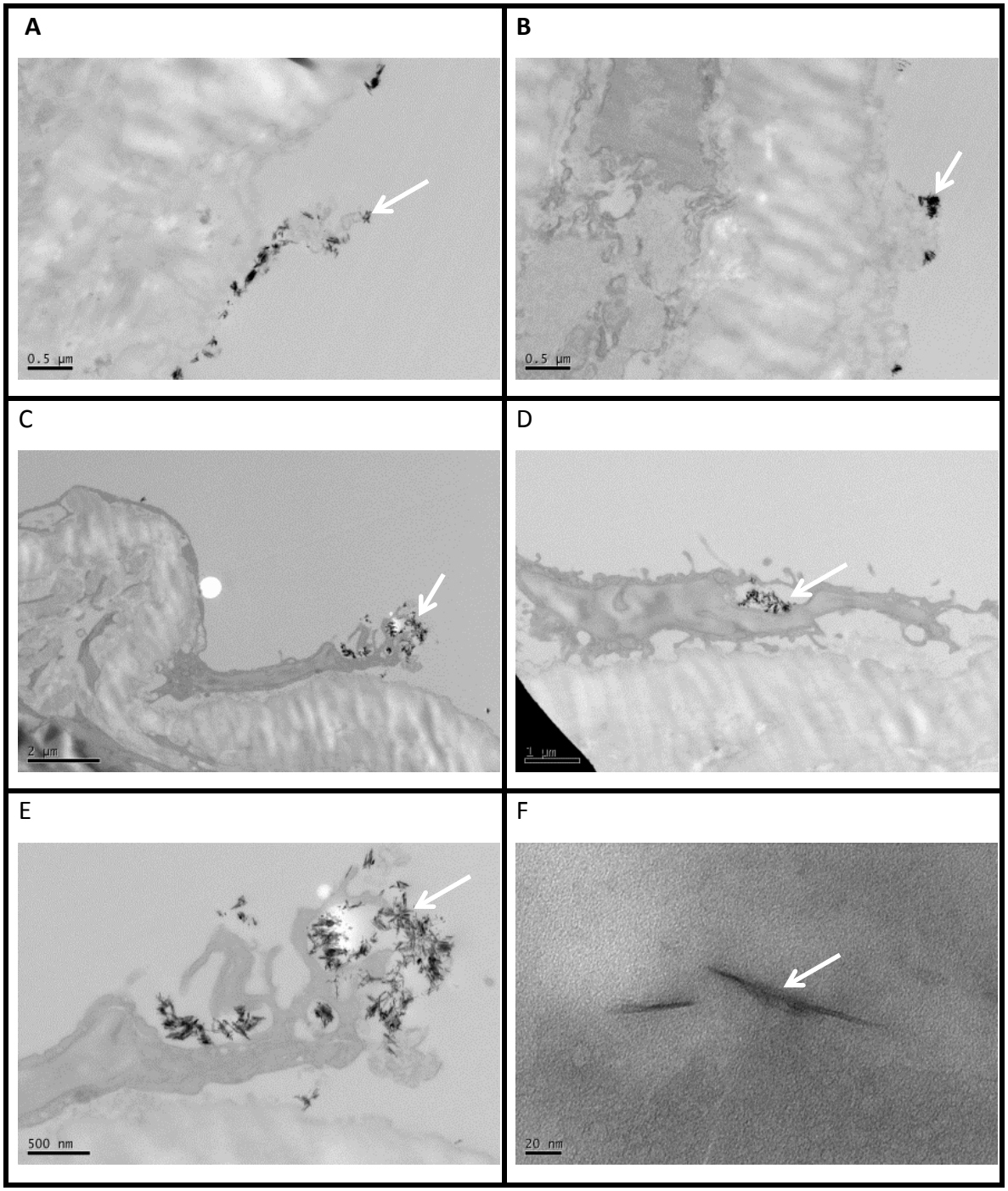

Figure 22. TEM images (A-F) illustrating the predominant presence of CNTs outside the vascular endothelium of the MAs after 30 minute of incubation. The CNTs are represented by black cylinder structures inside ECs (arrows).

1.5.2.4.2.2 Influence of CNTs on Vascular Responses

The influence of CNTs (at a calculated concentration of 1 mg/mL) on the vasoconstrictor and vasodilator responses of the mesenteric vessels were assessed *ex vivo*.

1.5.2.4.2.2.1 Vasoconstriction

Incubation in CNTs *ex vivo*, did not have an effect on the overall contractile responses of the vessels to Phe; (At 1 µM Phe, the mean percentage constriction was 68.09 ± 5.15% vs. 47.44 ± 6.56% after incubation in PSS and CNTs respectively, n=4 and 3 respectively, unpaired *t* test, NS; Figure 23).

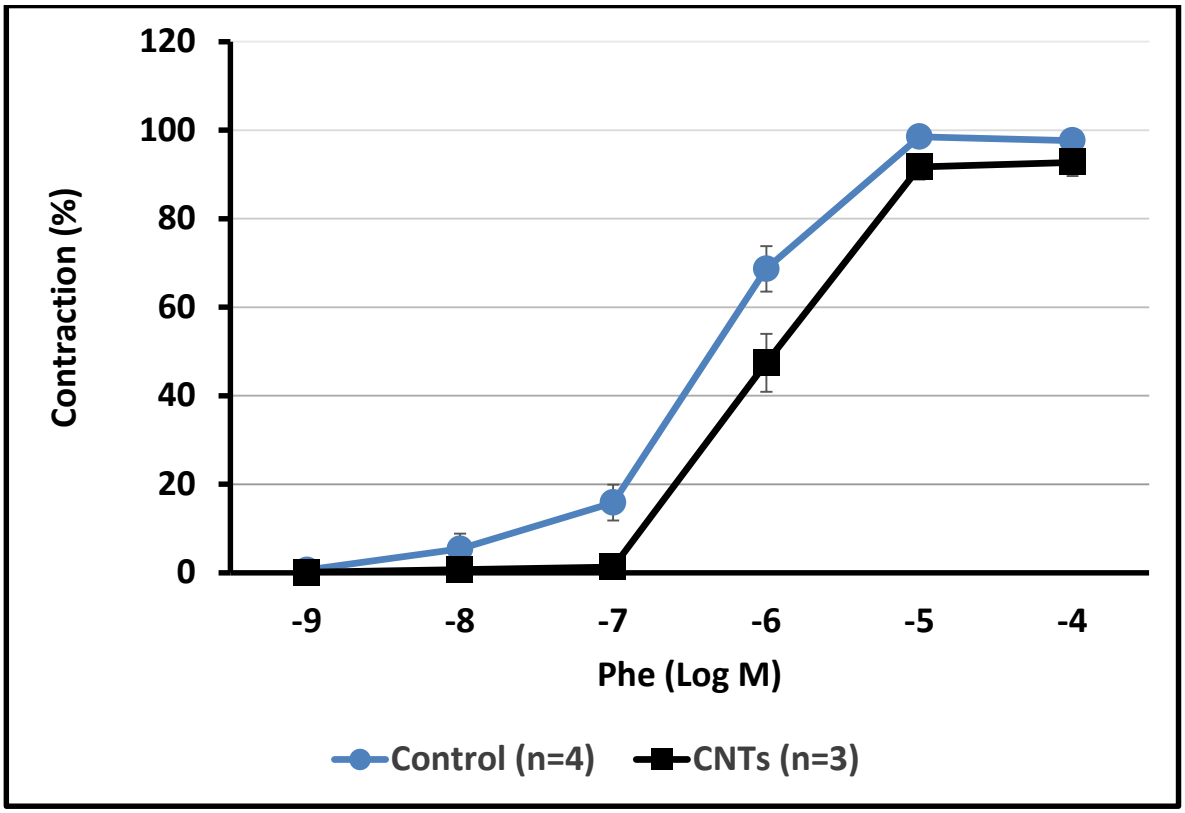

Figure 23. The influence of CNTs on the Phe-induced contraction. 'n' is number of vessels, error bars=SE.

1.5.2.4.2.2.2 Vasodilation

Incubation in CNTs *ex vivo*, had no overall effect on the magnitude of the endothelial-dependent dilator responses to ACh in Phe pre-constricted vessels; (At 100 nM ACh, the mean percentage dilation was 78.77 ± 8.58% vs. 71.87 ± 14.89% after incubation in PSS and CNTs respectively, n=6 and 3 respectively, unpaired *t* test, NS; Figure 24).

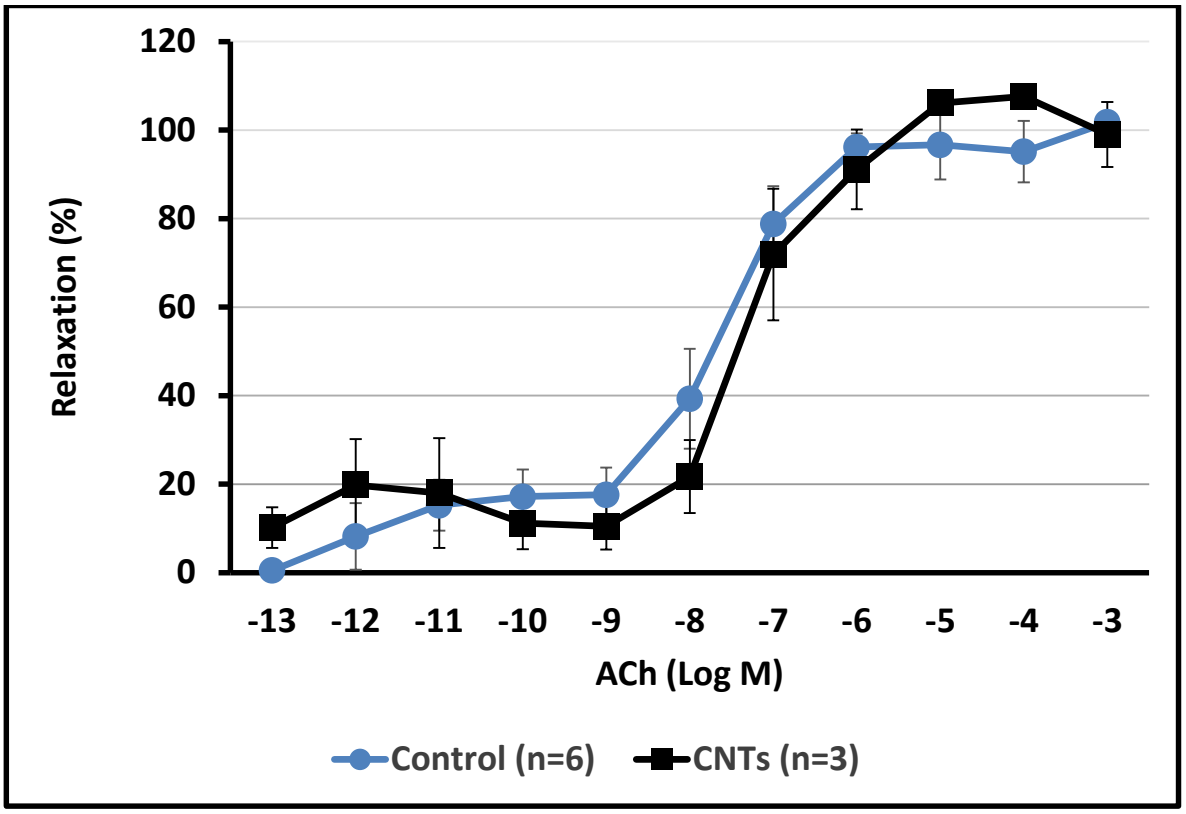

Figure 24. The influence of incubation in the CNTs on the ACh-induced relaxation in Phe pre-constricted vessels. 'n' is number of vessels, error bars=SE.

The was a trend of decrease in the endothelial-independent dilator responses to SNP following the incubation in CNTs infused *ex vivo* at SNP concentrations of 10^{-8} to 10^{-4} M but this reduction was not significant; (At 100 nM SNP, the mean percentage dilation was 102.30 ± 4.03% vs. 65.77 ± 11.26% after incubation in control and CNTs respectively, n=4 and 3 respectively, unpaired *t* test, NS; Figure 25).

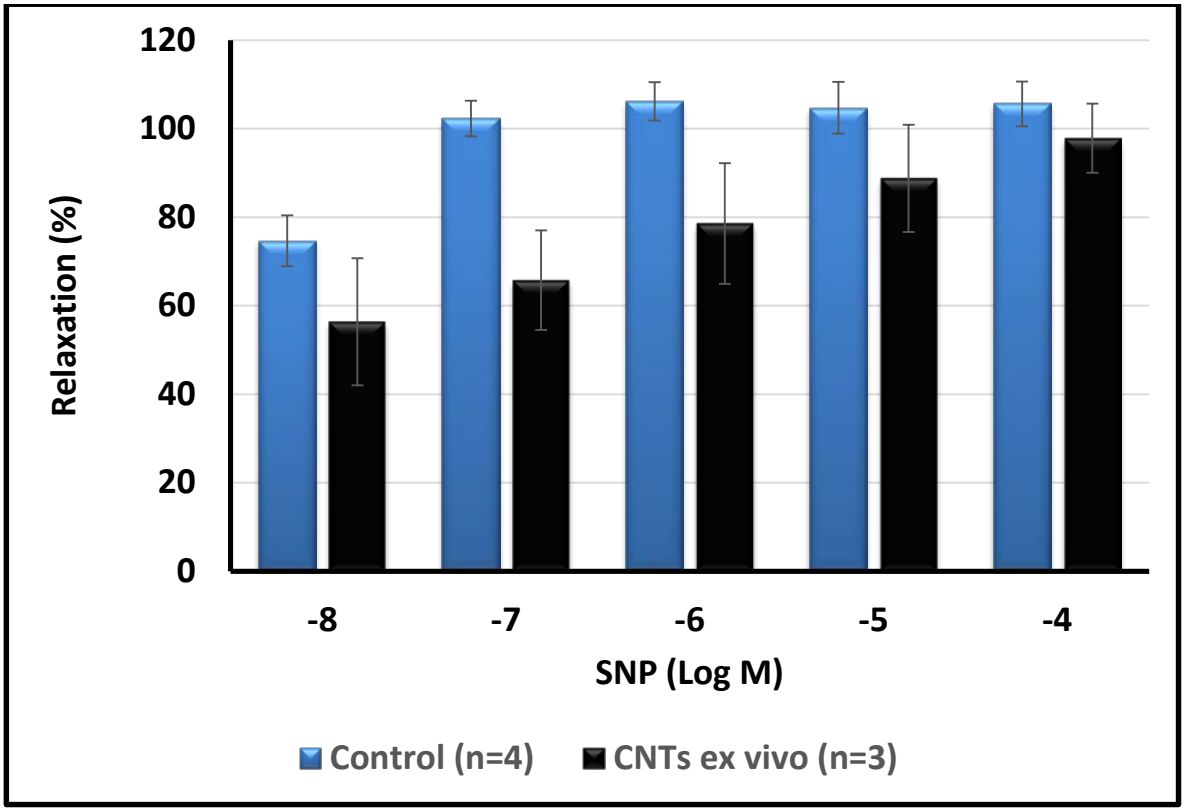

Figure 25. The influence of incubation in CNTs on the SNP-induced relaxation in Phe pre-constricted vessels. 'n' is number of vessels, error bars=SE.

No uptake of CNTs was observed by the ECs. This may explain the lack of any effects on vascular function. The influence of SNP responses may relate to direct interaction of CNTs with the SNP drug itself. Following their incubation intraluminally, CNTs were visualised mainly within the lumen of the vessel. CNTs did not affect Phe-induced contraction nor ACh-induced relaxation, but led to an overall trend of reduction to SNP-induced vasodilation. The slight compromise in SNP-related dilation may be due to the biomechanical influence of these nanotubes on the ECs and/or VSMCs function, as these were not visualised inside ECs surrounding the vascular lumen. The strong Van der Waals forces that attract carbon atoms together, may have caused CNTs to be aggregated and retained within the vascular lumen, hence surface functionalisation may not be sufficient for them to enter the vascular moiety and/or dissolve in the media. The biomechanical effect of the latter NPs may be translated by the interference with, and/or disruption of, the vascular relaxation in response to SNP. Our results contradict earlier studies indicating the detrimental effects of carbon black NPs on mesenteric artery function in response to

agonists (Vesterdal et al., 2012). The study by Vesterdal et al. suggested a significant decrease in the vasoconstrictor response to Phe as well as the vasodilator responses to ACh and SNP when mesenteric arteries were incubated in 100 µg/mL of carbon black NPs (of 14 nm size and surface area of 300 m^2/g) (Vesterdal et al., 2012). The uptake of the CNTs by ECs and the vessel wall has not been identified in this preliminary study, but the TEM images show the aggregation of these nanotubes in the vascular lumen. The uptake of the pristine CNTs into the mouse J774.1A macrophage-like cell line was previously demonstrated by Cherukuri et al. where the macrophage-like cells appeared to phagocytose CNTs at a rate of approximately one CNT per second, without cytotoxicity (Cherukuri et al., 2004). Further experiments are needed following the exposure to CNTs to identify their underlining effects, using appropriate surface coating or functionalisation, to prevent their aggregation. The influence of CNTs on SNP responses may also be due to their interference with the action of SNP, in a similar way to the effect of QDs on SNP responses (Shukur et al., 2013).

1.5.2.4.3 Dye-doped Silica Nanoparticles

An earlier research study conducted by Dr. Teba Mohamed from our nanovascular group at Manchester Metropolitan University demonstrated that intravascular exposure of dye doped silica nanoparticles led to their rapid uptake within ECs lining the MA blood vessel Figure 26).

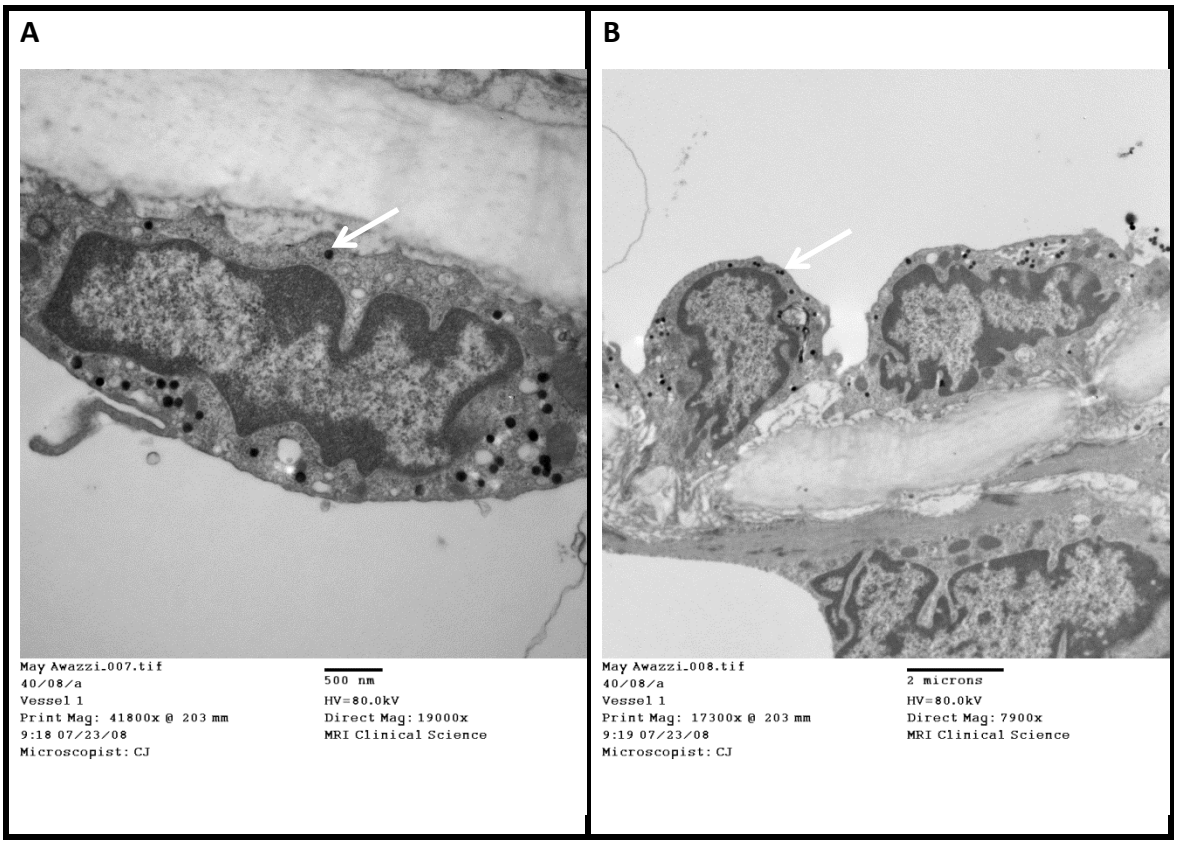

Figure 26. TEM images (A & B) illustrating the internalisation of dye doped SiNPs (100 nm) into the endothelial cell lining a mesenteric artery after a 30 minute incubation period. The SiNPs are represented by black spherical structures inside ECs (arrows). Images courtesy of Dr. T. Mohamed (MMU). The author gratefully acknowledge the support of Dr. Carolyn Jones (Maternal and Foetal Health, St. Mary's Hospital, Manchester) for the tissue processing and electron microscopy.

1.6 Gap in Understanding NP-Small vessel Interaction(s)

The approaches used to promote the safe application of NPs includes the enhancement of their biocompatibility (by optimisation of their dosage, chemical composition and/or surface chemistry) and their specific targeting to localised tissues within the body. To fulfil this goal, the behaviour, subsequent role (interaction and interference), impact, fate as well as the downstream mechanism(s) that accompany NP exposure and/or uptake need to be further established. SiNPs are of special clinical interest and will constitute the focus of this project. The influence of NPs at the physiological, cellular and molecular levels need to be addressed particularly in small arteries due to the limited information in this regard and their important role in regulating blood perfusion into organs and tissues.

1.7 Aim and Objectives

The aim of the current study was to investigate the direct influence of SiNPs on small arterial function and contractility. The ultimate goal of this research initiative was to highlight the potential benefits and/or risks associated with the vascular uptake of SiNPs and suggest alternative strategies to enable the future safe application of these agents *in vivo*. The scope of this study may, in part, display a platform for the translation of NP research into vascular biomedicine.

The main objectives of the current study:

1. To fabricate and characterise SiNPs using chemical techniques.

2. To examine the uptake and biodistribution of SiNPs in rat small mesenteric arteries and organs, using TEM and ICP analysis.

3. To investigate the influence of the intravascular infusion of NP on the physiological responses of small mesenteric arteries *ex vivo* as well as *in vivo*.

4. To determine the mechanism of any altered vascular responses induced by NP uptake using inhibition studies.

1.8 Hypothesis

The hypothesis of this current study states that SiNPs will compromise vascular responses to pharmacological agonists. This is due to their uptake and interaction with the vascular cells influencing specific cellular pathways related to the contractile and dilator machinery. The null hypothesis states that there is no significant change induced by the SiNPs on vascular responses.

Chapter 2.

Methodology

2.1 SiNP Synthesis

Mono-dispersed dye-encapsulated fluorescent SiNPs (SiO_2) of defined diameters were fabricated according to the Stöber sol-gel and Ismail (Stöber et al., 1968; Ismail et al., 2010) methods with some modifications (Table 2). The initial stages in the synthesis of SiNPs involved the incorporation of the rhodamine B isothiocyanate (RBITC) core within silica (Figure 27). Briefly 40 mg of RBITC dye was stirred with 600 µL of 3-aminopropyltrimethoxysilane (APS, as linking agent) at room temperature (~20℃) in a bijoux with a magnetic stirrer (flea). The reaction vessel was filled with nitrogen gas and mechanically stirred for 3-4 hours in the absence of light (covered with foil) until turned from dark red into orange. Ammonium hydroxide (NH_4OH) (taken from a bijoux on a zeroed balance; such that it read minus the required amount due to evaporation control), absolute ethanol, dH_2O and TEOS were magnetically stirred for 15 minutes. 50 µL of APS coupled with RBITC was added. SiNPs of varying diameter and morphology were obtained by reacting different molar ratio of the reagents (Table 2). The reaction solutions were centrifuged at 6000 rpm for 20 minutes and the supernatant solution discarded. Sedimented NPs were re-dispersed in absolute ethanol by vortex mixing and ultrasonication. The solution was re-centrifuged at 6000 rpm for further 20 minutes and the supernatant discarded again; NPs were re-dispersed in distilled water and then characterised (Figure 28). SiNP suspensions were subjected to sonication before their use.

Figure 27. An image of silica suspension; left) without RBITC dye and right) with RBITC dye.

Table 2. SiNP samples synthesised according to different methodologies and reactant concentrations.

NP Sample (Batch)	dH_2O	EtOH	NH_4OH	TEOS Solution	Stirring (hours)
1A	0.7938 g	100 mL	0.7032 g	8.3533 g	3 at 20℃
1I	1.9092 g	70.6663 g	4.8637 g	2.11 g	24 on at 62℃ on a hot plate
1B	0.8301 g		1.7684 g	4.1584 g	3 at 20℃
2A	0.883 g		1.7421 g	4.16 g	3 at 20℃
2I	1.9055 g	69.8784 g	4.58 g	2.1117 g	24 at 60℃
3A	1.7165 g	100 mL	0.7497 g	4.1637 g	4 at 20℃ at 5.8 mot
3B	1.7384 g	90 mL	3.6701 g	4.1684 g	3 at 20℃ at 4 mot
D1 without dye	2.985 mL	100 mL	4.85 mL	3.78 mL	3 at 20℃
D2 without dye	2.985 mL	100 mL	4.85 mL	3.78 mL	3 at 20℃
D2		60 mL	4 mL	3 mL	3 at 20℃ at 4.2 mot
D3		60 mL	4 mL	3 mL	3.5 at 20℃ at 5.8 mot
DA2		60 mL	4 mL	3 mL	3.5 at 20℃ at 5.8 mot
DA3		60 mL	4 mL	3 mL	3 at 20℃ at 5.8 mot
DA4		60 mL	4 mL	3 mL	2.5 at 20℃ at 5.8 mot
DA5		60 mL	4 mL	3 mL	2.5 at 20℃ at 5.8 mot
DA6		60 mL	4 mL	3 mL	2.5 at 20℃ at 5.8 mot
A2 without dye	2.99793 g	200 mL	4.8688 g	3.7768 g	3 at 20℃
A2	3.3346 g	200 mL	4.85 g	3.7909 g	3 at 20℃
A3	2.9775 g	250 mL	4.89 g	3.776 g	3 at 20℃ at 5 mot

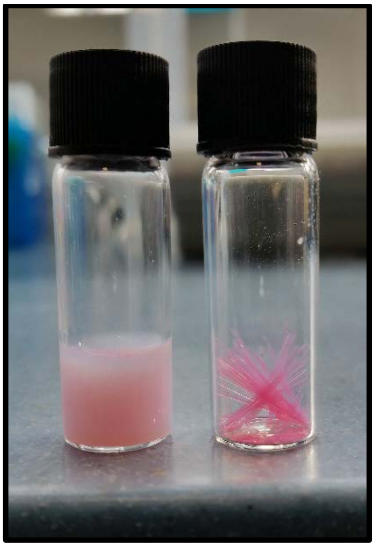

Figure 28. An image of A3 SiNP sample; left) in suspension and right) dry product.

2.1.1 Determination of RBITC Dye Present in SiNPs using Fluorescence Spectroscopy

The fluorescence measurement experiments were performed to confirm the presence of RBITC dye within the SiNPs suspensions used in this study. 4 mL of whole SiNPs suspensions (without dilution) were added into a specialised UV cuvette after sonication and placed inside the Hitachi fluorescence spectrophotometer F-2500 (Figure 19). Using the fluorescent emission (λem) mode, the λem from the silica samples was measured at an excitation wavelength (λex) of 540 or 554 nm.

2.2 SiNP Characterisation

NP size was determined by dynamic light scattering (DLS) also known as photon correlation spectroscopy using a Malvern Zetasizer Nano ZS instrument. Following SiNP suspension sonication, the NP solution was diluted 1:100 in dH_2O (10 µL of NP drop into 0.90 mL of dH_2O) and placed into a polystyrene cuvette. The instrument illuminates the particles with a laser, which results in intensity fluctuations in detected scattered light. The fluctuations are a consequence of Brownian motion of the particle, which is dependent on particle size, so analysis of the fluctuations allows calculation of particles size. The particles were dispersed in water or PSS for analysis and were allowed sonicated before size and Zeta potential analysis. NP size was also confirmed by scanning electron microscopy (SEM) at a working distance of 10 mm (just above 20 mm on the adjustment rotator) and transmission electron microscopy (TEM). A few drops of the NP solution within the Zeta machine cuvettes was dried onto a clean silicon surface in a 60℃ oven, imaged by SEM (Gemini-SEM 500 from Carl Zeiss Supra 40VP FEG), and coated with gold at 20 mAms voltage. Average NP size was determined by measuring particle diameters with reference to the typography scales on micrographs. TEM was also used to assess the size and closely observe the surface of SiNPs. SiNPs were added at a diluted dosage of 1:500 (50 µL into 4.95 mL of water) onto formvar-coated TEM copper grids (3.05 mm, 400 mesh; Agar scientific) for visualisation under TEM.

2.2.1 Determination of SiNPs Zeta Potential

SiNPs were redispersed in distilled water for analysis, as described above. SiNP Zeta potential was determined using the Malvern Zetasizer nano ZS instrument. The NP solution containing 0.02% weight was injected into the Malvern disposable Zeta capillary cell. The electrophoretic mobility was obtained by performing laser Doppler velocimetry. The Zeta potential was calculated using the electrophoretic mobility measurement. The Zeta potentials were measured in distilled water and in PSS.

2.3 Vascular Function Studies *Ex Vivo*

2.3.1 Animal Preparation

Male Wistar rats (150-250 g) were humanely euthanised in accordance with the 'Animals (Scientific Procedures) Act 1986' and Institutional guidelines, by stunning followed by cervical dislocation of the neck. The mesenteric bed of each rat was removed and placed on a clear glass dissecting dish containing a silicon base (pinned for dissection) in ice-cold physiological salt solution (PSS) [composition [mM]: 119 NaCl, 4.7 KCl, 1.2 $MgSO_4$, 7 de-ionised (dH_2O), 25 $NaHCO_3$, 1.17 $KHPO_4$, 0.03 K_2EDTA, 5.5 glucose, 1.6 $CaCl_2 2H_2O$; *pH* 7.4] (Figure 29). Water purified by Milli-Q purification system was utilised for all studies.

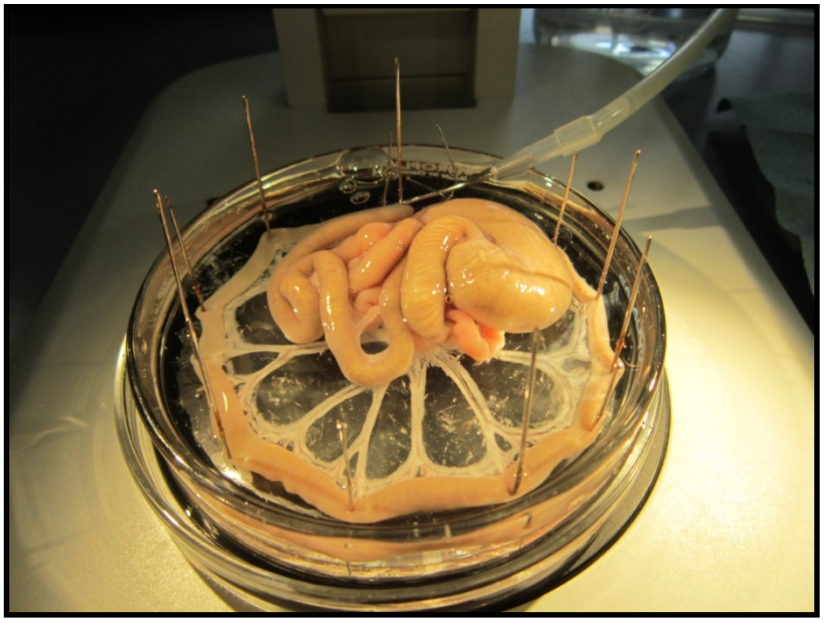

Figure 29. An image displaying a section of the mesentery excised from a Wistar Rat. The mesenteric vessels are seen surrounded by the perivascular tissue.

2.3.2 The pressure Myography System (Preparation and Cannulation)

Second- to third order arteries from the mesentery (145-300 µm initial diameter, 3-4 mm in length) were finely dissected (the fat tissue layer and connective tissue surrounding each vessel were also removed; Figure 30) and mounted between two glass cannulae (tied using fine thread), fixed in place on a modified pressure myography chamber (Living Systems Instrumentation, Burlington, VT, USA; Figure 31) (Shahid and Buys, 2013).

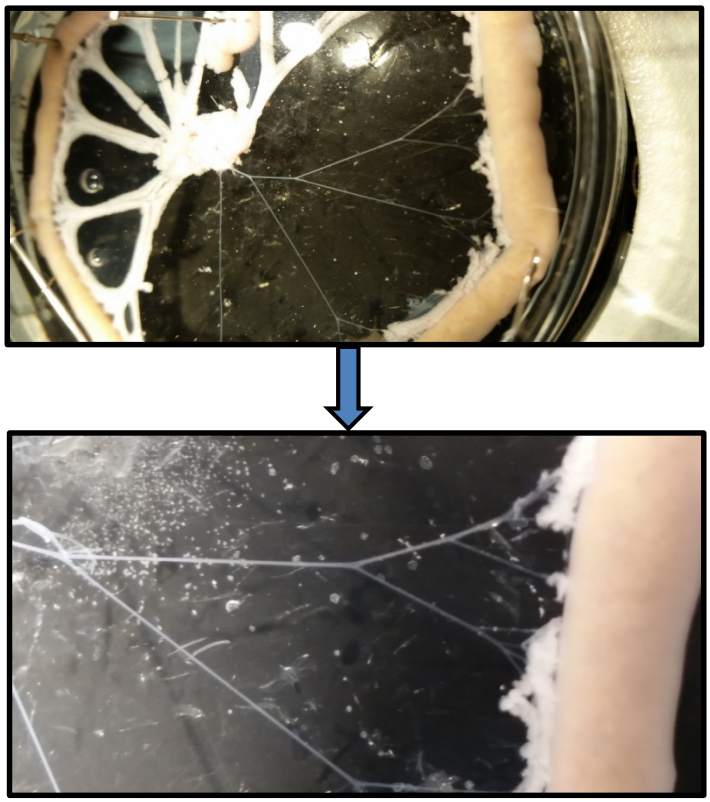

Figure 30. An image displaying the mesentery excised from a Wistar Rat [top] exposing the arteries after removal of the perivascular fat [bottom].

The mounting of the mesenteric artery on a pressure myograph chamber is a very delicate procedure and requires extensive practice to avoid any damage to the endothelial cell layer. Two knots of thread were tied on both cannulae, which were used to tie the mounted vessel and keep it in place. Arteries were initially pressurised to an intravascular (luminal) pressure (IvP) of 60 mmHg and maintained at that pressure using a pressure servo-control unit (Living Systems, Burlington, USA); the system tubing and valve systems was initially checked for leaks to ensure a sealed pressurised circuit.

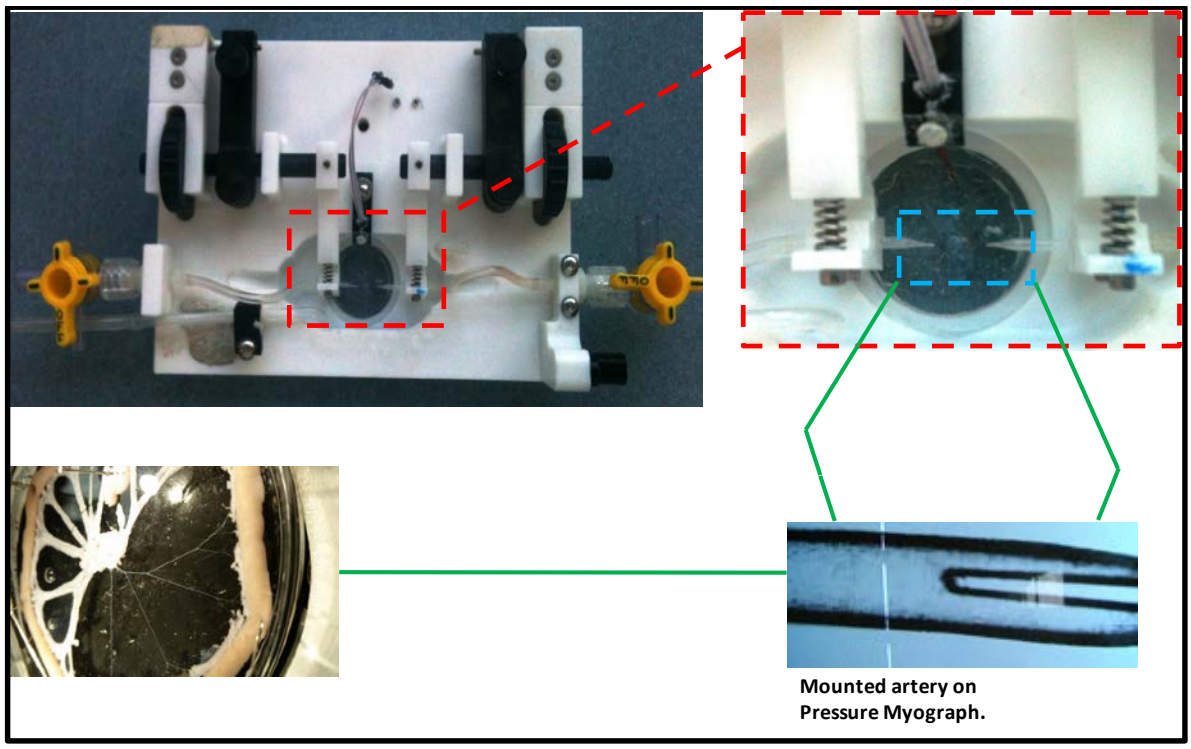

Figure 31. An image of the pressure myography vessel chamber illustrating the position of the cannulae [top right] and a mounted artery [bottom right].

All vessels were constantly superfused in a continuous source of PSS at 37°C, *pH* 7.4, and gassed with 95% air-5% CO_2 (from a standard gas cylinder), with the superfusate entering and leaving the chamber via luer connections in the side of the chamber. This was done under a Nikon inverted microscope to allow for optimal resolution in visualising the tissues (Figure 32).

Figure 32. An image of the pressure myography system, where the vessel chamber is placed on inverted microscope connected to a pressure servo system.

Lumen and internal diameters of the vessel were constantly measured using a video dimension analyser, with data recorded on the computer using Chartlab 5 software (Powerlab system, AD Instruments, UK) for later analysis (Figure 33). Where appropriate, arteries were superfused with Ca^{2+}-free PSS containing 2 mM EGTA for 20 - 30 minutes to obtain passive diameters and allow the vessel to relax completely.

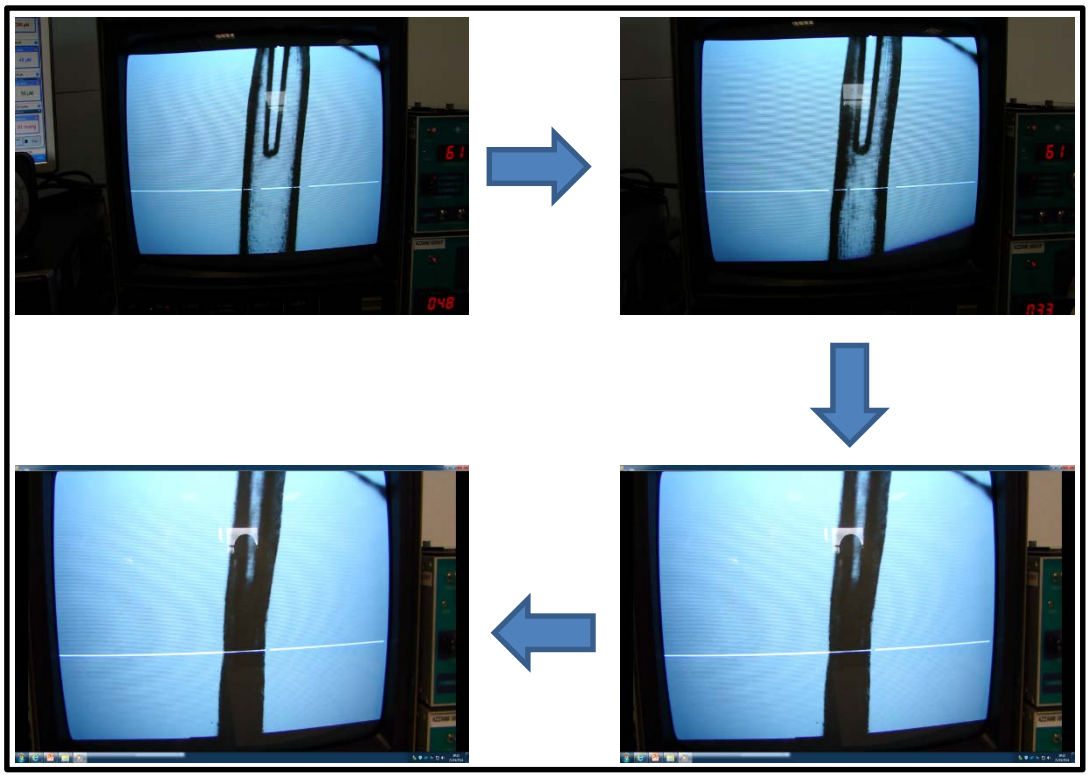

Figure 33. An image of the diameter of the vessel being constantly monitored, in real time, and diameter changes are recorded using chart lab recorder.

2.3.3 Experimental Protocols

The viability of the mesenteric arteries was assessed for their ability to constrict to a high potassium solution (KPSS; composition [mM]: 78.2 NaCl, 60 KCl, 1.2 $MgSO_4$, 7 dH_2O, 25 $NaHCO_3$, 1.17 $KHPO_4$, 0.03 K_2EDTA, 5.5 glucose, 1.6 $CaCl_2 2H_2O$; *pH* 7.4) and the constriction agonist phenylephrine (Phe). The influence of SiNPs on MAs was assessed by measuring the degree of changes in vascular contraction and relaxation in response to various vasoconstrictors and vasodilators before (in non-treated control vessels), and 30 minutes subsequent to intraluminal infusion and incubation in PSS (control) or SiNPs (at a flow rate of 50 µL/min). The intraluminal infusion was conducted as follows: The pressure servo-control unit was turned off and a 1 mL syringe was inserted into one end of the 3-way luer connection in the side of the pressure myograph chamber. 0.5 ml of diluted SiNP solution (in PSS) was slowly administered via the syringe. The 3-way luer valve was closed off and pressure increased to 60 mmHg, using the pressure servo unit. Vasoconstrictor responses (Phe, 10^{-9}-10^{-4} M and AVP, 10^{-13}-10^{-6} M) and endothelial-dependent (Acetylcholine (ACh), 10^{-13}-10^{-3} M) and -independent (sodium nitroprusside (SNP), 10^{-13}-10^{-3} M and papaverine (PAPA), 100 µM) dilator responses were used to assess the repeatability of the contractile and dilator responses of MAs before (initial responses; control) and after the incubation in PSS (second responses). All chemicals (such as Phe, AVP, ACh, SNP and PAPA and reagents (such as N^G-nitro-L-Arginine; L-N^G-Nitroarginine (L-NNA), apamin and TRAM-34) were obtained from Sigma-Aldrich (Poole, UK). Chemical molar concentrations were calculated as shown in appendix 5. Responses after incubation in PSS were used as controls to compare with SiNPs responses. Thus, initial responses were compared to second responses to PSS and second responses to PSS were compared to second responses to SiNPs. After each vessel reached its sub-maximal constriction (using Phe concentration range of 1-10 µM) and stabilised, an ACh dose-response concentration in KPSS or Phe were used and maximum dilation measurement was taken when the vessel was allowed to stabilise. PSS washout period was essential to allow the MA to revert its diameter back to the starting level (in full dilatory mode) before the next contraction.

2.3.4 Inhibition Studies

For the inhibition studies, in a separate set of experiments, vessels were mounted as before and responses to ACh were assessed before and 30 minutes after incubation in inhibitors including; L-NNA, apamin, TRAM-34 and indomethacin (Sigma-Aldrich, Poole, UK). Inhibitors were intraluminally infused into the MA as well as superfused continuously throughout the experiment. Dilator responses were assessed in the presence of inhibitors. Vessels were also co-incubated in L-NNA and SiNPs to assess the effects on function.

2.4 Vascular Function Studies *in Vivo*

In vivo experiments were carried out at UCL. Animal procedures were conducted in compliance with institutional guidelines and UK Home Office requirements (Project License 70/6616). Animals were given food and water ad libitum and housed in a 12 hours/12hours light dark cycle. The rat was anaesthetised in an induction chamber using 2% isoflurane. Maintenance of anaesthesia was achieved by the use of 1.5-2.0% isoflurane via a concentric oronasal mask connected to an anaesthetic circuit. Core body temperature was maintained at 37.0 ± 0.5℃ using a heating pad linked to a rectal temperature probe. The *in vivo* study involved the quick intravenous injection of SiNPs into the tail vein of a 300 g unconscious male Wistar rat. The appropriate volume of SiNPs stock solution was concentrated by spinning in a centrifuge and resuspended in a total volume of 100 µL in PSS for the iv injection. SiNPs were given at the same dosage used in our *ex vivo* studies (5.32 x 10^{11} NP/mL dosage), taking into consideration the blood volume, thus 5.32 x 10^{11} NP/mL of SiNPs per 1 mL of animal blood. Each Kg of animal weight corresponds to a circulatory blood volume of about 50 mL of blood; thus, a 300 g animal contained 15 mL of blood. After injection, the rat was monitored for a period of 2 hours and then terminated by cardiac catheterisation and scarified.

At the end of the *in vivo* experiment, the rat mesentery, and associated vessels (aortic and pulmonary) were dissected-away and placed in ice-cold PSS. Other tissues such as the brain, lung, heart, stomach, liver, spleen, small intestine, large intestine, kidneys, bladder,

tail and thyroid were also excised. The tissues were fixed in 2% gluteraldehyde for a period of 30 minutes to be further analysed. Additional tissues were snap frozen in liquid nitrogen and kept at -80℃. A small length of mesenteric vessel was excised and placed on ice for further physiological analysis. A first- or second order artery from the mesentery (200-400 µm initial diameter, 2-3 mm in length) from the SiNP-injected rat was dissected out using fine forceps and mounted between two glass cannulae fixed in place on a modified pressure myography chamber at 60 mmHg intra-vascular pressure (IvP) and constantly superfused with gassed PSS at 37℃, pH 7.4, as described above. The viability of the mesenteric artery was determined by its ability to constrict to a high potassium physiological salt solution (60 mM KCl). Constrictor responses to phenylephrine (Phe), 10^{-9}-10^{-4} M) was initially assessed, followed by the endothelial-dependent (ACh, 10^{-10}-10^{-3} M) and independent (Sodium Nitroprusside- SNP 10^{-10}-10^{-3} M) dilator response in a Phe-preconstricted vessel.

2.5 Tissue Fixation and TEM

At the end of the functional studies, vessels were carefully untied from the glass cannulae and immediately fixed in 2.5% glutaraldehyde in 0.1 M sodium cacodylate buffer (containing 4.8 g sodium cacodylate in 80 mL of dH_2O and made to reach pH 7.4 with 0.1 M HCL), *pH* 7.3 over 2 hours at 22℃. The samples were preserved in a wash buffer (containing 40 mL of 2.5% glutaraldehyde and 0.003 g calcium chloride ($CaCl_2$)) in the fridge before processing by TEM. The samples were postfixed with reduced osmium (1% OsO_4 + 1.5% $K_4Fe(CN)_6$) counterstain for 1 hour, then dehydrated in a series of alcohols, infiltrated with TAAB LV resin and polymerised for 24 hour at 60℃, as described previously (Akbar et al., 2011) (Appendix 5). Ultrathin 70 nm sections were cut with Leica 'Ultracut S' ultramicrotome and placed on copper grids. The grids were observed in Tecnai 12 Biotwin TEM at 80 kV. Direct visualisation of nanomaterials in the MAs and various tissues was carried out using TEM, which was used to verify the presence of nanomaterials in the vascular wall, vascular cells or other tissues and demonstrate the evidence and the extent of nanomaterial uptake (if any).

2.6 Inductively Coupled Plasma Mass Spectrometry

Inductively coupled plasma mass spectrometry (ICP-MS; Perkin Elmer, UK) was used in order to quantify and calculate the relative amount of the silica (Si) metal in a sample containing the *ex vivo*-relevant amount. The sample was diluted in 5 mL dH_2O and subjected to analysis using ICP-MS. Additionally, to verify SiNPs uptake by vessels and other organs (for the *in vivo* biodistribution studies), ICP-MS was used to measure Si concentration. Briefly, vessels were weighed and placed into 500 µL lysate buffer solution [containing 1% sodium dodecyl sulphate (SDS; Sigma, Japan, 0.5 g), 0.1 M NaCl (0.29 g), 0.05 M tris(hydroxylmethyl)aminomethane (0.03 g) and Tris (0.39 g) in 25 mL of dH_2O at *pH* 8; with 250 µL of the protease inhibitor cocktail] and allowed to digest over 48 hours at room temperature. The lysate was subsequently mixed in 1 mL high purity (70%) nitric acid (HNO3; Sigma, UK) in glass tubing and placed in an oil bath at 115℃, for 2-3 hours as described previously (Al-Jamal et al., 2009). The solution was made up to 5 mL in distilled water and analysed. A standard curve was used to quantify the amount of metal in the tissues, using standards (Sigma, UK), in the same background solution as that of the tissue solutions. The limit of Si quantification was 50 ng/mL.

2.7 Protein Phosphorylation Studies

2.7.1 Sample Preparation for Protein Extraction – Non-functional Studies

A non-functional study was performed by infusing PSS or SiNPs (at 5.32 x 10^{11} NP/mL) into the whole mesenteric tree of the rat (dissected from the rat mesentery) in a petri-dish containing gassed PSS and placed on a hot plate at 37℃ (Figures 34 and 35). The infusion of PSS or SiNPs was performed by the use a 1 mL syringe inserted into the cannula tubing end, where the arterial tree is attached. Following 30 minutes of incubation in SiNPs, MAs were stimulated with 10 µM of ACh for 5 minutes. Segments were pooled after experimentation, and 100 MA segments (first-sixth order MAs) were collected per experimental condition, from 4 animal mesenteries (from a total of 400 MAs and 16 animal mesenteries) (Figure 35).

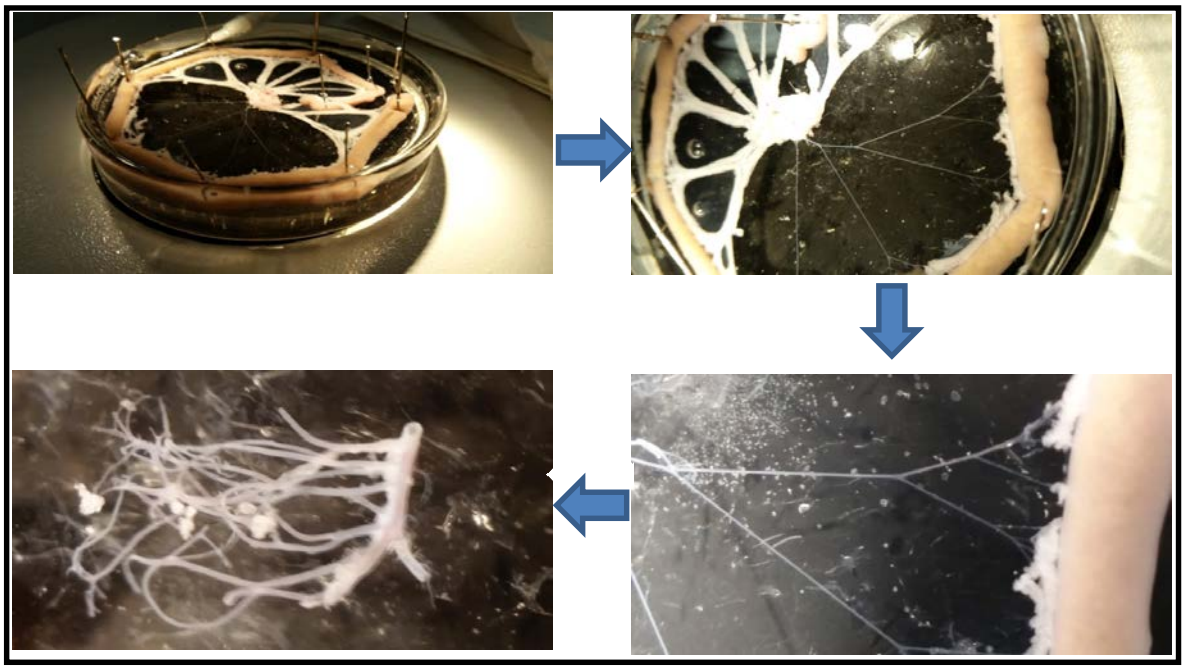

Figure 34. Vessel Pooling for non-functional studies and protein extraction.

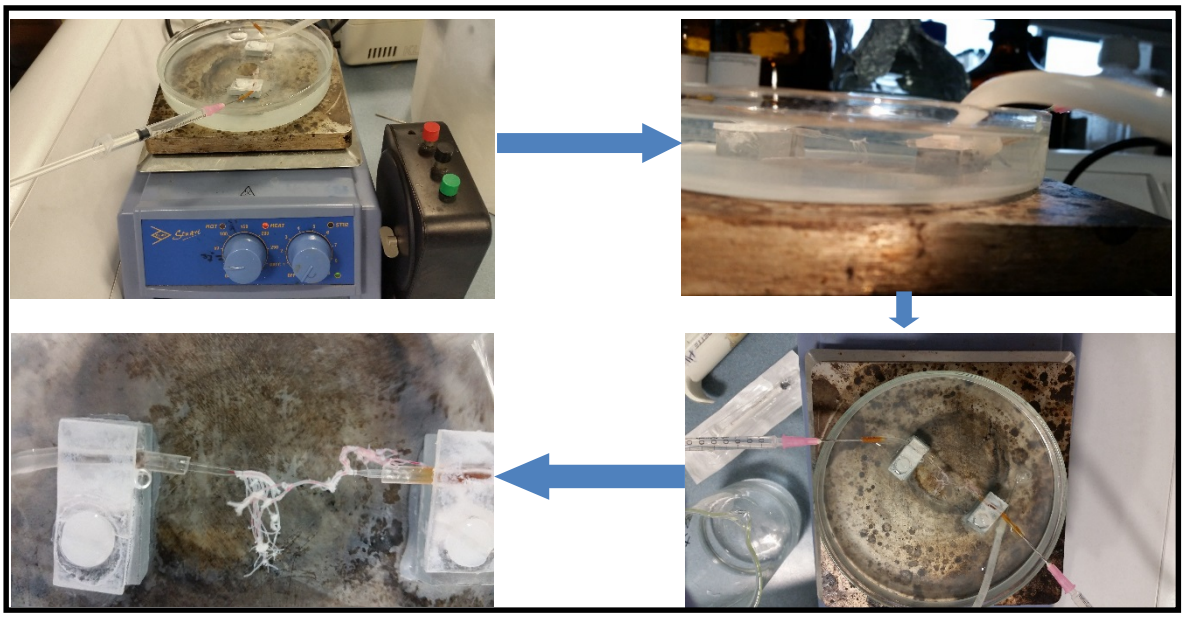

Figure 35. Non-functional on the whole rat mesentery studies including SiNPs infusion *ex vivo*.

2.7.2 Sample Lysis and Homogenisation

250 µL of lysis buffer obtained from the Proteome Profiler Human Phospho-Kinase Array (R&D Systems, Abingdon, UK) containing protein inhibitors cocktail was placed in each of the Eppendorf tubes corresponding to mesenteric vessels treated at a different condition. Samples were briefly sonicated three times for 5 seconds at 5 µm amplitude on ice. The tubes were incubated on ice in a rocker shaker placed in the cold room for 20 minutes. The vessels were placed in the sonicator for 5-10 seconds to break the DNA. Using the small Eppendorf tube homogeniser (Sigma, UK), the vessels were ground by rotation of the homogeniser in order to dissolve them in the buffer. Tissues were spun down at 13,000 rpm in a centrifuge for 20 minutes at 4℃ (the tubes were facing the inside of the centrifuge chamber). After spinning, the supernatant containing the total protein of the original sample was removed and placed into a fresh Eppendorf tube leaving the derbis and debris pullet. The procedure was repeated to maximise the protein yield from MAs.

2.7.3 Protein Quantification

The protein content of the samples was determined using the Pierce BCA protein assay kit (Reference number: 23225; Thermo SCIENTIFIC, UK). This protein assay is a dye-binding assay in which a differential colour change of a dye occurs in response to various concentrations of protein. The protein estimation technique was used to quantify the amount of solubilised proteins obtained in the tissue lysates from MAs allowing calculation of the volume of lysate necessary to perform a proteomics analysis. The protein standard dilutions were prepared as shown in appendix 6. Extra volume was prepared for bubble formation and/or pipetting errors. 10 µL aliquots of each dilution was pipetted in a 96-well flat-bottomed plate in triplicate. 10 µL volume from a total volume of 40 µL of each diluted (1:6) protein sample to quantify was pipetted in a 96-well flat-bottomed plate in triplicate; that is 6.67 µL of each protein sample added to 33.33 µL of lysis buffer. The dye solution was prepared by mixing 1 part of reagent A of the protein assay kit with 50 parts of reagent B in a 50 mL Falcon tube. As a blank to calculate background, 10 µL of the dye solution was pipetted into the plate in triplicate. The dye mixture was vortexed and filtered it using a 0.2 µm filter and a 20 mL syringe. The filtered volume was transferred into a different 50 mL Falcon tube. The dye solution was poured into a Gilson reagent reservoir and pipetted into

the 96-well plate at 190 µL per well using a multichannel pipette (both protein containing and blank wells). The plate was incubated for 30 minutes at 37°C. The plate was read in a Synergy HT microplate reader (Biotek, UK) using the Gen 5 2.05 software at an absorbance of 562 nm. The optical units read by the microplate reader were exported to an excel file to create an XY table with 3 replicates for each experimental point. The standard linear regression blot was used to create the line equation, R2 calculation and to interpolate unknown values, allowing the quantification of the protein content in the lysates in mg/mL (Appendix 6). The final protein concentration was calculated according to the dilution factor.

2.7.4 The Detection of Phosphorylated Proteins Patterns

A proteomic approach for the detection of the relative phosphorylation levels of 46 intracellular kinases was utilised using the Proteome Profiler Human Phospho-Kinase Array (Catalogue #ARY003B, R&D Systems, Abingdon, UK). This screening procedure was used to investigate the phosphorylation levels of proteins involved in mediating the actions of eNOS and EDHF in rat MAs following SiNP uptake. The phospho-protein expression levels were detected in 100 MAs after exposure to SiNPs at 5.32 x 10^{11} NP/mL for 30 minutes as part of a non-functional study using the proteome array kit according to the manufacturer's instructions. Briefly, capture and control antibodies were spotted in duplicate onto nitrocellulose membranes containing 46 kinase phosphorylation sites for the human phospho-kinase array (outlined in Table 3). 1 mL of array buffer was added to each well of the 8-well plate for blots in duplicates (to part A and B in duplicates; Figure 36). The blots were incubated in buffer for 1 hour (Figure 36). The buffer was aspirated from the plate. Tissue extracts containing 450 µg of total protein (form the recommended range of 200-600 µg of total protein per assay set) were diluted in lysis buffer (making a final volume of 2 mL) and incubated with the phospho-kinase array overnight at a volume of 950 µL per well of sample condition in duplicates. The array was washed to remove unbound proteins, followed by incubation with a cocktail of biotinylated detection antibodies. Streptavidin-HRP and chemiluminescent detection reagents were applied, and a signal was produced at each capture spot corresponding to the amount of protein bound, if any. After incubation, membranes were developed using enhanced chemiluminescence reagents (Hyperfilm ECL;

Amersham, UK) and immediately exposed to LI-COR scanner. Protein-positive spots on the mini-blots were visualised using the WestPico chemiluminescent substrate and quantified using ImageJ software (NCBI) and protein expression was normalised to a positive control, which was represented in each membrane.

Table 3. The 46-kinase phosphorylation sites for the human phospho-kinase array proteomics blot.

Akt (S473)	Hck (Y411)	PRAS40 (T246)
Akt (T308)	HSP27 (S78/S82)	Pyk2 (Y402)
AMPK alpha1 (T174)	HSP60	RSK1/2/3 (S380/S386/S377)
AMPK alpha2 (T172)	JNK pan (T183/Y185, T221/Y223)	Src (Y419)
beta-Catenin	Lck (Y394)	STAT2 (Y689)
Chk-2 (T68)	Lyn (Y397)	STAT3 (S727)
c-Jun (S63)	MSK1/2 (S376/S360)	STAT3 (Y705)
CREB (S133)	p27 (T198)	STAT5a (Y694)
EGF R (Y1086)	p38 alpha (T180/Y182)	STAT5a/b (Y694/Y699)
eNOS (S1177)	p53 (S15)	STAT5b (Y699)
ERK1/2 (T202/Y204, T185/Y187)	p53 (S392)	STAT6 (Y641)
FAK (Y397)	p53 (S46)	TOR (S2448)
Fgr (Y412)	p70 S6 Kinase (T421/S424)	WNK-1 (T60)
Fyn (Y420)	PDGF R beta (Y751)	Yes (Y426)
GSK-3 alpha/beta (S21/S9)	PLC gamma-1 (Y783)	

Figure 36. Images illustrating the procedure for mini-blots used in the proteomics array kit; where A) Labelling and preparing the mini-blots, B) Incubation of blots with the MA lysates, C) Incubation of the blots with the antibodies and D) Protein spot detection on a LI-COR platform.

2.8 Statistical Analysis

A generalised linear mixed model (GLMM) approach was performed for the statistical analysis of the data obtained using the IBM statistical package for social sciences (SPSS) version 19.0 (Breslow and Clayton, 1993). The GLMM that is used in this current study is an extension to the generalised linear model in which the linear predictor contains random effects, in addition to the usual fixed effects for sample effects regression analysis of grouped data. This model provides an extension of the linear mixed models to non-normal data (in our case % response values). This fixed-effects model of analysis of variance was applied due to the existence of different parameters or independent variables across different sets of experiments that can influence the dependent variable. The dependent variable in our case is the dilator response elicited by ACh and SNP which is expressed as percentage relaxation (corresponding to the increase from the pre-constricted maximal Phe value), or the constrictor response by Phe. The independent variables include: the number of the mesenteric vessel segments used, incubation type of the vessels [PSS, SiNPs at high dosage, SiNPs at low dosage, SiNPs with L-NNA, SiNPs with SOD, inhibitors (L-NNA, indomethacin, apamin and TRAM-34; alone or in combination] and chemical concentration (10^{-13} – 10^{-3} M) of the agonist used (Phe, ACh or SNP). As each vessel employed in this current study was repeatedly assessed (before as well as after incubation) for the different agonist concentration, we have also taken into the account the co-variant. The co-variant is the weight of each vessel i.e. how many occasions it was measured for either % contraction or relaxation. This allowed for the estimation of the ranges of response variable values that the independent factors would generate in a particular set of experiments. This whole analysis determined two factors, which are the 'incubation type' and the 'agonist concentration' to be responsible for the main significant effects contributing to the variation in vascular % responses (contraction or relaxation). This justified the use of repeated measures (one-, two-, three- or multi-variate) analysis of variance (ANOVA) for multiple sample mean comparisons due to the vessels being repeatedly measured for their responses to different agonist concentrations. The ANOVA test were performed to specify which incubation type is contributing to the significance of results (% response

measurements). The pairwise adjustments identified the particular dose(s) that lead to the significance of results among the different incubation types.

The number of mesenteric vessel segments is expressed as n, which represents the number of vessels utilised for each set of experiments. Data is represented as mean ± standard error of mean (SE). Concentration response curves were assessed using the appropriate ANOVA test with subsequent pairwise comparisons to determine the main effects of dose and incubation as well as the interaction of effects. Bonferroni adjustments were used to correct for multiple comparisons. If a main effect was observed, Student's paired or unpaired *t*-test (two tailed) was used to determine the locations of differences as appropriate. $p<0.05$ was considered to be statistically significant. The percentage dilation response of ACh and SNP was normalised to Phe constrictor responses and calculated as follows:

$$\frac{(\text{Dilation} - \text{Maximal Constriction})}{(\text{Original Diameter} - \text{Maximal Constriction})} X\ 100$$

Chapter 3.

The Chemical Characterisation of SiNPs

3.1 The Absorption Spectra of SiNPs Samples using Fluorescence Spectroscopy

The fluorescence absorption spectra of the A3 and DA3 SiNPs samples show peaks obtained at their expected wavelength (550-690 nm), confirming the presence of RBITC dye within the samples analysed (Figure 37). This is further illustrated by the pink colour observed with the A3 SiNPs substrate displaying a characteristic crystalline appearance in its dry form (Figure 28). In contrast, no absorption was detected by the A2 and DA1 SiNPs samples, which were prepared without dye (Figure 27).

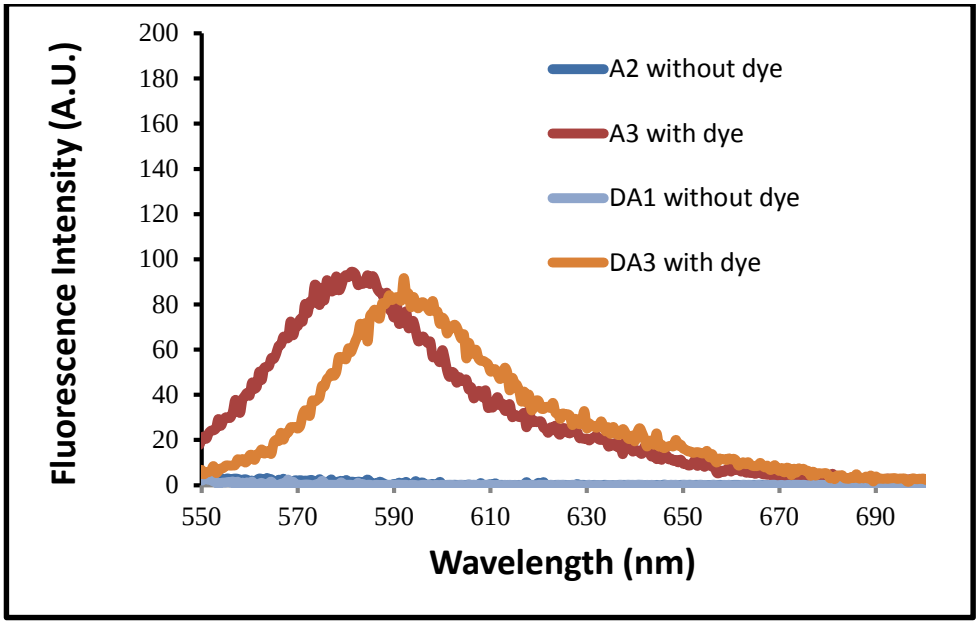

Figure 37.The fluorescence spectroscopy spectra indicating the presence of RBITC dye with an absorption of light at 550-690 nm wavelength region in different SiNPs samples with and without the dye.

3.2 SiNP Hydrodynamic Diameter

The DLS hydrodynamic diameter size for the different SiNPs samples synthesised according to the Stöber method measured between 94-2619 nm (Table 3). SiNPs with a DLS size distribution of above 200 displayed a higher tendency to sediment and aggregate in suspension (Table 4). There was a clear change in SiNPs size depending on the concentration of the reaction reagents. Thus, reaction flasks exposed to the same physical conditions were able to generate SiNPs with different size ranges depending on the concentration of reagent used (Table 2).

Table 4. The average hydrodynamic diameter size of different SiNP solutions in water or ethanol synthesised according to the Stöber method using the Malvern Zetasizer.

Sample	Size (nm)
1A	1085
1B	2619
2A	960
3A	225
3B	2174
D1 without dye	22400
D2 without dye	299
D2	315
D3	360
DA3	150
DA4	160
DA5	203
DA6	184
A2 without dye	103
A2	146
A3	138

3.3 SiNPs Topography and Morphology

The SEM images obtained for different dye-encapsulated SiNP samples are shown in Figure 38. The SEM images for DA5 and DA6 SiNPs samples shows mono-dispersed and uniform SiNPs with smooth spherical surfaces and an approximate overall relative diameter size in the range of 170-180 nm. In contrast, the SEM images for SiNP samples; 1Aa and 1B showed aggregation of NPs (Figure 38). The DLS measurements do not show agreement of size with the SEM images with slight differences of a factor of approximately 20-25 nm difference in favour of the DLS-measured samples. TEM analysis provides a more detailed and closer image to NP dispersion and size. Hence, the TEM diameter size was taken as the definitive SiNP size in contrast to the DLS size. NP size-related calculations are detailed in appendix 3.

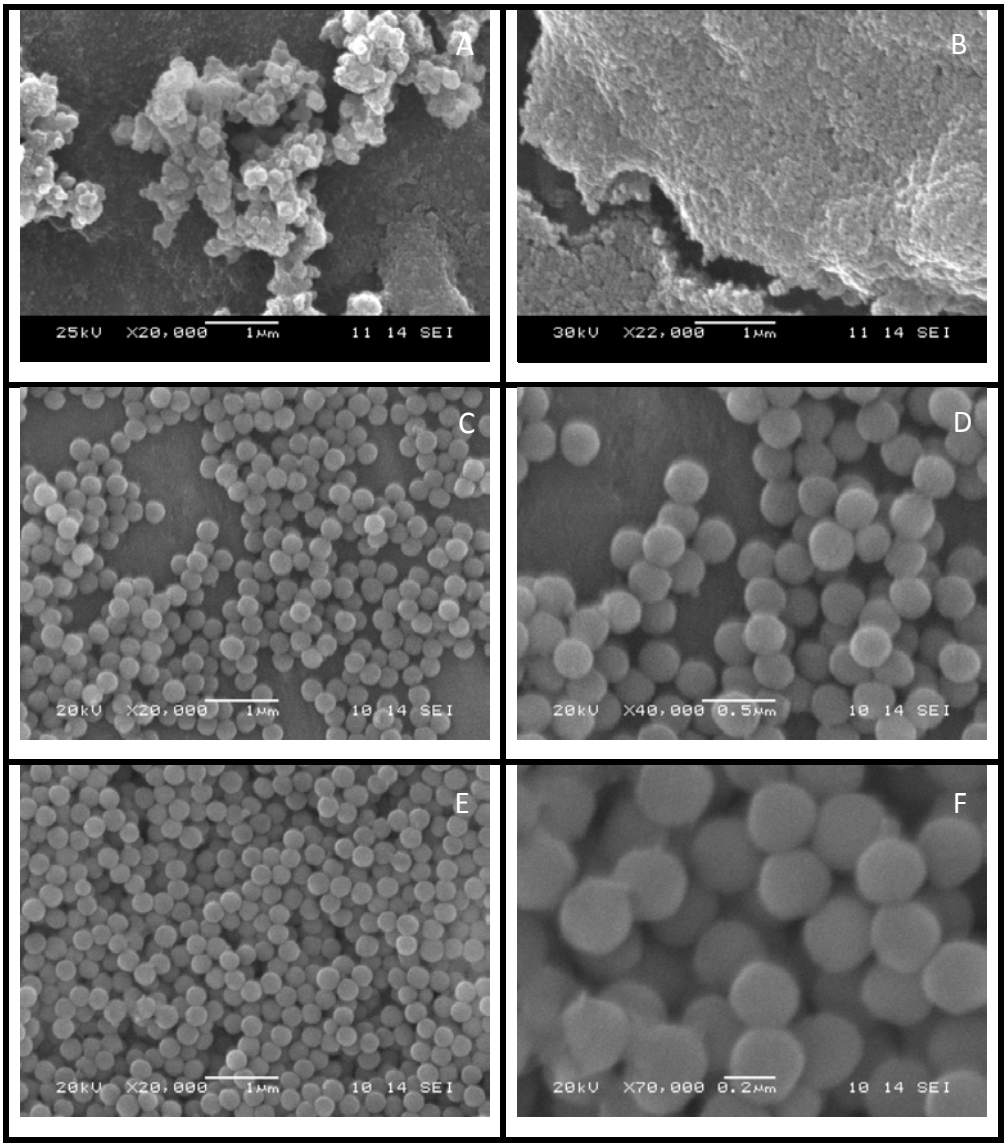

Figure 38. SEM images of the Samples: 1A (A), 1B (B), DA5 (C and D) and DA6 (E and F).

3.4 SiNPs in a Blood Sample

In order to examine SiNPs interaction with blood (if any); the changes to the DA3 SiNPs DLS size and Zeta potential were monitored after they were dispersed in a blood sample obtained from a 3 weeks old Wistar Rat (following DA3 centrifugation in water to remove ethanol). The latter SiNP sample was incubated in blood over 8 hours and size and Zeta potential was monitored in a sequential manner using the Malvern Zetasizer. There was a trend of increase in the size of D3 SiNPs in the blood after 4 hours of incubation reaching to 717 nm compared to 145 nm before incubation (100 runs in the Zetasizer; Figure 39). However, the D3 SiNPs size was reduced to 200 nm following 8 hours of incubation. The Zeta potential profile for the DA3 SiNPs in blood decreased from -32 to -37 mV for the 8-hour duration of incubation (Figure 40).

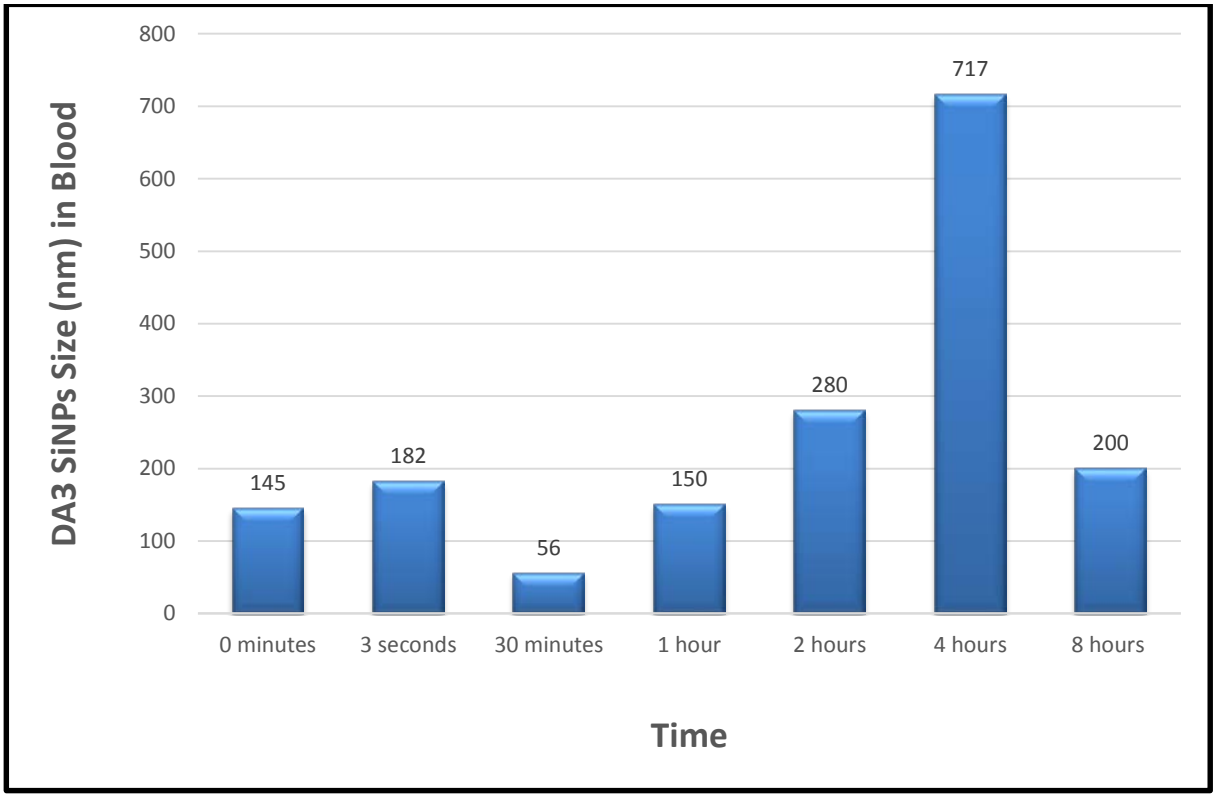

Figure 39. The changes in DA3 SiNPs size in a blood sample obtained from a 3 weeks old Wistar Rat over 8 hours using the Malvern Zetasizer. Values are an average of 100 readings performed by the Malvern Zetasizer machine.

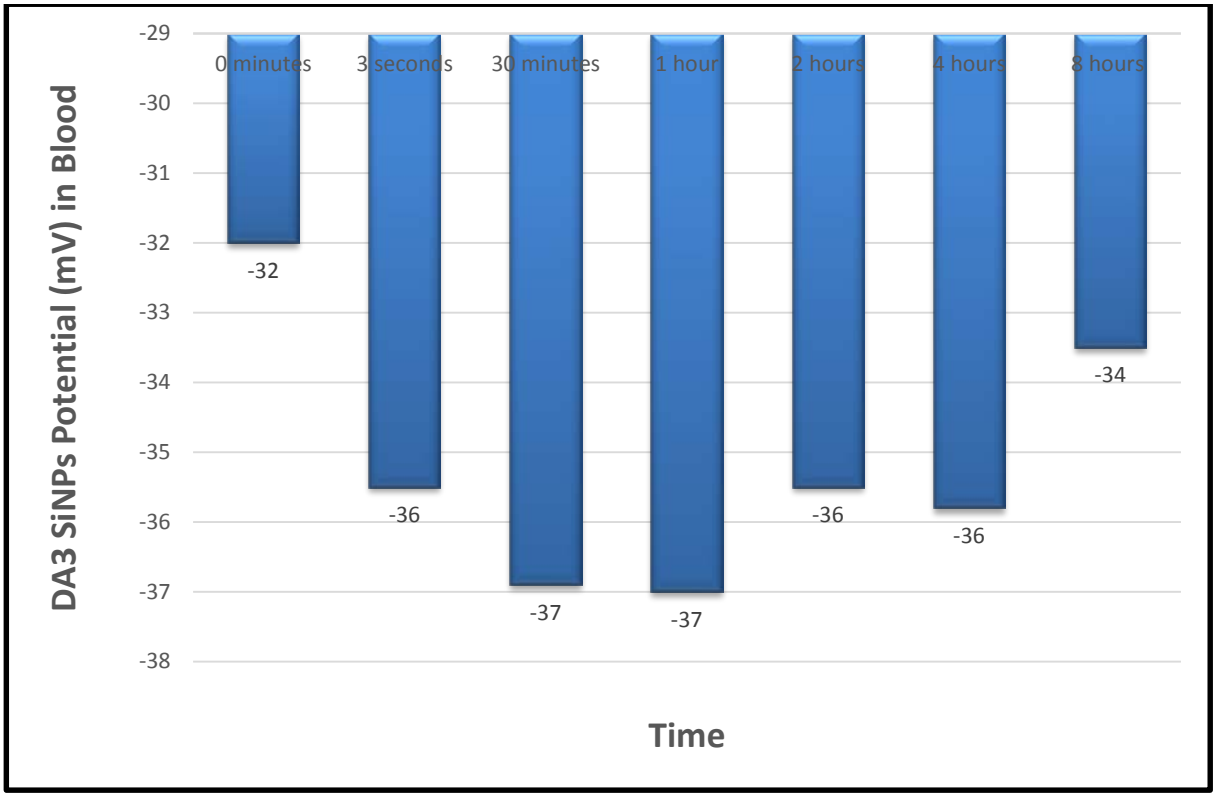

Figure 40. The changes DA3 SiNPs potential in a blood sample obtained from a 3 weeks old Wistar Rat over 8 hours using the Malvern Zetasizer. The mean of 100 runs is presented.

The TEM images obtained for SiNPs incubation in blood demonstrate the presence of aggregated SiNPs (Figure 41).

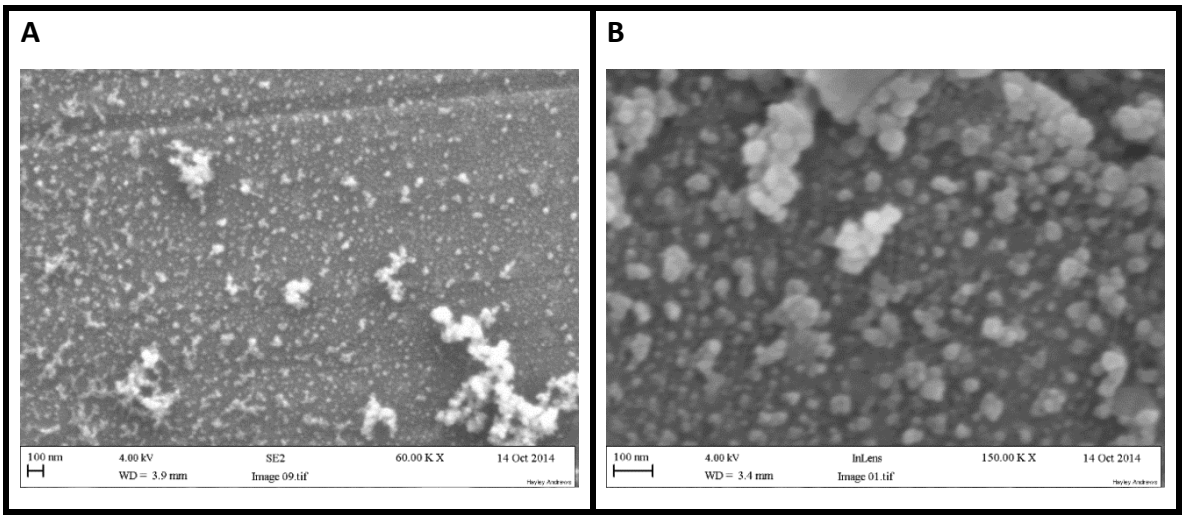

Figure 41. TEM images of the DA3 SiNPs in blood sample following 8 hours of incubation.

3.5 The Shelf-life for DA3 and A3 SiNPs Samples

DA3 (in ethanol) and A3 (in water and in PSS) SiNPs samples were specifically monitored over a time-course of 15 months in an attempt to predict their shelf-life *in vitro*. This may have an impact on the suitability of the storage medium used in this case, ethanol, water and PSS, and allow the understanding of NPs behaviour in an aqueous environment as applied to *in vivo*.

3.5.1 DA3 and A3 Morphology

The SEM and TEM images of the synthesised DA3 SiNPs sample stored in ethanol demonstrate that the NPs have a mono-disperse spherical morphology (Figures 42 and 43). The storage of the NPs over a one-year period has not affected the particle morphology, as the particle shape and size have remained similar (~110 nm).

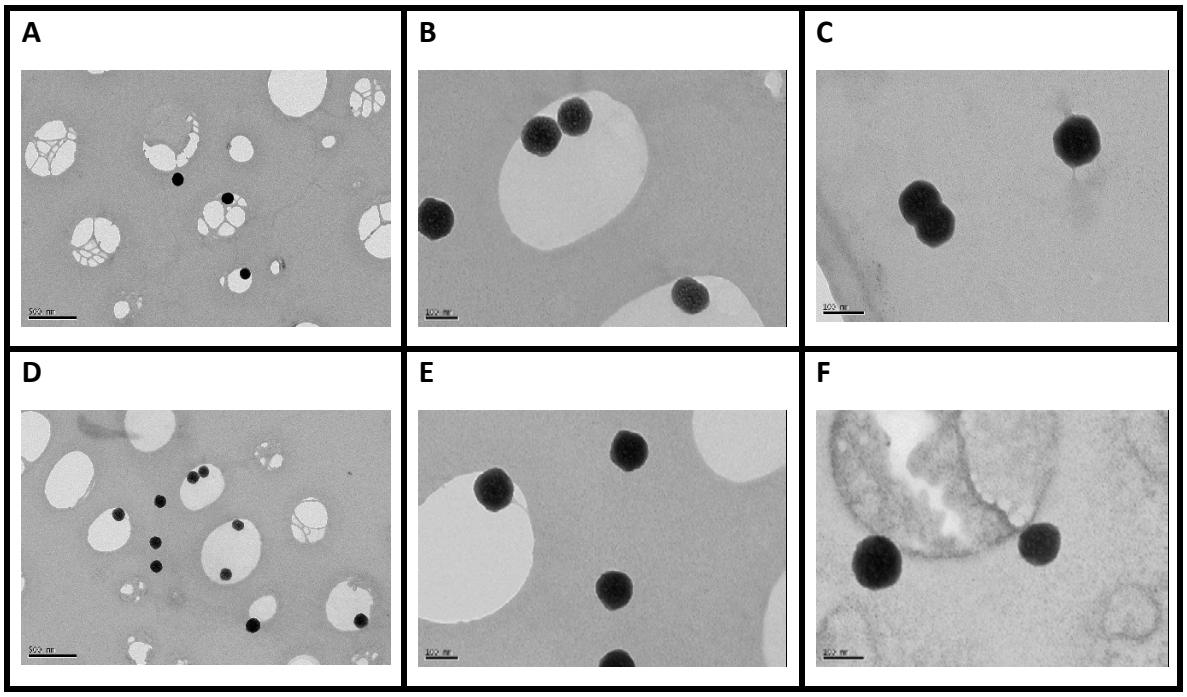

Figure 42. TEM images of the DA3 SiNPs sample at month 1 (A-C) and month 15 (D-F).

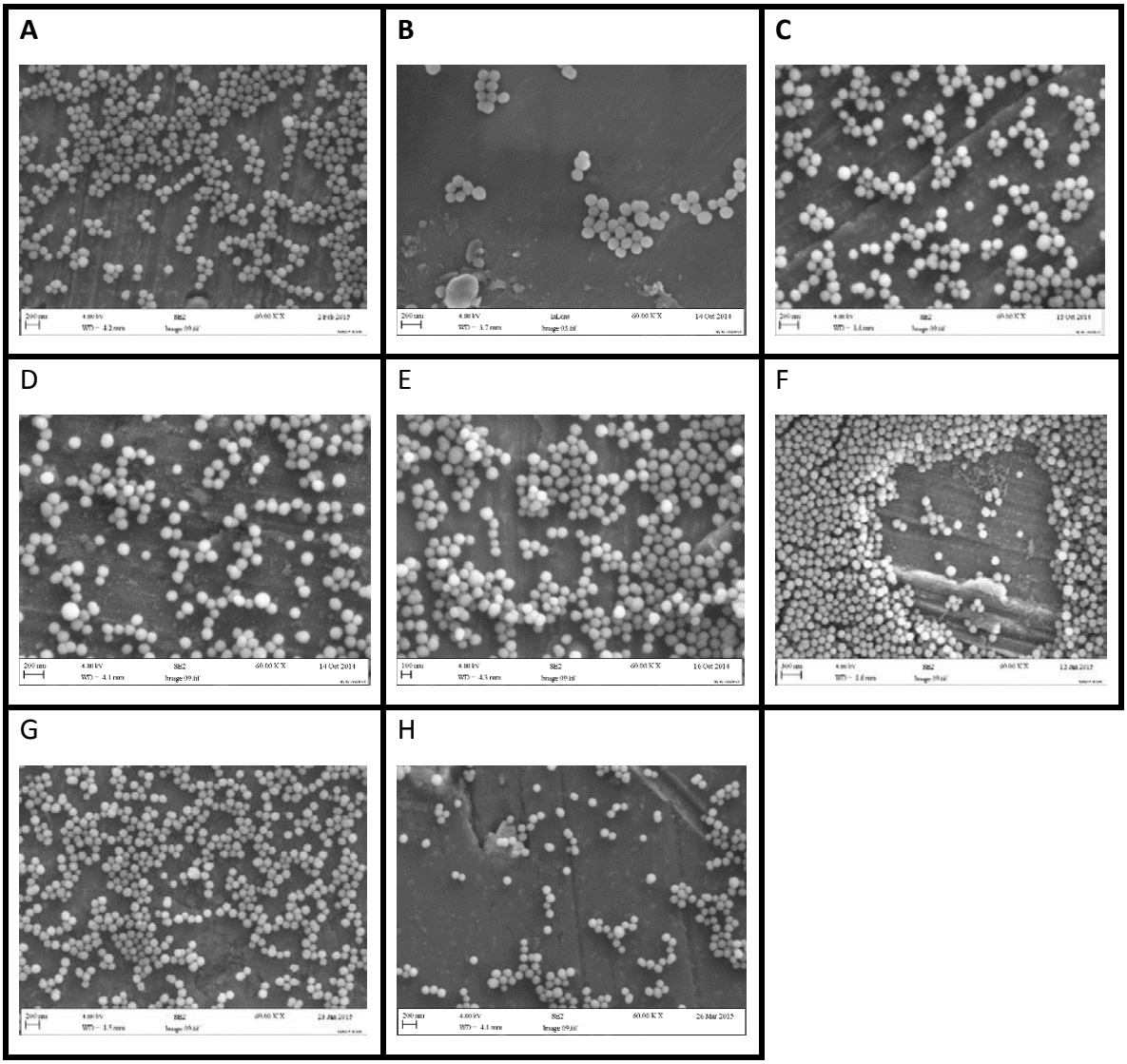

Figure 43. SEM images of DA3 SiNPs sample in ethanol over time, where A) month one; B) month three; C) month five; D) month seven; E) nine; F) month eleven; G) month thirteen and H) month fifteen.

TEM analysis confirmed the size of the A3 SiNPs sample as 97.85 ± 2.26 nm (~98 nm). Compared to the DA3 SiNP sample, the SEM and TEM images obtained for the A3 SiNPs sample stored in water show the aggregation and change in shape of the NPs over a 15-month period, from relatively smooth monodispersed NPs to more aggregated and rough or crunchy-looking NPs, with no significant changes to their size (Figures 44 and 45). A3 SiNPs seem to be aggregated with the presence of different sizes of other medium size and tiny NPs in suspension and in some cases surrounding the A3 SiNPs (Figure 44).

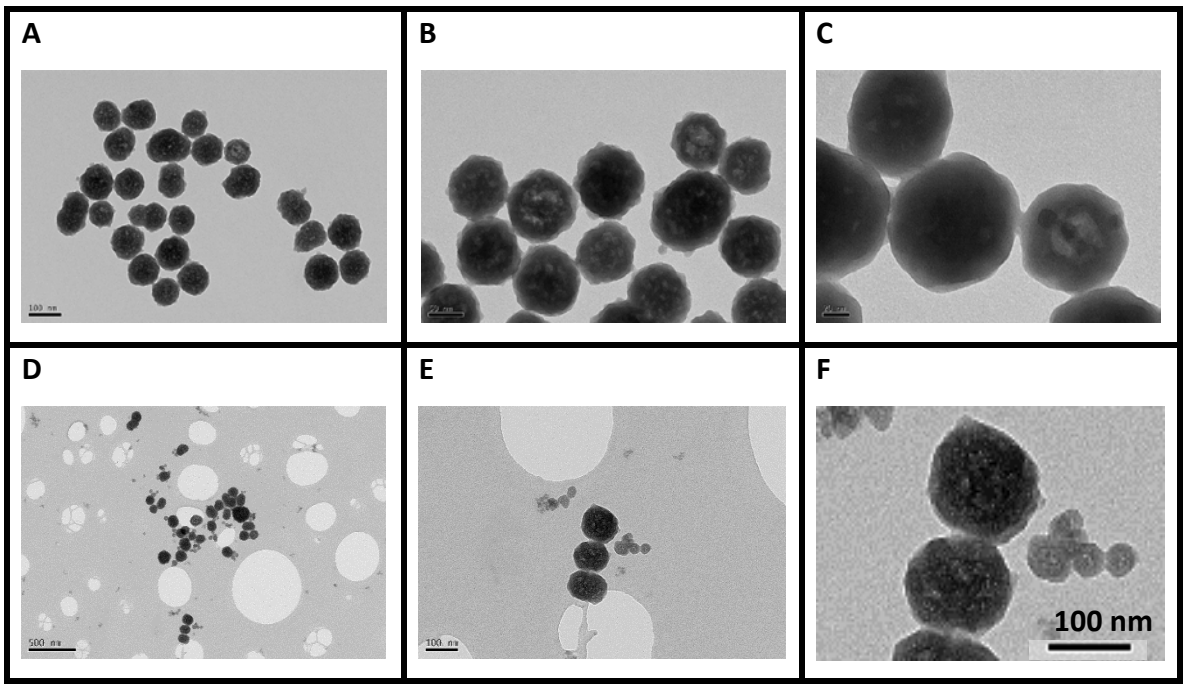

Figure 44. TEM images of the A3 SiNPs sample at month 1 (A-C) and month 15 (D-F).

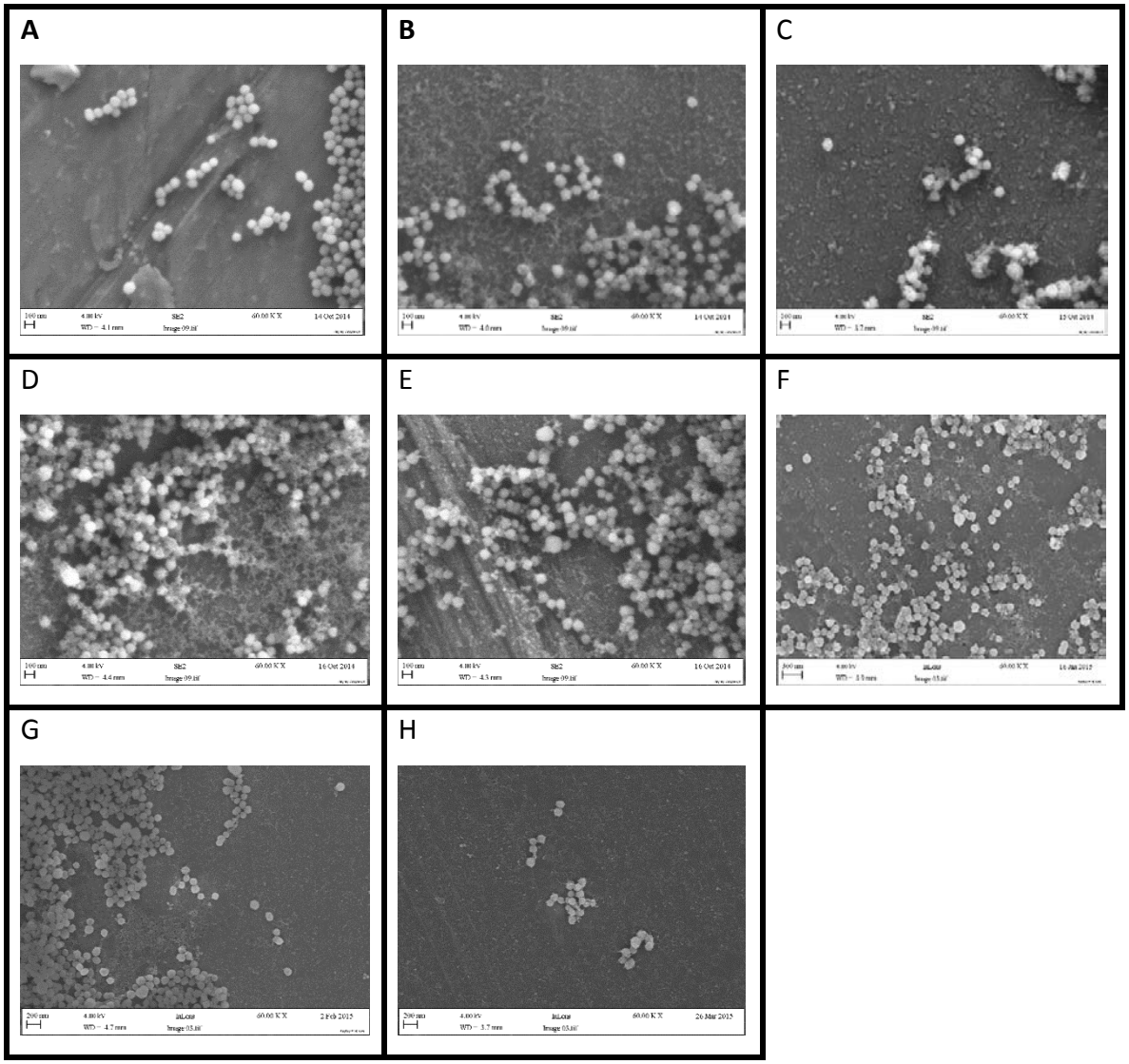

Figure 45. SEM images of sample A3 SiNPs sample in water over time, where A) month one; B) month three; C) month five; D) month seven; E) nine; F) month eleven; G) month thirteen and H) month fifteen.

The overall average hydrodynamic sizes of DA3 and A3 SiNPs samples were graphically presented for direct comparisons as stored in different media (Figures 46 and 47). There was no change in the size of A3 and DA3 SiNPs following 15 months of size measurements in water, ethanol and PSS (the mean size of A3 SiNPs sample in PSS was 128 ± 1.52 nm vs. 129 ± 2.75 nm after month 1 and 15 respectively, n=4, paired *t* test, NS; Figure 46).

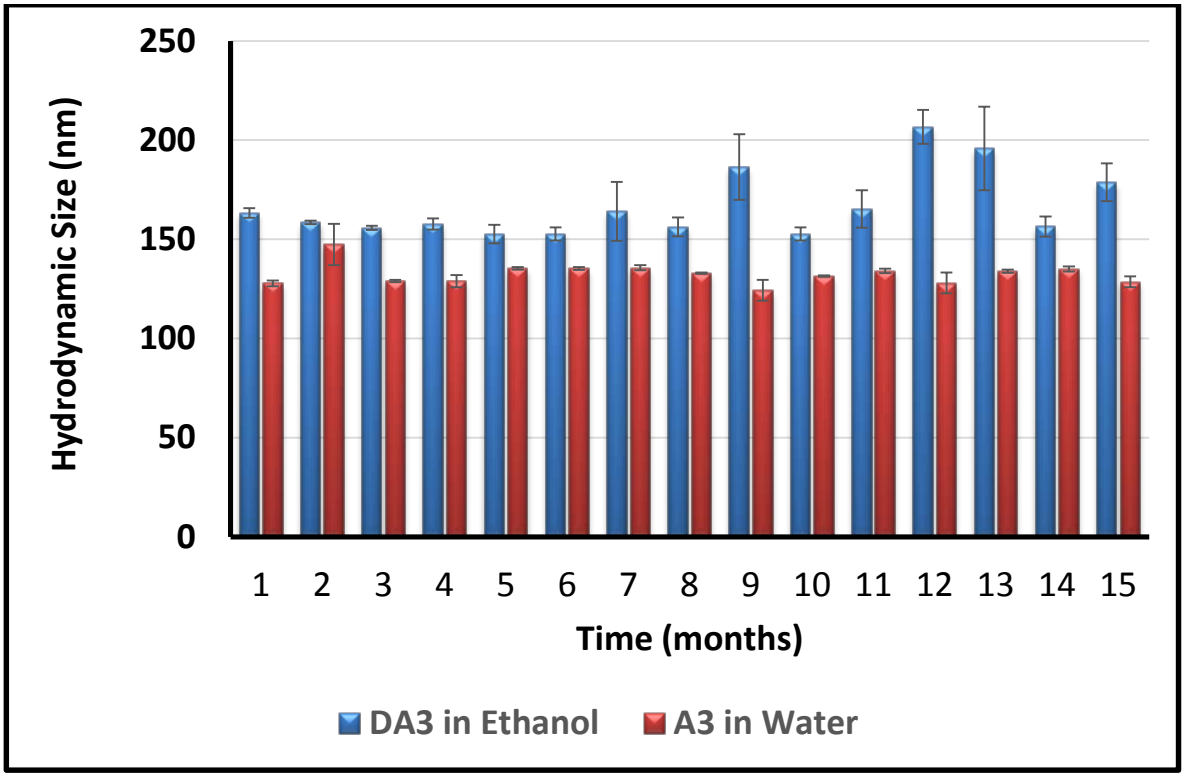

Figure 46. The repeated analysis of the hydrodynamic average size of DA3 SiNPs in Ethanol and A3 SiNPs in water for 15 months using the Malvern Zetasizer.

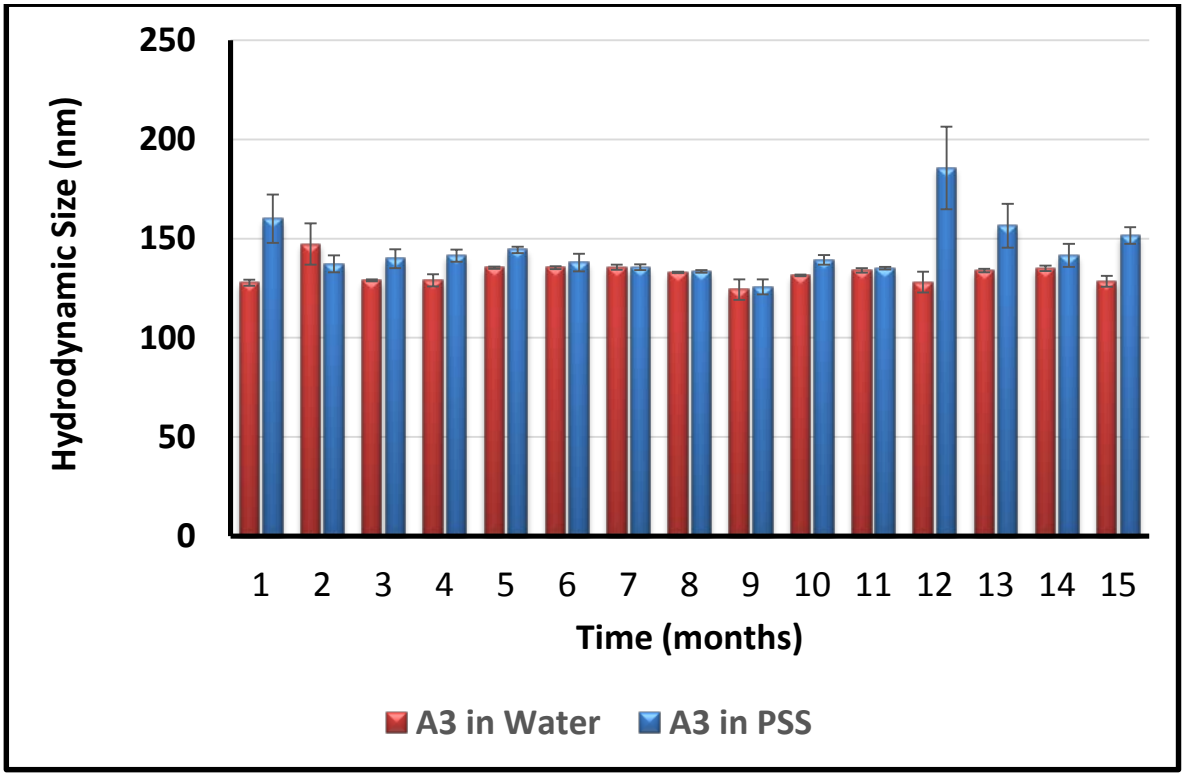

Figure 47. The repeated analysis of the hydrodynamic average size of DA3 SiNPs in Ethanol and A3 SiNPs in water for 15 months using the Malvern Zetasizer.

3.5.2 DA3 and A3 Charge and Stability

The DA3 and A3 SiNP samples were also monitored for their surface charge and stability in ethanol or water and PSS respectively over the course of 15 months (Appendix 4). There was a significant change in the Zeta potential of DA3 SiNPs sample in ethanol following 15 months of Zeta potential measurements (the mean Zeta potential of DA3 SiNPs sample in ethanol was -37 ± 0.85 mV vs. -24 ± 1.07 mV after month 1 and 15 respectively, n=4, paired *t* test, $p<0.0001$). The Zeta potential measurements for the A3 SiNPs displayed significant changes in PSS only for a course of 15 months with slight fluctuations in Zeta potential for the SiNPs dispersed in water during the 15 months period (the mean Zeta potential of A3 SiNPs sample in water was -41 ± 1.04 mV vs. -29 ± 5.57 mV after month 1 and 15 respectively, n=4, paired *t* test, NS; Figure 48 and that of PSS -12 ± 0.38 mV vs. -15 ± 0.25 mV after month 1 and 15 respectively, n=4, paired *t* test, $p<0.001$; Figures 49). Overall, SiNPs did not maintain their Zeta potential in ethanol and PSS as compared to water. However, the incubation in PSS increased SiNPs stability over time with the Zeta potential becoming more negative.

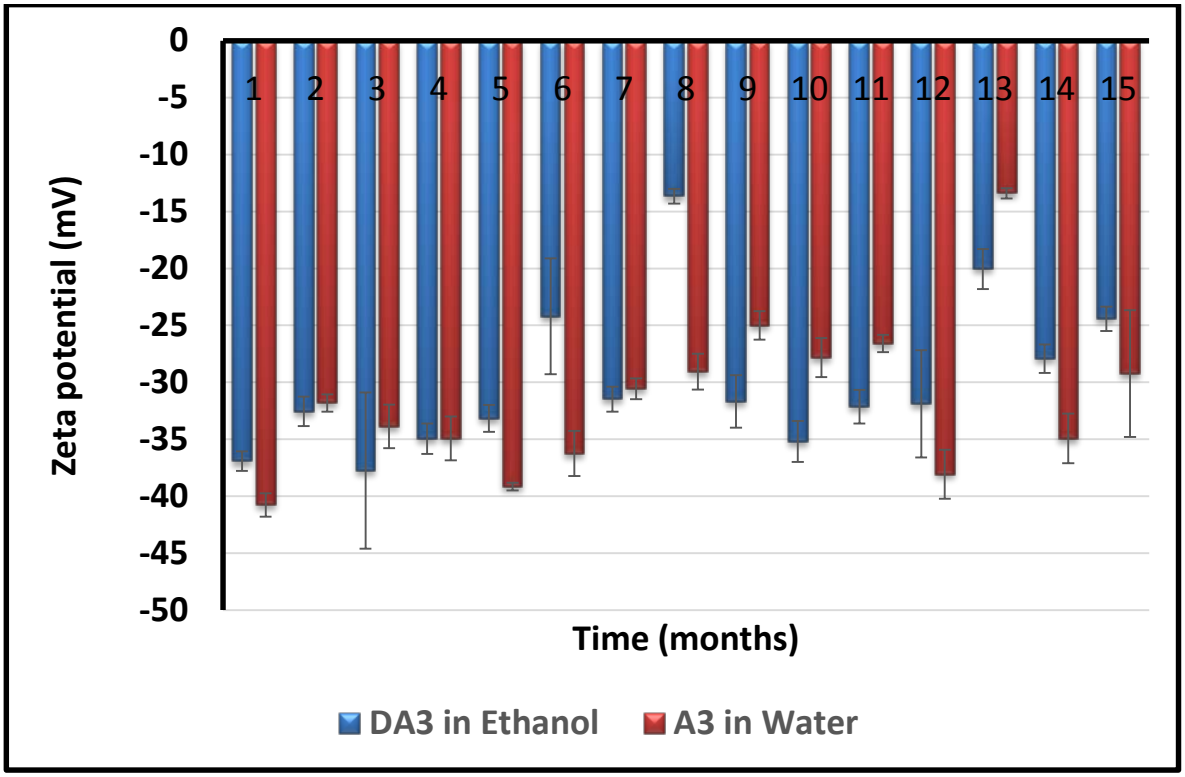

Figure 48. The repeated analysis of the Zeta potential average of DA3 SiNPs in Ethanol and A3 SiNPs in water for 15 months using the Malvern Zetasizer.

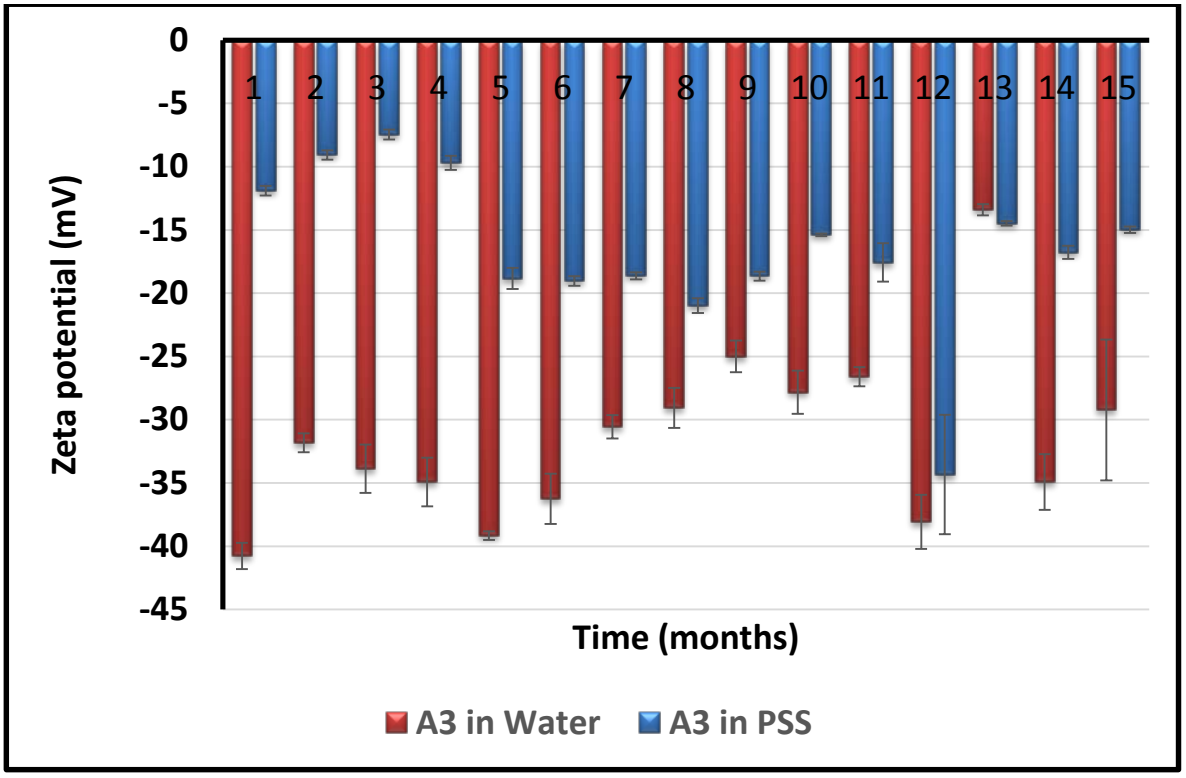

Figure 49. The repeated analysis of the Zeta potential average of A3 SiNPs in water and PSS for 15 months using the Malvern Zetasizer.

3.6 Discussion

3.6.1 Fabrication and Characterisation of SiNPs

The SiNP size and morphologies of the different sizes were determined by DLS, TEMs, SEMs and Zeta potentials using the Malvern Zetasizer and electron microscopy. The Derjaguin-Landau-Verwey-Overbeek (DLVO) theory (Derjaguin and Landau, 1941; Verwey et al., 1948) describes colloidal dispersions stability. The theory describes that the total interaction energy between two particles is given by the sum of the attraction due to Van der Waals interactions and the electrostatic repulsion originating from the overlap of the charged diffuse layers. The Zeta potential provides a charge for the surface potential and can be used to indicate particle stability. A number of sol-gel precipitation methods were employed in the present study to synthesise SiNPs, based on the Stöber and Ismael methods (Stöber et al., 1968; Ismail et al., 2010). These yielded small aggregated NPs, which may be due to the experimental conditions explained by a narrow variation in the temperature and stirring conditions used. Thus, the methods were not repeatable but the synthesis of NPs using the modified Stöber method with different reagent ratios generated more desirable NP sizes and morphologies. In contrast to other samples made, the A3 SiNPs sample was prepared by using a slightly higher dilution of silica reagents in ethanol; namely TOES. The results suggest that using a large reaction vessel (250 mL) and a larger volume of ethanol (250 mL; acting as a medium for the interaction of silica precursors) enhanced the optimal dispersion for TEOS to nucleate more silica seeds. Improved monodispersity of silica seed growth and finer spherical morphology was achieved with an increase in the size of silica particles (~200 nm), which were achieved in the absence of water and lower volume of TEOS to ethanol (1:20 ratio). This finding was similar to a pervious study by Zhang et al., which suggested that the TEOS dilution in ethanol before its drop-wise addition (in a 2-hour time-intervals) can suppress the generation of new nuclei and the aggregation or adhesion of particles. Thus, TEOS dilution in a drop-wise fashion can improve monodispersity of silica spheres (Zhang et al., 2003). In agreement with the study by Canton et al., we were able to produce smaller SiNPs dimensions by incremental changes to the reagents and the addition of more ethanol in a continuous drop-wise addition. Thus, increasing the ratio of water to hydrated ammonia used in the synthesis of the range of

SiNP samples, as well as the reduction of TOES, yielded smaller size NPs. These changes in silica precursor concentrations yielded small SiNPs that were approximately 100 nm in size, although with crunchy shell due to the characteristic appearance of ultra-fine silica seeds surrounding the silica surface as with the A3 SiNPs sample (Figure 44). Hence, the production of fine SiNPs surrounding the silica surface may be prevented by further optimising the method for making smooth SiNPs taking into account all the factors mentioned above. Thus, the synthesis of SiNPs requires fine-tuning of the reagents as well as experimental conditions to achieve the desired NP sizes and morphologies (Zhang et al., 2003).

The SEM images obtained for different SiNP samples confirm the fabrication of colloidal and monodispersed SiNPs despite the presence of aggregated NPs due to the variation in the reactant concentrations used. As previously recommended the addition of TEOS at a controlled rate (Nozawa et al., 2005) resulted in small particle size with a polydispersity index (PDI) values of less than 0.7, indicating that the A3 and DA3 samples were monodispersed. The optimisation of TEOS and NH_3 concentrations, the type of solvent or media (H_2O and ethanol) and the reaction temperature can hence control SiNPs size distribution and Zeta potential measurements (Rahman and Padavettan, 2012). For instance, increasing the amount of ammonia resulted in an increase of silanol groups on the SiNPs surface thereby causing the size of SiNPs to increase.

3.6.2 The Stability of DA3 and A3 SiNPs over Time

The RBITC dye-encapsulated monodispersed SiNPs samples; DA3 and A3 SiNPs were characterised over a 15-month period in different media (ethanol, water and PSS). The granular appearance of the A3 SiNPs, after a 15-month period, may have been caused by the silica seeds surrounding the individual SiNPs. In contrast, the DA3 SiNPs maintained their smooth surface characteristics in ethanol over time. The polydispersity index (PDI) of the DA3 and A3 SiNP samples did not significantly change over the 15-month storage period, with PDI values scoring below 0.3 nm, confirming the monodispersity of the samples. The A3 SiNP sample, however, became aggregated and rough in its outer surfaces

with time. Silica is known to decompose into silicic acid (DIACONU et al., 2010). During prolonged storage of the A3 SiNPs in water suspension, silicic acid release may have contributed to their aggregation with time. The latter may also be responsible for raising the *pH* of the storage medium, which can contribute further to the A3 SiNP changes in characteristics. The breakage of the Van der Waal forces keeping the nanospheres in shape and the distortion of the lattice structures of these NPs may be one cause. The other possible explanation for the variation in the morphology of A3 SiNPs sample over time may be due to the dissolution of these NPs in water with time. The dissolution of the SiNPs may give rise to silica seeds and enhance the aggregation of the NPs as well the responsibility of the crunchy-looking surface due to the surrounding tiny seeds. Dissolution is a process where a solution is formed after a solute is added to a solvent. The dissolution mechanism of SiNPs initially undergoes the dissociation of the sianol group ($\equiv$SiO-H $\leftrightharpoons$ SiO^- + H^+). Then Si^{+4} atom undergoes a nucleophilic attack by water molecules to form a silica intermediate, ($Si_2O(OH)_7^-$). Followed by the breaking of the siloxane bond $\equiv$Si-O-Si$\equiv$. Thus, distorting and breaking the nanosphere structure. The dissolution of the silica may have been initiated by the NPs (surface area, concentration) and/or water media over time. The large surface area due to the relatively small size of our A3 SiNPs sample, may have contributed to the enhanced dissolution of the NPs due to the greater accessibility to water molecules, thereby reducing the Zeta potential. This phenomenon was previously demonstrated in mesoporous SiNPs (Finsy, 2004; Huang et al., 2014). Other factors such as; temperature, *pH*, silicate concentration and metal oxide formation, all can affect the dynamic equilibrium between silicate dissolution and decomposition (Bass et al., 2007).

Our results show that the Zeta potentials of the A3 SiNPs samples were unaffected by storage in water, suggesting that water maintains SiNP stability. The Zeta potential measurements of the DA3 SiNPs sample in ethanol significantly decreased, suggesting that ethanol may not maintain the stability of silica samples overtime. The neutralisation effect of PSS on the SiNPs surfaces may have decreased its negativity of the Zeta potential, which is expected due to a decrease in the extension of the diffuse repulsive layer caused by counter ion screening. The existence of the surface charge on SiNPs may be due to the deprotonation of silanol groups projecting from the SiNPs surfaces. An increase in cation

concentration causes an exchange of the hydrogens on the silanol groups ($SiOH \leftrightharpoons SiO^- + H^+$) (Derjaguin and Landau, 1993). The other possibility is that PSS may compete for SiNPs with water molecules and lead to reduced hydration layer formation. However, PSS over the course of 15 months improved the stability of SiNPs.

Chapter 4.

The Influence of SiNPs on Arterial Function, *Ex Vivo*

4.1 Control Vascular Responses (Repeatability)

The results indicate that there was no overall significant difference before and after the incubation in PSS alone without nanomaterial(s) present.

4.1.1 Repeatability of Responses to High Potassium Solution (KPSS)

The incubation of mesenteric vessels in PSS alone over a 30-minute period led to no change in the vasoconstrictor responses to KPSS at 60 mM concentration (Figure 50; unpaired *t* test, NS). Most mesenteric vessels constricted in response to KPSS. The use of KPSS allowed for over 50% constriction by most mesenteric vessels *ex vivo* (Figure 50) confirming their viability. The vessel viability cut off value for inclusion was 50% KPSS constriction or over. Vessels that failed to reach 50% constriction by KPSS were excluded from further experimentation. The incubation in PSS alone had no overall effect on the KPSS contractile responses as compared to before incubation; (At 60 mM KPSS, the mean percentage constriction was 67.43 ± 3.51% vs. 78.49 ± 7.13% before (control) and 30 minutes after incubation in PSS respectively, n=56 and 7 respectively, unpaired *t* test, NS; Figure 50).

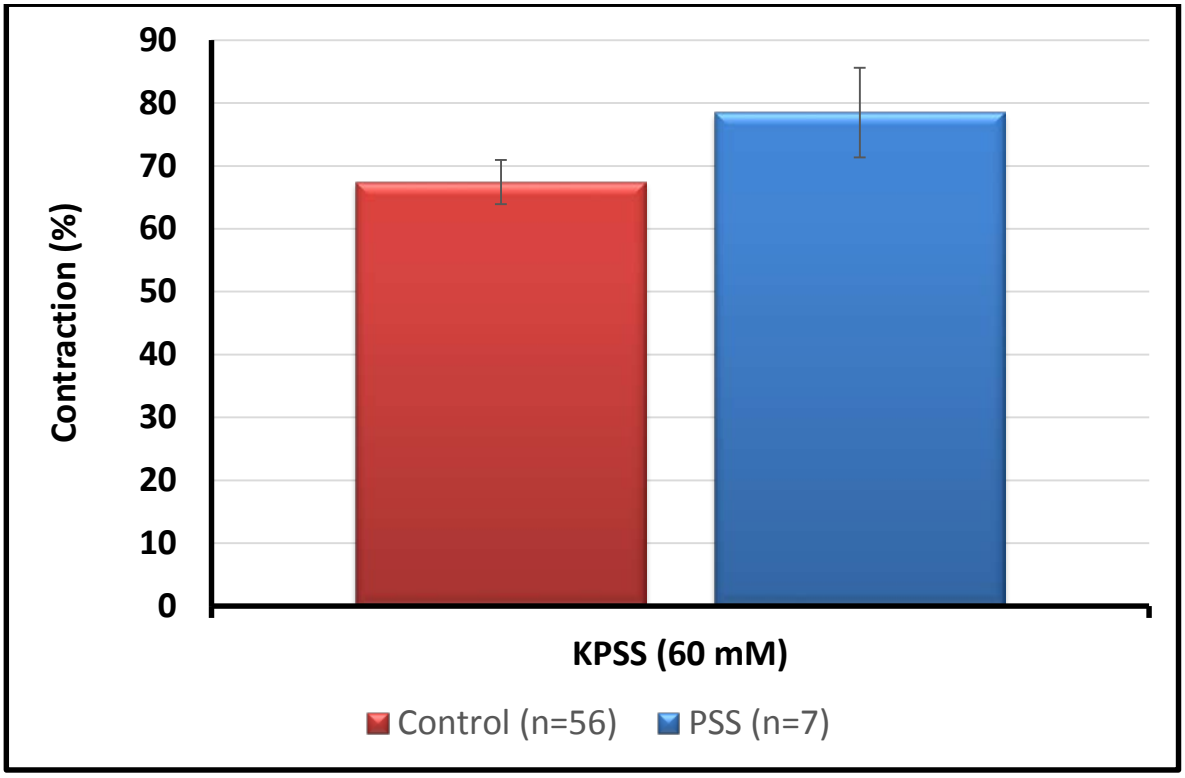

Figure 50. Responses to KPSS-induced Contraction, before (Control) and after incubation in PSS. 'n' is number of vessels, error bars=SE.

4.1.2 Repeatability of Responses to Phe

Similarly, the incubation in PSS alone had no overall effect on the Phe contractile responses as compared to before incubation. At the submaximal concentration of Phe (1 µM), the mean percentage constriction was 78.68 ± 3.78% vs. 68.69 ± 5.15% before (control) and 30 minutes after incubation in PSS respectively, n=27 and 4 respectively, unpaired *t* test, NS; Figure 51). Some vessels developed episodes of continuous vasomotions upon the addition of the maximal concentrations of Phe, in some instances for a period of 20-30 minutes.

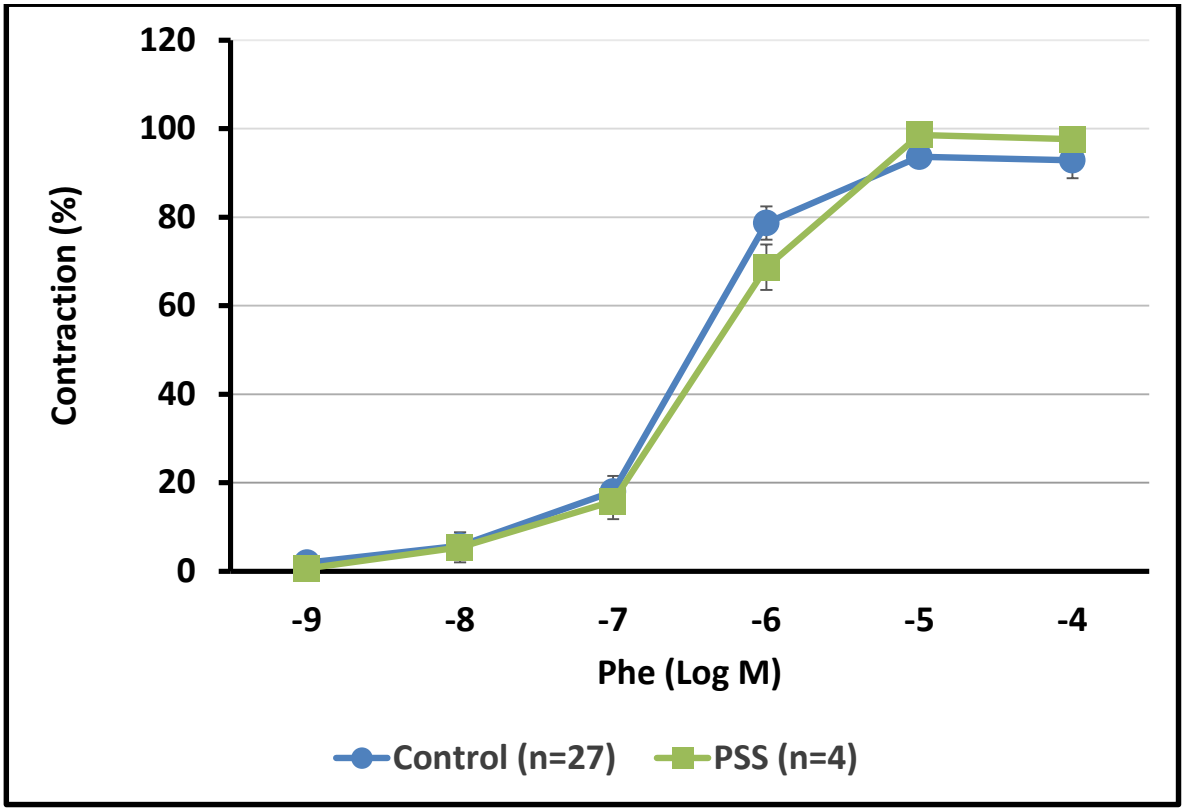

Figure 51. Responses to Phe-induced contraction, before (Control) and after incubation in PSS. 'n' is number of vessels, error bars=SE. One-factor repeated measures ANOVA. P values correspond to comparisons between PSS incubation vs. control Phe responses of MAs.

4.1.3 Repeatability of Responses to ACh

ACh induced a concentration-dependent increase in the dilator response in all pre-constricted vessels reaching optimal dilation at ACh concentration of 100 nM in control and PSS incubated vessels (Figure 52). There was no overall effect on the endothelial-dependent ACh dilator responses following KPSS pre-constriction after the incubation in PSS as compared to before incubation. The effect of the incubation in PSS on the submaximal concentration of ACh (10 µM) was unaffected; (At 10 µM ACh, the mean percentage dilation was 86.44 ± 3.59 % vs. 70.78 ± 9.79% before (control) and 30 minutes after incubation in PSS respectively, n=9 and 4 respectively, unpaired *t* test, NS; Figure 52).

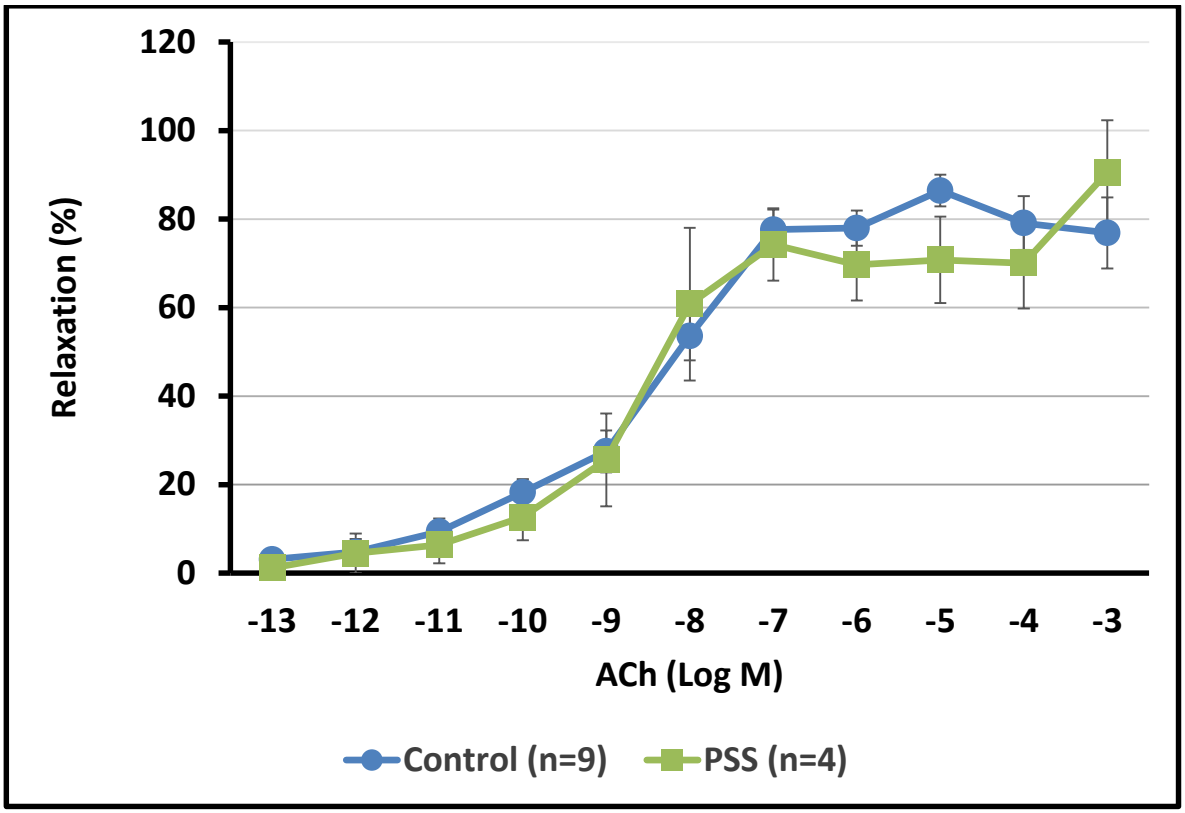

Figure 52. Responses to ACh-induced relaxation in KPSS pre-constricted vessels, before (Control) and after incubation in PSS. 'n' is number of vessels, error bars=SE. One-factor repeated measures ANOVA. P values correspond to comparisons between PSS incubation vs. control ACh responses of MAs.

The incubation in PSS alone had no overall effect on the endothelial-dependent ACh dilator responses following Phe pre-constriction as compared to before incubation; (At 1 µM ACh, the mean percentage dilation was 97.35 ± 3.55 % vs. 96.15 ± 3.11% before (control) and 30 minutes after incubation in PSS respectively, n=7 and 6 respectively, unpaired *t* test, NS; Figures 53 and 54). The effect of the incubation in PSS on the submaximal concentration of ACh (10 µM) was unaffected (At 10 µM ACh, the mean percentage dilation was 101.67 ± 3.02% vs. 96.68 ± 7.82% before (control) and 30 minutes after incubation in PSS respectively, n=7 and 6 respectively, unpaired *t* test, NS; Figure 54). At an ACh concentration of 1 mM; the maximum concentration of ACh used, the vessels achieved more than 100% dilation; (At 1 mM ACh, the mean percentage dilation was 105.64 ± 6.41 % vs. 101.76 ± 0.69% before (control) and after incubation in PSS respectively, n=7 and 6 respectively, unpaired *t* test, NS; Figure 54).

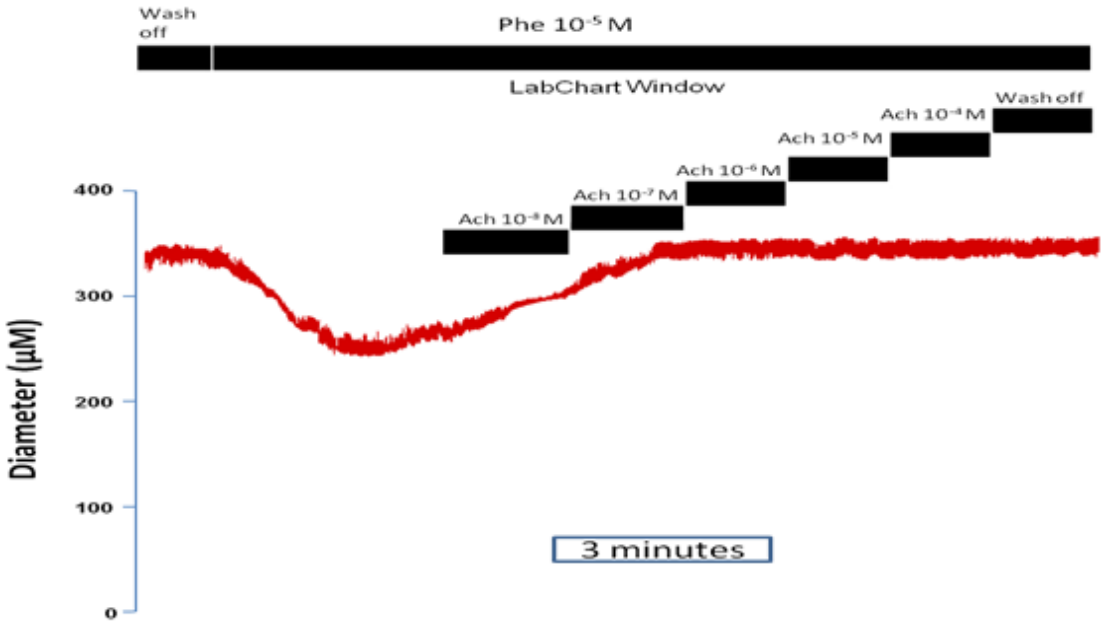

Figure 53. A representative trace of the responses to ACh in Phe pre-constricted vessels after incubation in PSS *ex vivo*.

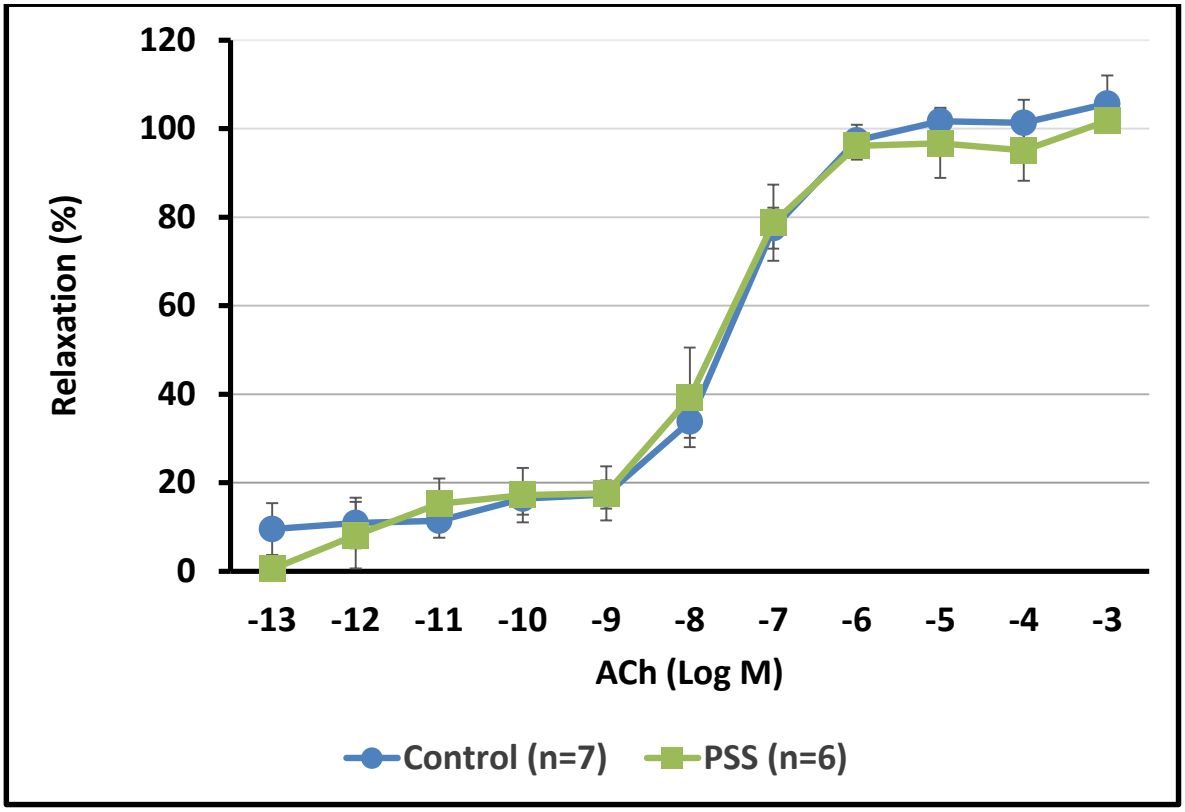

Figure 54. Responses to ACh-induced relaxation in Phe pre-constricted vessels, before (Control) and after incubation in PSS. 'n' is number of vessels, error bars=SE. One-factor repeated measures ANOVA. P values correspond to comparisons between PSS incubation vs. control ACh responses of MAs.

4.1.4 The Influence of Incubation in PSS on MA Integrity *ex vivo*

The mechanical luminal infusion of PSS through 1 mL syringe into the MA had no effect on the intact MA cellular layers as indicated in Figure 55.

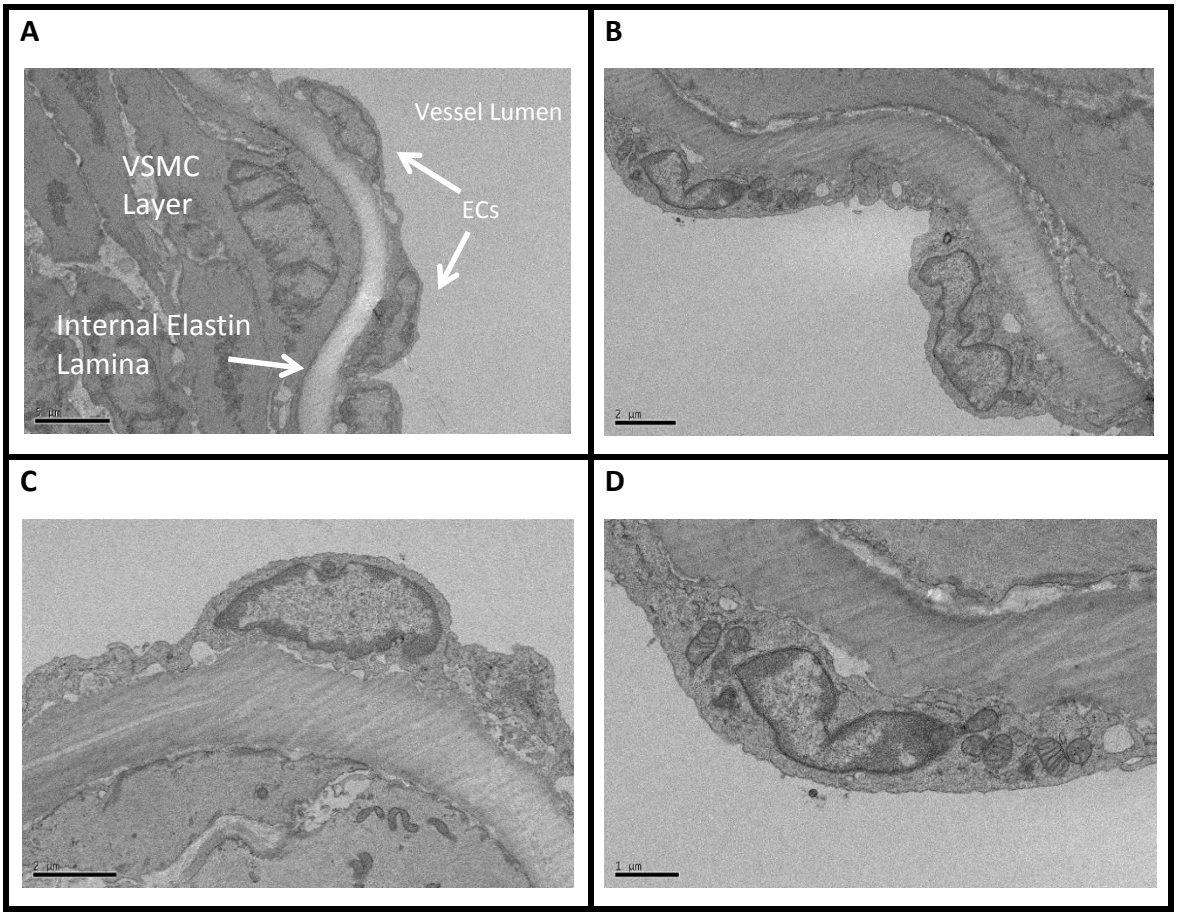

Figure 55. TEM images (A-D) representing the different cellular layers in a second order MA after 30 minute of incubation in PSS.

4.2 Influence of SiNPs on Vascular Responses

The vasoconstrictor and vasodilator responses of the mesenteric vessels was assessed using the SiNPs at a concentration of 5.32 x 10^{11} NP/mL. Data analysed within the mixed model produced a significant differences associated mainly with the incubation types. Thus, the null hypothesis, that "there is no difference before or after the incubation with the nanomaterials (SiNPs and CNTs)" was rejected.

4.2.1 Vasoconstrictor Responses

4.2.1.1 KPSS Responses

Incubation in SiNPs *ex vivo*, at 5.32 x 10^{11} NP/mL, had no overall influence on the contractile responses of vessels to KPSS; (the mean percentage constriction was 78.49 ± 7.13% vs. 65.80 ± 7.04% after incubation in control and SiNPs respectively, n=7 and 10 respectively, unpaired *t* test, NS; Figure 56).

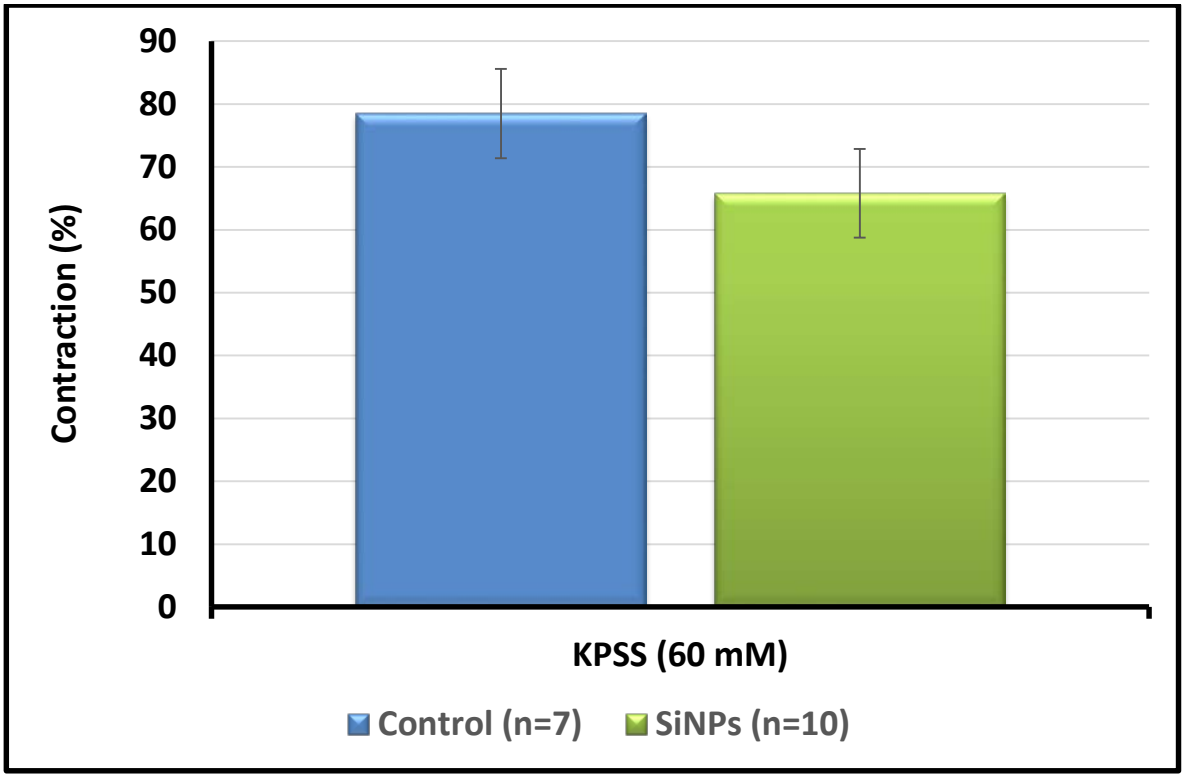

Figure 56. The influence of SiNPs infused *ex vivo* on constriction responses to KPSS. 'n' is number of vessels, error bars=SE.

4.2.1.2 Phe Responses

Incubation in SiNPs *ex vivo*, at 5.32 x 10^{11} NP/mL, led to a significant reduction in the contractile responses of vessels to Phe, at specific concentrations (1, 10 and 100 µM); (At 10 µM Phe, the mean percentage constriction was 98.55 ± 1.45% vs. 36.51 ± 11.17% after incubation in PSS and SiNPs respectively, n=4 and 5 respectively, unpaired *t* test, $p<0.05$; Figure 57). The submaximal constriction to Phe was reduced when the vessels were incubated in SiNPs; (At 1 µM Phe, the mean percentage constriction was 68.69 ± 5.15% vs. 36.47 ± 6.85% after incubation in PSS and SiNPs respectively, n=4 and 5 respectively, unpaired *t* test, NS; Figure 57). In contrast, incubation in a diluted dosage (1x) of SiNPs at 1.01 x 10^{11} NP/mL (i.e. 5x less concentrated) did not affect the contractile responses of the vessels to Phe. The 1x SiNPs produced a dose-dependent increase in the level of responses to Phe (10^{-7} to 10^{-4} M) similar to control; (At 1 µM Phe, the mean percentage constriction was 68.69 ± 5.15% vs. 76.37 ± 5.15% after incubation in PSS and 1x SiNPs respectively, n=4 and 3 respectively, unpaired *t* test, NS; Figure 57).

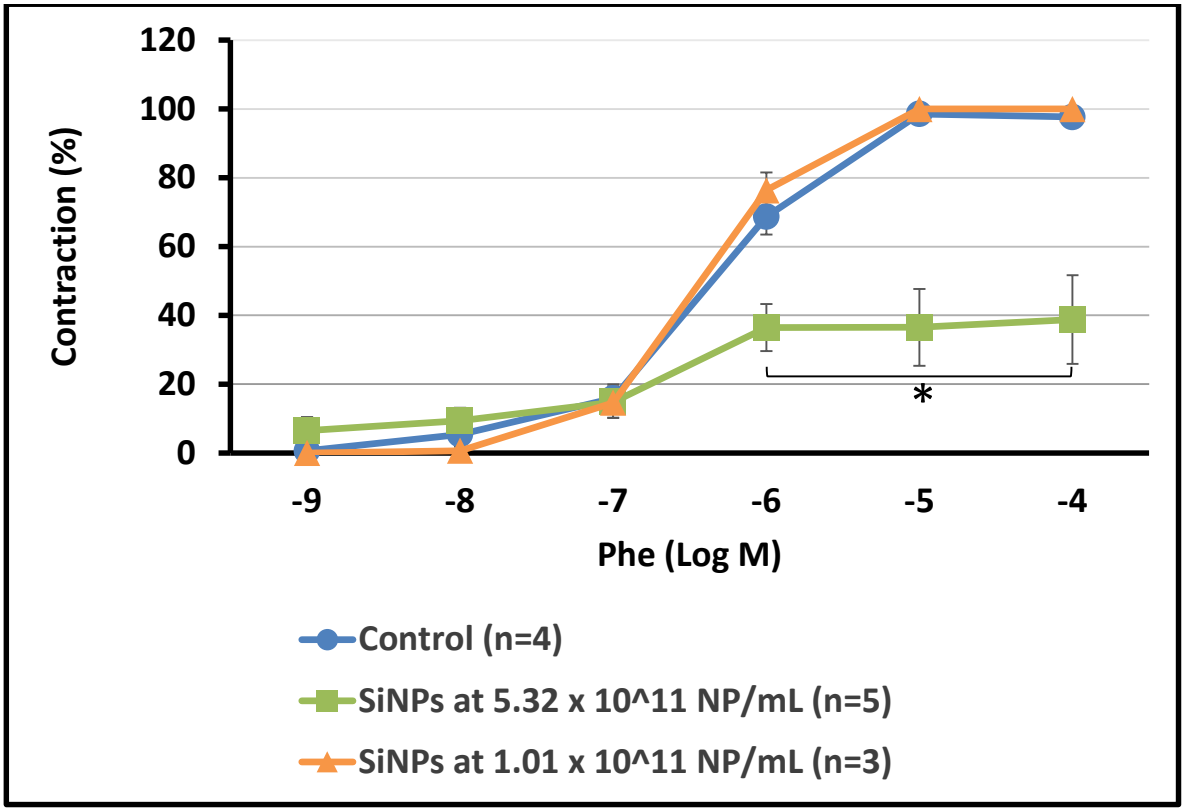

Figure 57. The influence of SiNPs infused *ex vivo* at two different concentrations (5.32 x 10^{11} and 1.01 x 10^{11} NP/mL) on the Phe-induced contraction. 'n' is number of vessels. *p<0.05, error bars=SE. Two-factor repeated measures ANOVA. P values correspond to comparisons between SiNPs incubated either at high or low dosage vs. control Phe responses of MAs.

4.2.1.3 AVP Responses

All vessels constricted to AVP in a dose-dependent manner (Figure 58). In contrast to Phe, a similar behaviour of constriction to AVP was found when the vessels were incubated in SiNPs. The incubation in SiNPs had no overall effect on the contractile responses to AVP despite a significant decrease in the magnitude of constriction at 10 nM concentration of AVP; (At 10 nM AVP, the mean percentage constriction was 90.41 ± 2.10% vs. 97.40 ± 1.74% after incubation in control and SiNPs respectively, n=4, paired *t* test, $p<0.05$; Figure 58). Thus, SiNPs slightly reduced the contractile responses of the vessels to AVP in contrast to control vessels.

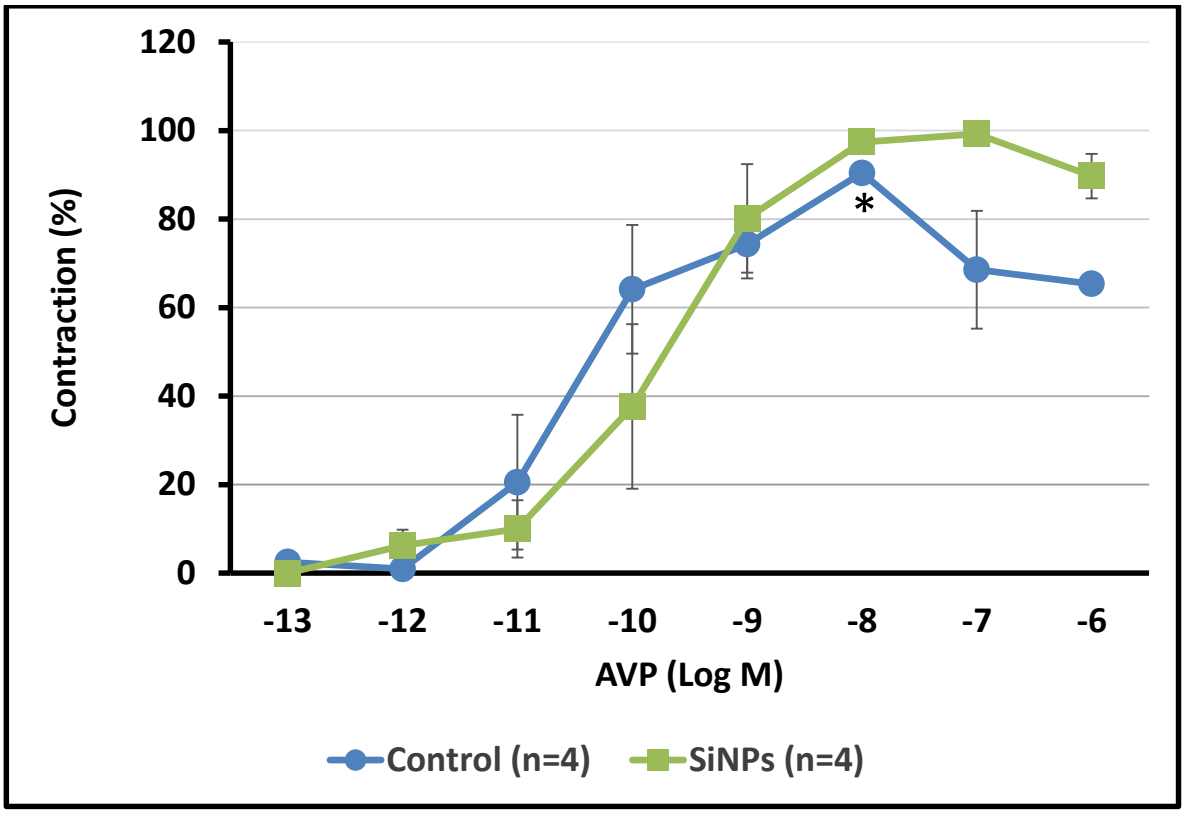

Figure 58. The influence of SiNPs infused *ex vivo* on the AVP-induced contraction. 'n' is number of vessels. *p<0.05, error bars=SE. One-factor repeated measures ANOVA. P values correspond to comparisons between SiNPs incubated *ex vivo* vs. control AVP responses of MAs.

4.2.2 Vasodilator Responses

4.2.2.1 Endothelial-dependent (ACh) Responses

Incubation in SiNPs *ex vivo*, at 5.32 x 10^{11} NP/mL, led to a significant attenuation in the magnitude of the endothelial-dependent dilator responses to ACh following KPSS pre-constriction, at specific concentrations (10^{-7} to 10^{-4} M ACh); (At 100 nM ACh, the mean percentage dilation was 74.25 ± 8.17% vs. 31.33 ± 8.72% after incubation in control and SiNPs respectively, n=4 and 5 respectively, unpaired *t* test, p<0.05; Figure 59).

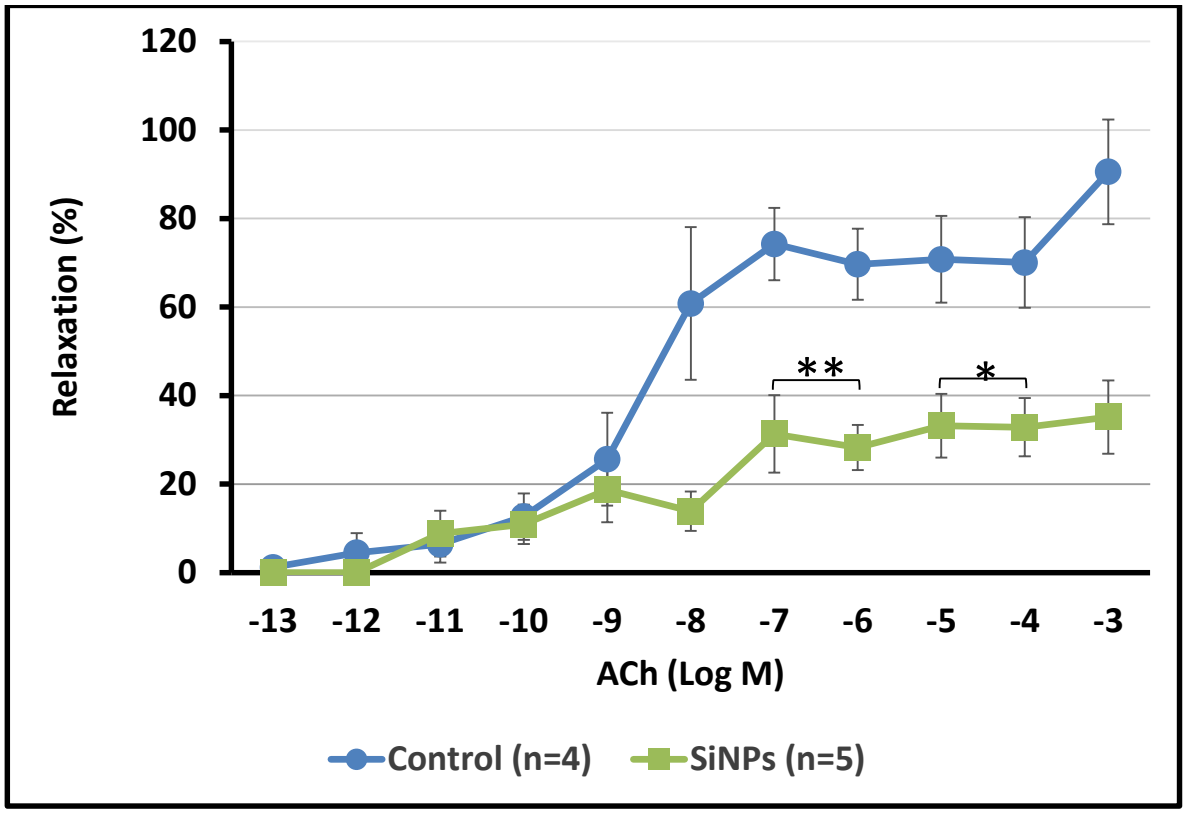

Figure 59. The influence of SiNPs infused *ex vivo* on the ACh-induced relaxation in KPSS pre-constricted vessels. 'n' is number of vessels. *p<0.05 and **p<0.01, error bars=SE. One-factor repeated measures ANOVA. P values correspond to comparisons between SiNPs incubated *ex vivo* vs. control ACh responses of MAs.

Incubation in SiNPs *ex vivo*, at 5.32 x 10^{11} NP/mL, led to a significant attenuation in the dilator responses to ACh following Phe pre-constriction, at specific concentrations (10^{-7} to 10^{-3} M); (At 1 µM of ACh, the mean percentage dilation was 96.15 ± 3.11% vs. 27.82 ± 5.13% after incubation in PSS and SiNPs at 5.32 x 10^{11} NP/mL respectively, n=6 and 11 respectively, unpaired *t* test, p<0.0001; Figure 60). The dilator responses were improved when the vessels were incubated with a lower dose of SiNPs (1.01 x 10^{11} NP/mL) in contrast to the more concentrated sample. The incubation in SiNPs at 1.01 x 10^{11} NP/mL produced no effects on higher concentrations of ACh (10^{-6} to 10^{-3} M), despite a significant decrease at the ACh concentration of 100 nM; (At 100 nM ACh, the mean percentage dilation was 78.77 ± 8.58% vs. 37.07 ± 9.44% after incubation in control and SiNPs at 1.01 x 10^{11} NP/mL respectively, n=6, paired *t* test, p<0.05; Figure 60).

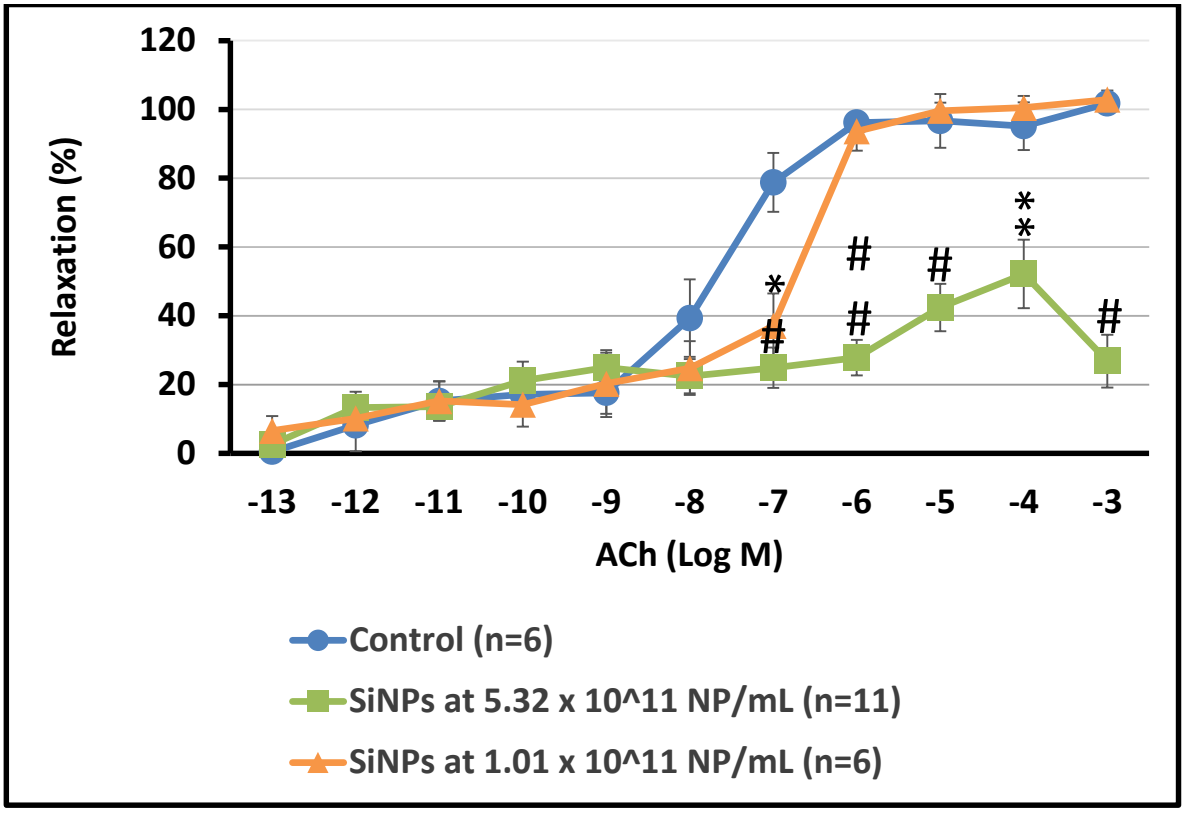

Figure 60. The influence of SiNPs infused *ex vivo* at two different concentrations (5.32 x 10^{11} and 1.01 x 10^{11} NP/mL) on the ACh-induced relaxation in Phe pre-constricted vessels. 'n' is number of vessels. *p<0.05, **p<0.01, $^{\#}$p<0.001 and $^{\#\#}$p<0.0001, error bars=SE. Two-factor repeated measures ANOVA. P values correspond to comparisons between SiNPs incubated either at high or low dosage vs. control ACh responses of MAs.

4.2.2.2 Endothelial-independent (SNP) Responses

The endothelial-independent dilator responses to the NO donor, SNP were unaffected by incubation in SiNPs (at 5.32 x 10^{11} NP/mL) at SNP concentrations of 10^{-8} to 10^{-4} M, despite a slight trend of decrease (At 1 µM ACh, the mean percentage dilation was 106.17 ± 4.36% vs. 67.95 ± 16.48% after incubation in PSS and SiNPs respectively, n=4 and 6 respectively, unpaired *t* test, NS; Figure 61).

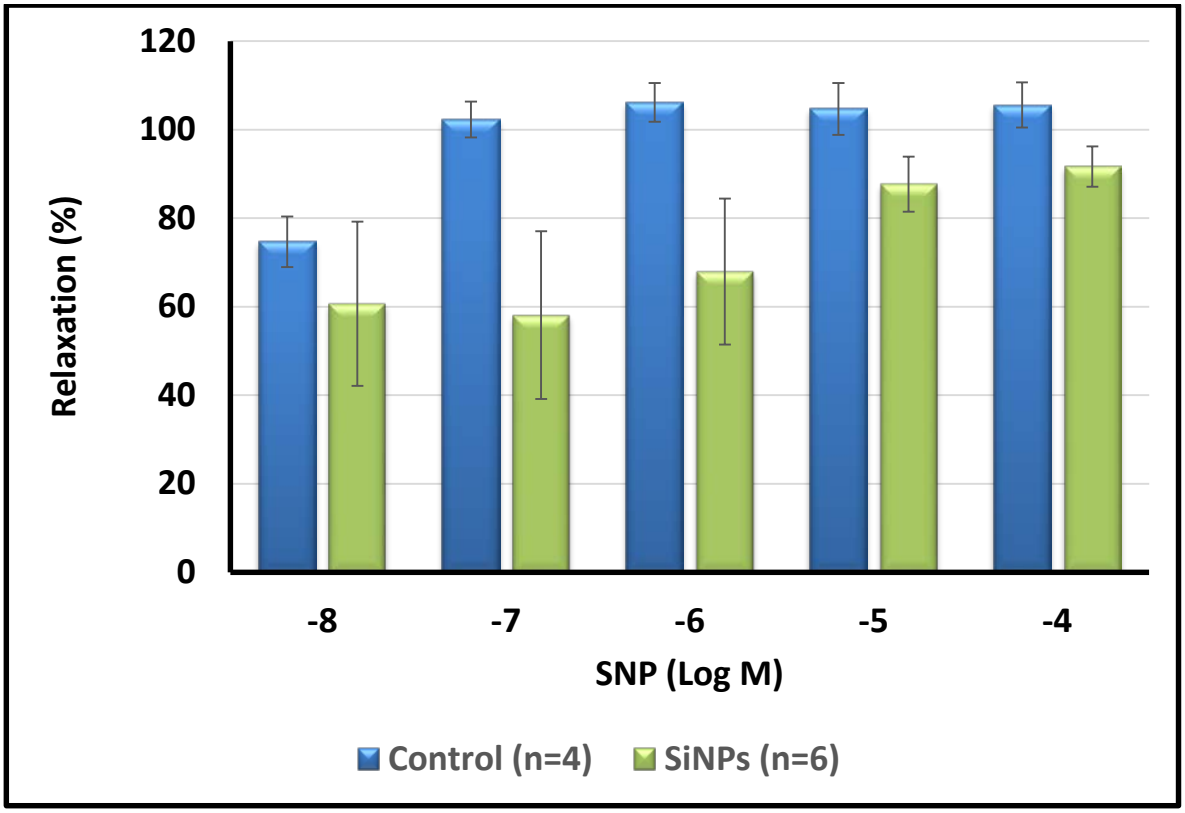

Figure 61. The influence of SiNPs infused *ex vivo* on the SNP-induced relaxation in Phe pre-constricted vessels. 'n' is number of vessels, error bars=SE. One-factor repeated measures ANOVA. P values correspond to comparisons between SiNPs incubated either *ex vivo* or *in vivo* vs. control SNP responses of MAs.

4.2.2.3 Responses to PAPA

The dilator responses to PAPA were unaffected by the infusion of SiNPs at 5.32 x 10^{11} NP/mL *ex vivo* but showed a slight increase compared to control (At 10 µM concentration of PAPA, the mean percentage dilation was 89.04 ± 12.53% vs. 105.07 ± 2.79% after incubation in control and SiNPs respectively, n=3, unpaired *t* test, NS; Figure 62).

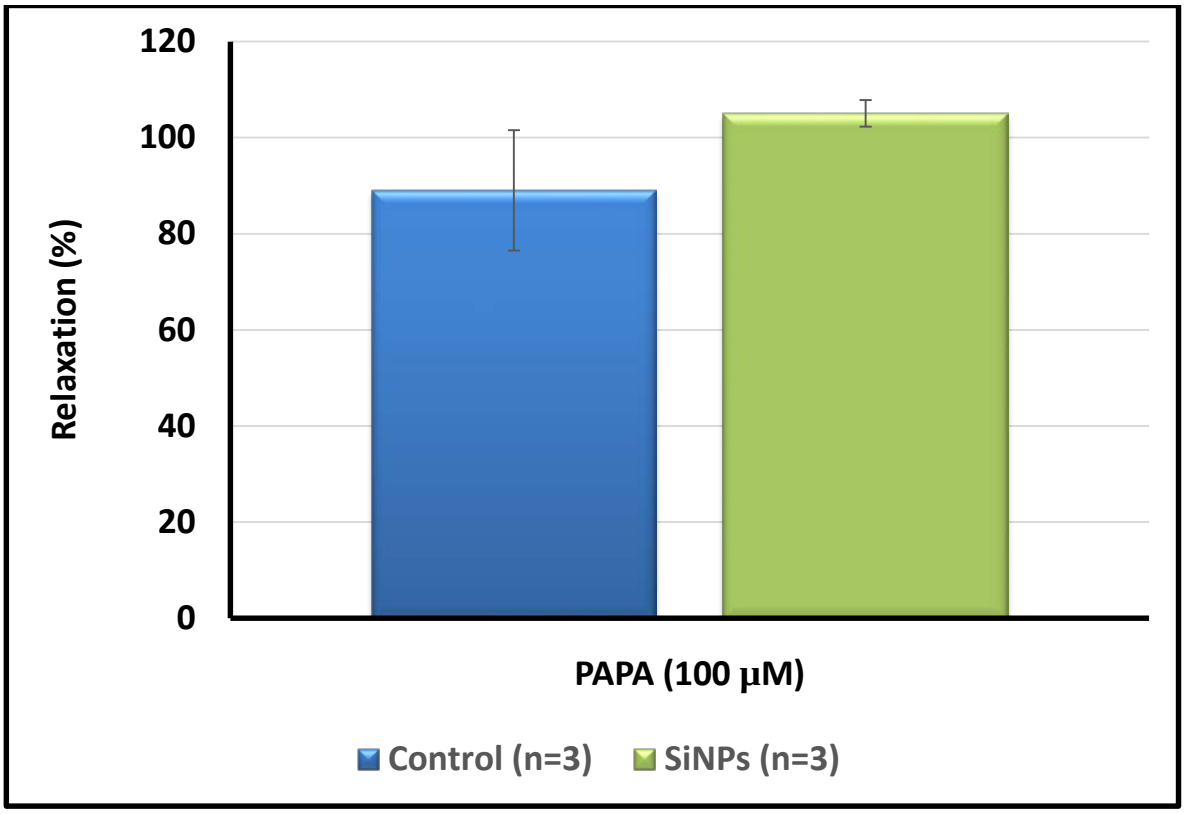

Figure 62. The influence of SiNPs infused *ex vivo* on the PAPA-induced relaxation in Phe pre-constricted vessels. 'n' is number of vessel, error bars=SE.

4.3 Cellular Uptake of SiNPs into the MAs

4.3.1 SiNPs Uptake at 4℃

Examination of the TEM sections demonstrate the presence of a large number of SiNPs of ~100 nm in size, outside ECs of the mesenteric vessels after 30 minute of incubation (at 5.32 x 10^{11} NP/mL), along the EC layer and inside the vessel lumen (Figure 63). There are also a number of SiNPs near EC membranes. Very few NPs were endocytosed inside ECs (Figure 63).

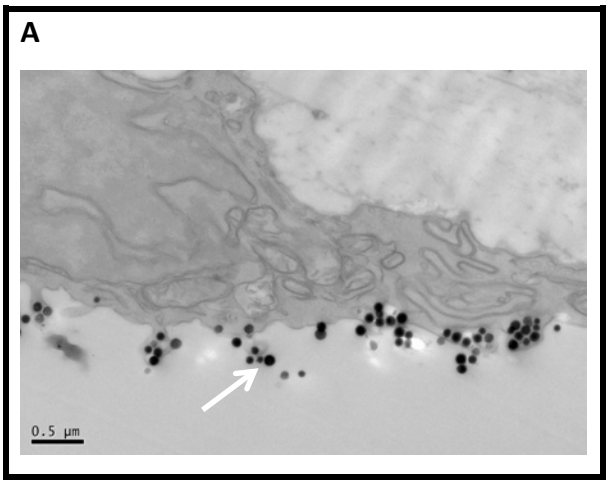

Figure 63. TEM image illustrating the predominant presence of SiNPs outside the vascular endothelium of the MAs after 30 minute of incubation. The SiNPs are represented by black spherical structures inside ECs (arrows).

4.3.2 SiNPs Uptake at 37℃

Examination of the TEM sections demonstrate the presence of SiNPs inside ECs of the mesenteric vessels after 30 minute of incubation (at 5.32 x 10^{11} NP/mL) (Figure 64). They were unevenly distributed and dispersed throughout the cytoplasm of ECs, but none were apparent in the nucleus. SiNPs were located either singly or in small clusters and were predominantly membrane-bound within vesicle structures, that may be of endosomal or lysosomal origin (Figure 64F), suggesting that an endocytotic pathway of uptake may be involved (Figure 64). SiNP may have also caused EC damage and full cell detachment (Figure 65A) forming cellular debris in the regions lining the vascular lumen. SiNPs adhered to the basal lamina of the vascular wall (Figure 65B) and were found in regions near the VSMC layer and/or areas of VSMC damage (Figure 65C). In addition; in one section a total of 9 SiNPs were able to penetrate the basal lamina and were found inside VSMCs (Figure 65C and -D), perhaps due to the disruption of the EC layer. The translocation of SiNPs into the latter regions coincided with areas of cellular damage in some instances. The 6 SiNP sizes found within the MA in the TEM images shown in Figure 64B measured 120, 120, 110, 110, 110 and 130 nm respectively.

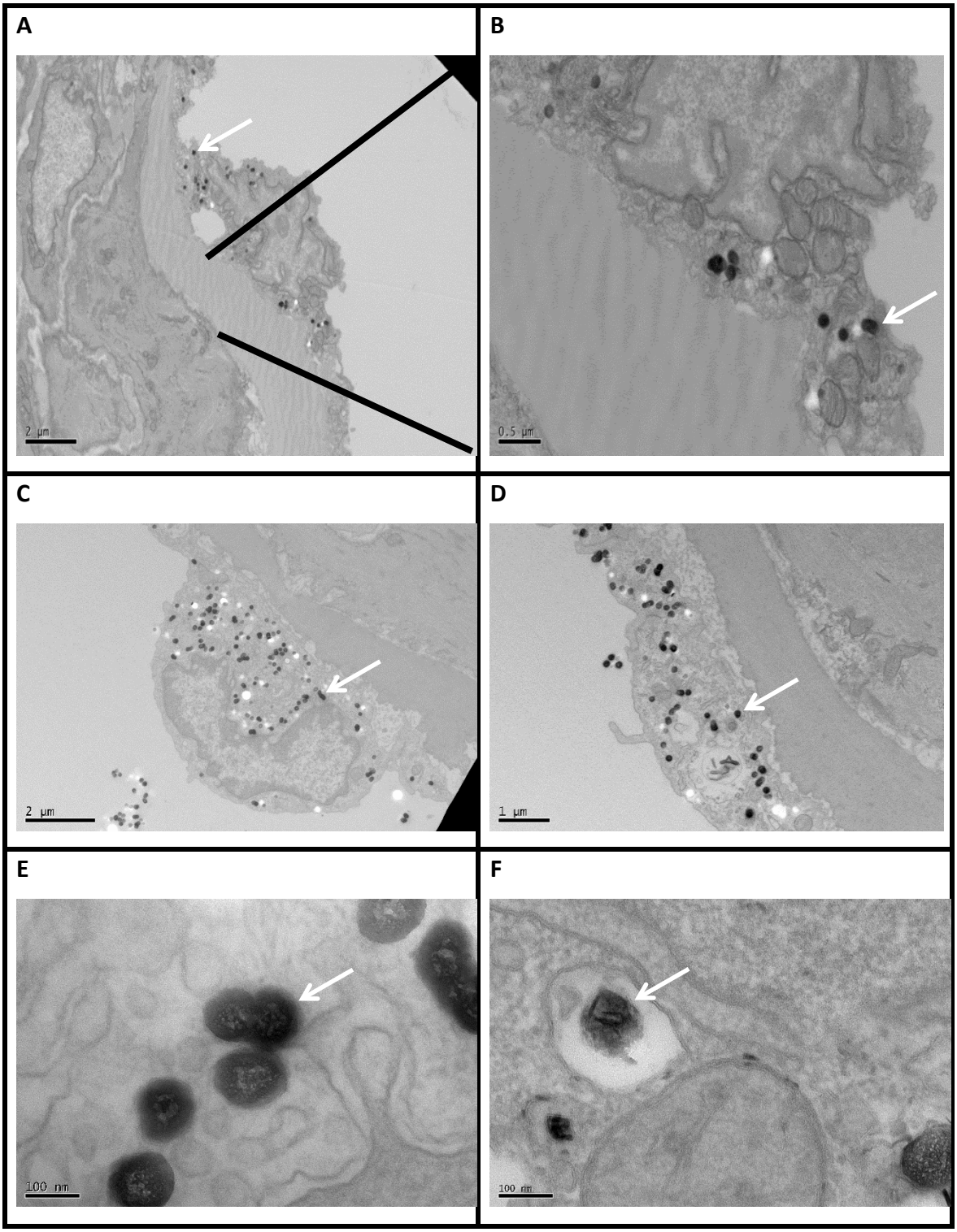

Figure 64. TEM images (A-F) illustrating the internalisation of SiNPs into the vascular endothelium of the MAs after 30 minute of incubation. The SiNPs are represented by black spherical structures inside ECs (arrows).

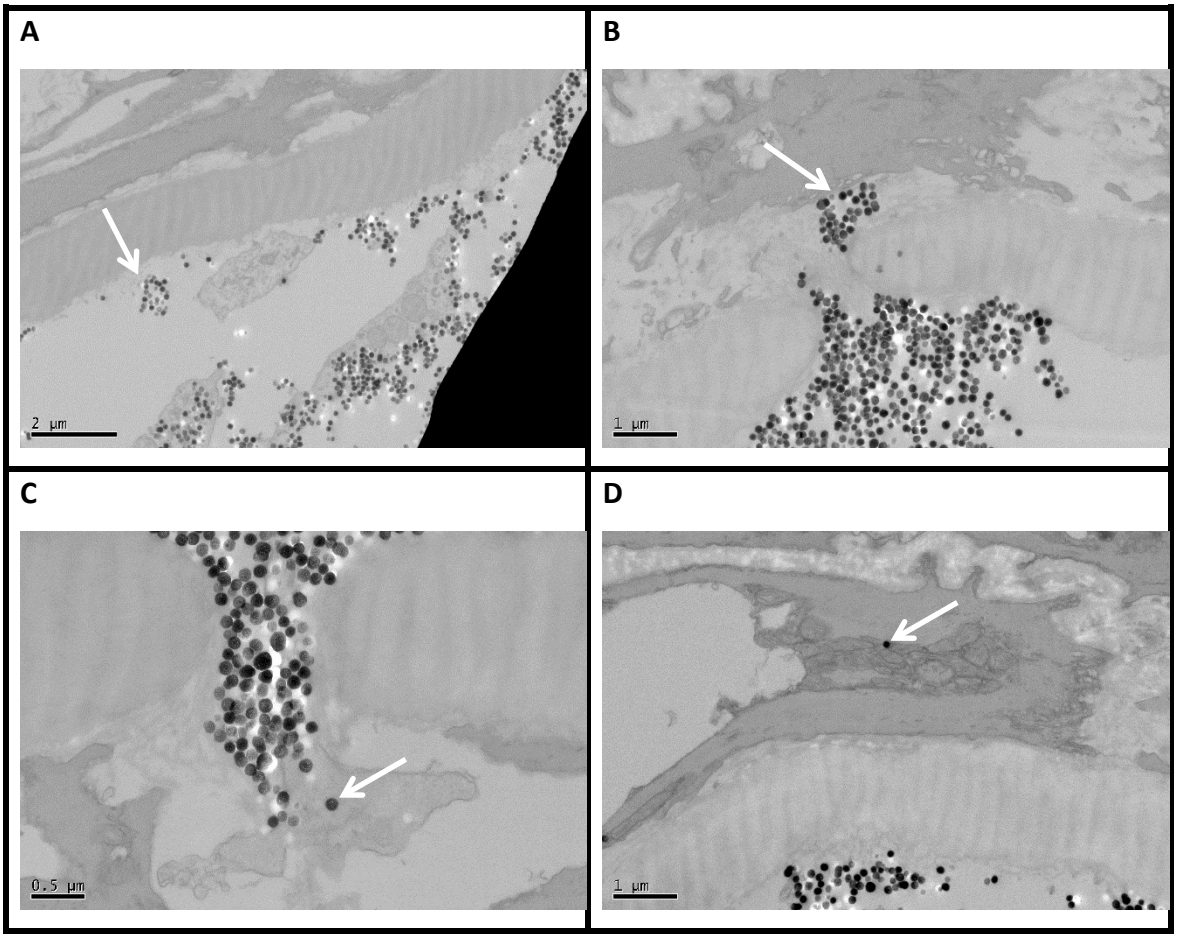

Figure 65. TEM images (A-D) illustrating the internalisation of SiNPs into the basal lamina and vascular smooth muscle cell layer of the MAs after 30 minute of incubation. The SiNPs are represented by black spherical structures inside ECs (arrows).

At elevated pressure (100 mmHg), there was no evidence of SiNPs uptake in the VSMC layer, but the occasional SiNPs (2 NPs) were found near areas of VSMC damage (Figure 66). The uptake of SiNPs was accompanied by functional effects on the MA, although this was examined only in one vessel.

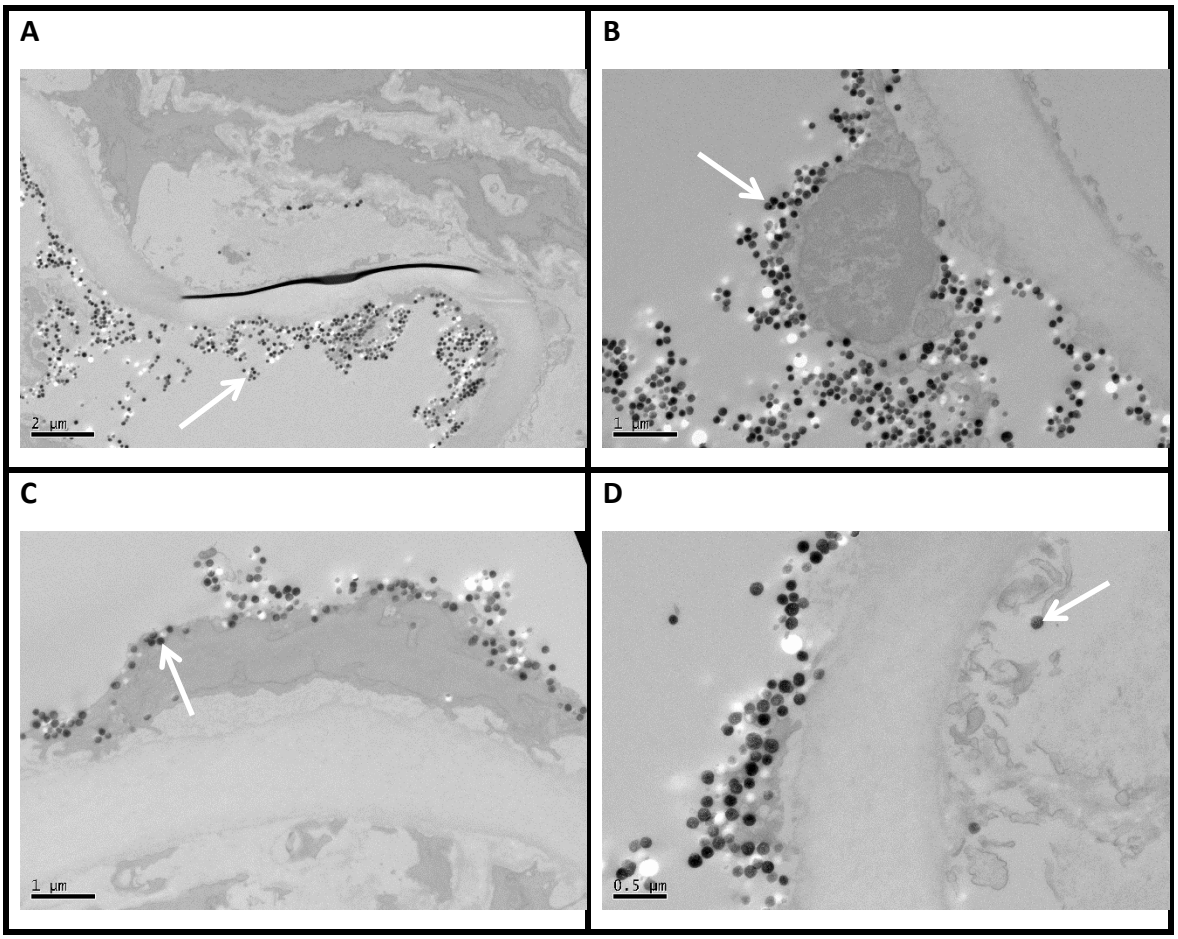

Figure 66. TEM images (A-D) illustrating the internalisation of SiNPs into the basal lamina and vascular smooth muscle cell layer of the MAs after 30 minute of incubation at elevated pressure of 100 mmHg. The SiNPs are represented by black spherical structures inside ECs (arrows).

4.4 Discussion

4.4.1 Control Experiments

KPSS acts by causing VSMC membrane depolarisation, bypassing the signal transduction pathways, due to the presence of extracellular potassium ions. The change in the PM potential activates Ca^{2+} channels in the membrane leading to an influx of extracellular Ca^{2+} and hence an increase in intracellular concentration of Ca^{2+}. The fact that Phe induces higher vascular contractile response as compared to KPSS is because the former also mobilises intracellular Ca^{2+} from intracellular stores, leading to calcium influx and VSMC contraction in control and PSS-incubated vessels. While the role of Phe is mediated via its stimulation of the α1 adrenergic receptor, it is also suggested to suppress K^{+}-induced hyperpolarisation in the rat MAs (Richards et al., 2001). KPSS was used to assess the viability of the vessels. All vessels constricted after incubation in KPSS. The non-viable or non-responsive vessels were excluded and these might have been damaged during or after dissection of the rats. Infusion in PSS and incubation for 30 minutes did not affect the contractile (KPSS and Phe) and dilator responses (ACh) of mesenteric vessels. Thus, the mechanical infusion, the pressure applied intravascularly while infusing with PSS as well as the incubation in PSS alone can be excluded as factors that may influence the vessel behaviour after the incubation in SiNPs. Hence, SiNPs are responsible in principle for the changes observed in the response of the vessels to the vasoconstrictors and vasodilators.

The variability of vascular responses to the vasoconstrictors and vasodilators may be due to the small variation in the ages of the rats (in days) from which vessels were derived, slight variation in the size of the arterial segments mounted on the pressure myograph and the differential responses of the specific chosen segment along the arterial vessel (Kitazawa and Kitazawa, 2012).

4.4.2 SiNPs Vascular-Uptake Studies

The 30-minute incubation period in SiNPs led to their cellular uptake as was evident by the TEM images obtained (Figures 64 and 65). The SiNPs were freely localised within ECs, inside the cytoplasm and in some cases inside vesicles without affecting cellular integrity in some of the electron micrographs obtained (Figure 64). However, in some cases, SiNPs were able to cause EC damage and detachment from the basal layer (Figure 65A and -B). This behaviour was accompanied by the translocation of SiNPs to the basal lamina of the vessel wall and a small number to the VSMC layer. This may be due to 1) Endothelial damage and/or detachment or 2) The capability of these NPs to cross different cellular barriers and tight junction proteins reaching to various vascular regions. To investigate proposal 2 in more detail, further experiments are required with increased incubation periods for SiNPs. Perhaps the SiNPs incubation period was insufficient to cause more nanoparticles to translocate from the endothelium to the smooth muscle layer.

The non-specific uptake of SiNPs may be related to an engulfment through pinocytosis, endocytosis and/or phagocytosis by the extracellular matrix constituents. It will be interesting to examine the uptake of SiNPs at low concentration to determine whether the uptake of these NPs is related to the observed physiological effects and/or the dependence of SiNPs uptake concentration of the NPs. Previous studies have emphasised the importance of NP size in determining the pathway of cellular entry (Vivero-Escoto et al., 2010). Barbé et al. reported the internalisation and passage of SiNPs smaller than 50 nm but not above 300 nm through small intercellular openings in normal blood vessel walls *in vivo* (Barbé et al., 2004). A study by Shapero et al. detected the accumulation of amorphous SiNPs of 50 and 100 nm in size in lysosomes of lung epithelial cells after 24 hours of incubation (Shapero et al., 2011). It was also found that amorphous SiNPs at 2 x 10^{11} NP/mL with different sizes (30, 70 and 300 nm) were localised within human microvascular ECs and human lung adenocarcinoma cells, inside specialised flotillin-1- and flotillin-2-bearing endocytic vesicles (Kasper et al., 2013). The latter vesicles contain flotillin-1 and flotillin-2 lipid raft proteins and thought to display a marker for late endosomal or lysosomal structures (Dermine et al., 2001; Glebov et al., 2006) and appear to exhibit a clathrin- or

caveolae-independent mode of endocytosis (Kasper et al., 2013; Langhorst et al., 2008; Ait-Slimane et al., 2009).

At physiological *pH*, the surface charge on SiNPs is predominantly negative (due to the presence of the carbonyl groups (COO^-)). Some SiNPs seemed to form aggregates near the surface of ECs and were seen inside vesicle structures near the edges of the vesicles. It is assumed that due to the predominant negative charge on the SiNPs (not neutralised by ECs), this may have caused their repulsion from EC surfaces, perhaps via their negative membrane phospholipidic groups (Gamucci et al., 2014). The overall negative charge on the ECs layer may correspond to the ECM proteins, integrins and TJ proteins. The dependence of the nanomaterial surface polarity or charge on the non-targeted uptake was previously studied but yielded conflicting results; reviewed in Fröhlich (Frohlich, 2012). The other possibility for accumulation of SiNPs outside ECs is that they may have stimulated some form of an immune response (Fruijtier-Pölloth, 2012) from the ECs leading to the secretion of specialised vesicles to engulf the NPs, although these vesicles do not seem to be internalised or processed further inside the ECs. We assume that SiNPs have either become neutralised or gained positive charge or both by ECs secretions, ECM proteins, forming protein corona (Gamucci et al., 2014) and/or the ionic species found in PSS. The latter may have increased the overall size to charge ratio of SiNPs, altered their overall charge of and/or induced structural changes within their lattice structures in a fashion that facilitated their uptake into ECs.

The mechanism whereby the nanoparticles enter and penetrate the PM is not fully understood, but alternative pathways may also be involved. However, in our study no uptake of SiNPs was evident at 4°C, suggesting that the uptake was an active process. Various studies have demonstrated the ability of SiNPs to penetrate tissues and cells in a manner that is dependent upon their material composition, surface charge and shape (Nabeshi et al., 2011). The internalisation of SiNPs by the ECs may be mediated through receptors that are specific or preferential to anionic ligands or through those favouring cationic ligands such as cell surface proteoglycans (Payne et al., 2007). The fact that the hydrodynamic size (size to charge ratio) of the SiNPs utilised for this study 98 nm, make

them prone to cholesterol-laden low-density lipoprotein (LDL) receptor or scavenger receptor-mediated internalisation (Zhang and Monteiro-Riviere, 2009) as these were previously suggested to possess similar size to charge ratio to LDL or acetylated LDL, normally recognised by these receptors. The suppression of the mechanisms for cellular uptake (Bakalova et al., 2008) (through inhibitors) may provide a new model for SiNPs-cellular delivery mechanism. Inhibition *in vitro* and *in vivo* studies suggest four main pathways for the delivery of NPs into viable mammalian cells in particular; non-specific endocytosis and pinocytosis, microinjection, electroporation and peptide-induced transport (Dubertret et al., 2002; Mattheakis et al., 2004; Jaiswal et al., 2003; Chen and Gerion, 2004; Derfus et al., 2004). The localisation of our SiNPs within endocytic compartments may cause SiNP instability inside these targeted vesicles due to the presence of variable *pH* gradient across different intracellular compartments. The *pH* value in early endosomes is between 5.9 to 6.0 (Mukherjee et al., 1997), hence the stable *pH* may cause the SiNPs with their polar groups to expel each other and stay dispersed. The drop in *pH* to 5.0-5.5 (Ryman-Rasmussen et al., 2007) and in some cases 4 (Mukherjee et al., 1997; Asokan and Cho, 2002) in lysosomes, may allow the carbonyl groups on the SiNP surface to become protonated. The protonation of SiNPs surfaces may result in an increase of intra-endosomal *pH* and a charge gradient provoking a water influx and endosomal swelling and disintegration, resulting in the escape of SiNPs from the endo-lysosomal compartment (Nabiev et al., 2007). This may revert the SiNPs to neutral species resulting in SiNPs aggregation inside or outside of these vesicles and cause their subsequent damage. The damage to these SiNP-bearing vesicles may block their access to other proteins inside the EC cytoplasm leading to disrupted protein trafficking inside ECs. Together with the possible SiNPs aggregation inside ECs cytoplasm, the former may explain the impairment in endothelial-dependent dilation following SiNPs uptake and ultimately cause EC dysfunction and/or promote mechanism for cellular apoptosis. However, these speculations need to be further investigated and analysed on microvascular EC cultures *in vitro*.

NP uptake was rapid and evident within 10 minutes of incubation. Decreasing or increasing the incubation period may result in different cellular uptake scenarios. Some of these may involve the uptake of SiNPs via more specialised mechanisms for cellular delivery following

extended incubation periods, the localisation and/or targeted delivery of nanomaterials to the VSMC layer or a reverse transport mechanism of internalised NPs out of cells into the vascular lumen. The uptake of SiNPs may involve special cellular adaptation strategy that may in part involve the gene expression of specialised vesicle structures for targeted internalisation, though there is no evidence to support such theory. Hence more detailed analysis would be necessary to account for all possibilities specifically nanomaterial trafficking, uptake, processing (localisation, targeting and/or metabolism) and nanomaterial-dependent roles (e.g. that of nanomaterial-induced entry, protein modification, transcription factor regulation and/or cellular gene expression). It is also essential to measure whether there is a time-dependent uptake i.e. a build-up of nanomaterial gradient as a function of time. This could also be useful in assessing the efficiency of the cellular uptake machinery and the factors that may account for their involvement in the nanomaterial-internalisation process. Such factors may be related to time-dependent or -independent vesicle formation, signalling pathways and/or downstream cellular effectors in addition to the type, size and concentration of the nanomaterial involved. One critical issue to consider is whether the internalised nanomaterials are dependent upon intracellular hydrodynamics and hence move down a concentration gradient in a disordered manner or whether they exhibit a more defined and uniform ordered pathway(s) that may or may not involve intracellular interactions and movement to other cellular layers. Hence, it will be worthwhile measuring the entropy change (Atkins, 2005) that couples such nanomaterial behaviour and assess the direction of nanomaterial route of adherence inside and outside cells whether in extracellular spaces, cellular paracellular spaces, tight-junctions and/or other cell types accounting for morphological and physiological changes accompanying such route.

It is also not clear whether the prolonged incubation in NPs may enable their uptake into the nucleus of cells and/or in other organelles. Previous studies using QDs, suggest that a period of 4 hours was insufficient for the NPs to enter the nuclei of cells (Bakalova et al., 2008). Hence, the absence of SiNPs from the nucleus may be due to insufficient time of exposure to the latter NPs, lack of an independent nuclear-related pathway of entry and/or a possible repulsion from the negatively charged DNA histones within the nucleus. Further

evidence and experimental approaches are needed to investigate this phenomenon. Thus the uptake-associated damage and/or toxicity to vascular function and integrity is possible and needs to be further tested *in vivo* as well as *in vitro* on endothelial microvascular cell cultures.

4.4.3 The Influence of SiNPs on Vascular Function

4.4.3.1 Effects of SiNPs on Vasoconstriction

This is the first study to examine the effect of NPs on constrictor function of MAs. Phe acts via α1-adrenoceptors located on the membrane surface of the VSMCs to activate a Ca^{2+}-dependent sensitising pathway during the sustained late-phase contraction (Kitazawa and Kitazawa, 2012). The action of Phe is thought to be mediated via PKC leading to the phosphorylation and inhibition of myosin light chain phosphatase and subsequent sacroplasmic Ca^{2+} release and voltage-dependent Ca^{2+} influx (Kitazawa and Kitazawa, 2012). Hence, the compromise of the Phe-induced constriction and the unsustained constriction of the vessels at maximal Phe doses by SiNPs may be due to the random or the specific targeting and blockage of Phe receptor (thus acting as antagonist) and/or the enzymes, mediators and adaptor proteins involved in mediating the action of Phe. SiNPs may specifically target pathways leading to stimulation of VSMCs via α1-adrenoceptors, since no effects of SiNPs were observed on AVP responses. AVP acts via V1a vasopressin receptors which function via a different mechanism of contraction to that of Phe (Trandafir and Kaufman, 2007).

4.4.3.2 Effects of SiNPs on Vasodilation

4.4.3.2.1 Effects of SiNPs on ACh responses

SiNPs significantly reduced ACh-related dilation of mesenteric vessels at specific doses. Previous studies have suggested that the vasodilation component in rat MAs may be elicited largely by EDHF (Crane et al., 2003). Consequently, the attenuation in dilation may be due to 1) the indirect or the direct role of SiNPs in targeting specific extracellular, intracellular and downstream factors involved in the EDHF-dependent pathway in ECs and 2) the inability of NO to compensate for the loss in EDHF action due to the delayed NO production and/or the influence of SiNPs on eNOS or other factors involved in NO synthesis

and action. Additionally, the effect of SiNPs on EC function may be related to the interaction, disruption and/or blockage of the rat-specific muscarinic (M)-3 ACh receptors on ECs surface (Phillips et al., 1996), voltage-gated channels, gene expression as well as protein synthesis, trafficking and transport of the vasodilator machinery. Although in the case of the present study, effect on gene expression is excluded due to the acute nature of the study involving 30 minutes of NP incubation. SiNP surface may also generate ROS and that could quench NO, hence affecting vasodilation (Farooq et al., 2013).

The inhalation studies of TiO_2 NPs by Nurkiewicz group, suggesting NP's detrimental effects on the microvascular function in the lungs with blunted arteriolar dilations and induced constrictions (Nurkiewicz et al., 2008) may be due to the disruption in NO signalling (Nurkiewicz et al., 2009) (support our findings). The TiO_2 NPs were also capable of translocating into coronary arteries causing the impairment of the endothelium-dependent vasodilation in subepicardial arterioles from the coronary microvascular bed in rats (LeBlanc et al., 2009). A recent study by Nemmar et al., suggested a significant reduction in the endothelium-dependent relaxation (at ACh concentration of 0.1 µM) of rat small MAs (third-branches) following exposure to amorphous SiNPs (of 50 and 500 nm size respectively, at 50 µg/mL) *in vitro* using the wire myography system (Nemmar et al., 2014). Previous findings from our group also showed similar effects of SiNPs on the dilation of large rat aortic vessels. However, the study by Akbar et al. demonstrated that an acute exposure of rat aortic vessels to SiNPs of 100 and 200 nm nonmodified and positively charged NPs (at 1.1×10^{11} NP/mL) resulted in their uptake by the lining ECs with no detrimental effect on conduit arterial function (Akbar et al., 2011). Although the 100 nm and positively charged SiNPs had a greater degree of attenuation on the dilator responses of the aortic vessels in contrast to the unmodified 200 nm particles, these changes were not significant (Akbar et al., 2011). We suggest that our NPs have larger surface area to size ratio and can be surrounded by positive ions from PSS due to their negative surfaces (as determined by Zeta potential measurements) and hence interact more efficiently with the vascular ECs. Another study by Farooq et al. demonstrated the attenuation of endothelial-dependent vasodilator responses by 30 and 70 nm SiNPs and dye-encapsulated SiNPs (1.96

× 10^{12} NP/mL) in aortic vessels whereby the degree of attenuation was related to NP surface area rather than size (Farooq et al., 2013).

A previous study using a wide range of negatively surface-charged SiNPs (of a Zeta potential more than -30 mV) sizes (10, 50, 150 and 500 nm) resulted in SiNPs penetration of PMs and stimulated generation of NO by HUVECs and correlated with endothelial inflammation and necrosis (Corbalan et al., 2011). The generation of NO was followed by the production of oxidant and cytotoxic $ONOO^-$, which is regarded as a major component of oxidative stress (Corbalan et al., 2011). This action of SiNPs was directly related to NP dosage specifically for the smaller-sized NPs (10 and 50 nm); thus with increased SiNPs dose, there was a rapid exponential rate of $ONOO^-$ release from ECs, possibly due to the large surface area in smaller SiNPs as opposed to larger ones (Corbalan et al., 2011). Hence, the production of $ONOO^-$ following SiNPs exposure significantly reduced the ratio of [NO]/[$ONOO^-$] in a size-dependent manner shifting the balance of maximal [NO]/[$ONOO^-$] unfavourably with this being more effective at the smallest SiNP (10 nm) concentration of at 10 μg/mL (Corbalan et al., 2011). In contrast, our study used larger sized SiNPs of approximately 100 nm with an effect on vascular dilation in a wider context, where ECs were lining the vascular lumen as opposed to HUVECs *in vitro*, thus contributing to the different mechanism(s) of ECs damage. Therefore, the increased nitroxidative/oxidative stress may not directly relate to the impairment in ACh responses.

The toxicity effect of rhodamine B dye that encapsulate SiNPs was previously studied and found to decrease the number of vascular ECs from the bovine aorta and VSMCs from murine aorta after 72 hours of incubation *in vitro* and inhibit the proliferation of human lip fibroblasts (Kaji et al., 1991). Although the dye molecules did not influence cellular detachment in the latter study, we suggest that the dye molecules may have a role in mediating SiNP-induced damage to ECs of the vessel lining hence inhibiting cellular proliferation (Figure 65A). This was previously supported by Kaji et al. where human lip fibroblasts experienced a degenerative change of their nuclei and an irregular shape of the cells as well as a decrease in their cell number following the incubation in 50 μg/mL of the

rhodamine B dye (Kaji et al., 1991). The direction and extent of such interference needs to be further investigated via molecular studies on MAs and cellular cultures.

4.4.3.2.2 Effects of SiNPs on SNP responses

The results from the SNP experiments in the present study suggest that the NO-independent pathways for mesenteric vessels are unaffected by the action of SiNPs suggesting that smooth muscle sensitivity to NO was unaffected by SiNP exposure. This finding was supported by other studies from our group, in large vessels described earlier.

SiNPs uptake, delivery, localisation and distribution may have a biophysical as well as biochemical impact on cellular functions. These may include the disruption of the integrity of cellular paracellular pathways and/or TJ components, obstruction of cell trafficking (by e.g. blocking the accommodation of certain signalling molecules to their receptors) and the disturbance to cell membrane permeability to certain electrolytes. These changes may be due to the biophysical presence of the NP themselves inside the cells, their thermodynamic and hydrodynamic impact and the change in free energy (entropy change) (Atkins, 2005). All of these factors may influence the haemostasis of vascular tissue integrity and physiology. The state and fate of the NPs is also important such as the aggregation status of the NPs or their possible interactions, excretion and clearance.

Chapter 5.

The Influence of SiNPs on Arterial Function, *in Vivo* (Vascular Function and Biodistribution Study)

5.1 Effects of SiNPs on Vascular Responses *in vivo*

The intravenous injection of SiNPs (calculated at 5.32 x 10^{11} NP/mL) *in vivo* for a period of 2 hours produced similar results to the *ex vivo*, mimicking the control vascular responses to Phe and ACh (in Phe pre-constricted vessels). However, there was a high variability with a high standard error of mean across the *in vivo* experiments.

5.1.1 Vasoconstrictor Responses

There was no overall change in the constrictor responses in MAs from the *in vivo* injected rat when superfused in high potassium solution (KPSS) at 60 mM concentration as compared to control, similar to *ex vivo*; (The mean percentage constriction was 78.49 ± 7.13% vs. 71.29 ± 17.39% after incubation in control and SiNP injection respectively, n=7 and 4 respectively, unpaired *t* test, NS; Figure 67).

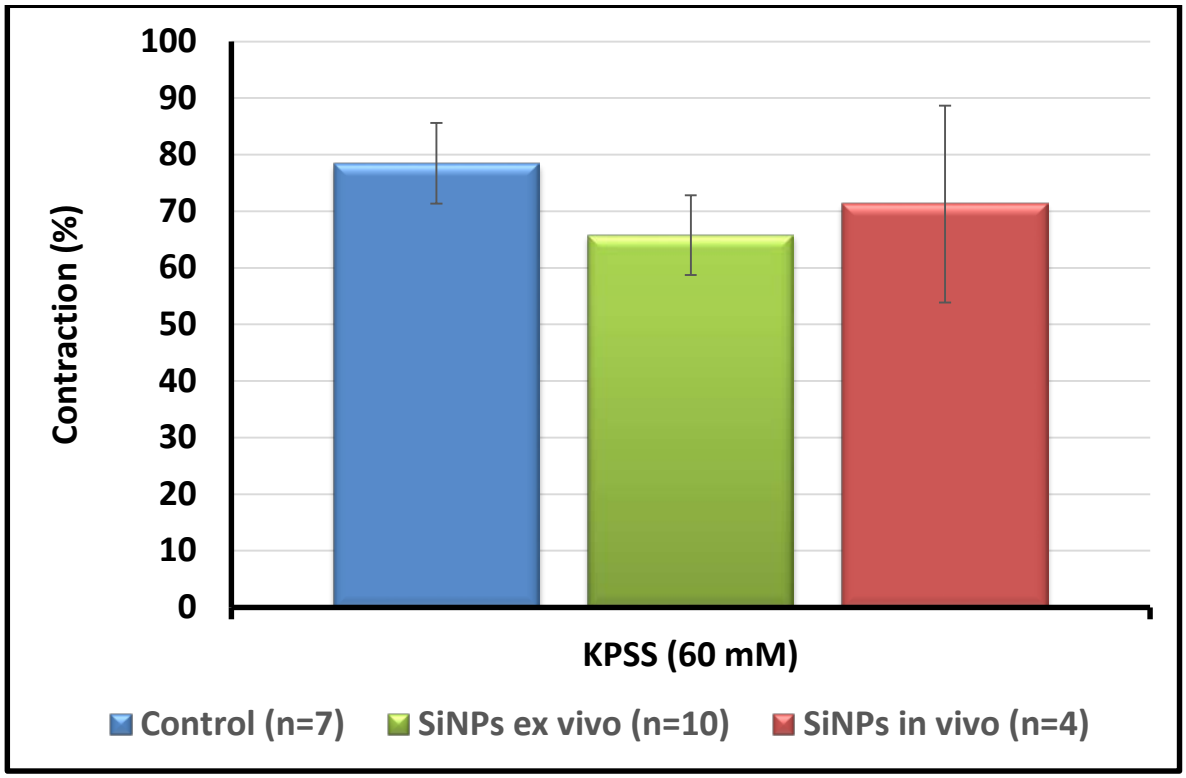

Figure 67. The influence SiNPs injected *in vivo*, on the KPSS-induced contraction. 'n' is number of vessels, error bars=SE.

There was no overall change in the Phe constrictor responses in MAs from the *in vivo* injected rat at lower concentrations of Phe (from 1 nM to 1 µM) as compared to control; (At 100 nM Phe, the mean percentage constriction was 15.85 ± 4.05% vs. 19.48 ± 13.57% after incubation in control and SiNPs respectively, n=4 and 3 respectively, unpaired *t* test, NS; Figure 68). However, intravenously-injected SiNPs caused an attenuation to Phe constrictor responses at higher concentrations (10 µM and 100 µM) compared to control, mimicking the *ex vivo* responses with the latter being more significant the 10 µM concentration of Phe; (At 10 µM Phe, the mean percentage constriction was 98.55 ± 1.45 % vs. 81.30 ± 5.90 % after incubation in control and SiNP injection respectively, n=4 and 3, unpaired *t* test, $p<0.05$; Figure 68).

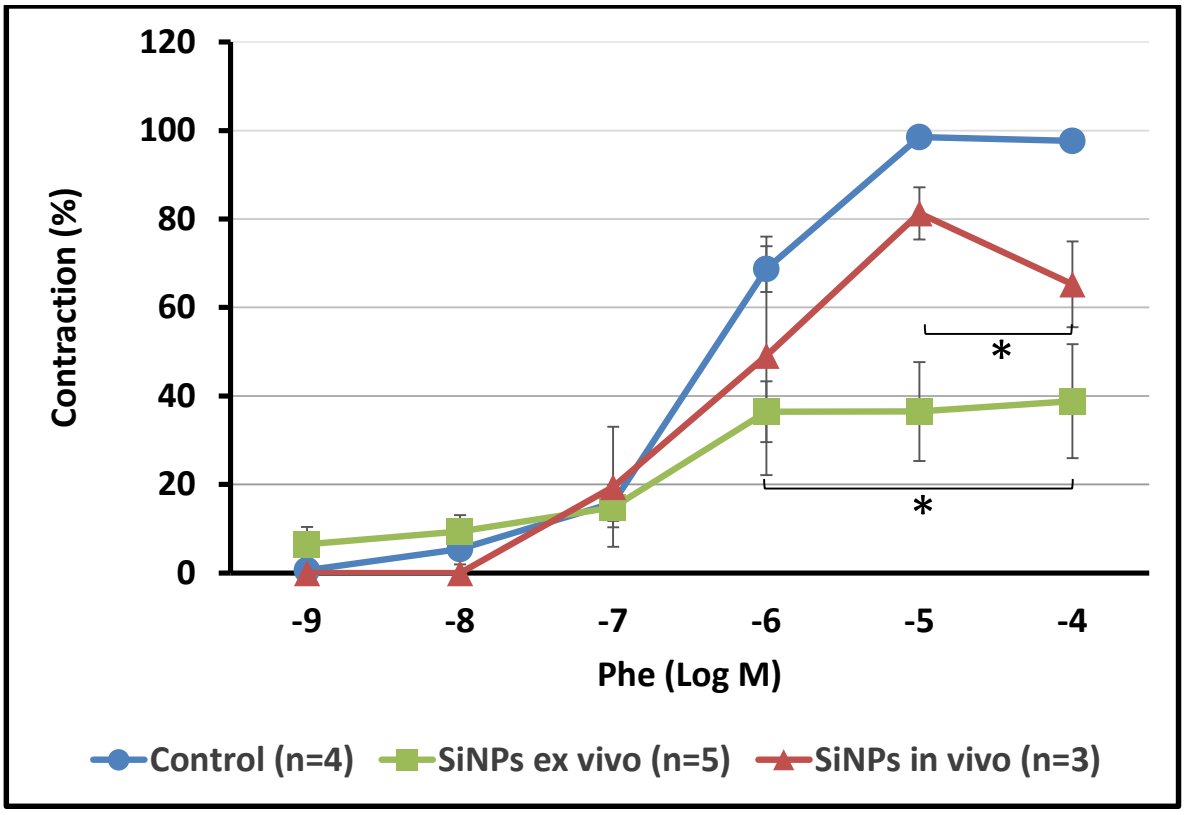

Figure 68. The influence of SiNPs injected *in vivo*, on the Phe-induced contraction. 'n' is number of vessels. *p<0.05, error bars=SE. Two-factor repeated measures ANOVA. P values correspond to comparisons between SiNPs incubated either *ex vivo* or *in vivo* vs. control Phe responses of MAs.

5.1.2 Vasodilator Responses

5.1.2.1 Endothelial-dependent (ACh) Responses

The injection of SiNPs *in vivo*, at a final dosage of 5.32 x 10^{11} NP/mL, led to an overall trend of reduction in the magnitude of dilator responses to ACh specially at lower concentrations of ACh (10^{-13} to 10^{-8} M; similar to *ex vivo* responses), including the maximal concentration of ACh (1 mM). *In vivo* injected NPs however, produced significant reduction in the magnitude of ACh-induced dilation only at specific concentrations (100 nM and 1 mM of ACh; similar to *ex vivo*) following Phe pre-constriction of MAs. For instance at 100 nM concentration of ACh, the mean percentage dilation was 78.77 ± 8.58% vs. 16.42 ± 7.96% after incubation in control and SiNP injection respectively (n=6 and 3 respectively, unpaired *t* test, $p<0.01$; Figure 69). The dilator responses were improved at high ACh concentrations (1 µM – 100 µM) *in vivo* compared to *ex vivo* following SiNP injection. For instance, at 1 µM concentration ACh, the mean percentage dilations were 91.52 ± 12.80% vs. 27.82 ± 5.13% for *in vivo* and *ex vivo* exposure respectively (n=11 and 3 respectively, unpaired *t* test, $p<0.0001$; Figure 69). Despite the recovery of the dilator responses *in vivo*, the incubation in SiNPs significantly reduced the dilation of the vessels at the highest concentration of ACh (1 mM); (At 1 mM concentration of ACh, the mean percentage dilation was 101.76 ± 0.69% vs. 93.81 ± 1.80% after incubation in control and SiNP injection respectively, n=6 and 3 respectively, unpaired *t* test, $p<0.01$; Figure 69). Hence, the injection of NPs *in vivo* displayed less detrimental effect compared to *ex vivo*.

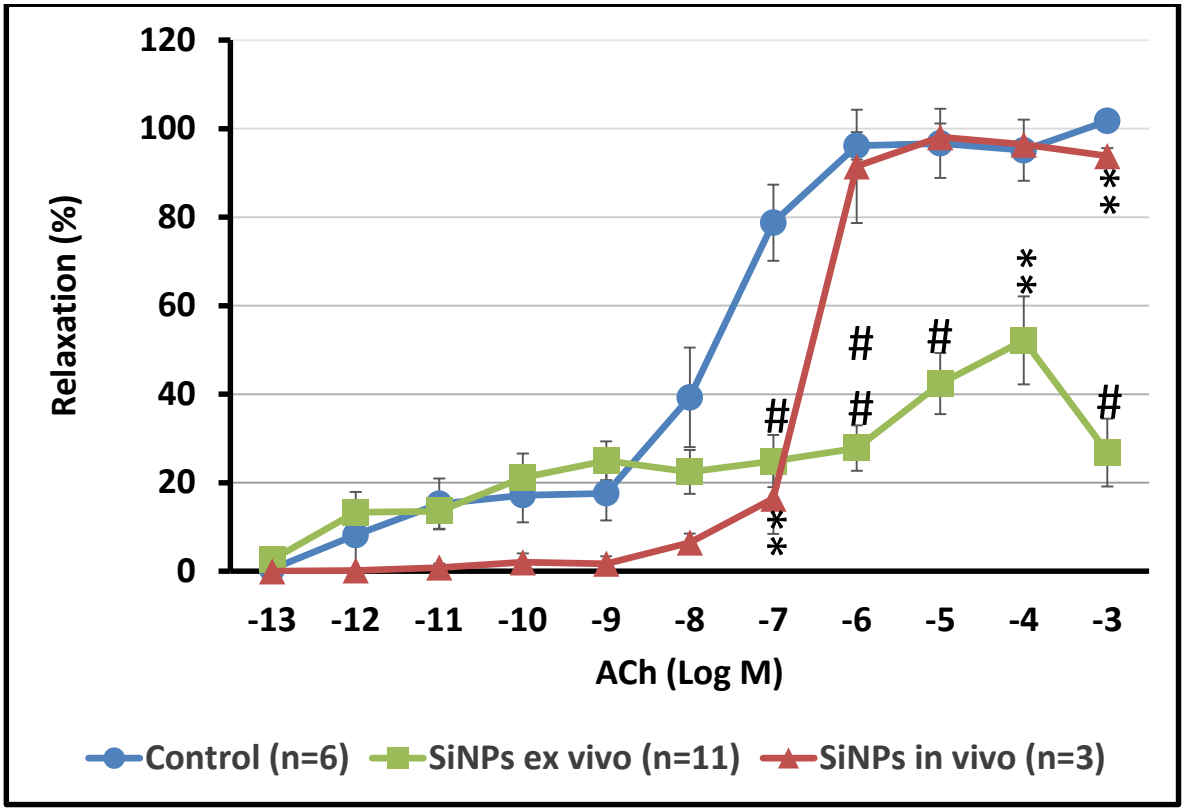

Figure 69. The influence of SiNPs injected *in vivo*, on the ACh-induced relaxation in Phe pre-constricted vessels. 'n' is number of vessels. **p<0.01, #p<0.001 and ##p<0.0001, error bars=SE. Two-factor repeated measures ANOVA. P values correspond to comparisons between SiNPs incubated either *ex vivo* or *in vivo* vs. control ACh responses of MAs.

5.2.2.2 Endothelial-independent (SNP) Responses

The endothelial-independent dilator responses to the NO donor, SNP were significantly affected by SiNPs that were injected *in vivo* at specific SNP concentrations (10 and 100 nM); (At 10 nM concentration of SNP, the mean percentage dilation was 74.67 ± 5.74% vs. 4.20 ± 2.80% after incubation in control and SiNP injection respectively, n=4 and 3 respectively, unpaired *t* test, p<0.001; Figure 70). The submaximal concentration of SNP also displayed a significant reduction in dilation in SiNPs-injected rat; (At 100 nM concentration of SNP, the mean percentage dilation was 102.20 ± 4.03% vs. 15.21 ± 13.40% after incubation in control and SiNP injection respectively, n=4 and 3 respectively, unpaired *t* test, p<0.01; Figure 70). Dilator responses were unaffected at higher SNP concentrations (1 µM, 10 µM and 100 µM) following SiNPs injection *in vivo* (n=3, NS; Figure 70).

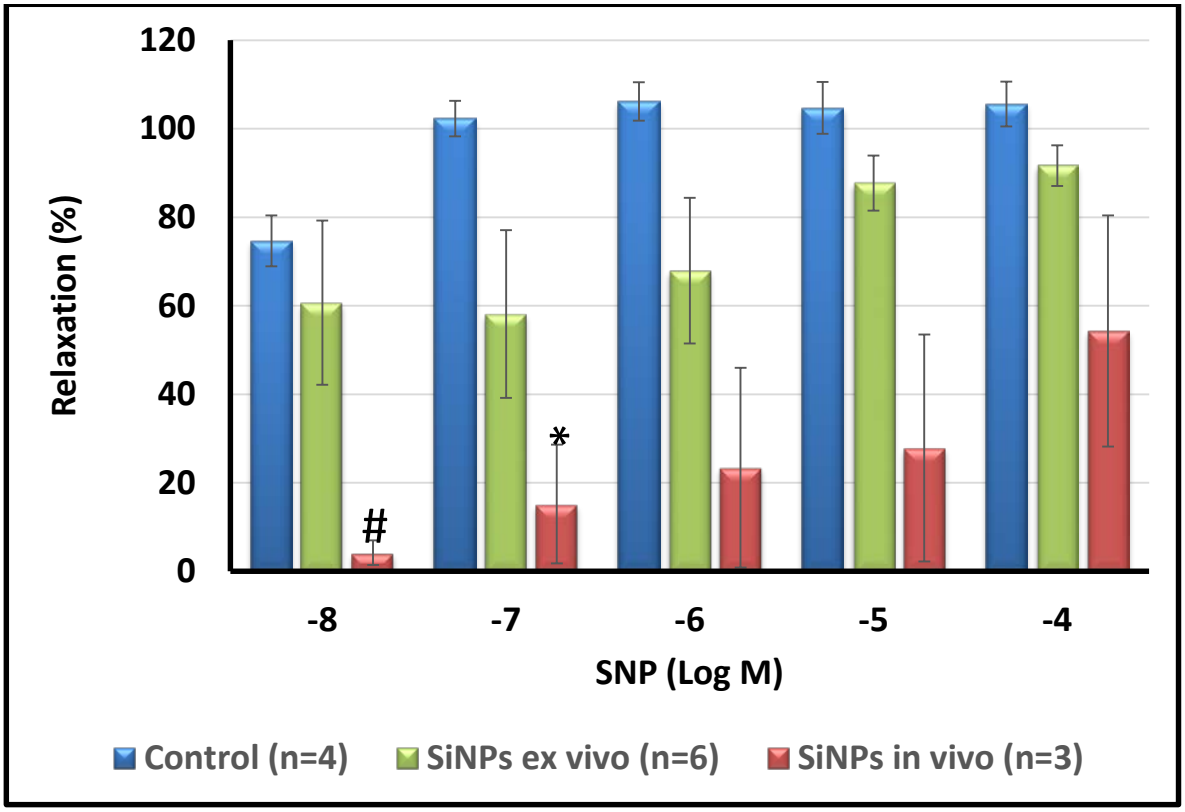

Figure 70. The influence of SiNPs injected *in vivo*, on the SNP-induced relaxation in Phe pre-constricted vessels. 'n' is number of vessels. *p<0.05, and #p<0.001, error bars=SE. Two-factor repeated measures ANOVA. P values correspond to comparisons between SiNPs incubated either *ex vivo* or *in vivo* vs. control SNP responses of MAs.

5.2.2.3 Responses to PAPA

The vasodilator responses to the smooth muscle cell relaxant, papaverine were not affected by SiNPs injection *in vivo*; (At 100 µM concentration of SNP, the mean percentage dilation was 89.04 ± 12.53% vs. 104.53 ± 4.32% after incubation in control and SiNP injection respectively, n=3, paired *t* test, NS; Figure 71).

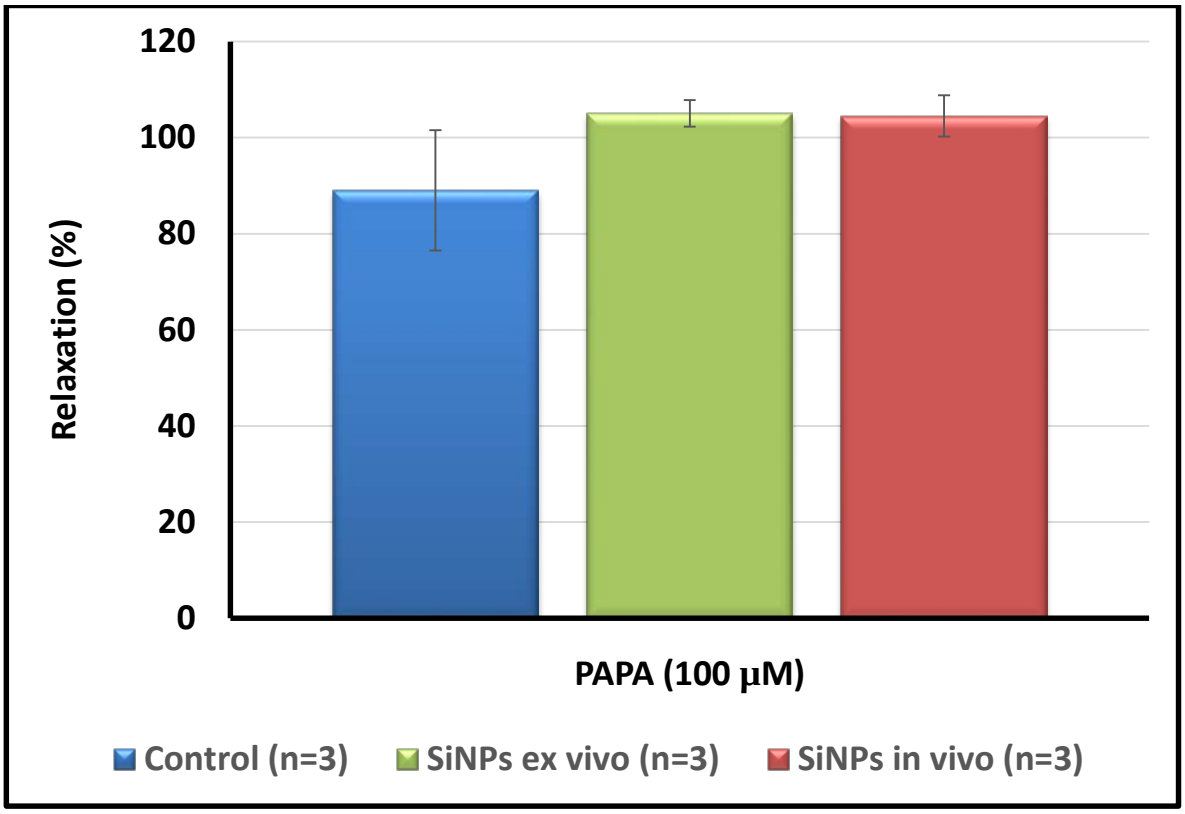

Figure 71. The influence of SiNPs injected *in vivo*, on the PAPA-induced relaxation in Phe pre-constricted vessels. 'n' is number of vessel, error bars=SE.

5.2 Determination of SiNPs Uptake, Concentration and Biodistribution

TEM and ICP analysis was used to verify and quantify SiNP uptake by the rat mesenteric arteries as well as their biodistribution within major organs (such as the lung, heart, aorta, mesenteric artery, liver, spleen and kidneys). The concentration of SiNPs was determined in NP samples, biological media (PSS) and samples (tissues and organs from *in vivo* tissues) using ICP. The measurements were mean values from three readings per sample per experiment. The ICP determined the relative amount of SiNPs when injected at 0.217 g for the A3 SiNPs and 0.103 g for the DA3 SiNPs samples respectively to obtain a final concentration of 5.32×10^{11} NP/mL of blood of the rat. These results were used to quantify the actual concentration SiNPs within solutions in ppm/mL by considering the estimated dilution factor. The uptake concentrations were expressed as percentage.

5.2.1 Cellular Uptake of SiNPs

Examination of the TEM sections demonstrated the presence of SiNPs inside various tissues (Figure 72). TEM sections were taken from a random tissue section related to one tissue type. Within the spleen, two SiNPs were identified of 106 and 94 nm in size respectively. In the kidney, NPs were located in connective tissues. In one section, examined at random, one SiNP (240 nm diameter) was identified inside a fibroblast cell within the kidney tubules.

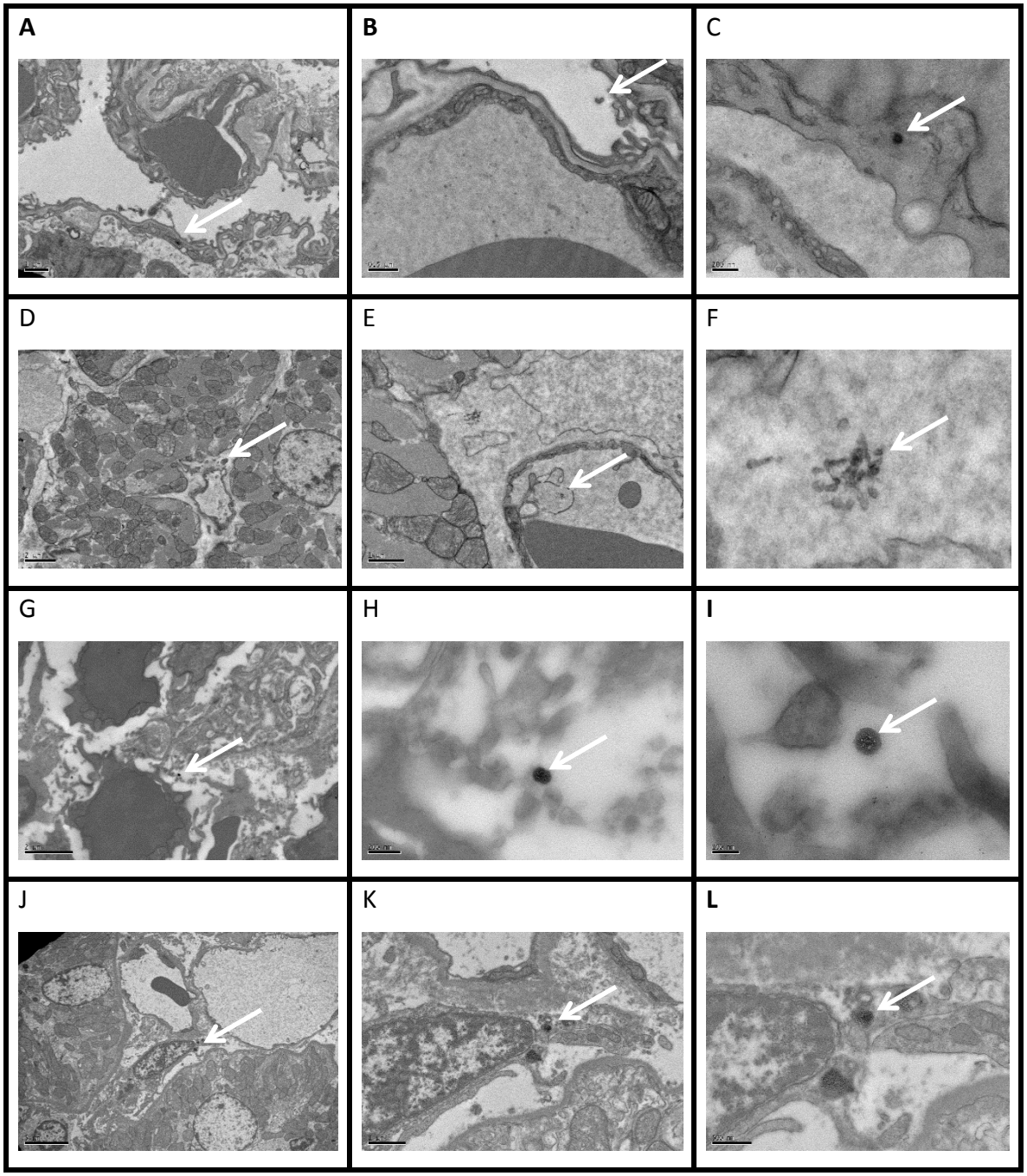

Figure 72. TEM images of SiNP uptake by the lungs (A-C), heart (D-F), spleen (G-I) and kidney (J-L) from the *in vivo* injected rat. The SiNPs are represented by black spherical structures inside various tissues (arrows).

Within the aorta, SiNPs were identified within ECs. In one TEM section, examined at random, 8 SiNPs were present within the cytosol of ECs (Figure 73).

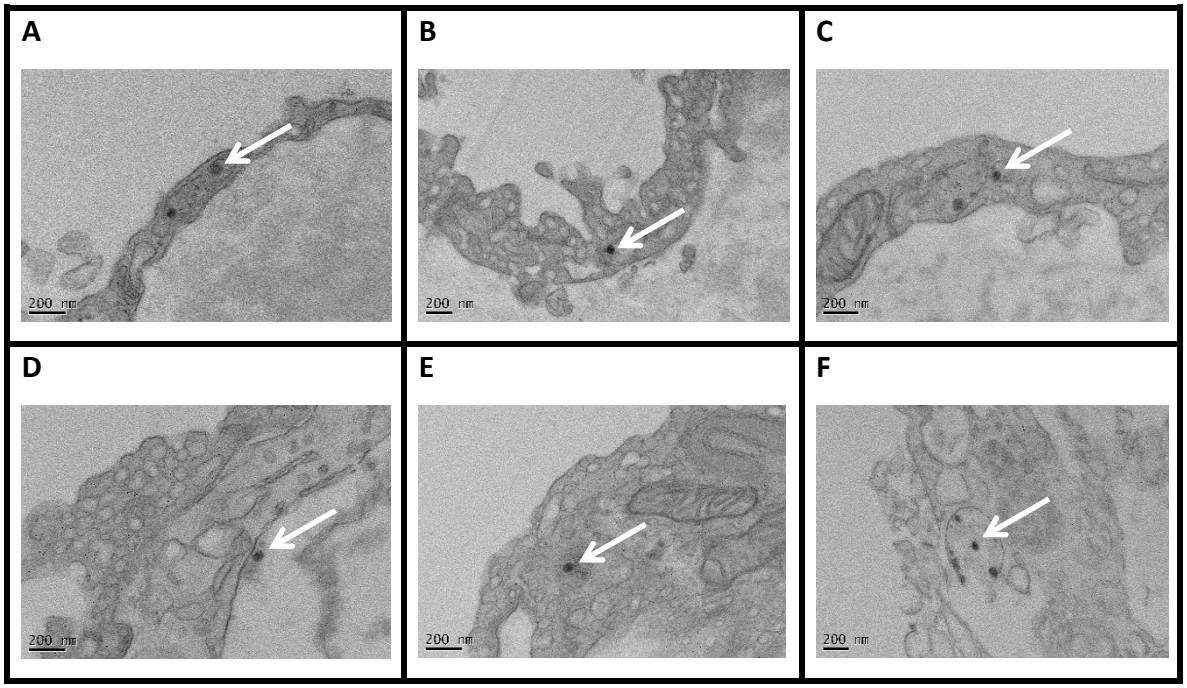

Figure 73. TEM images of SiNP uptake by the aorta from the *in vivo* injected rat (A-F). The SiNPs are represented by black spherical structures inside ECs (arrows).

Within the MAs, A few SiNPs (two of 80 nm in size and one at a 100 nm) were identified within the cytoplasm of ECs with none being identified in the nucleus, VSMC layer or the adventitia in a random TEM section (Figure 74).

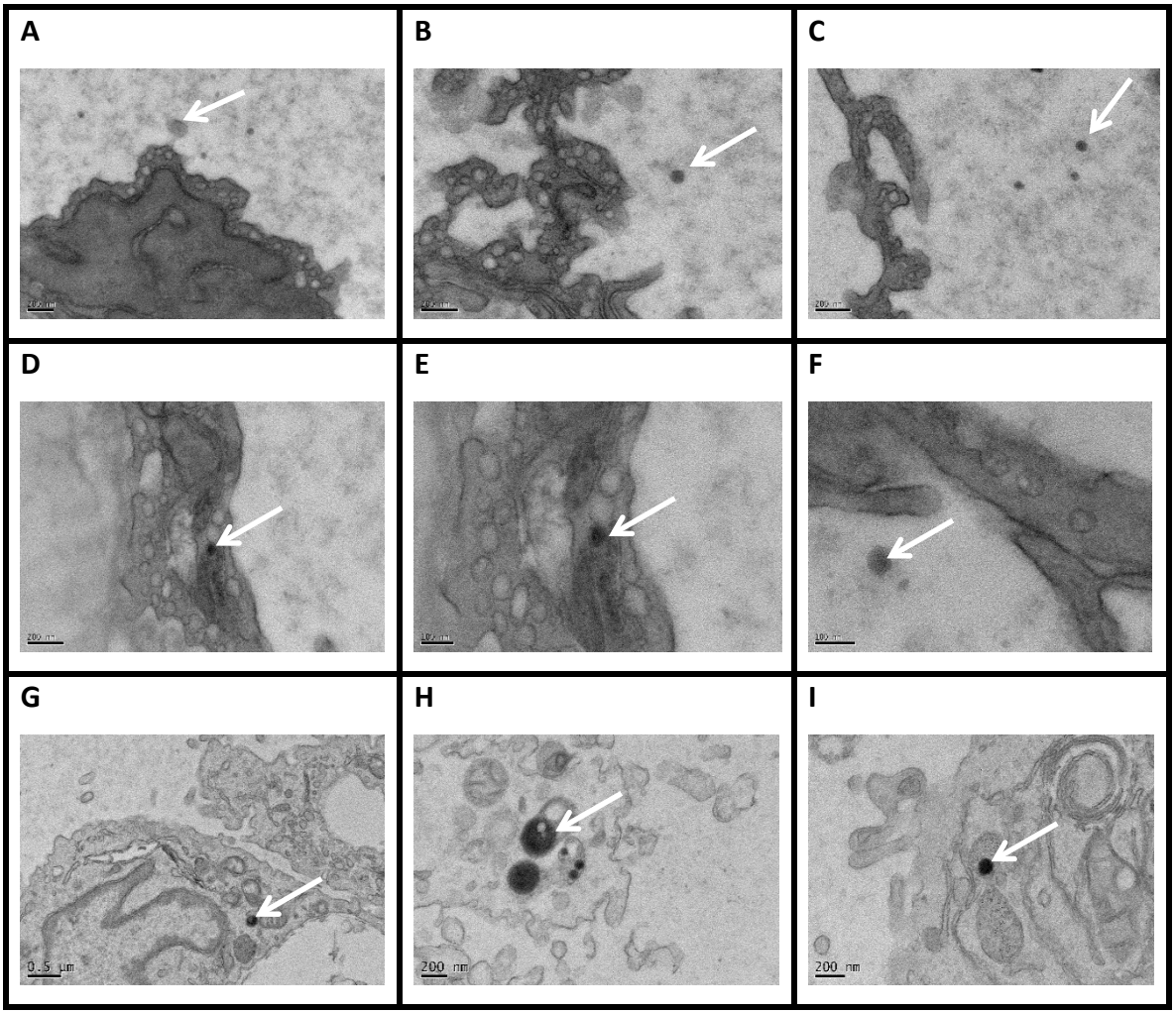

Figure 74. TEM images of SiNP uptake by MAs *in vivo* injected rat (A-I). The SiNPs are represented by black spherical structures inside ECs (arrows).

5.2.2 SiNP Biodistribution within Tissues and Organs.

The ICP results confirmed the internalisation of SiNPs within various tissues and organs after their injection *in vivo* (Figures 75). A small fraction of 6% of the SiNPs administered *in vivo* were localised into various tissues including; lungs, heart, aorta, mesentery, liver, spleen and kidney. The percentages for their distribution into different tissues as determined by ICP are illustrated in Figure 76. Despite the minimal concentration of SiNPs internalised into different tissues, the largest fraction of uptake was observed within the MA tissue with the latter accounting for nearly 5% of SiNPs injected *in vivo* (Figure 75).

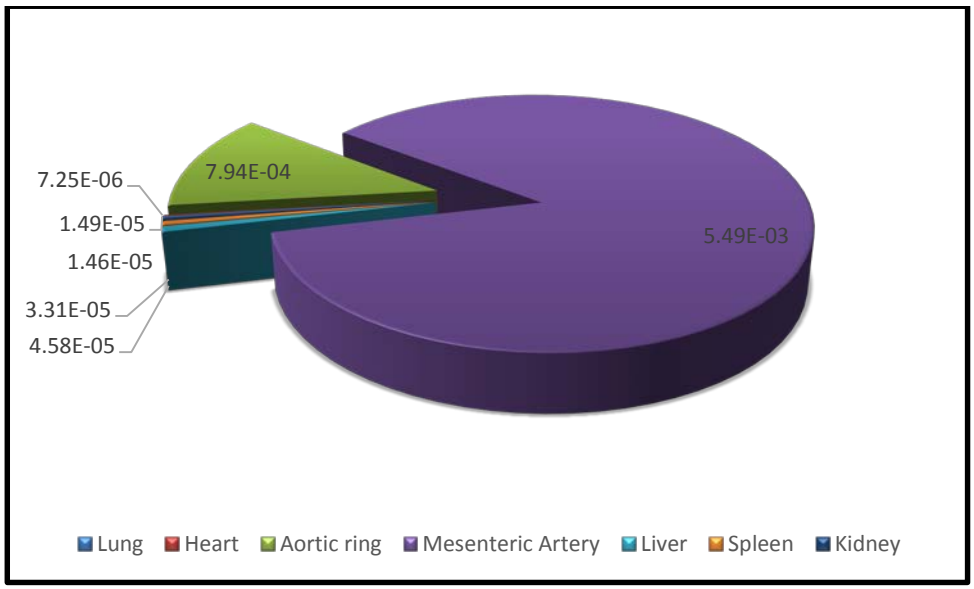

Figure 75. The mean normalised silicon oxide concentration (g) per 1 g of *in vivo* tissue. The pie chart illustrates how the 6% fraction of internalised SiNPs was distributed within tissues.

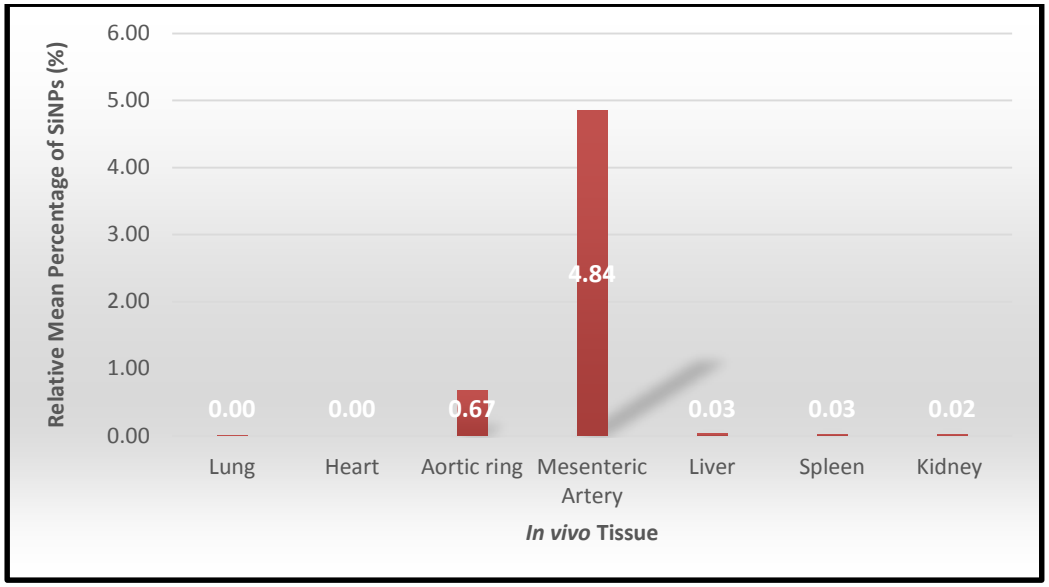

Figure 76. Mean percentage of SiNPs present in *in vivo* tissues. Expressed as a mean percentage of the actual dose injected (100%).

5.3 Discussion

SiNPs injected *in vivo*, had no overall effect on Phe-induced contraction (at the higher doses) contrary to the results found after *ex vivo* infusion of SiNPs. This may be due to the corona formation after the SiNPs are injected into the blood (Tenzer et al., 2011), thus preventing their interaction with the α1-adrenergic receptors. Although SiNPs injected *in vivo*, induced a significant reduction in ACh dilator responses at the lower doses, there was no overall detrimental reduction in dilation at the high doses. Again, this may relate to corona formation. Whilst having no overall effect on SNP responses *ex vivo*, SiNPs injected *in vivo*, significantly reduced SNP-induced dilator responses at a lower dosage. Thus SiNPs may have an impact on the clinical use of NO donors in different settings including NO-releasing NPs (Naghavi et al., 2013) and NO-releasing polymers for vascular stents (Seabra et al., 2008). The ability of PAPA to induce relaxation of VSMCs after the *in vivo* SiNPs injection (attributed to its direct action on the smooth muscle layer independent of the endothelium) suggests that SiNPs had no overall effect on the contractile machinery, or the integrity of VSMCs. Indeed, previous studies suggest the involvement of PAPA in the suppression of the L-type Ca^{2+} currents in VSMCs (Iguchi et al., 1992) through the blockage of voltage-dependent L-type Ca^{2+} channels (Bolton, 1979).

The uptake of SiNPs by ECs was confirmed by TEMs and quantified by ICP, involving rigorous calculation, which took into account all factors including the presence of silica in natural tissues. TEM images may not account for all tissue cross-sections and hence may miss out SiNPs localised into any plane of the tissue and/or organ section. ICPs results suggest that SiNPs had largely accumulated in MAs *in vivo*. The mesentery represents the highest proportion of ECs, in comparison to other tissues e.g. the heart. Hence, the presence of larger proportion of ECs on small- and microvessels per surface area compared to other tissues may account for more uptake in vivo.

Two batches of SiNPs were used for the *in vivo* study. These were used at the same dosage (NP/mL), but were of slightly different sizes 98 nm vs. 110 nm). The corresponding weight and surface area difference may have added a factor in the small variation observed

between the 3 different experiments. Since our group has previously demonstrated that it is NP number (hence surface area) rather than mass that affects vascular function. The results obtained *in vivo* need to be established with further experiments due to the limited *n* number (n=3). Also additional variable factors may be considered to account for extended SiNP exposure time of the rats, hence more circulatory time of NPs as well as real-time imaging of the fate of SiNPs, using the luminescent dye as a tracking material. A similar *in vivo* study by Borak et al. found that only 36% of the introduced SiNPs (150 nm) were excreted with urine after four days of iv injection (Borak et al., 2012). The remaining particles were accumulated in the lung air sacs and kidney glomerulus (Borak et al., 2012). Smaller size SiNPs (70 and 35 nm; but not 300 and 100 nm ones) were demonstrated to cross the placenta barrier in pregnant mice resulting in retarded uterus and foetus formation and caused pregnancy complications (Yamashita et al., 2011).

Due to their predominant negative charge, SiNPs may have sequestered in the liver as indicated previously by Souris et al. (Souris et al., 2010). The neutralisation of the negative change or the possible change of surface charge to positive by corona formation in circulation, may have led to SiNP hepatobiliary excretion from the liver into the gastrointestinal tract (Souris et al., 2010). The corona formation of SiNPs are suggested to be charge-dependent and involve the adsorption of serum proteins facilitating hepatobiliary excretion (Souris et al., 2010). The excretion of SiNPs by the liver may explain the absence of SiNPs presence in the latter tissue in our present study.

The fluorescent rhodamine B dye used to encapsulate our dye-encapsulated SiNPs, had previously demonstrated its ability to form a thiourea bond with thyroxine (T4) and triiodothyronine (T3) (Ermolenko et al., 1992). This phenomenon may have been implicated in the *in vivo* study, where dye molecules may have formed conjugates with plasma and/or serum proteins leading to blood corona formation and reducing the effects they have on blood vessels as in *ex vivo*.

The presence of SiNPs in circulation may make them prone to corona formation and altered surface characteristics. The corona concept was previously demonstrated through a rapid

and extensive interaction between human serum albumin and SiNPs with a characteristic distributed adhesion of the protein and particle (Ang et al., 2014). The extent of NP damage was suggested to be related not only to the electrostatic effects of SiNPs and protein affinity but also to the hydrodynamic size of the latter NPs rather to than their concentration and/or protein size or charge (Tenzer et al., 2011). Although the effects of such phenomenon have not been tested in our study, further experiments using larger SiNP may provide some clues. Corona formation may lead to varied interaction with the surrounding tissues, proteins and receptors, improving their biocompatibility. However, the corona may also lead to a change in hydrodynamic size in the serum and/or their subsequent aggregation. This could possibly lead to the blockage or closure of microvessels such as arterioles and capillaries. The aggregation of NPs formed in the blood was previously suggested to cause obstruction in the capillaries of the lung, resulting in acute embolism (Muzykantov, 2005). A previous study by Yu et al. suggested a mechanical obstruction in the vasculature caused by the iv injection of 170 nm non-porous SiNPs at 450 mg/Kg (Yu, Greish, et al., 2012). The latter resulted in congestion in major organs, lesion formation and subsequently organ failure (Yu, Greish, et al., 2012). This phenomenon is critical as applied to *in vivo*; as it indicates that the physical impact of SiNPs on the vasculature rather than their mediated cellular-toxicity effects and may limits their safety.

Chapter 6.

The Molecular Mechanisms of SiNP-induced Attenuated Dilation

Findings from the present study suggest that SiNPs have a detrimental effect on endothelial-dependent (ACh) dilator responses. In order to elucidate the mechanisms involved, a series of experiments were conducted including; the characterisation of the dilator component, the influence of superoxide dismutase and the analysis the cellular signalling pathway. We examined two theories; concerning 1) The involvement of ROS in mediating SiNPs-induced impairment to vascular function and 2) the role of inhibitors such as L-NNA, apamin, TRAM-34 and indomethacin in elucidating the pathways SiNPs may target to mediate their effects. Firstly, however, the dilator component within the rat MAs were elucidated using inhibitor studies.

6.1 Characterisation of the Dilator Component (Inhibition Studies)

6.1.1 Influence of L-NNA

The inhibition of NO synthesis via a NO synthase-inhibitor; L-NNA (at 100 µM) *ex vivo* caused a drastic reduction of ACh-induced dilator responses in KPSS pre-constricted vessels, with this being significant at all ACh concentrations tested (10^{-9} to 10^{-5} M). At the submaximal ACh concentration (100 nM) the mean percentage dilation was 74.25 ± 8.17% vs. 10.95 ± 6.44% after incubation in control and SiNPs respectively (n=4 and 5 respectively, unpaired *t* test, p<0.0001; Figure 77).

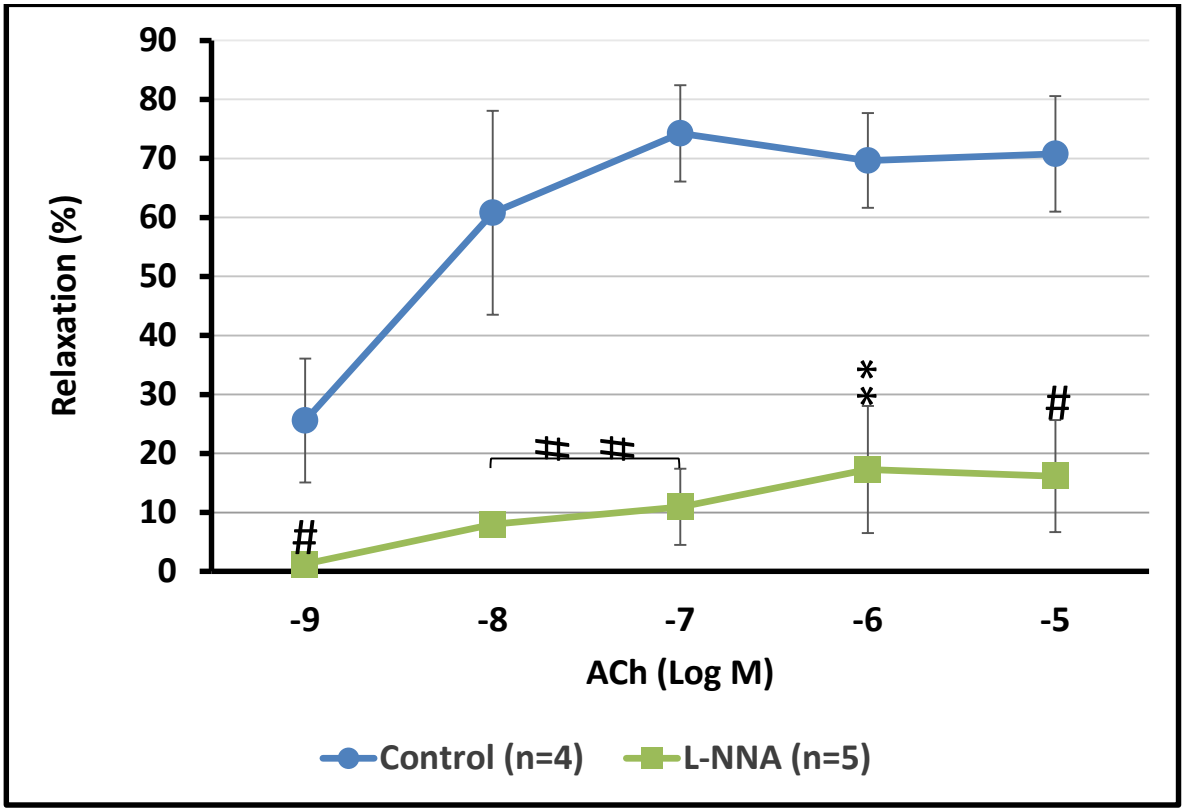

Figure 77. The influence of incubation in L-NNA superfused in PSS and luminally-infused *ex vivo* on the ACh-induced relaxation in KPSS pre-constricted vessels. 'n' is number of vessels. **p<0.01, #p<0.001 and ##p<0.0001, error bars=SE. One-factor repeated measures ANOVA. P values correspond to comparisons between L-NNA-incubated vs. control ACh responses of MAs.

In contrast to KPSS-reconstricted vessels, the 30 minutes inhibition of NO synthesis and release had no overall effect on the ACh-induced dilator responses in Phe pre-constricted vessels. This is despite a significant decrease in dilation to ACh at 10 nM; (At 10 nM ACh, the mean percentage dilation was 39.30 ± 11.25% vs. 8.78 ± 4.86% after incubation in control and LNNA respectively, n=6, paired *t* test, p<0.05; Figure 78), while the dilations to 1 nM, submaximal (100 nM) and higher (1 µM and 10 µM) ACh concentrations were preserved.

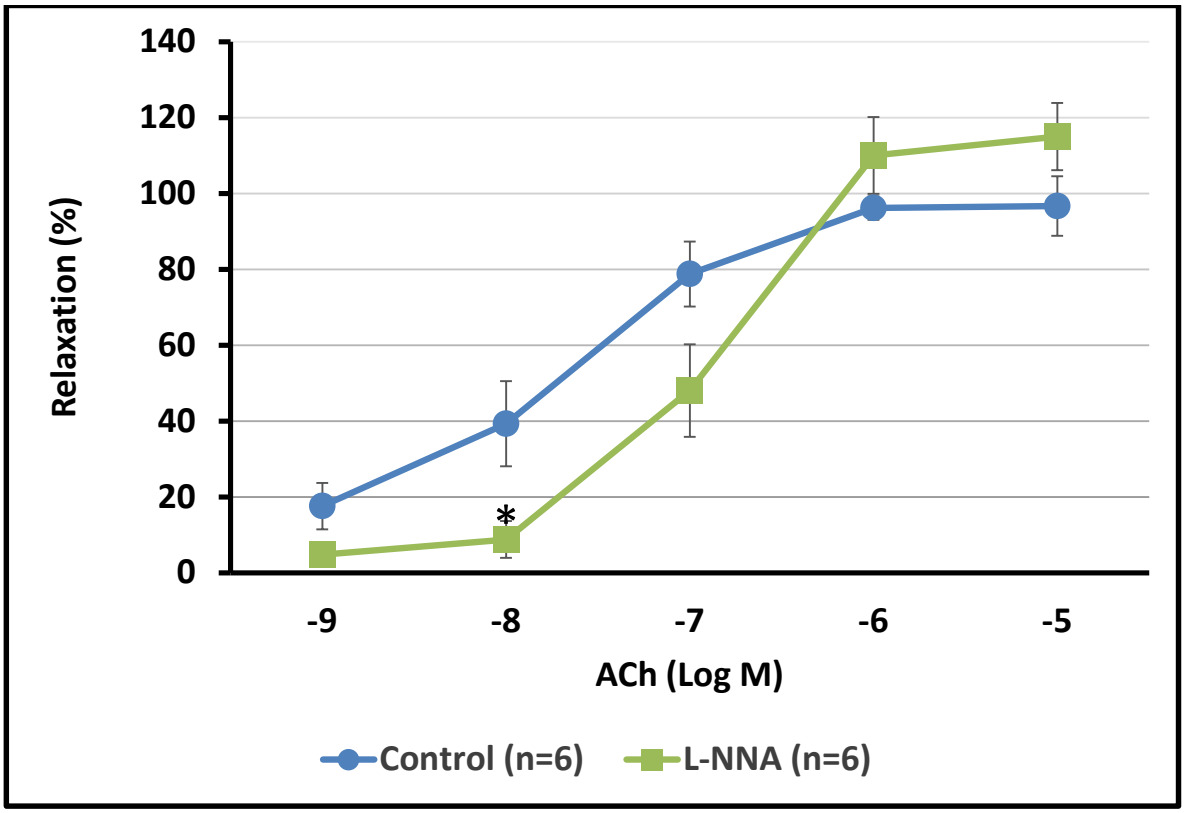

Figure 78. The influence of incubation in L-NNA on the ACh-induced relaxation in Phe pre-constricted vessels. 'n' is number of vessels. *p<0.05, error bars=SE. One-factor repeated measures ANOVA. P values correspond to comparisons between L-NNA-incubated vs. control ACh responses of MAs.

6.1.2 Influence of Apamin and TRAM-34

The vascular incubation in apamin (at 100 nM) and TRAM-34 (at 1 µM) alone for 30 minutes significantly decrease the dilator responses at specific ACh concentrations (1 nM, 10 nM and 100 nM). At 100 nM ACh, the mean percentage dilations were 78.77 ± 8.58% vs. 6.99 ± 5.71% and 12.17 ± 4.99% after incubation in control, apamin and TRAM-34 respectively (n=6 and 4 respectively, unpaired *t* test, $p<0.05$; Figure 79). The dilatory responses were recovered at higher ACh concentrations (1 µM and 10 µM) (Figure 79). The co-incubation of MA in apamin and TRAM-34 however, significantly reduced and almost abolished the vasodilator responses to ACh in contrast to apamin or TRAM alone (Figure 79). At 100 nM ACh, the mean percentage dilation was 78.77 ± 8.58% vs. 17.09 ± 12.99% after incubation in control and apamin with TRAM-34 respectively, n=6 and 4 respectively, unpaired *t* test, $p<0.05$; Figure 79).

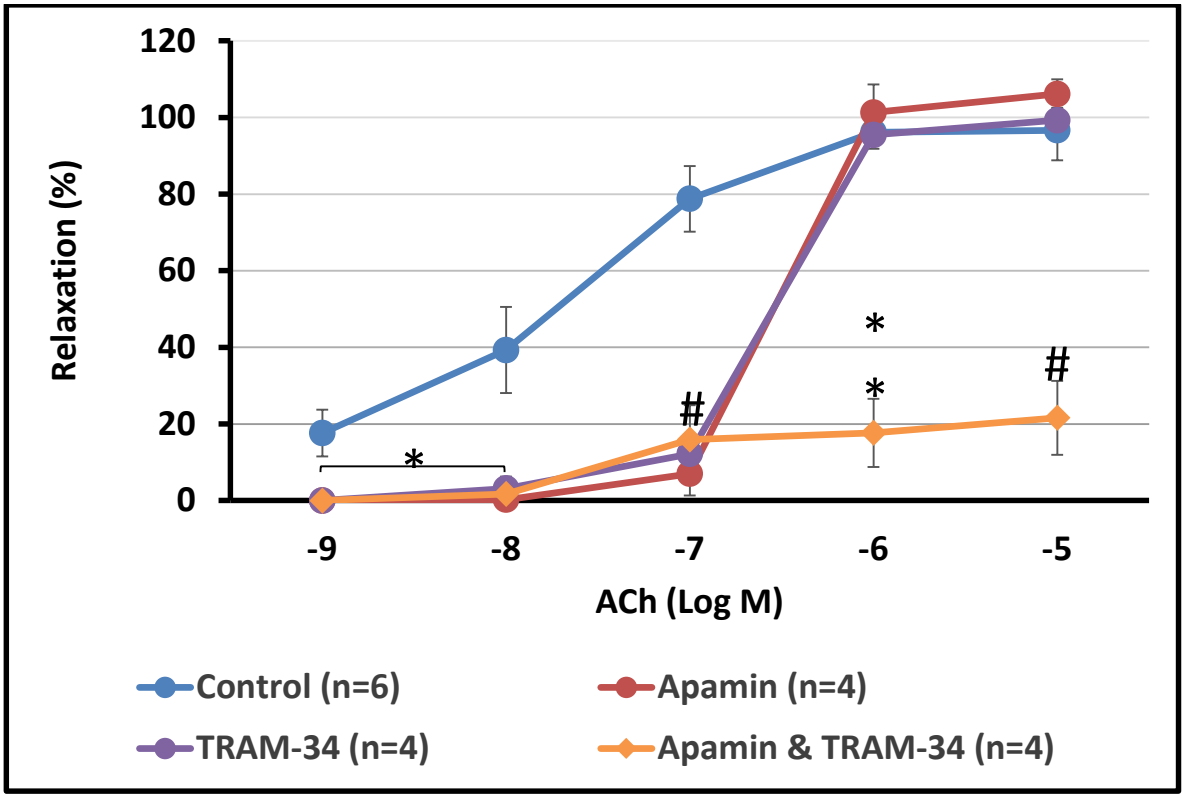

Figure 79. The influence of co-incubation in apamin and TRAM-34 on the ACh-induced relaxation in Phe pre-constricted vessels. 'n' is number of vessels. *p<0.05, **p<0.01, #p<0.001 and ##p<0.0001, error bars=SE. Three-factor repeated measures ANOVA. P values correspond to comparisons between inhibitor-incubated vs. control ACh responses of MAs.

6.1.3 Influence of All Inhibitors (including indomethacin)

The use of an inhibitor cocktail containing L-NNA, apamin and TRAM-34 attenuated the vasodilator responses to ACh despite a minimal degree of dilation of 7.96-10.98% that was sustained at the maximal ACh concentration of 1 μM and 10 μM, respectively (Figure 80). To investigate whether a NO-independent pathway is involved in mediating the small degree of dilation that is present following the inhibition in L-NNA, apamin and TRAM-34, we have used a cyclooxygenase inhibitor; indomethacin (at 10 μM). The inhibition of the COX with indomethacin for 30 minutes had no overall effect on the ACh-induced dilator responses in Phe pre-constricted vessels; (At 100 nM ACh, the mean percentage dilation was 78.77 ± 8.58% vs. 84.41 ± 10.97% after incubation in control and indomethacin respectively, n=6 and 4 respectively, unpaired *t* test, $p<0.05$; Figure 80). However, the use of all inhibitors including indomethacin abolished the vasodilator responses to ACh (Figure 80).

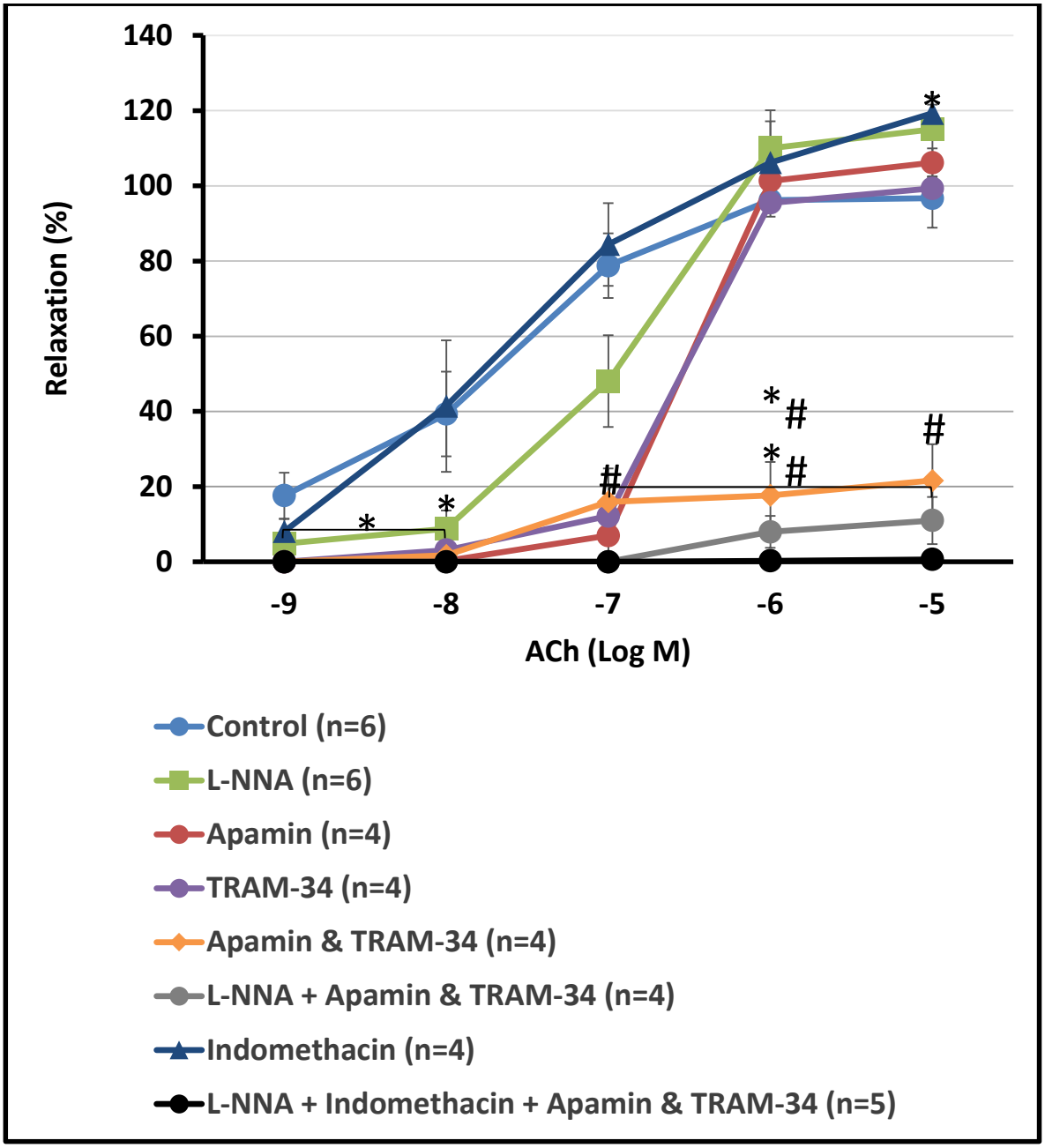

Figure 80. The influence of the inhibitor cocktail of L-NNA, apamin and TRAM-34 as well as indomethacin on the ACh-induced relaxation in Phe pre-constricted vessels. 'n' is number of vessels. *p<0.05, **p<0.01, $^{\#}$p<0.001 and $^{\#\#}$p<0.0001, error bars=SE. Multi-variate repeated measures ANOVA. P values correspond to comparisons between inhibitor-incubated vs. control ACh responses of MAs.

The vasodilator responses to the NO donor, SNP were not affected by incubation in all inhibitors *ex vivo* (At 100 nM concentration of SNP, the mean percentage dilation was

102.30 ± 4.03% vs. 114.97 ± 5.28% after incubation in control and all inhibitors respectively, n=3, paired *t* test, NS).

6.2 The Influence of Co-incubation of SiNPs with Inhibitors

The co-incubation of SiNPs (5.32 x 10^{11} NP/mL) in the presence of L-NNA completely abolished the dilator responses to ACh at all concentrations tested (Figure 81). The most drastic effects were observed at the submaximal (100 nM), maximal (1 µM) and highest (10 µM) ACh concentrations (At 100 nM ACh, the mean percentage dilation was 78.77 ± 8.58% vs. 3.09 ± 1.48% after incubation in control and SiNPs with L-NNA respectively, n=6 and 7 respectively, unpaired *t* test, p<0.0001; Figure 81).

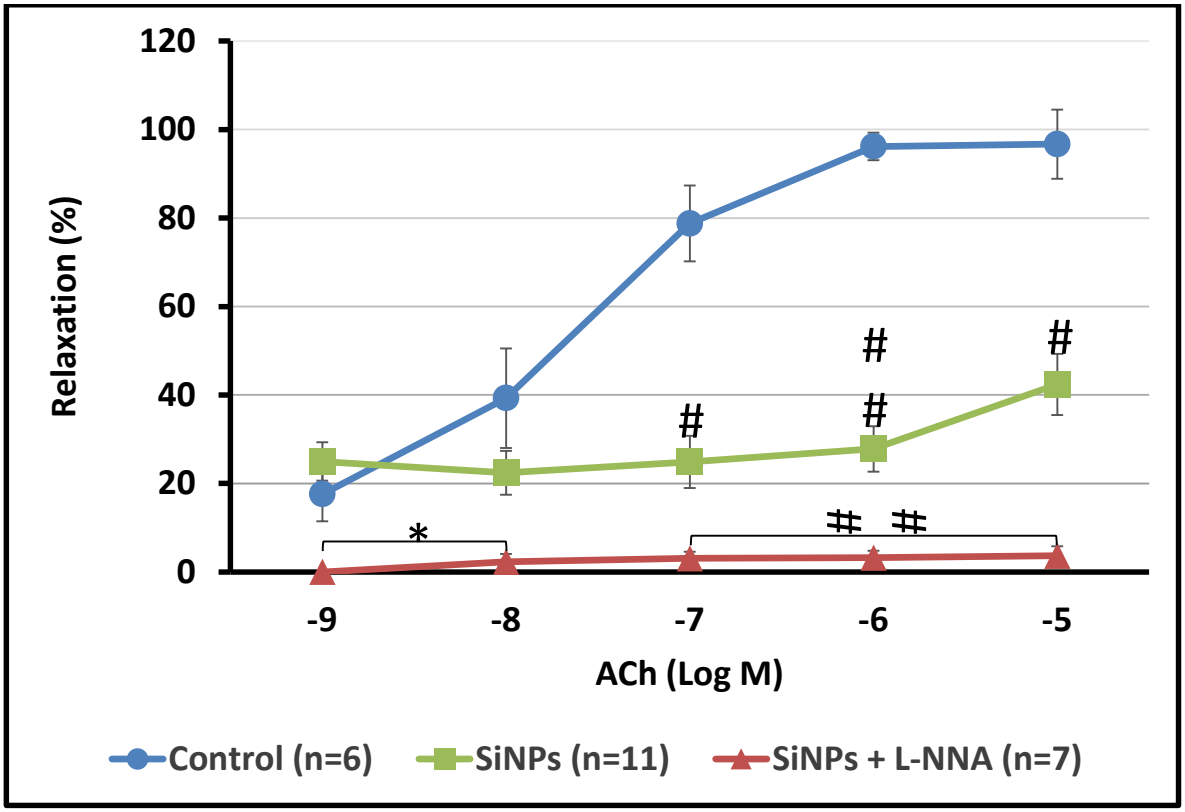

Figure 81. The influence of co-incubation in SiNPs and L-NNA on the ACh-induced relaxation in Phe pre-constricted vessels. 'n' is number of vessels. *p<0.05, #p<0.001 and ##p<0.0001, error bars=SE. Two-factor repeated measures ANOVA. P values correspond to comparisons between either SiNPs incubated *ex vivo* or with L-NNA vs. control ACh responses of MAs.

6.3 Influence of Superoxide Dismutase

When the vessels were co-incubated in SiNPs (at 5.32 x 10^{11} NP/mL) and SOD dilation of Phe pre-constricted vessels was not restored but led to further reductions in the ACh dilator responses specially at higher ACh doses (10^{-5} to 10^{-3} M) (At 10 µM ACh, the mean percentage dilation was 96.68 ± 7.82% vs. 35.58 ± 3.51% after incubation in PSS and SiNPs with SOD respectively, n=6 and 5 respectively, unpaired *t* test, p<0.0001; Figure 82).

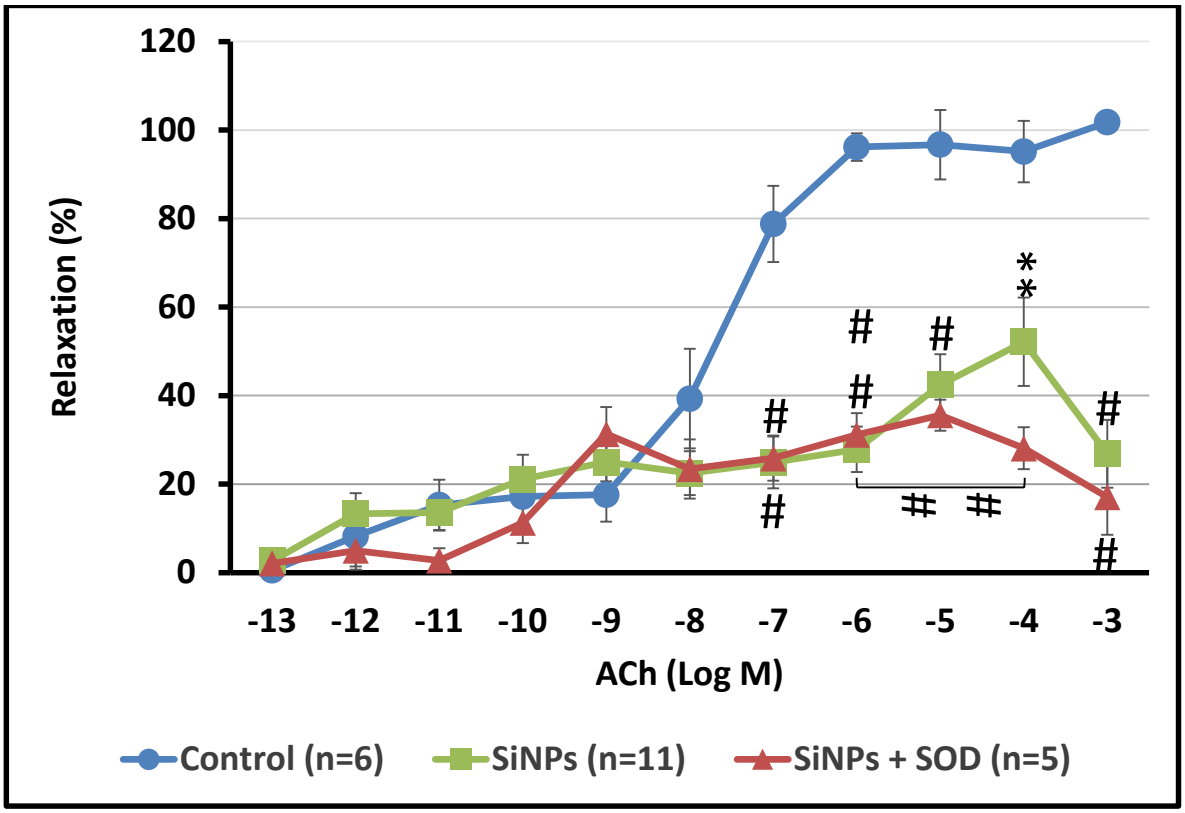

Figure 82. The influence of co-incubation in SiNPs (at 5.32 x 10^{11} NP/mL) and SOD on the ACh-induced relaxation in Phe pre-constricted vessels. 'n' is number of vessels. **p<0.01, #p<0.001 and ##p<0.0001, error bars=SE. Two-factor repeated measures ANOVA. P values correspond to comparisons between either SiNPs incubated *ex vivo* or with SOD vs. control ACh responses of MAs.

6.4 Analysis of the Cellular Signalling Pathway

The influence of SiNPs at the physiological level may translate into a change in the levels and/or the phosphorylation or de-phosphorylation pattern of certain proteins or regulatory proteins involved in mediating and/or facilitating vasodilation. These proteins may involve regulatory factors, adaptor proteins, enzymes and ion channels directly associated with the NO and/or EDHF-related pathways leading to the relaxation of small arteries. Hence, phosphorylated protein detection was carried out using the Proteomics Screening approach.

100 MA segments (first-sixth order MAs) were collected per experimental condition, excluding the superior MA, and incubated in various conditions including: negative control (PSS only), positive control (ACh-stimulated), SiNPs control (NP only) and NPs with ACh-stimulated vessels for the duration of 30 minutes. The latter tissues were processed as mentioned previously in the methodology. We examined whether SiNPs had an effect on the phosphorylated levels or form of key protein targets involved in the vasodilatory pathway in the rat MAs and arterioles. Initially a screening method was accomplished to screen over a number of protein targets within the vascular relaxation pathway using the Human Phospho-Kinase Antibody Array (Catalogue Number: #ARY003B, R&D Systems, Abingdon, UK) according to manufacturers' instructions. The array was used for the detection of the relative phosphorylation levels of 46 intracellular kinases using a simple two-site sandwich assay principle. Proteins were visualised using chemiluminescence (Hyperfilm ECL; Amersham), scanned using a Syngene densitometer and analysed using the GeneSnap software (Syngene). The 5 minutes stimulation with 10 µM of ACh had led to the increase in the levels of phospho-ERK (p-ERK 1/2) and phospho-Akt (p-Akt 1/2/3) in isolated MAs compared to control (PSS only) (Figure 83). In contrast, the incubation in SiNPs for normal vessels (NPs only) or stimulated vessels (NP with ACh) had reduced the levels of p-ERK and p-Akt compared to the levels detected in control vessels (Figure 83). The reduction in the phosphorylated pattern of ERK was more pronounced in the NP only-treated vessels as compared to stimulated ones (Figure 83). This gives an insight into the mechanism of attenuated vasodilation. Further molecular work is beyond the scope of the present study.

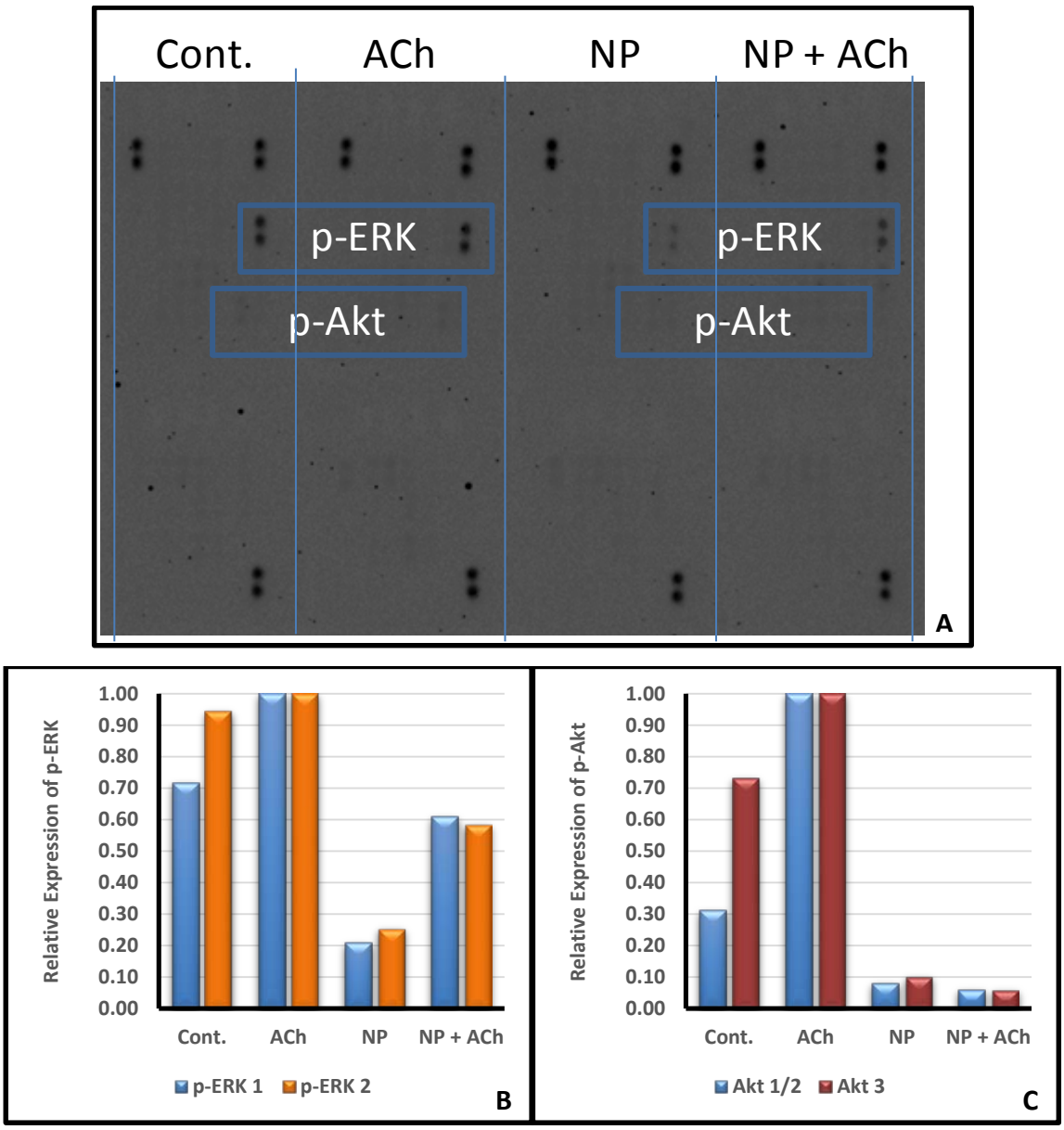

Figure 83. A) The effect of SiNPs on the phosphorylated levels of protein targets involved in mediating ACh-induced vasodilatation. A representative proteomics blot for the protein samples extracted from the pooled MAs from the Wistar Rat. The intensity of the dots shown above represent the quantity of the phosphorylated kinase present. B) A quantitative analysis of the p-ERK 1/2 blot shown in A. C) A quantitative analysis of the p-Akt 1/2/3 blot shown in A.

6.5 Discussion

In order to elucidate the mechanisms by which SiNPs attenuate vasodilator responses, it was necessary first to determine what mediators were responsible for the dilator component in MAs. L-NNA is known as a competitive inhibitor of eNOS (Griffith and Kilbourn, 1996; Garvey et al., 1994), due to its ability to bind to enzyme pockets that in turn prevents other NO substrates from binding, thus blocking the NOS action and ultimately preventing NO generation (Clark et al.). The inhibition studies demonstrate that; 1) in depolarised vessels (KPSS preconstriction), NO was the major dilator component. 2) In Phe-preconstricted vessels, the vasodilator response was influenced by all inhibitors tested (L-NNA and potassium channel blockers), thus demonstrating that both NO and EDHF contribute to the vasodilator response in MAs. Therefore, the incubation of MAs in L-NNA may have partially compromised vasodilation because of reduced NO bioavailability (Joshi and Woodman, 2012). This suggests that NO may only partly contribute to the vasodilator component of MAs (Figure 77). The co-incubation of SiNPs in the presence of L-NNA completely abolished the dilator responses to ACh (Figure 80). This suggests that SiNPs may directly affect the EDHF pathway. Hence, EDHF act as an important dilator for MAs. This is further demonstrated by the use of the potassium channels inhibitors (apamin and TRAM-34) alone and in combination. The results from the potassium channel inhibitors studies indicate the dependence of the mesenteric artery on both the SK_{Ca} and IK_{Ca} channels mediating the dilatory responses to ACh as previously suggested (Crane et al., 2003). Furthermore, there may be a cross-talk between the pathways leading to potassium channel activation within the endothelium such that the absence of the small potassium channels are compensated functionally by the intermediate channel partners. Our inhibition studies were previously supported by Jane and Langton who used apamin and TRAM-39 (at 50 nM) and demonstrated that the abolition of EDHF required the presence of both SK_{Ca} and IK_{Ca} channels using rat isolated MAs mounted on a wire myography system (Hinton and Langton, 2003). In rat mesenteric arteries, the stimulation of ECs results in the activation of endothelial calcium-sensitive potassium channels and leads to the generation of the hyperpolarising event. The resulting efflux of K^+ from ECs via SK_{Ca} and IK_{Ca} channels (Edwards et al., 1998), regarded as the hyperpolarisation current, propagates or spreads

passively via myoendothelial gap junctions (Sandow and Hill, 2000; Sandow et al., 2002) to accumulate in the myoendothelial space where it stimulates the Na^+/K^+ ATPase pumps and voltage-gated potassium channels (K_v; e.g. $K_v1.5$ and $K_v2.1$ (Hald et al., 2012)) in VSMCs (Edwards et al., 1998). This results in the EDHF-attributed hyperpolarisation in VSMCs. Hence, the EC-VSMC electrical coupling (Little et al., 1995) is characterised by endothelial potassium channels that influence smooth muscle cell contractile activity by reducing Ca^{2+} influx via voltage-operated Ca^{2+} channels and by suppression of key enzymes involved in agonist-induced transduction pathways (Itoh et al., 1992). Thus it is logical to suggest that SK_{Ca} and IK_{Ca} channels are located and constitutively expressed in abundance on ECs in rat mesenteric arteries (Parkington et al., 2002), and their opening is voltage-independent but sensitive to a rise in endothelial Ca^{2+} (Gluais et al., 2005) (Figure 84). Previous studies determined the endothelium as being the specific site of action for apamin (Doughty et al., 1999). Hence, we suggest that the SK_{Ca} channels affected here are related specifically to the action of apamin on ECs. The contribution of SK_{Ca} and IK_{Ca} channels to EDHF-mediated dilation as confirmed by our inhibition studies was also previously suggested to be more pronounced than the contribution made by other potassium channels such as K_v channels (Waldron and Garland, 1994). Taken together; with the fact that SiNPs uptake was only evident in ECs lining the blood vessels and that inhibitors were applied intravascularly inside the MA vessel lumen, we suggest that the SiNPs significantly affected dilation related to SK_{Ca} and IK_{Ca} channels of endothelium origin. Our results from the inhibition studies provide further support to the belief that SK_{Ca} and IK_{Ca} channels are most abundant in endothelial cells, but not VSMCs from mesenteric arteries.

It would be interesting to examine whether the incubation of 11,12-EET with MAs (Potente et al., 2003) will improve the dilator responses to ACh following SiNP incubation. This will determine the impact and contribution of an exogenously applied EDHF-derived precursor to the dilation responses of mesenteric vessels. The dilation of MAs in the presence of the inhibitor cocktail (L-NNA, apamin and TRAM-34) was not sufficient to completely abolish the dilator response of the MA and was able to maintain a very minimal dilation (the dilation of MAs were 8 and 11% at high ACh concentrations of 1 µM and 10 µM, respectively). This may suggest the presence of minimal degree of residual relaxation

despite the use of all inhibitors and the possible contribution from other pathway(s) in mediating vasodilation in second order rat MAs in particular, which may also be affected by SiNPs. Although the use of the cylcooxygenase inhibitor (indomethacin) did not have an overall effect on dilation, however its co-incubation with L-NNA, apamin and TRAM-34 abolished the dilatory response of the MA. The latter suggests a minor additional contribution from prostanoids from the cyclooxygenase pathway to the dilator component of mesenteric arteries (Honing et al., 2000). Previous reports also suggest the participation of connexins (37, 40 and 43; reviewed in (Griffith et al., 2001)) from Chaytor paper 2005); in mediating the endothelial-dependent hyperpolarisation via myoendothelial gap junctions in different vascular beds (Taylor et al., 1998; Chaytor et al., 2005; de Wit and Griffith, 2010). These gap junctions may have alternative potassium channels to the apamin/TRAM-34-sensitive calcium-activated potassium ones and/or rely on other pathways that lead to vasodilation including cAMP (Chaytor et al., 2002).

The rationale for using SOD as a ROS scavenger was an attempt to examine the involvement of ROS in mediating SiNPs damage as previously suggested (Fubini, 1997). Due to the dependence of the endothelium-derived NO factor in causing vasodilation, an elevation in ROS may quench NO, leading to impaired vasodilator responses (J. Kim et al., 2011). Furthermore; a study by Zhao et al. suggested the impairment of EDHF-related vasodilation in the MAs of the rat via ROS-dependent mechanism (Zhao et al., 2013). Hence, we have assumed that the attenuated vasodilatory function of the MAs upon the exposure to SiNPs may be mediated via the production of ROS. However, the data obtained show that SOD worsened dilation and no improvements were apparent when co-incubated with SiNPs. Hence, in light of results from vessels co-incubated in SiNPs and SOD (inability of SOD to restore vasodilation), we suggest that the mechanism for SiNPs impairment of vasodilation is ROS-independent and may involve alternative mechanisms. This finding contradicts other studies reporting the effects of SiNPs on inducing endothelial cells dysfunction through oxidative stress via JNK-, p53- and NF-κB-related pathways (Liu and Sun, 2010) or the induction of antioxidant enzymes (catalase, lutathione stransferase and thioredoxin reductase) by 100 nm SiNPs through ROS-dependent pathways (Passagne et al., 2012).

To determine whether SiNPs effects were on the basal phosphorylated forms of ERK and Akt and/or their expression levels, our findings suggest that under stimulated conditions there is a reduction (and/or down regulation in expression) of p-ERK and p-Akt levels following SiNPs uptake by first- to sixth order-MAs *ex vivo*. This highlights the critical role of phosphorylated ERK and Akt in mediating ACh-induced dilation of small arteries. The effect of SiNPs on MAs may be mediated through their effects on blocking the NO and EDHF-related signalling pathway at least in part via their ability to reduce the phosphorylated levels of both ERK and Akt. The latter may act independently or together to limit the action (if there are existing basal levels) and/or our expression of both eNOS and EDHF causing the compromise in the dilator responses of MAs to ACh *ex vivo*. Since EDHF is the principal dilator in MAs (Hilgers et al., 2006; Hilgers and Webb, 2007), we suggest that this is mostly affected by SiNPs, although the use of the whole mesentery (namely first to sixth order MAs) may reflect other components such as NO. The more pronounced role of EDHF in small MAs (specifically second to fourth order arteries) compared with medium sized and large conduit arteries such as the superior MA and the aorta is attributed to the action of IK_{Ca} and SK_{Ca} channels in ACh-induced relaxations (Chen and Cheung, 1997; Hilgers et al., 2006). However, the decrease of p-Akt levels also suggest an additional effect of SiNPs in preventing the backup role of NO to revert MA-dilator responses to normal levels or maintain the levels resulting from compromised EDHF action(s) following SiNPs infusion *ex vivo*. The actions of ERK are mediated via its action on regulating the activity of eNOS (Salerno et al., 2014) and EET-related signalling cascade (11,12- and 14,15-EETs CYP metabolites (Fleming, Fisslthaler, Michaelis, et al., 2001)) leading to eNOS-induced H_2O_2 production (that upregulates ERK) and subsequent hyperpolarisation of VSMCs. The decreased levels of p-ERK by SiNPs may thus be in part responsible for the impairment in the vasodilator function of MAs. Upon ACh stimulation, Akt is thought to be produced via two pathways; 1) the overproduction of EDHF and 2) when EDHF is compromised. When produced, Akt is involved in the upstream regulation of NO production via serine 1177 phosphorylation (Zhang et al., 2009) and promoting its action(s) on ECs (Dimmeler et al., 1999). The decreased levels of p-Akt by SiNPs may thus be in part responsible for the impairment in the vasodilator function of MAs through the blockage of NO production by eNOS. This is because NO acts as a backup to EDHF when the

latter is also compromised by SiNPs. The mechanism through which SiNPs decrease p-ERK and Akt may be due to their direct interaction with the latter proteins due to their abundance and role in mediating MA-dilation. The study by Yu et al. have reiterated this finding by suggesting the effect of SiNPs on lowering the haemoglobin levels in the blood of mice injected with non-porous Stöber SiNPs (115 ± 13 nm; at 600 mg/kg) (Yu, Greish, et al., 2012). SiNPs may also induce irreversible conformational change (Turci et al., 2010) to the protein structures resulting in protein de-phosphorylation and/or misfolding. ERK can stimulate eNOS, calcium-dependent potassium channels and BK_{Ca} channels, and on the long-term, induce ECs and VSMCs proliferation. Due to the limitations in our study, there may be further SiNP disruptive, obstructive, blockade and/or inhibitory actions (if any) on MAs, however these may have not been accounted for due to limitation in detecting all protein isoforms specific to the rat species and/or the difficulty in obtaining the more protein yield from more samples, hence sample size. Further investigation is required to account for other targets for SiNPs actions. This may include the specific CYP2C11 isoform associated with the rat MAs, as a different isoform was shown to be affected by SiNPs in a human liver and fibroblast cellular model (Christen and Fent, 2012).

It is generally difficult to detect phospho-proteins in blood vessel lysates and the process may require incubation in the primary antibody for over a few days to obtain denser protein bands and/or the use of a stronger chemi-luminescent signal of Western blot detection. The main limitation of the proteomics study related to the fact that not all kinases cross-reacted and/or were specific to the particular isoforms present in the rat MAs. Furthermore, the kit from R&D lacked a number of key targets such as cPLA2, PLCγ, CYP4A, and CYP2C11 involved in mediating MA-mediated vasodilation and hence these were not accounted for in the present studies and need to be further investigated in future studies.

Chapter 7.

Summary of Results, General Discussion and Conclusion

7.1 Summary of Results

7.1.1 The Synthesis and Characterisation of SiNPs

Dye-encapsulated SiNPs were fabricated using the Stöber method and characterised by DLS, Zeta potential and TEM. Two batches of SiNPs (DA3 and A3) were monitored for 15 months following their initial synthesis, in ethanol and water respectively. The results are summarised as follows:

1. The presence of rhodamine dye was confirmed by fluorescence microscopy.

2. The DLS technology using the ZetaSizer provided an overall SiNPs size of 124.1 nm with a stability of -34.5 mV (A3 sample). The size was confirmed by TEM analysis to be 98 nm in diameter.

3. The SEM and TEM images of the synthesised DA3 SiNPs sample stored in ethanol demonstrate that the NPs have spherical morphology 15 months after their initial synthesis. The storage of the NPs over one year period did not affect the particle morphology, as the particle shape and size remained similar. In contrast, the A3 SiNPs sample displayed more a granular appearance over time with some aggregation in morphology.

4. There was a significant decrease in the Zeta potential of DA3 SiNPs sample following 15 months of storage in ethanol. The potential for the A3 SiNPs displayed significant changes in PSS (only after 15 months) with slight fluctuations in Zeta potential when dispersed in water for the 15-month period.

7.1.2 Effects of SiNPs on MAs *Ex Vivo*

Ex vivo vascular studies demonstrated that:

1. The acute 30-minute exposure of MAs to SiNPs (at 5.32 x 10^{11} NP/mL) resulted in their uptake by ECs lining the vascular lumen and free localisation in the cytoplasm.

2. SiNP uptake caused a significant reduction in contractile responses to Phe at specific concentrations without affecting the contractile machinery of MAs (high potassium solution).

3. SiNPs uptake also attenuated the endothelium-dependent (ACh) vasodilator responses at specific concentrations (10^{-7} to 10^{-3} M).

4. The dilator responses were improved when the vessels were incubated with a lower dose of SiNPs (1.01 x 10^{11} NP/mL).

5. The endothelium-independent (SNP) vasodilator responses were unaffected by the incubation in SiNPs.

7.1.3 Effects of SiNPs on MAs *in Vivo*

In vivo vascular studies demonstrated that:

1. A small fraction (approx. 6%) of the SiNPs administered *in vivo* were localised into various tissues including; lungs, heart, aorta, mesentery, liver, spleen and kidney. Despite the minimal concentration of SiNPs internalised into different tissues, the largest fraction of uptake was observed within the MA tissue with the latter accounting for approximately 5% of SiNPs injected *in vivo*

2. SiNPs injected *in vivo*, had no overall effect on Phe-induced contraction contrary to the results found after *ex vivo* infusion of SiNPs.

3. Although SiNPs injected *in vivo*, induced a significant reduction in ACh dilator responses at specific concentrations (100 nM and 1 mM), there was no overall detrimental reduction in dilation at the high doses (1 μM – 100 μM).

4. SiNPs injected *in vivo*, significantly reduced SNP-induced dilator responses at a lower dosage (10 and 100 nM).

7.1.4 Mechanisms Mediating SiNPs Effects

Molecular Studies involving the use of inhibitors, SOD and the analysis of signalling pathways demonstrated that:

1. The vasodilator response of MAs was significantly reduced after vessels were incubated in L-NNA and potassium channel blockers, thus demonstrating that both NO and EDHF contribute to vasodilator response in MAs.

2. The co-incubation of SiNPs in the presence of L-NNA completely abolished the dilator responses to ACh, suggesting the direct effect of SiNPs on the EDHF pathway.

3. The co-incubation in SOD did not reverse the actions of the SiNPs, indicating that a reactive oxygen species (ROS)-independent mechanism may mediate SiNPs actions in MAs.

4. SiNPs uptake in MAs caused a reduction in the phosphorylated levels of ERK and Akt.

7.2 General Discussion

In the present study, RBITC dye-encapsulated monodispersed SiNPs were carefully fabricated and characterised, and their shelf life evaluated in various media (ethanol, water and PSS) over a 15-month period. SiNPs were selected as the nanomaterial of choice due to their ability to decompose into silicic acid which is a relatively harmless by-product, in comparison nanomaterials that are not metabolised such as gold NPs and CNTs (DIACONU et al., 2010). This property makes the silica an attractive metal of choice for NP fabrication and application. Our findings suggest that these SiNPs when stored in water, they show morphological changes over the 15-month time course. The granular appearance and rough outer surfaces of SiNPs in water, after the 15 month period, may have been caused by the silica seeds surrounding the individual SiNPs, generated by the water "dissolution-effect" (Finsy, 2004) and/or silica decomposition into silicic acid (DIACONU et al., 2010), which promoted SiNP aggregation overtime. When dispersed in ethanol, no morphological changes were apparent as SiNPs maintained their smooth surface characteristics; however, SiNPs did not maintain stability (significant alteration in Zeta potential) over the 15-month period. SiNPs dispersed in PSS led to a significant increase in both hydrodynamic diameter and stability. Consequently, the long-term storage of SiNPs in water or ethanol is not recommended due to the change in their characteristics overtime. Incubating the SiNPs in blood resulted in an increase in the size of SiNPs and a greater decrease in Zeta potential (hence increased stability) after 8 hours of incubation. This may be due to corona formation and serum protein adsorption onto their surface (Gamucci et al., 2014).

In addition to their application as contrast agents in medical imaging, SiNPs (in their mesoporous forms) can also be used as targeted delivery platforms for drugs, specific RNA and as gene carriers (Ferrari, 2008). This is due to their ability to accommodate thousands of luminescent molecules, protecting dye molecules from photodegradation (Roche et al., 2006) and/or become functionalised or tagged by different receptor agonists and/or antibodies (Arruebo et al., 2009) directed towards specific sites *in vivo* for guided diagnostic and therapeutic interventions. Furthermore; due to their unique features, SiNPs are favoured over conventional diagnostic and therapeutic tools, for the delivery of drugs and cancer therapy. For instance; SiNPs are more stable than liposomes (which are composed

of lipid mixtures typical of cellular PMs), as drug nanocarriers (Mu et al., 2012). SiNPs have been shown to be superior in a number of diagnostic methods, *in vitro*. For example, in the study by Ekrami et al. on sputum specimens obtained from patients who were suspected to have pulmonary tuberculosis, the use of bioconjugated fluorescent SiNPs displayed higher diagnostic sensitivity and specificity in detecting *Mycobacterium tuberculosis* compared to conventional methods based on culture, microscopic analysis and polymerase chain reaction (PCR) (Ekrami et al., 2011). *In vivo*, the improved image contrast of ultrasound devices has been demonstrated due to the acoustic behaviour of SiNPs (Casciaro et al., 2010). It was suggested that SiNPs of 330 nm in size at 1-2 x 10^{11} NP/mL were ideal for ultrasound imaging being detectable at high sensitivity at conventional diagnostic frequencies *in vitro* using with agarose phantoms (Casciaro et al., 2010). The ultrasound backscatter amplitude values increased as particle size increased from 160 nm to 330 nm (Casciaro et al., 2010). A further study by Lui et al. showed that systemically administering 100 nm SiNPs into mice could generate a detectable ultrasound response and regarded the latter size of SiNPs as being ideal for such purpose (Liu et al., 2006). The high contrast encountered by the use of SiNPs can overcome the limitation in visualising cancer cells, which are located beyond the capillary vasculature, undetected by encapsulated gas microbubbles (few μm in size) (Casciaro et al., 2010). An additional advantage of using SiNPs over commercial liposomal lipid/polymeric formulations as a contrast agent in ultrasound imaging is their slow degradation and potential for high *in vivo* stability makes them ideal for long-term imaging thereby overcoming the need for high dosages or volumes of traditional contrast agents (Liberman et al., 2014). In a very recent study by Gao et al., the use of rhodamine B dye-encapsulated SiNPs increased the absorption of acoustic energy by ultrasound devices (Gao et al., 2015). According to previous studies from our group, the acute exposure to SiNPs of 100 nm in size had no detrimental effects on the vasodilator responses of large conduit arteries (Akbar et al., 2011). Therefore, our aim was to investigate the effects of SiNPs of approx. 100 nm on the small size arterial function *ex vivo* and *in vivo* using a rat model.

In the present study, we demonstrate the rapid uptake of SiNPs by ECs lining the mesenteric arteries. The neutralisation effect of PSS to SiNPs negative surfaces may have decreased their negative charge and facilitated their uptake into ECs. Incubation of SiNPs for longer periods may promote their uptake into the nucleus of ECs and/or VSMCs; hence, more functional and molecular consequences may become apparent as a consequence. Our findings contradict those from a previous study by Asefa and Tao, suggesting that SiNPs (in their mesoporous form) of less than 100 nm can avoid absorption by the reticuloendothelial system following their iv administration (Asefa and Tao, 2012). The latter may be due to the NP type that they used (mesoporous vs. non-porous SiNPs), hence the ability to accommodate and adsorb different ionic species and serum proteins within the blood *in vivo*. The localisation of our SiNPs in late endosomes indicates their processing to endocytotic pathways, however, a considerable number of particles seem to have used a different route of cellular entry and trafficking. While we cannot exclude that some SiNPs may have been shuttled back to the endothelial PM for extrusion, the majority of nanoparticles remained localised intracellularly and accumulated in the cytoplasm even after 3 hours of incubation.

In the present study, we demonstrated that SiNP uptake by ECs *ex vivo* influences both constrictor and dilator responses. Phe contractile responses *ex vivo* were compromised at high Phe doses by SiNPs. This significant reduction in constriction seems to be specific to the pathways leading to stimulation of VSMCs via α1-adrenoceptors, since no significant effect of SiNPs were observed on AVP responses or KPSS. SiNPs significantly attenuated the vasodilator responses to endothelium-dependent agonist (ACh), while endothelium independent dilation by SNP was unaffected. This may be related to SiNP uptake being evidenced in ECs with no observed entry into VSMCs; hence, VSMCs' sensitivity to NO remained intact.

In the present study, an attempt was made to elucidate the mechanisms leading to attenuated endothelial dependent dilator responses by SiNP uptake, using inhibition and molecular studies. The data obtained from our SOD studies suggest an alternative (ROS independent) mechanism of action of SiNPs characterised by the potential effect(s) of SiNPs interference (interaction, cross-linking, binding and/or cytotoxicity) on the vasodilatory pathway accompanying ACh-induced relaxations. Additional simple physical effects of SiNP presence within cells cannot be excluded. Since EDHF is an important contributor in the dilatory process of small vessels (Hinton and Langton, 2003), (also demonstrated here in), any effects of SiNPs could be mediated through their interference with and/or the block of EDHF action. These effects are hypothesised to be mediated via a direct interaction between SiNPs and cellular ions, organelles, proteins and/or DNA and/or the latter affinity to SiNPs. SiNPs may also affect the basal NO release thereby blocking the vasodilator function of NO and/or its EET-mediated EDHF-backup role (Simonsen et al., 1999). Likewise, SiNPs may impair basal protein levels (for both NO and EDHF pathways, as both contribute to small vessel dilation (Leo et al., 2011)) and/or mRNA and subsequent protein product and/or yield if the vessels are exposed to these NPs for longer periods.

SiNPs may directly and/or indirectly interfere with, disrupt (leading to defective translocation) and/or block SK_{Ca} and IK_{Ca} channels involved in modulating the EDHF signalling and hence inhibit EDHF-mediated relaxation. The potential targets that may be affected by SiNPs are detailed in Table 5 and illustrated in Figure 84. Indirect effects of SiNPs may include physical and/or mechanical effect on the cell membranes of ECs leading to the disruption of the EC membranes as previously reported by Yu et al. (Yu et al., 2009) and altering membrane fluidity (Zhao et al., 2011). The latter membrane changes were previously suggested to have a significant impact on human red blood cells model using mesoporous SiNPs at a size range of 100-200 nm (Zhao et al., 2011). On the other hand, SiNPs adhesion to ECs may cause membrane bending and interaction (obstruct, accommodate, bind and/or block) with ECM, TJ proteins, ion channels and cell surface receptors in addition to being able to accumulate inside cells and deposit within organelles (e.g. endosomes as evident in the current study). Membrane bending of ECs and/or lipid vesicles in response to SiNPs adhesion and/or uptake may lead to mechanical or

morphological changes in lipid vesicles embedded in membranes and hence impaired cellular function(s). This can lead to disruption of the caveolin-rich lipid microdomains (and/or the caveolar caveolin-1) within ECs membranes thereby affecting potassium channels and connexins that reside within these structures and hence influence vasodilation. Caveolae microdomains consist of cholesterol and glycosphingolipids together with self-associating caveolins (Parton and Simons, 2007). The caveolae provide a matrix for compartmentation as they act as mechanotransducers by clamping enzymes such as eNOS and accommodating SK_{Ca} channels in close proximity on ECs membranes and myoendothelial TJs and spaces (Rath et al., 2009). They also promote the coupling between Ca^{2+} (TRPV4) and K^{+} (SK_{Ca}) channels to permit Ca^{2+} entry, which is required to open SK_{Ca} channels on ECs (when reaching Ca^{2+} threshold required), thereby facilitating the generation of PM hyperpolarisation (Rath et al., 2009). Additionally, SiNPs once taken up by ECs, may act indiscriminately in obstructing intracellular receptors and/or pathways leading to protein trafficking, protein misfolding, protein denaturation, protein de-phosphorylation (ERK and Akt as demonstrated in our study) and protein modification defects rather than their direct targeted interaction with cellular compartments and/or molecules. SiNPs may also affect the basal EET or NO release thereby blocking the vasodilator function of EDHF and NO. The above scenarios may prevent the influx of ions such as potassium, disrupt cellular processes and protein trafficking and induce a conformational change to proteins and enzymes causing protein misfolding, cross-linking and/or dephosphorylate proteins leading to their denaturation.

Table 5. Potential targets that may be affected by SiNPs.

SiNPs Target	Target Function(s)	Localisation	Reference
Potassium channels (SK_{Ca} and IK_{Ca})	Mediate the downstream actions of EDHF and are involved in allowing K^+ efflux	SK_{Ca} channels reside within caveolae, whereas IK_{Ca} channels are present in cavelin-1-independent EC fractions	(Absi et al., 2007)
PLA2	Liberates AA from PM	EC PM	(Graziani et al., 2004)
CYP 2C11 (inhibited by sulfaphenazole)	EETs synthesis from AA precursors	ECs' cytosols	
Caveolae microdomains	1. Accommodate SK_{Ca} channels on ECs PMs and TJs. 2. Facilitate the generation of PM hyperpolarisation	ECs PMs, myoendothelial TJs & VSMCs PMs	(Rath et al., 2009)
Caveolin-1 protein	1. Act as regulatory scaffold for numerous signalling proteins 2. Involved in endothelial connexins shuttling to the PM and myoendothelial gap-junction formation. 4. Spread of the electric current mediating the EDHF	Within caveolae	(Saliez et al., 2008)
Connexins (Cx37, -40, and -43)	Modulate EDHF-related pathway & interact with caveolin-1	Lipid raft domains and caveolae	(Schubert et al., 2002)

Thus, the physicochemical interaction of SiNPs with cellular organelles and molecular species such as proteins (in our case; ERK and Akt) need to be fully investigated to determine the underlying cause of the SiNP-mode of action observed *ex vivo* as well as *in vivo* at the physiological and molecular levels. Furthermore, SiNP adhesion to the vascular endothelium as well as their uptake in late endosomes (Figure 64F) may contribute to increased membrane bending of ECs and/or lipid vesicles. This may lead to mechanical or morphological changes in lipid vesicles and hence impaired cellular function(s).

A comparison between the *ex vivo* and *in vivo* findings suggests that the functional effects of SiNPs are more pronounced *ex vivo*. Whilst in the *ex vivo* vessels there was a significant reduction in ACh dependent dilator responses at most concentrations, the attenuated dilation was only apparent at the lower ACh concentrations, *in vivo*. This was similar for Phe induced constrictor responses. This may be because, *in vivo*, the injected nanoparticles adsorb proteins from the serum (Ang et al., 2014). This leads to corona formation, evidenced in the present study by the altered SiNPs size, Zeta potential and morphology over time when the SiNPs were incubated in whole blood (Figures 39-41), and consequently altered surface characteristics of the nanoparticles such that they have less detrimental effect on vascular function. In contrast, for endothelial independent responses, the *in vivo* injected SiNPs induced a significant reduction in SNP induced dilation, as we have previously demonstrated for the QDs (Shukur et al., 2013). This has important medical implications, as SNP based drugs are used in heart disease patients. Hence, strategies would have to be developed to avoid such effects of SiNPs (Discussed in the future work section).

7.3 Conclusion

This is a novel study implicating the influence of nanomaterials on small rat mesenteric arterial function. The experimental protocols implemented in the present study enabled the fabrication and characterisation of SiNPs and the assessment of vascular function in response to various agonists after acute exposure to luminescent SiNPs both *ex vivo* and *in vivo*. The main findings of this study indicate that rapid uptake of SiNPs by ECs lining the vasculature can alter the physiological function of rat mesenteric vessels, depending on their dosage. A schematic illustration summarising the effects of SiNPs on the vasodilator function of the mesenteric artery with the potential key targets within the vasodilatory mechanisms involved in mediating their behaviour *ex vivo* are outlined in figure 84. SiNPs may interfere with the EDHF and NO pathways leading to potassium channel inactivation (SK_{Ca} and IK_{Ca}, in particular) as well as decreased availability of NO and/or H_2O_2 (Figure 84). The mode of action of SiNPs may be mediated via their potential effects in altering cell surface receptors, enzymes and/or kinases, dephosphorylation of enzymes (Erk and Akt), interference with enzymatic substrate pockets and/or competition, interaction with the components of TJs ad well as simple physical effects (Figure 84).

In addition to contributing to future medical diagnostics and therapeutics, NPs may also provide a useful tool to studying small arterial function at both the physiological and biochemical levels through their capacity to integrate and interfere with various molecular and cellular processes within the vasculature. Due to their promising role in biomedical applications, QDs, SiNP and CNTs biocompatibility and long-term safety and clearance must be carefully evaluated in preclinical studies before they could be translated for clinical use. This strategy will ensure the safe administration of these agents *in vivo* and guide their use in medical applications.

Our findings highlight the importance of assessing the biosafety of NPs for use in imaging diagnostics and medical interventions such as therapeutics, in order to minimise their toxicological influence on vessel contractility and function. One approach may involve the use of SiNPs at a lower dosage, which in our study resulted in less detrimental impact of vascular function *ex vivo*.

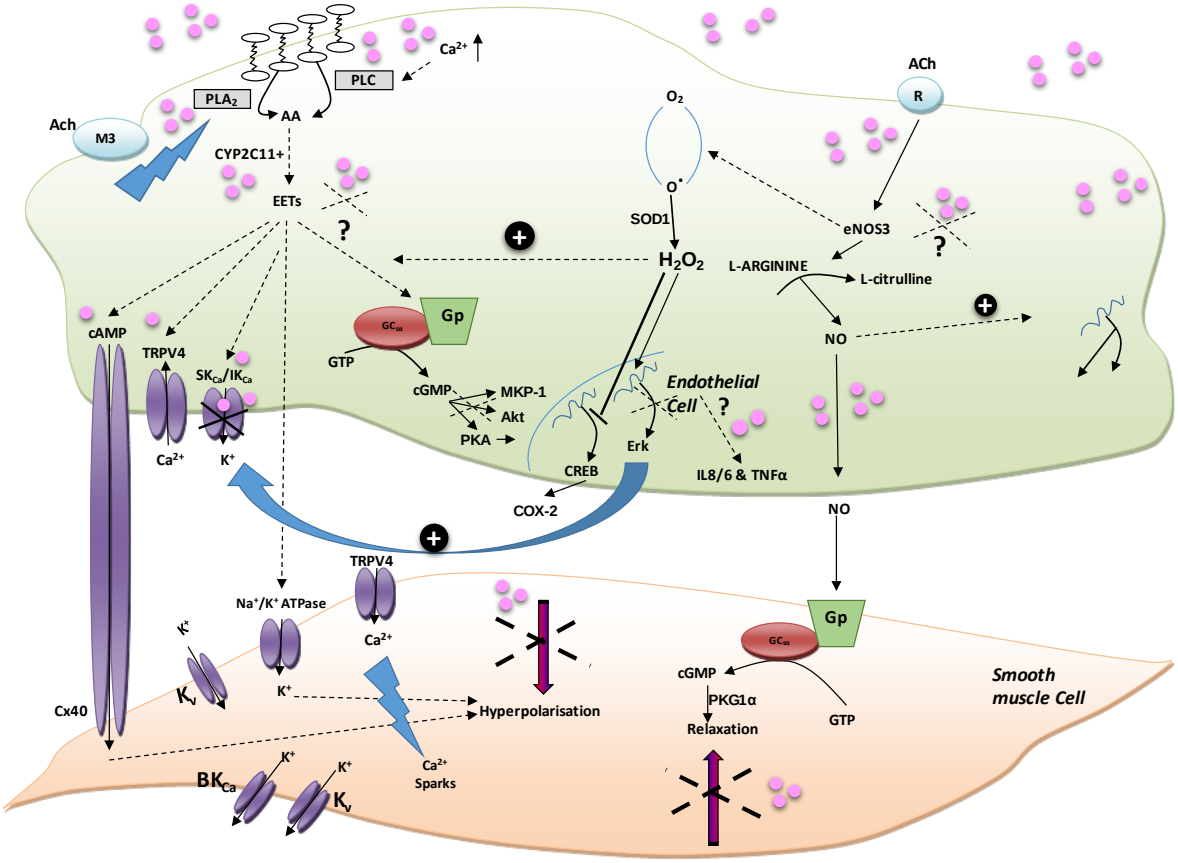

Figure 84. A schematic illustration summarising the effect of SiNPs on the vasodilator function of ECs and VSMCs of the MA and the proposed and potential associated mechanisms involved mediating their behaviour *ex vivo*. EDHF; endothelial-derived hyperpolarising factor (EDHF), eNOS; endothelial-derived NO synthase, SiNPs; silica nanoparticles. SiNPs may directly interfere with the EDHF pathway by inactivating the SK_{Ca} and IK_{Ca} channels. Author originated.

Chapter 8.

Future Work

SiNPs have potential use in imaging diagnostics. However, our study suggests that dye-encapsulated SiNPs have detrimental effects on vascular function, attributed to their properties, including their chemical composition (dye molecules encapsulated within SiNPs), surface area and dosimetry. Furthermore, we have demonstrated that SiNPs influence vascular function by affecting the cascade of NO/EDHF production within the vascular endothelial cells through the down-regulation of ERK and Akt. Future work may involve a number of investigations, as follows:

8.1 SiNPs

In the current study SiNPs stability were characterised in water, ethanol, PSS and blood. Initial future work using SiNPs (with and without dye) will be needed to characterise their size, morphology and stability in blood, in real time as well as in cell media (to permit cell culture studies).

8.2 Functional Studies

8.2.1 *In Vivo* Studies

More *in vivo* studies will need to be carried out to increase the n number of experiments and also account for the following;

1. The effect of a range of SiNPs dosages on small MA function as well as large conduit arteries (aortic vessel) to determine the minimum dosage of SiNPs required for safe administration *in vivo*.
2. The effects of SiNPs on ageing rats. This is relevant to older patients suffering from vascular disease, as they will require diagnostic and/or therapeutic interventions involving SiNPs.

8.2.2 *Ex Vivo* Studies

More *ex vivo* studies will need to be carried out to examine for the following;

1. SiNPs uptake and influence under flow and elevated pressure conditions: A preliminary experiment was carried out to determine the influence of SiNPs on mesenteric artery function under flow conditions and high intra-luminal pressure (100 mmHg) (Figures 85 and 66). The latter experiments provided a similar pattern to SiNPs effects as *ex vivo* under static conditions and at 60 mmHg pressure in terms SiNPs uptake into ECs and attenuated vasodilator responses. Because increased uptake is suggested under elevated pressure, this is of important relevance for patients with hypertension and needs to be further investigated.
2. A comparison between the effects of dye-encapsulated vs. bare SiNPs on vascular function: There is a need to assess the function of bare SiNPs without dye on mesenteric artery function *ex vivo* to exclude the role of the dye in mediating the effects of dye-encapsulated SiNPs on mesenteric function.
3. The influence of SiNPs on signal transduction pathways: The proteomics experiment results obtained will need to be confirmed further using the Western blotting technique targeting the expression levels of both ERK and Akt. The proteomics results can also be confirmed by the use of antibodies to specifically target the level of phosphorylation of the protein isoforms related to the rat MAs and thought to be affected through the SiNPs injury to the vascular homeostasis. Table 6 lists the main receptors, enzymes, adapter proteins and transcription factors involved in mediating the contractile and dilator responses in MAs *ex vivo*. This further investigation may suggest the detailed molecular mechanism underlining SiNPs action(s) involving its effects on the upstream signalling cascade and downstream regulators of genetic regulation and expression (if any).
4. The long-term or chronic influence of SiNPs on vascular function: Although the physiological effects of SiNPs uptake are apparent 30 minutes after incubation, however a change in the level of expression of the targets listed in Table 6, which may be affected by SiNPs may require longer incubation periods. Hence,

time-course experiments are needs with changes (if any) being accounted for using real-time PCR. Time-course experiments can also provide information on whether SiNPs can be translocated and deposited in VSMCs. This may determine whether that lack of effects of SiNPs on VSMCs was simply due insufficient time for SiNPs to penetrate the VSMC layer or whether there is a physical barrier to SiNPs entry.

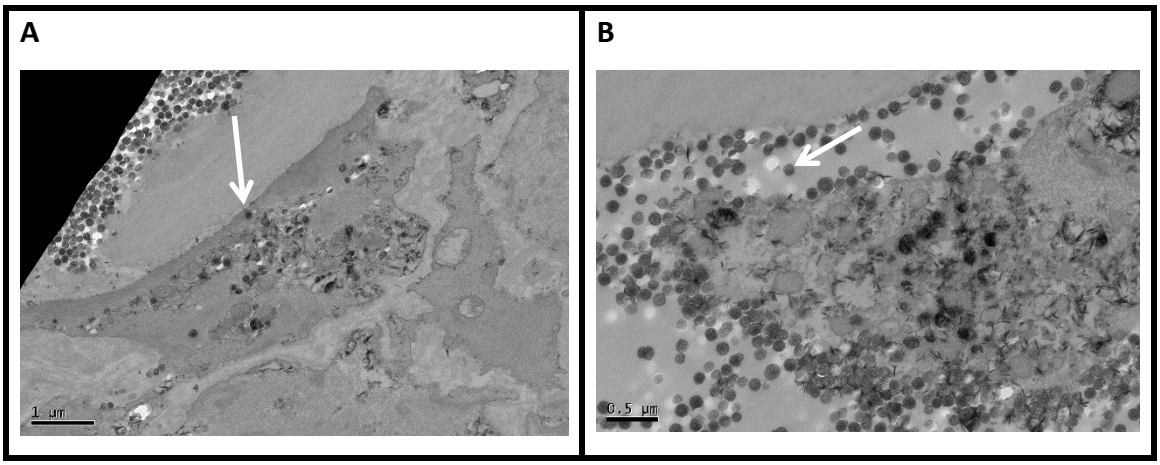

Figure 85. TEM images (A-D) illustrating the internalisation of SiNPs into the vascular endothelium of the MAs after 30 minute of incubation in SiNPs under flow conditions. The SiNPs are represented by black spherical structures inside ECs (arrows).

8.3 Cellular and Molecular Studies

Due to time limitation and the length and effort required to perform the physiological studies, it did not permit the examination of SiNPs on isolated human cardiac microvascular endothelial cells (HCMECs), complicated by the difficulty of growing and expanding the latter cells *in vitro*. The purpose of using the HCMECs was to provide a model for translating the results obtained *ex vivo* into a human *in vitro* model using cell culture. The design for a series of experiments using the HCMECs is detailed in Appendix 7. Other cell types can also be used. These may include human aortic endothelial cells to provide a model for SiNPs interaction with large arteries. The effect of bare or dye-encapsulated SiNPs uptake on cell proliferation and apoptosis can then be determined. In addition, different concentrations of the RBITC dye on cell proliferation will be analysed. The influence of dosage and size of SiNPs as well as dye encapsulation of SiNPs can be established.

8.3.1 To Determine the Influence of SiNPs Uptake on HCMECs Function (effect of SiNPs size and dosage)

Cell-lines from HCMECs (obtained from PromoCell) from frozen will be cultured in Dulbecco's Modified Eagles growth medium using standard cell culture techniques. SiNP suspensions of a range of concentrations (1 x $10^{9\text{-}12}$ NP/mL) can be preprepared in cell culture medium. Cells seeded in a 24-well plate at a density of 5 x 10^4 cells per well can then be exposed to SiNPs for different time-points (10 minutes, 30 minutes, 1, 2, 6, 8, 15, 24, 48 and 72 in hours) and following agonist stimulation. Cells can then be incubated in SiNPs while maintained at 37℃ in a 5% CO_2 humidified environment. SiNPs uptake by HCMECs will be visualised using confocal fluorescence microscopy (Leica SP2 laser scanning confocal microscope). However, more detailed analysis of the localisation of SiNPs in relation to the morphology of the cells can be examined under TEM. For TEM analysis; SiNP suspensions containing the appropriate sizes and dosage of SiNPs can be applied to the cells seeded in 6-well plates at a density of 2 × 10^5 cells per well, at 37℃ in a 5% CO_2 humidified environment for different time courses. Cells can then be trypsinised and then centrifuged to remove the trypsin. The pellets can be fixed in a Karnovsky's fixative containing phosphate buffered 2% glutaraldehyde and 2.5% paraformaldehyde.

Microwave fixation can be used with this primary fixative and the pellets washed in cacodylate buffer with no further additives. Samples can then be fixed and processed for TEM as previously described by Kim et al. (Kim et al., 2015). SiNP uptake into cells can also be quantified by ICP. The Influence of SiNPs on cell proliferation and viability can be assessed using 3-(4,5-Dimethylthiazol-2-yl)-2,5-diphenyltetrazolium bromide (MTT, Sigma-Aldrich, St Louis, MO) reduction. After exposure of cells to SiNPs of each size at the selected concentrations, the medium can be removed and the cells can be washed with PBS. The cells can then be incubated in fresh serum-free medium containing 0.5 mg/mL of MTT for 4 hours 37℃. The resulting formazan product can then be dissolved in DMSO, and the collected samples cab be centrifuged at 12,000 rpm for 5 minutes to remove any remaining SiNPs. 100 µL of the supernatant can then be transferred to a fresh well of a 96-well plate and absorbance can be measured at 570 nm using a microplate reader (Synergy-HT, BioTek, Winooski, VT) (Kim et al., 2015). The lactate dehydrogenase (LDH) assay can also be performed to assess membrane disruption caused by SiNPs. The assay can be conducted using the CytoTox96® Non-Radioactive Cytotoxicity Assay kit (Promega, Madison, WI). Following the incubation in SiNPs, cells can be prepared for the LDH assay and the absorbance can be measured at 490 nm using a microplate reader (Synergy-HT, BioTek, Winooski, VT). This will examine the level of LDH release by cells following SiNPs incubation.

8.3.2 To Investigate the Pathway for SiNP-dependent Uptake by HCMECs

Inhibitor experiments can be conducted to identify the uptake route used by SiNPs using e.g. endocytic inhibitors that specifically block individual cellular uptake pathways (Qualmann et al., 2000). For instance, chlorpromazine is a cationic amphiphilic inhibitor which is known to block the clathrin-mediated pathway, where it reversibly translocases clathrin and its adapter proteins from the cell surface to intracellular vesicles (Vercauteren et al., 2010; Wang et al., 1993). Whereas, Cytochalasin D acts to disrupt the actin filaments within the cytoskeleton by inducing ATP hydrolysis in actin subunits, leading to an accumulation of ADP containing actin monomers and increasing the ratio of actin-ADP/acting-ATP (Goddette and Frieden, 1986). Likewise, nocodazole is also involved in depolymerising the microtubule network by stimulating the hydrolysis of GTP in tubulin monomers and thereby leading to incorporation of GDP-tubulin into the filaments (Vasquez

et al., 1997). Markers for cathrin- and caveolin-mediated uptake such as glycoprotein transferrin and sphingolipid lactosylceramide respectively (Conner and Schmid, 2003; Vercauteren et al., 2010), can be used in investigating the path of NP-dependent entry to cellular compartments. We can also test whether the disruption of microtubules or actin network (Dausend et al., 2008; Raghu et al., 2009) by nocodazole or cytochalasin D respectively may influence the cellular uptake of SiNPs.

8.3.3 To determine ROS Generation Induced by SiNPs Uptake

The intracellular levels of ROS within the cultured cells following SiNPs uptake can be determined from cells exposed to various sizes and dosage of SiNPs using the cell-permeable fluorogenic probe, 2,7-dichlorodihydrofluorescein diacetate (DCFH-DA). DCFH-DA can diffuse into cells, where it can react with ROS to form the highly fluorescent product 2,7-dichlorodihydrofluorescein (DCF). Cells can be seeded into a 96-well plate at a density of 1.0×10^4 cells per well and pre-treated with DCFH-DA stock solution for 30 minutes before the administration of SiNPs. The fluorescence of oxidised DCF can be measured on a microplate reader (Synergy-HT, BioTek, Winooski, VT) at excitation and emission wavelengths of 480 nm and 530 nm, respectively (Kim et al., 2015).

8.3.4 To Determine the Mechanism of Attenuated Dilation Induced by SiNPs

There is no information on the mechanism of attenuated dilation in small arteries by the uptake of SiNPs, as far as we are aware. Hence, the future work will attempt to fulfil this gap and investigate further the molecular mechanisms underpinning the NP's-physiological effects on the vasculature. The aim of the molecular study is to determine the molecular mechanisms of SiNP-associated effects on isolated arteries (aortic and mesenteric arterial segments) and cell cultures. In addition to their role in compromising vasodilation, SiNPs may trigger an immune response by the vascular ECs (Abbot et al., 1992; Scott and Bicknell, 1993). The uptake of SiNPs may provoke an immunological response by ECs lining the vascular lumen causing EC dysfunction, damage and necrotic cell death through caspases 3 and 7-dependent pathway (Bauer et al., 2011). Previous studies highlighted the release of IL-8 by ECs as a response to NP uptake (Hetland et al., 2001; Cho et al., 2007). NPs may further activate the EC-coagulation system thus switching the vessel wall into a pro-

thrombotic and inflammatory surface (Wagner and Frenette, 2008), which can potentially trigger vascular disease due to the loss of the anti-thrombotic and anti-inflammatory properties of ECs (Spiel et al., 2008). Thus, mRNA extraction (Hilgers et al., 2006), real-time quantitative PCR array analysis and Western blotting techniques will be used to monitor the up- or down regulation in expression of potential target genes and the levels of proteins involved in the EDHF and NO-mediated pathways (Table 6). These techniques will be performed on snap-frozen homogenised vessels (Saitoh et al., 2012) as well as the cell cultures. GenBank will be searched for the DNA sequences related to the gene targets list involved in mediating vascular dilation and inflammatory responses. The intracellular gene or protein candidates that are likely to be affected by SiNPs and will include inflammatory cytokine, receptors, adapter proteins, kinases and enzymes (Table 6). These targets are involved in mediating and facilitating vasodilator and inflammatory pathways that accompany vessel function. For the isolated arteries, the influence of uptake of SiNPs (at 5.32×10^{11} NP/mL) on the gene and protein targets will be tested following the acute (30 minutes) and longer term exposure to SiNPs following the stimulation by agonists.

Table 6. Potential protein or gene target list for the vasodilatory and inflammatory pathways in ECs including; potassium channels, receptors, kinases, enzymes, cytokines, cytokine receptors and inflammatory markers.

Cytokines: IL-1, 4, 6 and 15	**Cytokine Receptors: for IL-1, IL-6, IL-6 signal transducer (IL-6ST), TNFα and γ-IFN.**	**α1-adrenergic receptor and muscarinic M3 receptor**
Kinases: PKG, PKG1α, CaMKKβ, PKA, PKC, MAPK (1,8 and 14), ERK and Akt	**Enzymes: eNOS, CaM, CaMKII, COX-2, 3MST, CBS, CSE, PLA2, PLC, Endothelial adenylyl cyclase, CYP epoxygenases and monooxygenase, CYP4A, SOD1 and Catalytic, α-polypeptide (PIK3CA)**	**TRPV4 channel**
Potassium Channels: K_{Ca}^{+}, SK_{Ca} (SK_{Ca}2.3), IK_{Ca} (K_{Ca} 3.1) and BK_{Ca}	**Rat-specific voltage-gated potassium channels: rv-K_{IR}6.1, rvK_{IR}6.2, rvK_{IR}SUR1 and rvSUR2B**	**Transcription Factors: CREB, NF-κB, PPAR-α, PPAR-γ and FABPs**

8.3.5 To investigate the Strategies to Enhance SiNPs Biocompatibility *in vivo*

To enhance the biocompatibility of SiNPs a number of strategies can be adopted. One of which may involve the use of an inorganic core or shell of nanostructured magnetic iron oxide (Abbas et al., 2014), such as magnetite (Fe_3O_4), and maghemite (γ-Fe_2O_3) (Mahdavi et al., 2013) with SiNPs. Iron oxide NPs may be prone to clearance from the body, perhaps through iron processing in the spleen, hence SiNPs attachment or incorporation may bypass SiNPs effects *in vivo* (e.g. tissue deposition and bioaccumulation) as well as enhancing their chemical stability (Nidhin et al., 2008). Such superparamagnetic NPs may also enhance the use of the iron oxide-SiNPs hybrids in magnetic resonance imaging (MRI) as diagnostic probes (B. H. Kim et al., 2011). Another approach may involve the coating of SiNPs with micelles (Huo et al., 2006), peptides, polysaccharides or polymers of biocompatible nature such as dextran (Hong et al., 2008), chitosan (Li et al., 2008), poly(ethylenimine) (PEI) (Yiu et al., 2010) and PEG (Mukhopadhyay et al., 2012) to stabilise and safely process SiNPs *in vivo*. The coating of SiNPs with PEG lipids was previously suggested to increase their blood circulation lifetime and prevent SiNPs from aggregation, and hence the clogging of capillaries in the lung and liver of SiNP-injected mice (van Schooneveld et al., 2008). The conjugation of SiNPs with peptides or proteins such as antibodies (Tsagkogeorgas et al., 2006) may minimise their non-specific off-target interaction and enhance their selective targeting *in vivo*. Furthermore; a study by Ma et al. suggested the improvement of SiNPs compatibility, using HUVECs cell line, following the incorporation of the liposomal architecture into cerasomes made from SiNPs core structures (Ma et al., 2011). Hence, there is a need to further assess the biosafety of SiNPs and enable their safe administration *in vivo*.

References

Abbas, M., Ramulu, S., Torati, S. R., Lee, C. S., Rinaldi, C. and Kim, C. (2014) 'Fe3O4/SiO2 Core/Shell Nanocubes: Novel Coating Approach with Tunable Silica Thickness and Enhancement in Stability and Biocompatibility.' *J Nanomed Nanotechnol* 5, Nov 23, p. 244.

Abbot, S. E., Kaul, A., Stevens, C. R. and Blake, D. R. (1992) 'Isolation and culture of synovial microvascular endothelial cells. Characterization and assessment of adhesion molecule expression.' *Arthritis Rheum*, 35(4), Apr, pp. 401-406.

Absi, M., Burnham, M. P., Weston, A. H., Harno, E., Rogers, M. and Edwards, G. (2007) 'Effects of methyl beta-cyclodextrin on EDHF responses in pig and rat arteries; association between SK(Ca) channels and caveolin-rich domains.' *Br J Pharmacol*, 151(3), Jun, pp. 332-340.

Abu-Soud, H. M. and Stuehr, D. J. (1993) 'Nitric oxide synthases reveal a role for calmodulin in controlling electron transfer.' *Proceedings of the National Academy of Sciences*, 90(22), November 15, 1993, pp. 10769-10772.

Adeagbo, A. S. and Henzel, M. K. (1998) 'Calcium-dependent phospholipase A2 mediates the production of endothelium-derived hyperpolarizing factor in perfused rat mesenteric prearteriolar bed.' *J Vasc Res*, 35(1), Jan-Feb, pp. 27-35.

Aillon, K. L., Xie, Y., El-Gendy, N., Berkland, C. J. and Forrest, M. L. (2009) 'Effects of nanomaterial physicochemical properties on in vivo toxicity.' *Adv Drug Deliv Rev*, 61(6), Jun 21, pp. 457-466.

Ait-Slimane, T., Galmes, R., Trugnan, G. and Maurice, M. (2009) 'Basolateral internalization of GPI-anchored proteins occurs via a clathrin-independent flotillin-dependent pathway in polarized hepatic cells.' *Mol Biol Cell*, 20(17), Sep, pp. 3792-3800.

Akbar, N., Mohamed, T., Whitehead, D. and Azzawi, M. (2011) 'Biocompatibility of amorphous silica nanoparticles: Size and charge effect on vascular function, in vitro.' *Biotechnol Appl Biochem*, 58(5), Sep-Oct, pp. 353-362.

Akhtar, M. J., Ahamed, M., Kumar, S., Siddiqui, H., Patil, G., Ashquin, M. and Ahmad, I. (2010) 'Nanotoxicity of pure silica mediated through oxidant generation rather than glutathione depletion in human lung epithelial cells.' *Toxicology*, 276(2) pp. 95-102.

Akitoshi, Y. (2005) 'Silica Nucleation, Polymerization, and Growth Preparation of Monodispersed Sols.' *In Colloidal Silica*. CRC Press, pp. 47-56.

Al-Jamal, W. T., Al-Jamal, K. T., Cakebread, A., Halket, J. M. and Kostarelos, K. (2009) 'Blood Circulation and Tissue Biodistribution of Lipid−Quantum Dot (L-QD) Hybrid Vesicles Intravenously Administered in Mice.' *Bioconjugate Chemistry*, 20(9), 2009/09/16, pp. 1696-1702.

Allen, M., Law, F. and Rushton, N. (1994) 'The effects of diamond-like carbon coatings on macrophages, fibroblasts and osteoblast-like cells in vitro.' *Clin Mater*, 17(1), /, pp. 1-10.

Allen, M., Myer, B. and Rushton, N. (2001) 'In vitro and in vivo investigations into the biocompatibility of diamond-like carbon (DLC) coatings for orthopedic applications.' *J Biomed Mater Res*, 58(3), May 1, pp. 319-328.

Alonso, D. and Radomski, M. W. (2003) 'Nitric oxide, platelet function, myocardial infarction and reperfusion therapies.' *Heart Fail Rev*, 8(1), Jan, pp. 47-54.

Andersson, N., Alberius, P. C. A., Pedersen, J. S. and Bergstrom, L. (2004) 'Structural features and adsorption behaviour of mesoporous silica particles formed from droplets generated in a spraying chamber.' *Microporous and Mesoporous Materials*, 72(1-3), Jul 8, pp. 175-183.

Ang, J. C., Henderson, M. J., Campbell, R. A., Lin, J. M., Yaron, P. N., Nelson, A., Faunce, T. and White, J. W. (2014) 'Human serum albumin binding to silica nanoparticles - effect of protein fatty acid ligand.' *Phys Chem Chem Phys*, Mar 5,

Arap, W., Pasqualini, R., Montalti, M., Petrizza, L., Prodi, L., Rampazzo, E., Zaccheroni, N. and Marchio, S. (2013) 'Luminescent Silica Nanoparticles for Cancer Diagnosis.' *Current Medicinal Chemistry*, 20(17), Jun, pp. 2195-2211.

Archer, S. L., Huang, J. M. C., Hampl, V., Nelson, D. P., Shultz, P. J. and Weir, E. K. (1994) 'Nitric-Oxide and Cgmp Cause Vasorelaxation by Activation of a Charybdotoxin-Sensitive K-Channel by Cgmp-Dependent Protein-Kinase.' *Proceedings of the National Academy of Sciences of the United States of America*, 91(16), Aug 2, pp. 7583-7587.

Arruebo, M., Valladares, M. and Gonzalez-Fernandez, A. (2009) 'Antibody-Conjugated Nanoparticles for Biomedical Applications.' *Journal of Nanomaterials*,

Asefa, T. and Tao, Z. M. (2012) 'Biocompatibility of Mesoporous Silica Nanoparticles.' *Chemical Research in Toxicology*, 25(11), Nov, pp. 2265-2284.

Ashcroft, F. M. (1988) 'Adenosine 5'-triphosphate-sensitive potassium channels.' *Annu Rev Neurosci*, 11, /, pp. 97-9118.

Asokan, A. and Cho, M. (2002) 'Exploitation of intracellular pH gradients in the cellular delivery of macromolecules.' *J Pharm Sci*, 91 pp. 903 - 913.

Atkins, P. W. (2005) The Second Law. *Physical chemistry*. 8th ed., pp. 76-109. New York: W.H. Freeman and Co.

Azzawi, M. and Austin, C. (2006) 'Extravascular pressure modulates responses of isolated rat coronary arteries to vasodilator, but not vasoconstrictor, stimuli.' *Am J Physiol Heart Circ Physiol*, 290(3), Mar, pp. H1151-1156.

Baalousha, M., Kammer, F. V. D., Motelica-Heino, M., Hilal, H. S. and Le Coustumer, P. (2006) 'Size fractionation and characterization of natural colloids by flow-field flow fractionation coupled to multi-angle laser light scattering.' *Journal of Chromatography A*, 1104(1-2), Feb 3, pp. 272-281.

Bachschmid, M., Schildknecht, S. and Ullrich, V. (2005) 'Redox regulation of vascular prostanoid synthesis by the nitric oxide-superoxide system.' *Biochem Biophys Res Commun*, 338(1), Dec 9, pp. 536-542.

Badr, G., Sayed, D., Maximous, D., Mohamed, A. O. and Gul, M. (2014) 'Increased Susceptibility to Apoptosis and Growth Arrest of Human Breast Cancer Cells Treated by a Snake Venom-Loaded Silica Nanoparticles.' *Cellular Physiology and Biochemistry*, 34(5) pp. 1640-1651.

Bakalova, R., Zhelev, Z., Aoki, I., Masamoto, K., Mileva, M., Obata, T., Higuchi, M., Gadjeva, V. and Kanno, I. (2008) 'Multimodal silica-shelled quantum dots: direct intracellular delivery, photosensitization, toxic, and microcirculation effects.' *Bioconjug Chem*, 19(6), Jun, pp. 1135-1142.

Baktur, R., Patel, H. and Kwon, S. (2011) 'Effect of exposure conditions on SWCNT-induced inflammatory response in human alveolar epithelial cells.' *Toxicol In Vitro*, 25(5), Aug, pp. 1153-1160.

Barbé, C., Bartlett, J., Kong, L., Finnie, K., Lin, H. Q., Larkin, M., Calleja, S., Bush, A. and Calleja, G. (2004) 'Silica Particles: A Novel Drug-Delivery System.' *Advanced Materials*, 16(21) pp. 1959-1966.

Barlow, R. S., El-Mowafy, A. M. and White, R. E. (2000) 'H(2)O(2) opens BK(Ca) channels via the PLA(2)-arachidonic acid signaling cascade in coronary artery smooth muscle.' *Am J Physiol Heart Circ Physiol*, 279(2), 08/, pp. 475-483.

Barratt, G. (2003) 'Colloidal drug carriers: achievements and perspectives.' *Cellular and Molecular Life Sciences*, 60(1), Jan, pp. 21-37.

Barshan-Tashnizi, M., Ahmadian, S., Niknam, K., Torabi, S.-F. and Ranaei-Siadat, S.-O. (2009) 'Covalent immobilization of Drosophila acetylcholinesterase for biosensor applications.' *Biotechnol Appl Biochem*, 52(18570631) pp. 257-264.

Bass, J. D., Grosso, D., Boissiere, C., Belamie, E., Coradin, T. and Sanchez, C. (2007) 'Stability of Mesoporous Oxide and Mixed Metal Oxide Materials under Biologically Relevant Conditions.' *Chemistry of Materials*, 19(17), 2007/08/01, pp. 4349-4356.

Bauer, A. T., Strozyk, E. A., Gorzelanny, C., Westerhausen, C., Desch, A., Schneider, M. F. and Schneider, S. W. (2011) 'Cytotoxicity of silica nanoparticles through exocytosis of von Willebrand factor and necrotic cell death in primary human endothelial cells.' *Biomaterials*, Aug 12,

Bauersachs, J., Popp, R., Hecker, M., Sauer, E., Fleming, I. and Busse, R. (1996) 'Nitric oxide attenuates the release of endothelium-derived hyperpolarizing factor.' *Circulation*, 94(12), Dec 15, pp. 3341-3347.

Beckman, J. S., Beckman, T. W., Chen, J., Marshall, P. A. and Freeman, B. A. (1990) 'Apparent hydroxyl radical production by peroxynitrite: implications for endothelial injury from nitric oxide and superoxide.' *Proc Natl Acad Sci U S A*, 87(4), Feb, pp. 1620-1624.

Bellien, J., Thuillez, C. and Joannides, R. (2008) 'Contribution of endothelium-derived hyperpolarizing factors to the regulation of vascular tone in humans.' *Fundam Clin Pharmacol*, 22(4), Aug, pp. 363-377.

Bellien, J., Iacob, M., Gutierrez, L., Isabelle, M., Lahary, A., Thuillez, C. and Joannides, R. (2006) 'Crucial role of NO and endothelium-derived hyperpolarizing factor in human sustained conduit artery flow-mediated dilatation.' *Hypertension*, 48(6), Dec, pp. 1088-1094.

Bernanke, D. H. and Velkey, J. M. (2002) 'Development of the coronary blood supply: Changing concepts and current ideas.' *Anat Rec*, 269(4) pp. 198-208.

Birdi, K. S. (2009) 'Colloidal Systems.' *In Surface and Colloid Chemistry*. CRC Press, pp. 141-159.

Blatter, L. A. and Wier, W. G. (1994) 'Nitric oxide decreases [Ca2+]i in vascular smooth muscle by inhibition of the calcium current.' *Cell Calcium*, 15(2), Feb, pp. 122-131.

Bogush, G. H. and Zukoski, C. F. (1991) 'Studies of the Kinetics of the Precipitation of Uniform Silica Particles through the Hydrolysis and Condensation of Silicon Alkoxides.' *Journal of Colloid and Interface Science*, 142(1), Mar 1, pp. 1-18.

Bogush, G. H., Tracy, M. A. and Zukoski, C. F. (1988) 'Preparation of Monodisperse Silica Particles - Control of Size and Mass Fraction.' *Journal of Non-Crystalline Solids*, 104(1), Aug, pp. 95-106.

Bolton, T. B. (1979) 'Mechanisms of action of transmitters and other substances on smooth muscle.' *Physiol Rev*, 59(3), Jul, pp. 606-718.

Borak, B., Biernat, P., Prescha, A., Baszczuk, A. and Pluta, J. (2012) 'In Vivo Study on the Biodistribution of Silica Particles in the Bodies of Rats.' *Advances in Clinical and Experimental Medicine*, 21(1), Jan-Feb, pp. 13-18.

Borm, P. J. A. and Müller-Schulte, D. (2006) 'Nanoparticles in drug delivery and environmental exposure: same size, same risks?' *Nanomedicine*, 1(2), 2006/08/01, pp. 235-249.

Bottini, M., Cerignoli, F., Dawson, M. I., Magrini, A., Rosato, N. and Mustelin, T. (2006) 'Full-length single-walled carbon nanotubes decorated with streptavidin-conjugated quantum dots as multivalent intracellular fluorescent nanoprobes.' *Biomacromolecules*, 7(8), Aug, pp. 2259-2263.

Breslow, N. E. and Clayton, D. G. (1993) 'Approximate Inference in Generalized Linear Mixed Models.' *Journal of the American Statistical Association*, 88(421) pp. 9-25.

Brodde, O. E. (1994) 'Adrenoceptors and their signal transduction mechanisms.' *J Auton Pharmacol*, 14(1) pp. 3-4.

Burnham, M. P., Johnson, I. T. and Weston, A. H. (2006) 'Impaired small-conductance Ca2+-activated K+ channel-dependent EDHF responses in Type II diabetic ZDF rats.' *Br J Pharmacol*, 148(4), Jun, pp. 434-441.

Burns, A., Ow, H. and Wiesner, U. (2006) 'Fluorescent core-shell silica nanoparticles: towards "Lab on a Particle" architectures for nanobiotechnology.' *Chemical Society Reviews*, 35(11) pp. 1028-1042.

Busse, R., Trogisch, G. and Bassenge, E. (1985) 'The role of endothelium in the control of vascular tone.' *Basic Res Cardiol*, 80(3000343) pp. 475-490.

Bychkov, R., Burnham, M. P., Richards, G. R., Edwards, G., Weston, A. H., Feletou, M. and Vanhoutte, P. M. (2002) 'Characterization of a charybdotoxin-sensitive intermediate conductance Ca2+-activated K+ channel in porcine coronary endothelium: relevance to EDHF.' *Br J Pharmacol*, 137(12466245) pp. 1346-1354.

Byers, C. H., Harris, M. T. and Williams, D. F. (1987) 'Controlled Microcrystalline Growth-Studies by Dynamic Laser-Light-Scattering Methods.' *Industrial & Engineering Chemistry Research*, 26(9), Sep, pp. 1916-1923.

Campbell, J. H. and Campbell, G. R. (1986) 'Endothelial cell influences on vascular smooth muscle phenotype.' *Annu Rev Physiol*, 48(3518616) pp. 295-306.

Campbell, W. B., Gebremedhin, D., Pratt, P. F. and Harder, D. R. (1996) 'Identification of epoxyeicosatrienoic acids as endothelium-derived hyperpolarizing factors.' *Circ Res*, 78(3), Mar, pp. 415-423.

Canton, G., Carmignato, S., Ricco, R., Marinello, F. and Enrichi, F. (2011) 'Modified Stöber synthesis of highly luminescent dye-doped silica nanoparticles.' *J Nanopart Res*, May

Cao, K., Tang, G., Hu, D. and Wang, R. (2002) 'Molecular basis of ATP-sensitive K+ channels in rat vascular smooth muscles.' *Biochem Biophys Res Commun*, 296(2), Aug 16, pp. 463-469.

Cardillo, C., Kilcoyne, C. M., Quyyumi, A. A., Cannon, R. O. and Panza, J. A. (1997) 'Decreased Vasodilator Response to Isoproterenol During Nitric Oxide Inhibition in Humans.' *Hypertension*, 30(4), October 1, 1997, pp. 918-921.

Carl, A., Lee, H. K. and Sanders, K. M. (1996) 'Regulation of ion channels in smooth muscles by calcium.' *American Journal of Physiology - Cell Physiolog*, 271(1), 1996-07-01 07:00:00, pp. C9-C34.

Casciaro, S., Conversano, F., Ragusa, A., Malvindi, M. A., Franchini, R., Greco, A., Pellegrino, T. and Gigli, G. (2010) 'Optimal Enhancement Configuration of Silica Nanoparticles for Ultrasound Imaging and Automatic Detection at Conventional Diagnostic Frequencies.' *Investigative Radiology*, 45(11), Nov, pp. 715-724.

Casscells, W. (1992) 'Migration of smooth muscle and endothelial cells. Critical events in restenosis.' *Circulation*, 86(1516183) pp. 723-729.

Cedervall, T., Lynch, I., Lindman, S., Berggård, T., Thulin, E., Nilsson, H., Dawson, K. A. and Linse, S. (2007) 'Understanding the nanoparticle-protein corona using methods to quntify exchange rates and affinities of proteins for nanoparticles.' *Proceedings of the National Academy of Sciences of the United States of America*, 104(7), //, pp. 2050-2055.

Chang, C. L. and Fogler, H. S. (1997) 'Controlled formation of silica particles from tetraethyl orthosilicate in nonionic water-in-oil microemulsions.' *Langmuir*, 13(13), Jun 25, pp. 3295-3307.

Chaytor, A. T., Taylor, H. J. and Griffith, T. M. (2002) 'Gap junction-dependent and -independent EDHF-type relaxations may involve smooth muscle cAMP accumulation.' *American Journal of Physiology-Heart and Circulatory Physiology*, 282(4), Apr, pp. H1548-H1555.

Chaytor, A. T., Bakker, L. M., Edwards, D. H. and Griffith, T. M. (2005) 'Connexin-mimetic peptides dissociate electrotonic EDHF-type signalling via myoendothelial and smooth muscle gap junctions in the rabbit iliac artery.' *British Journal of Pharmacology*, 144(1), Jan, pp. 108-114.

Chen, F. and Gerion, D. (2004) 'Fluorescent CdSe/ZnS Nanocrystal−Peptide Conjugates for Long-term, Nontoxic Imaging and Nuclear Targeting in Living Cells.' *Nano Lett*, 4(10) pp. 1827-1832.

Chen, G. and Cheung, D. W. (1997) 'Effect of K(+)-channel blockers on ACh-induced hyperpolarization and relaxation in mesenteric arteries.' *Am J Physiol*, 272(5 Pt 2), May, pp. H2306-2312.

Chen, G., Yamamoto, Y., Miwa, K. and Suzuki, H. (1991) 'Hyperpolarization of arterial smooth muscle induced by endothelial humoral substances.' *Am J Physiol*, 260(6 Pt 2), Jun, pp. H1888-1892.

Chen, M. Y., Chen, Z. Z., Wu, L. L., Tang, H. W. and Pang, D. W. (2013) 'Goat anti-rabbit IgG conjugated fluorescent dye-doped silica nanoparticles for human breast carcinoma cell recognition.' *Analyst*, 138(24), Nov 12, pp. 7411-7416.

Chen, Y. J., Gu, H. C., Zhang, D. S. Z., Li, F., Liu, T. Y. and Xia, W. L. (2014) 'Highly effective inhibition of lung cancer growth and metastasis by systemic delivery of siRNA via multimodal mesoporous silica-based nanocarrier.' *Biomaterials*, 35(38), Dec, pp. 10058-10069.

Cherukuri, P., Bachilo, S. M., Litovsky, S. H. and Weisman, R. B. (2004) 'Near-infrared fluorescence microscopy of single-walled carbon nanotubes in phagocytic cells.' *J Am Chem Soc*, 126(48), Dec 8, pp. 15638-15639.

Cheung, D. W., Chen, G., MacKay, M. J. and Burnette, E. (1999) 'Regulation of vascular tone by endothelium-derived hyperpolarizing factor.' *Clin Exp Pharmacol Physiol*, 26(2), Feb, pp. 172-175.

Cho, E. C., Xie, J., Wurm, P. A. and Xia, Y. (2009) 'Understanding the role of surface charges in cellular adsorption versus internalization by selectively removing gold nanoparticles on the cell surface with a I2/KI etchant.' *Nano Lett*, 9(3), Mar, pp. 1080-1084.

Cho, M., Cho, W. S., Choi, M., Kim, S. J., Han, B. S., Kim, S. H., Kim, H. O., Sheen, Y. Y. and Jeong, J. (2009) 'The impact of size on tissue distribution and elimination by single intravenous injection of silica nanoparticles.' *Toxicol Lett*, 189(3), Sep 28, pp. 177-183.

Cho, W. S., Choi, M., Han, B. S., Cho, M., Oh, J., Park, K., Kim, S. J., Kim, S. H. and Jeong, J. (2007) 'Inflammatory mediators induced by intratracheal instillation of ultrafine amorphous silica particles.' *Toxicol Lett*, 175(1-3), Dec 10, pp. 24-33.

Choi, H. and Chen, I. W. (2003) 'Surface-modified silica colloid for diagnostic imaging.' *J Colloid Interface Sci*, 258(2), Feb 15, pp. 435-437.

Choi, S., Na, H. Y., Kim, J. A., Cho, S. E. and Suh, S. H. (2013) 'Contradictory Effects of Superoxide and Hydrogen Peroxide on KCa3.1 in Human Endothelial Cells.' *Korean J Physiol Pharmacol*, 17(3), Jun, pp. 181-187.

Christen, V. and Fent, K. (2012) 'Silica nanoparticles and silver-doped silica nanoparticles induce endoplasmatic reticulum stress response and alter cytochrome P4501A activity.' *Chemosphere*, 87(4), Apr, pp. 423-434.

Christofidou-Solomidou, M., Kennel, S., Scherpereel, A., Wiewrodt, R., Solomides, C. C., Pietra, G. G., Murciano, J. C., Shah, S. A., Ischiropoulos, H., Albelda, S. M. and Muzykantov, V. R. (2002) 'Vascular immunotargeting of glucose oxidase to the endothelial antigens induces distinct forms of oxidant acute lung injury: targeting to thrombomodulin, but not to PECAM-1, causes pulmonary thrombosis and neutrophil transmigration.' *Am J Pathol*, 160(3), Mar, pp. 1155-1169.

Churaev, N. V. (1999) 'The DLVO theory in Russian colloid science.' *Advances in Colloid and Interface Science*, 83(1-3), Dec 1, pp. 19-32.

Chutkow, W. A., Simon, M. C., Le Beau, M. M. and Burant, C. F. (1996) 'Cloning, tissue expression, and chromosomal localization of SUR2, the putative drug-binding subunit of cardiac, skeletal muscle, and vascular KATP channels.' *Diabetes*, 45(10), 10/, pp. 1439-1445.

Cines, D. B., Pollak, E. S., Buck, C. A., Loscalzo, J., Zimmerman, G. A., McEver, R. P., Pober, J. S., Wick, T. M., Konkle, B. A., Schwartz, B. S., Barnathan, E. S., McCrae, K. R., Hug, B. A., Schmidt, A.-M. and Stern, D. M. (1998) 'Endothelial Cells in Physiology and in the Pathophysiology of Vascular Disorders.' *Blood*, 91(10), May 15, 1998, pp. 3527-3561.

Clark, C. B., Zhang, Y., Martin, S. M., Davies, L. R., Xu, L., Kregel, K. C., Miller, F. J., Jr., Buettner, G. R. and Kerber, R. E. 'The nitric oxide synthase inhibitor NG-nitro-l-arginine decreases defibrillation-induced free radical generation.' *Resuscitation*, 60(3) pp. 351-358.

Coats, P., Johnston, F., MacDonald, J., McMurray, J. J. and Hillier, C. (2001) 'Endothelium-derived hyperpolarizing factor : identification and mechanisms of action in human subcutaneous resistance arteries.' *Circulation*, 103(12), Mar 27, pp. 1702-1708.

Conner, S. D. and Schmid, S. L. (2003) 'Regulated portals of entry into the cell.' *Nature*, 422(6927), Mar 6, pp. 37-44.

Cook, D. L. and Hales, C. N. (1984) 'Intracellular ATP directly blocks K+ channels in pancreatic B-cells.' *Nature*, 311(5983), 09/20, pp. 271-273.

Corbalan, J. J., Medina, C., Jacoby, A., Malinski, T. and Radomski, M. W. (2011) 'Amorphous silica nanoparticles trigger nitric oxide/peroxynitrite imbalance in human endothelial cells: inflammatory and cytotoxic effects.' *Int J Nanomedicine*, 6 pp. 2821-2835.

Corbalan, J. J., Medina, C., Jacoby, A., Malinski, T. and Radomski, M. W. (2012) 'Amorphous silica nanoparticles aggregate human platelets: potential implications for vascular homeostasis.' *Int J Nanomedicine*, 7 pp. 631-639.

Courtois, A., Andujar, P., Ladeiro, Y., Baudrimont, I., Delannoy, E., Leblais, V., Begueret, H., Galland, M. A., Brochard, P., Marano, F., Marthan, R. and Muller, B. (2008) 'Impairment of NO-dependent relaxation in intralobar pulmonary arteries: comparison of urban particulate matter and manufactured nanoparticles.' *Environ Health Perspect*, 116(10), Oct, pp. 1294-1299.

Cowart, L. A., Wei, S., Hsu, M.-H., Johnson, E. F., Krishna, M. U., Falck, J. R. and Capdevila, J. H. (2002) 'The CYP4A isoforms hydroxylate epoxyeicosatrienoic acids to form high affinity peroxisome proliferator-activated receptor ligands.' *J Biol Chem*, 277(38), 09/20, pp. 35105-35112.

Crane, G. J., Neild, T. O. and Segal, S. S. (2004) 'Contribution of active membrane processes to conducted hyperpolarization in arterioles of hamster cheek pouch.' *Microcirculation*, 11(5), Jul-Aug, pp. 425-433.

Crane, G. J., Gallagher, N., Dora, K. A. and Garland, C. J. (2003) 'Small- and intermediate-conductance calcium-activated K+ channels provide different facets of endothelium-dependent hyperpolarization in rat mesenteric artery.' *Journal of Physiology-London*, 553(1), Nov 15, pp. 183-189.

Cui, D., Tian, F., Ozkan, C., Wang, M. and Gao, H. (2005) 'Effect of single wall carbon nanotubes on human HEK293 cells.' *Toxicol Lett*, 155 pp. 73 - 85.

Dausend, J., Musyanovych, A., Dass, M., Walther, P., Schrezenmeier, H., Landfester, K. and Mailander, V. (2008) 'Uptake Mechanism of Oppositely Charged Fluorescent Nanoparticles in HeLa Cells.' *Macromolecular Bioscience*, 8(12), Dec 8, pp. 1135-1143.

Davda, J. and Labhasetwar, V. (2002) 'Characterization of nanoparticle uptake by endothelial cells.' *Int J Pharm*, 233(1-2), Feb 21, pp. 51-59.

Davies, P. F. (1986) 'Vascular cell interactions with special reference to the pathogenesis of atherosclerosis.' *Lab Invest*, 55(1) pp. 5-24.

Davis, M. J. and Hill, M. A. (1999) 'Signaling mechanisms underlying the vascular myogenic response.' *Physiol Rev*, 79(2), Apr, pp. 387-423.

Davis, M. J., Wu, X., Nurkiewicz, T. R., Kawasaki, J., Davis, G. E., Hill, M. A. and Meininger, G. A. (2001) 'Integrins and mechanotransduction of the vascular myogenic response.' *Am J Physiol Heart Circ Physiol*, 280(4), Apr, pp. H1427-1433.

Dawes, M., Chowienczyk, P. J. and Ritter, J. M. (1997) 'Effects of Inhibition of the L-Arginine/Nitric Oxide Pathway on Vasodilation Caused by ß-Adrenergic Agonists in Human Forearm.' *Circulation*, 95(9), May 6, 1997, pp. 2293-2297.

de Matos, M. B., Piedade, A. P., Alvarez-Lorenzo, C., Concheiro, A., Braga, M. E. and de Sousa, H. C. (2013) 'Dexamethasone-loaded poly(varepsilon-caprolactone)/silica nanoparticles composites prepared by supercritical CO foaming/mixing and deposition.' *Int J Pharm*, Sep 2,

De Mello, W. C. (2013) 'Intracellular angiotensin II increases the total potassium current and the resting potential of arterial myocytes from vascular resistance vessels of the rat. Physiological and pathological implications.' *J Am Soc Hypertens*, 7(3), May-Jun, pp. 192-197.

de Wit, C. and Griffith, T. M. (2010) 'Connexins and gap junctions in the EDHF phenomenon and conducted vasomotor responses.' *Pflugers Archiv-European Journal of Physiology*, 459(6), May, pp. 897-914.

Delgado, A. V., Gonzalez-Caballero, E., Hunter, R. J., Koopal, L. K. and Lyklema, J. (2005) 'Measurement and interpretation of electrokinetic phenomena - (IUPAC technical report).' *Pure and Applied Chemistry*, 77(10), Oct, pp. 1753-1805.

Derfus, A. M., Chan, W. C. W. and Bhatia, S. N. (2004) 'Intracellular Delivery of Quantum Dots for Live Cell Labeling and Organelle Tracking.' *Advanced Materials*, 16(12) pp. 961-966.

Derjaguin, B. and Landau, L. (1993) 'Theory of the Stability of Strongly Charged Lyophobic Sols and of the Adhesion of Strongly Charged-Particles in Solutions of Electrolytes.' *Progress in Surface Science*, 43(1-4), May-Aug, pp. 30-59.

Derjaguin, B. and Landau, L. (1941) 'Theory of the stability of strongly charged lyophobic sols and of the adhesion of strongly charged particles in solutions of electrolytes.' *Acta Physico Chemica URSS*, 14 p. 633.

Dermine, J. F., Duclos, S., Garin, J., St-Louis, F., Rea, S., Parton, R. G. and Desjardins, M. (2001) 'Flotillin-1-enriched lipid raft domains accumulate on maturing phagosomes.' *J Biol Chem*, 276(21), May 25, pp. 18507-18512.

DIACONU, M., TACHE, A., EREMIA, S. A.-M. V., GATEA, F., LITESCU, Simona. and RADU, G. L. (2010) 'STRUCTURAL CHARACTERIZATION OF CHITOSAN COATED SILICON NANOPARTICLES –A FT-IR APPROACH.' *U.P.B. Sci. Bull., Series B*, 72(3).

Didion, S. P., Ryan, M. J., Didion, L. A., Fegan, P. E., Sigmund, C. D. and Faraci, F. M. (2002) 'Increased superoxide and vascular dysfunction in CuZnSOD-deficient mice.' *Circulation Research*, 91(10), //, pp. 938-944.

Dimmeler, S., Fleming, I., Fisslthaler, B., Hermann, C., Busse, R. and Zeiher, A. M. (1999) 'Activation of nitric oxide synthase in endothelial cells by Akt-dependent phosphorylation.' *Nature*, 399(6736), Jun 10, pp. 601-605.

Donaldson, K. and Tran, C. L. (2004) 'An introduction to the short-term toxicology of respirable industrial fibres.' *Mutat Res*, 553(1-2), Sep 3, pp. 5-9.

Donners, W. A. B., Rijnbout, J. B. and Vrij, A. (1977) 'Light scattering from soap films: I. Determination of double-layer repulsion forces.' *Journal of Colloid and Interface Science*, 61(2), 9//, pp. 249-260.

Dora, K. A. (2001) 'Cell-cell communication in the vessel wall.' *Vascular Medicine*, 6(1), February 1, 2001, pp. 43-50.

Doughty, J. M., Plane, F. and Langton, P. D. (1999) 'Charybdotoxin and apamin block EDHF in rat mesenteric artery if selectively applied to the endothelium.' *American Journal of Physiology-Heart and Circulatory Physiology*, 276(3), Mar, pp. H1107-H1112.

Du, Z., Zhao, D., Jing, L., Cui, G., Jin, M., Li, Y., Liu, X., Liu, Y., Du, H., Guo, C., Zhou, X. and Sun, Z. (2013) 'Cardiovascular toxicity of different sizes amorphous silica nanoparticles in rats after intratracheal instillation.' *Cardiovasc Toxicol*, 13(3), Sep, pp. 194-207.

Dubertret, B., Skourides, P., Norris, D. J., Noireaux, V., Brivanlou, A. H. and Libchaber, A. (2002) 'In vivo imaging of quantum dots encapsulated in phospholipid micelles.' *Science*, 298(5599), Nov 29, pp. 1759-1762.

Dumont, F., Warlus, J. and Watillon, A. (1990) 'Influence of the Point of Zero Charge of Titanium-Dioxide Hydrosols on the Ionic Adsorption Sequences.' *Journal of Colloid and Interface Science*, 138(2), Sep, pp. 543-554.

Edwards, G., Dora, K. A., Gardener, M. J., Garland, C. J. and Weston, A. H. (1998) 'K+ is an endothelium-derived hyperpolarizing factor in rat arteries.' *Nature*, 396(9834033) pp. 269-272.

Edwards, G., Thollon, C., Gardener, M. J., Feletou, M., Vilaine, J., Vanhoutte, P. M. and Weston, A. H. (2000) 'Role of gap junctions and EETs in endothelium-dependent hyperpolarization of porcine coronary artery.' *Br J Pharmacol*, 129(10725263) pp. 1145-1154.

Ehrenberg, M. S., Friedman, A. E., Finkelstein, J. N., Oberdorster, G. and McGrath, J. L. (2009) 'The influence of protein adsorption on nanoparticle association with cultured endothelial cells.' *Biomaterials*, 30(4), Feb, pp. 603-610.

Ekrami, A., Samarbaf-Zadeh, A. R., Khosravi, A., Zargar, B., Alavi, M., Amin, M. and Kiasat, A. (2011) 'Validity of bioconjugated silica nanoparticles in comparison with direct smear, culture, and polymerase chain reaction for detection of Mycobacterium tuberculosis in sputum specimens.' *International Journal of Nanomedicine*, 6 pp. 2729-2735.

Emerson, G. G., Neild, T. O. and Segal, S. S. (2002) 'Conduction of hyperpolarization along hamster feed arteries: augmentation by acetylcholine.' *Am J Physiol Heart Circ Physiol*, 283(1), Jul, pp. H102-109.

Ermolenko, M. N., Filchenkov, N. A. and Sviridov, O. V. (1992) 'Rhodamine-B Conjugates of Thyroid-Hormones as Fluorescent Ligands of Human Blood-Plasma Transport Proteins.' *Biochemistry-Moscow*, 57(8), Aug, pp. 880-884.

Faehling, M., Koch, E. D., Raithel, J., Trischler, G. and Waltenberger, J. (2001) 'Vascular endothelial growth factor-A activates Ca2+ -activated K+ channels in human endothelial cells in culture.' *Int J Biochem Cell Biol*, 33(4), 04/, pp. 337-346.

Fang, X., Kaduce, T. L., Weintraub, N. L. and Spector, A. A. (1997) 'Cytochrome P450 metabolites of arachidonic acid: rapid incorporation and hydration of 14,15-epoxyeicosatrienoic acid in arterial smooth muscle cells.' *Prostaglandins Leukot Essent Fatty Acids*, 57(4-5), Oct, pp. 367-371.

Fang, X., Kaduce, T. L., Weintraub, N. L., VanRollins, M. and Spector, A. A. (1996) 'Functional Implications of a Newly Characterized Pathway of 11,12-Epoxyeicosatrienoic Acid Metabolism in Arterial Smooth Muscle.' *Circulation Research*, 79(4), October 1, 1996, pp. 784-793.

Faraci, F. M. and Didion, S. P. (2004) 'Vascular protection: Superoxide dismutase isoforms in the vessel wall.' *Arteriosclerosis, Thrombosis, and Vascular Biology*, 24(8), //, pp. 1367-1373.

Farooq, A., Whitehead, D. and Azzawi, M. (2013) 'Attenuation of endothelial-dependent vasodilator responses, induced by dye-encapsulated silica nanoparticles, in aortic vessels.' *Nanomedicine (Lond)*, Feb 22,

Feletou, M. and Vanhoutte, P. M. (1988) 'Endothelium-dependent hyperpolarization of canine coronary smooth muscle.' *Br J Pharmacol*, 93(3), Mar, pp. 515-524.

Ferrante, M., Cicciu, F., Fallico, R., Sciacca, S. and Fiore, M. (2012) '[Nanotechnology and nanoparticles].' *Ig Sanita Pubbl*, 68(6), Nov-Dec, pp. 875-883.

Ferrari, M. (2008) 'Nanogeometry: Beyond drug delivery.' *Nat Nano*, 3(3), 03//print, pp. 131-132.

Finsy, R. (2004) 'On the Critical Radius in Ostwald Ripening.' *Langmuir*, 20 pp. 2975-2976.

Fisslthaler, B., Popp, R., Kiss, L., Potente, M., Harder, D. R., Fleming, I. and Busse, R. (1999) 'Cytochrome P450 2C is an EDHF synthase in coronary arteries.' *Nature*, 401(10519554) pp. 493-497.

Fleming, I. (2001) 'Cytochrome p450 and vascular homeostasis.' *Circ Res*, 89(9), Oct 26, pp. 753-762.

Fleming, I. (2004) 'Cytochrome P450 epoxygenases as EDHF synthase(s).' *Pharmacol Res*, 49(6), Jun, pp. 525-533.

Fleming, I. (2010) 'Molecular mechanisms underlying the activation of eNOS.' *Pflugers Arch*, 459(6), May, pp. 793-806.

Fleming, I. (2011) 'The cytochrome P450 pathway in angiogenesis and endothelial cell biology.' *Cancer Metastasis Rev*, 30(3-4), Dec, pp. 541-555.

Fleming, I. and Busse, R. (2006) 'Endothelium-Derived Epoxyeicosatrienoic Acids and Vascular Function.' *Hypertension*, 47(4), April 1, 2006, pp. 629-633.

Fleming, I., Fisslthaler, B., Dimmeler, S., Kemp, B. E. and Busse, R. (2001) 'Phosphorylation of Thr(495) regulates Ca(2+)/calmodulin-dependent endothelial nitric oxide synthase activity.' *Circ Res*, 88(11), Jun 8, pp. E68-75.

Fleming, I., Fisslthaler, B., Michaelis, U. R., Kiss, L., Popp, R. and Busse, R. (2001) 'The coronary endothelium-derived hyperpolarizing factor (EDHF) stimulates multiple signalling pathways and proliferation in vascular cells.' *Pflugers Arch*, 442(4), Jul, pp. 511-518.

Fok, H., Jiang, B., Clapp, B. and Chowienczyk, P. (2012) 'Regulation of vascular tone and pulse wave velocity in human muscular conduit arteries: selective effects of nitric oxide donors to dilate muscular arteries relative to resistance vessels.' *Hypertension*, 60(5), Nov, pp. 1220-1225.

Franca-Silva, M. S., Luciano, M. N., Ribeiro, T. P., Silva, J. S. F., Santos, A. F., Franca, K. C., Nakao, L. S., Athayde, P. F., Braga, V. A. and Medeiros, I. A. (2012) 'The 2-nitrate-1,3-dibuthoxypropan, a new nitric oxide donor, induces vasorelaxation in mesenteric arteries of the rat.' *European Journal of Pharmacology*, 690(1-3), Sep 5, pp. 170-175.

Franks, G. V. (2002) 'Zeta potentials and yield stresses of silica suspensions in concentrated monovalent electrolytes: Isoelectric point shift and additional attraction.' *Journal of Colloid and Interface Science*, 249(1), May 1, pp. 44-51.

Freese, C., Schreiner, D., Anspach, L., Bantz, C., Maskos, M., Unger, R. E. and Kirkpatrick, C. (2014) 'In vitro investigation of silica nanoparticle uptake into human endothelial cells under physiological cyclic stretch.' *Part Fibre Toxicol*, 11(1), Dec 24, p. 1.

Frieden, M., Sollini, M. and Beny, J. (1999) 'Substance P and bradykinin activate different types of KCa currents to hyperpolarize cultured porcine coronary artery endothelial cells.' *J Physiol*, 519 Pt 2, Sep 1, pp. 361-371.

Frohlich, E. (2012) 'The role of surface charge in cellular uptake and cytotoxicity of medical nanoparticles.' *International Journal of Nanomedicine*, 7 pp. 5577-5591.

Fruijtier-Pölloth, C. (2012) 'The toxicological mode of action and the safety of synthetic amorphous silica—A nanostructured material.' *Toxicology*, 294(2–3), 4/11/, pp. 61-79.

Fubini, B. (1997) 'Surface reactivity in the pathogenic response to particulates.' *Environmental Health Perspectives*, 105, Sep, pp. 1013-1020.

Fujiki, T., Shimokawa, H., Morikawa, K., Kubota, H., Hatanaka, M., Talukder, M. A., Matoba, T., Takeshita, A. and Sunagawa, K. (2005) 'Endothelium-derived hydrogen peroxide accounts for the enhancing effect of an angiotensin-converting enzyme inhibitor on endothelium-derived hyperpolarizing factor-mediated responses in mice.' *Arterioscler Thromb Vasc Biol*, 25(4), Apr, pp. 766-771.

Fujita, A. and Kurachi, Y. (2000) 'Molecular aspects of ATP-sensitive K+ channels in the cardiovascular system and K+ channel openers.' *Pharmacol Ther*, 85(1), Jan, pp. 39-53.

Fukai, T., Folz, R. J., Landmesser, U. and Harrison, D. G. (2002) 'Extracellular superoxide dismutase and cardiovascular disease.' *Cardiovascular Research*, 55(2), //, pp. 239-249.

Fulton, D., Gratton, J. P., McCabe, T. J., Fontana, J., Fujio, Y., Walsh, K., Franke, T. F., Papapetropoulos, A. and Sessa, W. C. (1999) 'Regulation of endothelium-derived nitric oxide production by the protein kinase Akt.' *Nature*, 399(6736), Jun 10, pp. 597-601.

Gallis, B., Corthals, G. L., Goodlett, D. R., Ueba, H., Kim, F., Presnell, S. R., Figeys, D., Harrison, D. G., Berk, B. C., Aebersold, R. and Corson, M. A. (1999) 'Identification of flow-dependent endothelial nitric-oxide synthase phosphorylation sites by mass spectrometry and regulation of phosphorylation and nitric oxide production by the phosphatidylinositol 3-kinase inhibitor LY294002.' *J Biol Chem*, 274(42), Oct 15, pp. 30101-30108.

Gamucci, O., Bertero, A., Gagliardi, M. and Bardi, G. (2014) 'Biomedical Nanoparticles: Overview of Their Surface Immune-Compatibility.' *Coatings*, 4(1), Feb, pp. 139-159.

Gao, H., Wen, D. S. and Sukhorukov, G. B. (2015) 'Composite silica nanoparticle/polyelectrolyte microcapsules with reduced permeability and enhanced ultrasound sensitivity.' *Journal of Materials Chemistry B*, 3(9) pp. 1888-1897.

Garland, C. J. and McPherson, G. A. (1992) 'Evidence that nitric oxide does not mediate the hyperpolarization and relaxation to acetylcholine in the rat small mesenteric artery.' *Br J Pharmacol*, 105(2), Feb, pp. 429-435.

Garvey, E. P., Tuttle, J. V., Covington, K., Merrill, B. M., Wood, E. R., Baylis, S. A. and Charles, I. G. (1994) 'Purification and Characterization of the Constitutive Nitric-Oxide Synthase from Human Placenta.' *Archives of Biochemistry and Biophysics*, 311(2), Jun, pp. 235-241.

Gaubert, M. L., Sigaudo-Roussel, D., Tartas, M., Berrut, G., Saumet, J. L. and Fromy, B. (2007) 'Endothelium-derived hyperpolarizing factor as an in vivo back-up mechanism in the cutaneous microcirculation in old mice.' *Journal of Physiology-London*, 585(2), Dec 1, pp. 617-626.

Gebremedhin, D., Harder, D. R., Pratt, P. F. and Campbell, W. B. (1998) 'Bioassay of an endothelium-derived hyperpolarizing factor from bovine coronary arteries: role of a cytochrome P450 metabolite.' *J Vasc Res*, 35(4), Jul-Aug, pp. 274-284.

Gellai, M., De Wolf, R., Fletcher, T. and Nambi, P. (1997) 'Contribution of endogenous endothelin-1 to the maintenance of vascular tone: role of nitric oxide.' *Pharmacology*, 55(6), Dec, pp. 299-308.

Geng, Y. J., Wu, Q. and Hansson, G. K. (1994) 'Protein kinase C activation inhibits cytokine-induced nitric oxide synthesis in vascular smooth muscle cells.' *Biochim Biophys Acta*, 1223(1), Aug 11, pp. 125-132.

Ghosh, S., Gachhui, R., Crooks, C., Wu, C., Lisanti, M. P. and Stuehr, D. J. (1998) 'Interaction between caveolin-1 and the reductase domain of endothelial nitric-oxide synthase. Consequences for catalysis.' *J Biol Chem*, 273(35), Aug 28, pp. 22267-22271.

Gierst, L. and Herman, P. (1966) 'On the desorption of pyridine at negative potentials in mercury-water systems.' *Fresenius' Zeitschrift für analytische Chemie*, 216(2), 1966/06/01, pp. 238-242.

Gierst, L., Vandenberghen, L., Nicolas, E. and Fraboni, A. (1966) 'Ion Pairing Mechanisms in Electrode Processes.' *Journal of The Electrochemical Society*, 113(10), October 1, 1966, pp. 1025-1036.

Giesche, H. (1994a) 'Synthesis of Monodispersed Silica Powders .2. Controlled Growth Reaction and Continuous Production Process.' *Journal of the European Ceramic Society*, 14(3) pp. 205-214.

Giesche, H. (1994b) 'Synthesis of Monodispersed Silica Powders .1. Particle Properties and Reaction-Kinetics.' *Journal of the European Ceramic Society*, 14(3) pp. 189-204.

Giri, S., Trewyn, B. G., Stellmaker, M. P. and Lin, V. S. Y. (2005) 'Stimuli-responsive controlled-release delivery system based on mesoporous silica nanorods capped with magnetic nanoparticles.' *Angew Chem Int Ed Engl*, 44(32), 08/12, pp. 5038-5044.

Glebov, O. O., Bright, N. A. and Nichols, B. J. (2006) 'Flotillin-1 defines a clathrin-independent endocytic pathway in mammalian cells.' *Nat Cell Biol*, 8(1), Jan, pp. 46-54.

Glencross, H., Ahmed, N. and Wang, Q. (2011) Biomedical science practice: experimental and professional skills. Vol. 7, pp. 1-342. Oxford: Oxford University Press.

Gluais, P., Edwards, G., Weston, A. H., Falck, J. R., Vanhoutte, P. M. and Feletou, M. (2005) 'Role of SKCa and IKCa in endothelium-dependent hyperpolarizations of the guinea-pig isolated carotid artery.' *British Journal of Pharmacology*, 144(4), Feb, pp. 477-485.

Goddette, D. W. and Frieden, C. (1986) 'Actin Polymerization - the Mechanism of Action of Cytochalasin-D.' *Journal of Biological Chemistry*, 261(34), Dec 5, pp. 5974-5980.

Gong, X., Yang, Y., Zhang, L., Zou, C., Cai, P., Chen, G. and Huang, S. (2010) 'Controlled synthesis of Pt nanoparticles via seeding growth and their shape-dependent catalytic activity.' *J Colloid Interface Sci*, 352(2), Dec 15, pp. 379-385.

Gopalakrishnan, M., Whiteaker, K. L., Molinari, E. J., Davis-Taber, R., Scott, V. E., Shieh, C. C., Buckner, S. A., Milicic, I., Cain, J. C., Postl, S., Sullivan, J. P. and Brioni, J. D. (1999) 'Characterization of the ATP-sensitive potassium channels (KATP) expressed in guinea pig bladder smooth muscle cells.' *J Pharmacol Exp Ther*, 289(1), Apr, pp. 551-558.

Gordon, J. L. and Martin, W. (1983) 'Endothelium-dependent relaxation of the pig aorta: relationship to stimulation of 86Rb efflux from isolated endothelial cells.' *Br J Pharmacol*, 79(2), Jun, pp. 531-541.

Goto, K., Rummery, N. M., Grayson, T. H. and Hill, C. E. (2004) 'Attenuation of conducted vasodilatation in rat mesenteric arteries during hypertension: role of inwardly rectifying potassium channels.' *J Physiol*, 561(Pt 1), Nov 15, pp. 215-231.

Govers, R. and Rabelink, T. J. (2001) 'Cellular regulation of endothelial nitric oxide synthase.' *Am J Physiol Renal Physiol*, 280(2), Feb, pp. F193-206.

Grahame, D. C. (1951) 'The Role of the Cation in the Electrical Double Layer.' *Journal of The Electrochemical Society*, 98(9), September 1, 1951, pp. 343-350.

Gratton, S. E. A., Ropp, P. A., Pohlhaus, P. D., Luft, J. C., Madden, V. J., Napier, M. E. and DeSimone, J. M. (2008) 'The effect of particle design on cellular internalization pathways.' *Proceedings of the National Academy of Sciences of the United States of America*, 105(33), Aug 19, pp. 11613-11618.

Graziani, A., Bricko, V., Carmignani, M., Graier, W. F. and Groschner, K. (2004) 'Cholesterol- and caveolin-rich membrane domains are essential for phospholipase A2-dependent EDHF formation.' *Cardiovasc Res*, 64(2), Nov 1, pp. 234-242.

Griendling, K. K., Sorescu, D. and Ushio-Fukai, M. (2000) 'NAD(P)H oxidase: role in cardiovascular biology and disease.' *Circ Res*, 86(5), Mar 17, pp. 494-501.

Griffith, O. W. and Kilbourn, R. G. (1996) 'Nitric oxide synthase inhibitors: Amino acids.' *Nitric Oxide, Pt a - Sources and Detection of No; No Synthase*, 268 pp. 375-392.

Griffith, T. M. (2004) 'Endothelium-dependent smooth muscle hyperpolarization: do gap junctions provide a unifying hypothesis?' *Br J Pharmacol*, 141(6), Mar, pp. 881-903.

Griffith, T. M., Chaytor, A. T. and Edwards, D. H. (2004) 'The obligatory link: role of gap junctional communication in endothelium-dependent smooth muscle hyperpolarization.' *Pharmacol Res*, 49(6), Jun, pp. 551-564.

Griffith, T. M., Chaytor, A. T., Berman, R. S. and Edwards, D. H. (2001) 'Heterogeneity of EDIT'-type relaxations of rabbit and rat arteries analysed with peptides homologous to the extracellular loops of connexins 37, 40 and 43.' *Edhf 2000*, pp. 62-74.

Griffith, T. M., Chaytor, A. T., Bakker, L. M. and Edwards, D. H. (2005) '5-Methyltetrahydrofolate and tetrahydrobiopterin can modulate electrotonically mediated endothelium-dependent vascular relaxation.' *Proceedings of the National Academy of Sciences of the United States of America*, 102(19), //, pp. 7008-7013.

Halcox, J. P., Narayanan, S., Cramer-Joyce, L., Mincemoyer, R. and Quyyumi, A. A. (2001) 'Characterization of endothelium-derived hyperpolarizing factor in the human forearm microcirculation.' *Am J Physiol Heart Circ Physiol*, 280(6), Jun, pp. H2470-2477.

Hald, B. O., Jacobsen, J. C., Braunstein, T. H., Inoue, R., Ito, Y., Sorensen, P. G., Holstein-Rathlou, N. H. and Jensen, L. J. (2012) 'BKCa and KV channels limit conducted vasomotor responses in rat mesenteric terminal arterioles.' *Pflugers Arch*, 463(2), Feb, pp. 279-295.

Harder, D. R., Roman, R. J. and Gebremedhin, D. (2000) 'Molecular mechanisms controlling nutritive blood flow: role of cytochrome P450 enzymes.' *Acta Physiol Scand*, 168(4), Apr, pp. 543-549.

Harris, M. B., Ju, H., Venema, V. J., Liang, H., Zou, R., Michell, B. J., Chen, Z. P., Kemp, B. E. and Venema, R. C. (2001) 'Reciprocal phosphorylation and regulation of endothelial nitric-oxide synthase in response to bradykinin stimulation.' *J Biol Chem*, 276(19), May 11, pp. 16587-16591.

Hartley, P. G., Larson, I. and Scales, P. J. (1997) 'Electrokinetic and direct force measurements between silica and mica surfaces in dilute electrolyte, solutions.' *Langmuir*, 13(8), Apr 16, pp. 2207-2214.

Heeba, G., Hassan, M. K. A., Khalifa, M. and Malinski, T. (2007) 'Adverse balance of nitric oxide/peroxynitrite in the dysfunctional endothelium can be reversed by statins.' *J Cardiovasc Pharmacol*, 50(4), 10/, pp. 391-398.

Hetland, R. B., Schwarze, P. E., Johansen, B. V., Myran, T., Uthus, N. and Refsnes, M. (2001) 'Silica-induced cytokine release from A549 cells: importance of surface area versus size.' *Hum Exp Toxicol*, 20(1), Jan, pp. 46-55.

Hilgers, R. H. and Webb, R. C. (2007) 'Reduced expression of SKCa and IKCa channel proteins in rat small mesenteric arteries during angiotensin II-induced hypertension.' *Am J Physiol Heart Circ Physiol*, 292(5), May, pp. H2275-2284.

Hilgers, R. H., Todd, J., Jr. and Webb, R. C. (2006) 'Regional heterogeneity in acetylcholine-induced relaxation in rat vascular bed: role of calcium-activated K+ channels.' *Am J Physiol Heart Circ Physiol*, 291(1), Jul, pp. H216-222.

Hill, M. A. and Davis, M. J. (2007) 'Coupling a change in intraluminal pressure to vascular smooth muscle depolarization: still stretching for an explanation.' *Am J Physiol Heart Circ Physiol*, 292(6), Jun, pp. H2570-2572.

Hinton, J. M. and Langton, P. D. (2003) 'Inhibition of EDHF by two new combinations of K+-channel inhibitors in rat isolated mesenteric arteries.' *Br J Pharmacol*, 138(6), Mar, pp. 1031-1035.

Hisamoto, K., Ohmichi, M., Kurachi, H., Hayakawa, J., Kanda, Y., Nishio, Y., Adachi, K., Tasaka, K., Miyoshi, E., Fujiwara, N., Taniguchi, N. and Murata, Y. (2001) 'Estrogen induces the Akt-dependent activation of endothelial nitric-oxide synthase in vascular endothelial cells.' *J Biol Chem*, 276(5), Feb 2, pp. 3459-3467.

Hoepfl, B., Rodenwaldt, B., Pohl, U. and De Wit, C. (2002) 'EDHF, but not NO or prostaglandins, is critical to evoke a conducted dilation upon ACh in hamster arterioles.' *Am J Physiol Heart Circ Physiol*, 283(3), Sep, pp. H996-H1004.

Hong, R. Y., Feng, B., Chen, L. L., Liu, G. H., Li, H. Z., Zheng, Y. and Wei, D. G. (2008) 'Synthesis, characterization and MRI application of dextran-coated Fe3O4 magnetic nanoparticles.' *Biochemical Engineering Journal*, 42(3), Dec 1, pp. 290-300.

Honing, M. L., Smits, P., Morrison, P. J. and Rabelink, T. J. (2000) 'Bradykinin-induced vasodilation of human forearm resistance vessels is primarily mediated by endothelium-dependent hyperpolarization.' *Hypertension*, 35(6), Jun, pp. 1314-1318.

Horiuchi, T., Dietrich, H. H., Hongo, K. and Dacey, R. G., Jr. (2002) 'Mechanism of extracellular K+-induced local and conducted responses in cerebral penetrating arterioles.' *Stroke*, 33(11), Nov, pp. 2692-2699.

Hrkach, J. S., Peracchia, M. T., Domb, A., Lotan, N. and Langer, R. (1997) 'Nanotechnology for biomaterials engineering: structural characterization of amphiphilic polymeric nanoparticles by 1H NMR spectroscopy.' *Biomaterials*, 18(1), Jan, pp. 27-30.

Hsiao, J.-K., Tsai, C.-P., Chung, T.-H., Hung, Y., Yao, M., Liu, H.-M., Mou, C.-Y., Yang, C.-S., Chen, Y.-C. and Huang, D.-M. (2008) 'Mesoporous silica nanoparticles as a delivery system of gadolinium for effective human stem cell tracking.' *Small*, 4(9), 09/, pp. 1445-1452.

Hsu, H. H., Duning, K., Meyer, H. H., Stolting, M., Weide, T., Kreusser, S., van Le, T., Gerard, C., Telgmann, R., Brand-Herrmann, S. M., Pavenstadt, H. and Bek, M. J. (2009) 'Hypertension in mice lacking the CXCR3 chemokine receptor.' *Am J Physiol Renal Physiol*, 296(4), Apr, pp. F780-789.

Huang, X., Young, N. and Townley, P. H. E. (2014) 'Characterization and Comparison of Mesoporous Silica Particles for Optimized Drug Delivery.' *Nanomater Nanotechnol*, 4(2)

Huo, Q., Liu, J., Wang, L. Q., Jiang, Y., Lambert, T. N. and Fang, E. (2006) 'A new class of silica cross-linked micellar core-shell nanoparticles.' *J Am Chem Soc*, 128(19), May 17, pp. 6447-6453.

Hurjui, L., Serban, I. L., Oprisa, C., Tucaliuc, E. S., Hogas, M. M., Tucaliuc, D., Hurjui, I., Luca, V. and Serban, D. N. (2011) 'The importance of EDHF in endothelium-dependent relaxation increases distally in mesenteric arteries depending upon the contracting agent.' *Rev Med Chir Soc Med Nat Iasi*, 115(1), Jan-Mar, pp. 168-170.

Hwa, J. J., Ghibaudi, L., Williams, P. and Chatterjee, M. (1994) 'Comparison of acetylcholine-dependent relaxation in large and small arteries of rat mesenteric vascular bed.' *American Journal of Physiology - Heart and Circulatory Physiology*, 266(3), March 1, 1994, pp. H952-H958.

Iguchi, M., Nakajima, T., Hisada, T., Sugimoto, T. and Kurachi, Y. (1992) 'On the mechanism of papaverine inhibition of the voltage-dependent Ca++ current in isolated smooth muscle cells from the guinea pig trachea.' *J Pharmacol Exp Ther*, 263(1), Oct, pp. 194-200.

Iler, R. K. (1979) *The Chemistry of Silica: Solubility, Polymerization, Colloid and Surface Properties and Biochemistry of Silica.* Wiley.

Imig, J. D. (2000) 'Eicosanoid regulation of the renal vasculature.' *American Journal of Physiology - Renal Physiology*, 279(6), 2000-12-01 08:00:00, pp. F965-F981.

Imig, J. D. and Roman, R. J. (1992) 'Nitric oxide modulates vascular tone in preglomerular arterioles.' *Hypertension*, 19(6 Pt 2), Jun, pp. 770-774.

Inagaki, N., Gonoi, T. and Seino, S. (1997) 'Subunit stoichiometry of the pancreatic beta-cell ATP-sensitive K+ channel.' *FEBS Lett*, 409(2), 06/09, pp. 232-236.

Inagaki, N., Gonoi, T., Clement, J. P., Wang, C. Z., Aguilar-Bryan, L., Bryan, J. and Seino, S. (1996) 'A family of sulfonylurea receptors determines the pharmacological properties of ATP-sensitive K+ channels.' *Neuron*, 16(5), May, pp. 1011-1017.

Ismail, A. M. I., A.A.F., Z. and Mohamed, A. S. (2010) 'Preparation of spherical silica nanoparticles: Stober silica.' *Journal of American Science*, 6(11), Oct, pp. 985-989.

Isomoto, S., Kondo, C., Yamada, M., Matsumoto, S., Higashiguchi, O., Horio, Y., Matsuzawa, Y. and Kurachi, Y. (1996) 'A novel sulfonylurea receptor forms with BIR (Kir6.2) a smooth muscle type ATP-sensitive K+ channel.' *J Biol Chem*, 271(40), 10/04, pp. 24321-24324.

Israelachvili, J. N. and Adams, G. E. (1978) 'Measurement of forces between two mica surfaces in aqueous electrolyte solutions in the range 0-100 nm.' *Journal of the Chemical Society, Faraday Transactions 1: Physical Chemistry in Condensed Phases*, 74(0) pp. 975-1001.

Itoh, T., Seki, N., Suzuki, S., Ito, S., Kajikuri, J. and Kuriyama, H. (1992) 'Membrane hyperpolarization inhibits agonist-induced synthesis of inositol 1,4,5-trisphosphate in rabbit mesenteric artery.' *The Journal of Physiology*, 451(1) pp. 307-328.

Jain, K. K. (2005) 'The role of nanobiotechnology in drug discovery.' *Drug Discov Today*, 10(21), Nov 1, pp. 1435-1442.

Jaiswal, J. K., Mattoussi, H., Mauro, J. M. and Simon, S. M. (2003) 'Long-term multiple color imaging of live cells using quantum dot bioconjugates.' *Nat Biotechnol*, 21(1), Jan, pp. 47-51.

Jani, P., Halbert, G. W., Langridge, J. and Florence, A. T. (1990) 'Nanoparticle uptake by the rat gastrointestinal mucosa: quantitation and particle size dependency.' *J Pharm Pharmacol*, 42(12), Dec, pp. 821-826.

Jin, Y., Kannan, S., Wu, M. and Zhao, J. X. (2007) 'Toxicity of Luminescent Silica Nanoparticles to Living Cells.' *Chem Res Toxicol*, 20(8) pp. 1126-1133.

Jokerst, J. V., Khademi, C. and Gambhir, S. S. (2013) 'Intracellular Aggregation of Multimodal Silica Nanoparticles for Ultrasound-Guided Stem Cell Implantation.' *Science Translational Medicine*, 5(177), Mar 20,

Joshi, A. and Woodman, O. L. (2012) 'Increased nitric oxide activity compensates for increased oxidative stress to maintain endothelial function in rat aorta in early type 1 diabetes.' *Naunyn-Schmiedebergs Archives of Pharmacology*, 385(11), Nov, pp. 1083-1094.

Ju-Nam, Y. and Lead, J. R. (2008) 'Manufactured nanoparticles: An overview of their chemistry, interactions and potential environmental implications.' *Science of the Total Environment*, 400(1-3), Aug 1, pp. 396-414.

Kagota, S., Yamaguchi, Y., Nakamura, K. and Kunitomo, M. (1999) 'Characterization of nitric oxide- and prostaglandin-independent relaxation in response to acetylcholine in rabbit renal artery.' *Clin Exp Pharmacol Physiol*, 26(10), Oct, pp. 790-796.

Kaji, T., Kawashima, T., Sakamoto, M., Kurashige, Y. and Koizumi, F. (1991) 'Inhibitory Effect of Rhodamine-B on the Proliferation of Human Lip Fibroblasts in Culture.' *Toxicology*, 68(1) pp. 11-20.

Kalinowski, L., Dobrucki, I. T. and Malinski, T. (2004) 'Race-specific differences in endothelial function: predisposition of African Americans to vascular diseases.' *Circulation*, 109(21), 06/01, pp. 2511-2517.

Kamouchi, M., Droogmans, G. and Nilius, B. (1999) 'Membrane potential as a modulator of the free intracellular Ca2+ concentration in agonist-activated endothelial cells.' *Gen Physiol Biophys*, 18(10517293) pp. 199-208.

Kapilov-Buchman, Y., Lellouche, E., Michaeli, S. and Lellouche, J. P. (2015) 'A unique surface modification of silica nanoparticles with polyethyleneimine (PEI) for siRNA delivery using cerium cation coordination chemistry.' *Bioconjug Chem*, Apr 1,

Kasper, J., Hermanns, M. I., Bantz, C., Koshkina, O., Lang, T., Maskos, M., Pohl, C., Unger, R. E. and Kirkpatrick, C. J. (2013) 'Interactions of silica nanoparticles with lung epithelial cells and the association to flotillins.' *Arch Toxicol*, 87(6), Jun, pp. 1053-1065.

Kaszuba, M. and Connah, M. T. (2006) 'Protein and nanoparticle characterisation using light scattering techniques.' *Particle & Particle Systems Characterization*, 23(2), Aug, pp. 193-196.

Kealey, D. and Haines, P. J. (2002) 'Instant notes: analytical chemistry.' *In*: BIOS Scientific Publishers Limited, pp. 1-342.

Kida, M., Sugiyama, T., Yoshimoto, T. and Ogawa, Y. (2012) 'Hydrogen Sulfide Increases Nitric Oxide Production with Calcium-dependent Activation of Endothelial Nitric Oxide Synthase in Endothelial Cells.' *Eur J Pharm Sci*, Nov 10,

Kim, B. H., Lee, N., Kim, H., An, K., Park, Y. I., Choi, Y., Shin, K., Lee, Y., Kwon, S. G., Na, H. B., Park, J. G., Ahn, T. Y., Kim, Y. W., Moon, W. K., Choi, S. H. and Hyeon, T. (2011) 'Large-scale synthesis of uniform and extremely small-sized iron oxide nanoparticles for high-resolution T1 magnetic resonance imaging contrast agents.' *J Am Chem Soc*, 133(32), Aug 17, pp. 12624-12631.

Kim, I. Y., Joachim, E., Choi, H. and Kim, K. (2015) 'Toxicity of silica nanoparticles depends on size, dose, and cell type.' *Nanomedicine*, 11(6), Aug, pp. 1407-1416.

Kim, J., Cao, L., Shvartsman, D., Silva, E. A. and Mooney, D. J. (2011) 'Targeted delivery of nanoparticles to ischemic muscle for imaging and therapeutic angiogenesis.' *Nano Lett*, 11(21192718) pp. 694-700.

Kingsley, J. D., Dou, H., Morehead, J., Rabinow, B., Gendelman, H. E. and Destache, C. J. (2006) 'Nanotechnology: a focus on nanoparticles as a drug delivery system.' *J Neuroimmune Pharmacol*, 1(3), Sep, pp. 340-350.

Kirby, B. J. and Hasselbrink, E. F., Jr. (2004) 'Zeta potential of microfluidic substrates: 1. Theory, experimental techniques, and effects on separations.' *Electrophoresis*, 25(2), Jan, pp. 187-202.

Kitazawa, T. and Kitazawa, K. (2012) 'Size-dependent heterogeneity of contractile Ca2+ sensitization in rat arterial smooth muscle.' *J Physiol*, 590(Pt 21), Nov 1, pp. 5401-5423.

Kjellander, R. (1996) 'Ion-ion correlations and effective charges in electrolyte and macroion systems.' *Berichte Der Bunsen-Gesellschaft-Physical Chemistry Chemical Physics*, 100(6), Jun, pp. 894-904.

Klein, J. (2007) 'Probing the interactions of proteins and nanoparticles.' *Proceedings of the National Academy of Sciences of the United States of America*, 104(7), //, pp. 2029-2030.

Knuckles, T. L., Yi, J. H., Frazer, D. G., Leonard, H. D., Chen, B. T., Castranova, V. and Nurkiewicz, T. R. (2012) 'Nanoparticle inhalation alters systemic arteriolar vasoreactivity through sympathetic and cyclooxygenase-mediated pathways.' *Nanotoxicology*, 6(7), Nov, pp. 724-735.

Kobayashi, M., Juillerat, F., Galletto, P., Bowen, P. and Borkovec, M. (2005) 'Aggregation and charging of colloidal silica particles: effect of particle size.' *Langmuir*, 21(13), Jun 21, pp. 5761-5769.

Koeppen, M., Feil, R., Siegl, D., Feil, S., Hofmann, F., Pohl, U. and de Wit, C. (2004) 'cGMP-dependent protein kinase mediates NO- but not acetylcholine-induced dilations in resistance vessels in vivo.' *Hypertension*, 44(6), Dec, pp. 952-955.

Koh, S. D., Bradley, K. K., Rae, M. G., Keef, K. D., Horowitz, B. and Sanders, K. M. (1998) 'Basal activation of ATP-sensitive potassium channels in murine colonic smooth muscle cell.' *Biophys J*, 75(4), 10/, pp. 1793-1800.

Kol'tsova, S. V., Baskakov, M. B. and Orlov, S. N. (2010) '[Myogenic tone of blood vessels in health and disease: role of purinergic signaling system and Na+, K+ 2Cl+ cotransport].' *Patol Fiziol Eksp Ter*, (4), Oct-Dec, pp. 3-10.

Koohestanian, A., Hosseini, M. and Abbasian, Z. (2004) 'The Separation Method for Removing of Colloidal Particles from Raw Water.' *American-Eurasian J. Agric. & Environ. Sci.*, 4(2) pp. 266-273.

Kvasnicka, T. (2003) '[NO (nitric oxide) and its significance in regulation of vascular homeostasis].' *Vnitr Lek*, 49(4), Apr, pp. 291-296.

Labbez, C., Jonsson, B., Skarba, M. and Borkovec, M. (2009) 'Ion-Ion Correlation and Charge Reversal at Titrating Solid Interfaces.' *Langmuir*, 25(13), Jul 7, pp. 7209-7213.

Labhasetwar, V., Song, C. X., Humphrey, W., Shebuski, R. and Levy, R. J. (1998) 'Arterial uptake of biodegradable nanoparticles: Effect of surface modifications.' *Journal of Pharmaceutical Sciences*, 87(10), Oct, pp. 1229-1234.

Langhorst, M. F., Reuter, A., Jaeger, F. A., Wippich, F. M., Luxenhofer, G., Plattner, H. and Stuermer, C. A. (2008) 'Trafficking of the microdomain scaffolding protein reggie-1/flotillin-2.' *Eur J Cell Biol*, 87(4), Apr, pp. 211-226.

LeBlanc, A. J., Cumpston, J. L., Chen, B. T., Frazer, D., Castranova, V. and Nurkiewicz, T. R. (2009) 'Nanoparticle inhalation impairs endothelium-dependent vasodilation in subepicardial arterioles.' *J Toxicol Environ Health A*, 72(24) pp. 1576-1584.

LeBlanc, A. J., Moseley, A. M., Chen, B. T., Frazer, D., Castranova, V. and Nurkiewicz, T. R. (2010) 'Nanoparticle inhalation impairs coronary microvascular reactivity via a local reactive oxygen species-dependent mechanism.' *Cardiovasc Toxicol*, 10(1), Mar, pp. 27-36.

Lefroy, D. C., Crake, T., Uren, N. G., Davies, G. J. and Maseri, A. (1993) 'Effect of inhibition of nitric oxide synthesis on epicardial coronary artery caliber and coronary blood flow in humans.' *Circulation*, 88(1), 07/, pp. 43-54.

Leo, C. H., Hart, J. L. and Woodman, O. L. (2011) 'Impairment of both nitric oxide-mediated and EDHF-type relaxation in small mesenteric arteries from rats with streptozotocin-induced diabetes.' *Br J Pharmacol*, 162(2), Jan, pp. 365-377.

Li, G. Y., Jiang, Y. R., Huang, K. L., Ding, P. and Chen, J. (2008) 'Preparation and properties of magnetic Fe3O4-chitosan nanoparticles.' *Journal of Alloys and Compounds*, 466(1-2), Oct 20, pp. 451-456.

Li, H. N., Mu, Y. W., Qian, S. S., Lu, J. S., Wan, Y. K., Fu, G. D. and Liu, S. Q. (2015) 'Synthesis of fluorescent dye-doped silica nanoparticles for target-cell-specific delivery and intracellular MicroRNA imaging.' *Analyst*, 140(2) pp. 567-573.

Liberman, A., Mendez, N., Trogler, W. C. and Kummel, A. C. (2014) 'Synthesis and surface functionalization of silica nanoparticles for nanomedicine.' *Surface Science Reports*, 69(2-3), Sep-Oct, pp. 132-158.

Linder, S., Pinkowski, W. and Aepfelbacher, M. (2002) 'Adhesion, cytoskeletal architecture and activation status of primary human macrophages on a diamond-like carbon coated surface.' *Biomaterials*, 23(3), 02/, pp. 767-773.

Little, T. L., Xia, J. and Duling, B. R. (1995) 'Dye Tracers Define Differential Endothelial and Smooth-Muscle Coupling Patterns within the Arteriolar Wall.' *Circulation Research*, 76(3), Mar, pp. 498-504.

Liu, J., Levine, A. L., Mattoon, J. S., Yamaguchi, M., Lee, R. J., Pan, X. L. and Rosol, T. J. (2006) 'Nanoparticles as image enhancing agents for ultrasonography.' *Physics in Medicine and Biology*, 51(9), May 7, pp. 2179-2189.

Liu, X. and Sun, J. A. (2010) 'Endothelial cells dysfunction induced by silica nanoparticles through oxidative stress via JNK/P53 and NF-kappa B pathways.' *Biomaterials*, 31(32), Nov, pp. 8198-8209.

Liu, Y., Zhao, H., Li, H., Kalyanaraman, B., Nicolosi, A. C. and Gutterman, D. D. (2003) 'Mitochondrial sources of H2O2 generation play a key role in flow-mediated dilation in human coronary resistance arteries.' *Circ Res*, 93(12919951) pp. 573-580.

Liu, Y., Zhang, Y., Schmelzer, K., Lee, T.-S., Fang, X., Zhu, Y., Spector, A. A., Gill, S., Morisseau, C., Hammock, B. D. and Shyy, J. Y. J. (2005) 'The antiinflammatory effect of laminar flow: the role of PPARgamma, epoxyeicosatrienoic acids, and soluble epoxide hydrolase.' *Proc Natl Acad Sci U S A*, 102(46), 11/15, pp. 16747-16752.

Lodish, H. F. (2000) 'Cell Motility and Shape I: Microfilaments.' *In Molecular cell biology*. 4th ed., New York: W.H. Freeman, pp. xxxvi, 1084, G-1017, I-1036 p.

Loesch, A., Milner, P., Anglin, S. C., Crowe, R., Miah, S., McEwan, J. R. and Burnstock, G. (1997) 'Ultrastructural localisation of nitric oxide synthase, endothelin and binding sites of lectin (from Bandeirea simplicifolia) in the rat carotid artery after balloon catheter injury.' *J Anat*, 190 (Pt 1)(9034885) pp. 93-9104.

Lu, J., Liong, M., Zink, J. I. and Tamanoi, F. (2007) 'Mesoporous silica nanoparticles as a delivery system for hydrophobic anticancer drugs.' *Small*, 3(8), Aug, pp. 1341-1346.

Luckhoff, A. and Busse, R. (1990) 'Calcium influx into endothelial cells and formation of endothelium-derived relaxing factor is controlled by the membrane potential.' *Pflugers Arch*, 416(3), May, pp. 305-311.

Lyklema, J. (2003) 'Lyotropic sequences in colloid stability revisited.' *Advances in Colloid and Interface Science*, 100, Feb 28, pp. 1-12.

Lyubimov, E. V. and Gotlieb, A. I. (2004) 'Smooth muscle cell growth in monolayer and aortic organ culture is promoted by a nonheparin binding endothelial cell-derived soluble factor/s.' *Cardiovasc Pathol*, 13(3), May-Jun, pp. 139-145.

Ma, Y., Dai, Z. F., Gao, Y. G., Cao, Z., Zha, Z. B., Yue, X. L. and Kikuchi, J. I. (2011) 'Liposomal architecture boosts biocompatibility of nanohybrid cerasomes.' *Nanotoxicology*, 5(4), Dec, pp. 622-635.

Mahdavi, M., Bin Ahmad, M., Haron, M. J., Namvar, F., Nadi, B., Ab Rahman, M. Z. and Amin, J. (2013) 'Synthesis, Surface Modification and Characterisation of Biocompatible Magnetic Iron Oxide Nanoparticles for Biomedical Applications.' *Molecules*, 18(7), Jul, pp. 7533-7548.

Malfatti, M. A., Palko, H. A., Kuhn, E. A. and Turteltaub, K. W. (2012) 'Determining the pharmacokinetics and long-term biodistribution of SiO2 nanoparticles in vivo using accelerator mass spectrometry.' *Nano Lett*, 12(11), Nov 14, pp. 5532-5538.

Malvern. (2013) Zetasizer nano user manual. (Apr) Vol. 3: Malvern Instruments Ltd.

Manolova, V., Flace, A., Saudan, P. and Bachmann, M. F. (2007) 'Nanoparticles target distinct dendritic cell populations according to their size.' *Swiss Medical Weekly*, 137, Mar 30, pp. 26s-26s.

Manolova, V., Flace, A., Bauer, M., Schwarz, K., Saudan, P. and Bachmann, M. F. (2008) 'Nanoparticles target distinct dendritic cell populations according to their size.' *European Journal of Immunology*, 38(5), May, pp. 1404-1413.

Marchenko, S. M. and Sage, S. O. (1993) 'Electrical properties of resting and acetylcholine-stimulated endothelium in intact rat aorta.' *J Physiol*, 462, Mar, pp. 735-751.

Marchesi, C., Ebrahimian, T., Angulo, O., Paradis, P. and Schiffrin, E. L. (2009) 'Endothelial nitric oxide synthase uncoupling and perivascular adipose oxidative stress and inflammation contribute to vascular dysfunction in a rodent model of metabolic syndrome.' *Hypertension*, 54(6), Dec, pp. 1384-1392.

Marchisio, D. L., Rivautella, L. and Barresi, A. A. (2006) 'Design and scale-up of chemical reactors for nanoparticle precipitation.' *Aiche Journal*, 52(5), May, pp. 1877-1887.

Marcus, Y. (1994) 'Viscosity B-Coefficients, Structural Entropies and Heat-Capacities, and the Effects of Ions on the Structure of Water.' *Journal of Solution Chemistry*, 23(7), Jul, pp. 831-848.

Marcus, Y. (2009) 'Effect of Ions on the Structure of Water: Structure Making and Breaking.' *Chemical Reviews*, 109(3), Mar, pp. 1346-1370.

Margolis, J., McDonald, J., Heuser, R., Klinke, P., Waksman, R., Virmani, R., Desai, N. and Hilton, D. (2007) 'Systemic nanoparticle paclitaxel (nab-paclitaxel) for in-stent restenosis I (SNAPIST-I): a first-in-human safety and dose-finding study.' *Clin Cardiol*, 30(4), Apr, pp. 165-170.

Mathison, R. and Davison, J. S. (1993) 'Altered vascular permeability responses to substance P in diabetic rats: interactions with a nitric oxide synthesis inhibitor.' *Eur J Pharmacol*, 240(2-3), Aug 24, pp. 163-168.

Matoba, T., Shimokawa, H., Kubota, H., Morikawa, K., Fujiki, T., Kunihiro, I., Mukai, Y., Hirakawa, Y. and Takeshita, A. (2002) 'Hydrogen peroxide is an endothelium-derived hyperpolarizing factor in human mesenteric arteries.' *Biochemical and Biophysical Research Communications*, 290(3), Jan 25, pp. 909-913.

Mattheakis, L. C., Dias, J. M., Choi, Y. J., Gong, J., Bruchez, M. P., Liu, J. and Wang, E. (2004) 'Optical coding of mammalian cells using semiconductor quantum dots.' *Anal Biochem*, 327(2), Apr 15, pp. 200-208.

McGiff, J. C. and Quilley, J. (1999) '20-HETE and the kidney: resolution of old problems and new beginnings.' *American Journal of Physiology - Regulatory, Integrative and Comparative Physiology*, 277(3), 1999-09-01 07:00:00, pp. R607-R623.

McNeish, A. J., Dora, K. A. and Garland, C. J. (2005) 'Possible role for K+ in endothelium-derived hyperpolarizing factor-linked dilatation in rat middle cerebral artery.' *Stroke*, 36(7), Jul, pp. 1526-1532.

Medebach, M., Moitzi, C., Freiberger, N. and Glatter, O. (2007) 'Dynamic light scattering in turbid colloidal dispersions: A comparison between the modified flat-cell light-scattering instrument and 3D dynamic light-scattering instrument.' *Journal of Colloid and Interface Science*, 305(1), Jan 1, pp. 88-93.

Mehrke, G. and Daut, J. (1990) 'The electrical response of cultured guinea-pig coronary endothelial cells to endothelium-dependent vasodilators.' *J Physiol*, 430, Nov, pp. 251-272.

Merrifield, C. J., Feldman, M. E., Wan, L. and Almers, W. (2002) 'Imaging actin and dynamin recruitment during invagination of single clathrin-coated pits.' *Nat Cell Biol*, 4(9), Sep, pp. 691-698.

Michael, L. H. and Zhuravlev, L. T. (2005) 'The Surface Chemistry of Silica ?Äì The Zhuravlev Model.' *In Colloidal Silica*. CRC Press, pp. 261-266.

Michaelis, U. R. and Fleming, I. (2006) 'From endothelium-derived hyperpolarizing factor (EDHF) to angiogenesis: Epoxyeicosatrienoic acids (EETs) and cell signaling.' *Pharmacol Ther*, 111(3), Sep, pp. 584-595.

Michell, B. J., Chen, Z., Tiganis, T., Stapleton, D., Katsis, F., Power, D. A., Sim, A. T. and Kemp, B. E. (2001) 'Coordinated control of endothelial nitric-oxide synthase phosphorylation by protein kinase C and the cAMP-dependent protein kinase.' *J Biol Chem*, 276(21), May 25, pp. 17625-17628.

Michell, B. J., Griffiths, J. E., Mitchelhill, K. I., Rodriguez-Crespo, I., Tiganis, T., Bozinovski, S., de Montellano, P. R., Kemp, B. E. and Pearson, R. B. (1999) 'The Akt kinase signals directly to endothelial nitric oxide synthase.' *Curr Biol*, 9(15), Jul 29-Aug 12, pp. 845-848.

Miller, C., Moczydlowski, E., Latorre, R. and Phillips, M. (1985) 'Charybdotoxin, a protein inhibitor of single Ca2+-activated K+ channels from mammalian skeletal muscle.' *Nature*, 313(6000), Jan 24-30, pp. 316-318.

Minarchick, V. C., Stapleton, P. A., Porter, D. W., Wolfarth, M. G., Ciftyurek, E., Barger, M., Sabolsky, E. M. and Nurkiewicz, T. R. (2013) 'Pulmonary Cerium Dioxide Nanoparticle Exposure Differentially Impairs Coronary and Mesenteric Arteriolar Reactivity.' *Cardiovasc Toxicol*, May 5,

Minneman, K. P. (1988) 'Alpha 1-adrenergic receptor subtypes, inositol phosphates, and sources of cell Ca2+.' *Pharmacological Reviews*, 40(2), June 1, 1988, pp. 87-119.

Miura, H. and Gutterman, D. D. (1998) 'Human coronary arteriolar dilation to arachidonic acid depends on cytochrome P-450 monooxygenase and Ca2+-activated K+ channels.' *Circ Res*, 83(5), Sep 7, pp. 501-507.

Miura, H., Liu, Y. and Gutterman, D. D. (1999) 'Human coronary arteriolar dilation to bradykinin depends on membrane hyperpolarization: contribution of nitric oxide and Ca2+-activated K+ channels.' *Circulation*, 99(10377076) pp. 3132-3138.

Miura, H., Wachtel, R. E., Liu, Y., Loberiza, F. R., Jr., Saito, T., Miura, M. and Gutterman, D. D. (2001) 'Flow-induced dilation of human coronary arterioles: important role of Ca(2+)-activated K(+) channels.' *Circulation*, 103(15), Apr 17, pp. 1992-1998.

Mombouli, J. V., Bissiriou, I., Agboton, V. D. and Vanhoutte, P. M. (1996) 'Bioassay of endothelium-derived hyperpolarizing factor.' *Biochem Biophys Res Commun*, 221(2), Apr 16, pp. 484-488.

Monopoli, M. P., Walczyk, D., Campbell, A., Elia, G., Lynch, I., Baldelli Bombelli, F. and Dawson, K. A. (2011) 'Physical-Chemical aspects of protein corona: Relevance to in vitro and in vivo biological impacts of nanoparticles.' *Journal of the American Chemical Society*, 133(8), //, pp. 2525-2534.

Monteiro-Riviere, N., Nemanich, R., Inman, A., Wang, Y. and Riviere, J. (2005) 'Multi-walled carbon nanotube interactions with human epidermal keratinocytes.' *Toxicol Lett*, 155 pp. 377 - 384.

Morikawa, K., Fujiki, T., Matoba, T., Kubota, H., Hatanaka, M., Takahashi, S. and Shimokawa, H. (2004) 'Important role of superoxide dismutase in EDHF-mediated responses of human mesenteric arteries.' *J Cardiovasc Pharmacol*, 44(5), Nov, pp. 552-556.

Morikawa, K., Shimokawa, H., Matoba, T., Kubota, H., Akaike, T., Talukder, M. A. H., Hatanaka, M., Fujiki, T., Maeda, H., Takahashi, S. and Takeshita, A. (2003) 'Pivotal role of Cu,Zn-superoxide dismutase in endothelium-dependent hyperpolarization.' *Journal of Clinical Investigation*, 112(12), //, pp. 1871-1879.

Mortensen, L. J., Oberdorster, G., Pentland, A. P. and Delouise, L. A. (2008) 'In vivo skin penetration of quantum dot nanoparticles in the murine model: the effect of UVR.' *Nano Lett*, 8(9), Sep, pp. 2779-2787.

Motwani, M. S., Rafiei, Y., Tzifa, A. and Seifalian, A. M. (2011) 'In situ endothelialization of intravascular stents from progenitor stem cells coated with nanocomposite and functionalized biomolecules.' *Biotechnol Appl Biochem*, 58(21446954) pp. 2-13.

Mu, Q. S., Hondow, N. S., Krzeminski, L., Brown, A. P., Jeuken, L. J. C. and Routledge, M. N. (2012) 'Mechanism of cellular uptake of genotoxic silica nanoparticles.' *Particle and Fibre Toxicology*, 9, Jul 23,

Mugge, A., Elwell, J. H., Peterson, T. E. and Harrison, D. G. (1991) 'Release of intact endothelium-derived relaxing factor depends on endothelial superoxide dismutase activity.' *American Journal of Physiology - Cell Physiology*, 260(2 29-2), //, pp. C219-C225.

Mukherjee, S., Ghosh, R. and Maxfield, F. (1997) 'Endocytosis.' *Physiol Rev*, 77 pp. 759 - 803.

Mukhopadhyay, A., Joshi, N., Chattopadhyay, K. and De, G. (2012) 'A Facile Synthesis of PEG-Coated Magnetite (Fe3O4) Nanoparticles and Their Prevention of the Reduction of Cytochrome C.' *Acs Applied Materials & Interfaces*, 4(1), Jan, pp. 142-149.

Mulvany, M. J. and Aalkjaer, C. (1990) 'Structure and function of small arteries.' *Physiol Rev*, 70(4), Oct, pp. 921-961.

Muzykantov, V. R. (2005) 'Biomedical aspects of targeted delivery of drugs to pulmonary endothelium.' *Expert Opin Drug Deliv*, 2(5), Sep, pp. 909-926.

Myit, S., Delafontaine, P., Bochaton-Piallat, M. L., Giraud, S., Gabbiani, G. and Brink, M. (2003) 'Different growth properties of neointimal and medial smooth muscle cells in response to growth factors.' *J Vasc Res*, 40(2), Mar-Apr, pp. 97-104.

Nabeshi, H., Yoshikawa, T., Arimori, A., Yoshida, T., Tochigi, S., Hirai, T., Akase, T., Nagano, K., Abe, Y., Kamada, H., Tsunoda, S., Itoh, N., Yoshioka, Y. and Tsutsumi, Y. (2011) 'Effect of surface properties of silica nanoparticles on their cytotoxicity and cellular distribution in murine macrophages.' *Nanoscale Res Lett*, 6(1) p. 93.

Nabiev, I., Mitchell, S., Davies, A., Williams, Y., Kelleher, D., Moore, R., Gun'ko, Y., Byrne, S., Rakovich, Y., Donegan, J., Sukhanova, A., Conroy, J., Cottell, D., Gaponik, N., Rogach, A. and Volkov, Y. (2007) 'Nonfunctionalized nanocrystals can exploit a cell's active transport machinery delivering them to specific nuclear and cytoplasmic compartments.' *Nano Lett*, 7 pp. 3452 - 3461.

Naghavi, N., de Mel, A., Alavijeh, O. S., Cousins, B. G. and Seifalian, A. M. (2013) 'Nitric oxide donors for cardiovascular implant applications.' *Small*, 9(1), Jan 14, pp. 22-35.

Nel, A. E., Madler, L., Velegol, D., Xia, T., Hoek, E. M. V., Somasundaran, P., Klaessig, F., Castranova, V. and Thompson, M. (2009) 'Understanding biophysicochemical interactions at the nano-bio interface.' *Nature Materials*, 8(7), Jul, pp. 543-557.

Nemmar, A., Hoylaerts, M. F., Hoet, P. H. and Nemery, B. (2004) 'Possible mechanisms of the cardiovascular effects of inhaled particles: systemic translocation and prothrombotic effects.' *Toxicol Lett*, 149(1-3), Apr 1, pp. 243-253.

Nemmar, A., Albarwani, S., Beegam, S., Yuvaraju, P., Yasin, J., Attoub, S. and Ali, B. H. (2014) 'Amorphous silica nanoparticles impair vascular homeostasis and induce systemic inflammation.' *Int J Nanomedicine*, 9 pp. 2779-2789.

Nidhin, M., Indumathy, R., Sreeram, K. J. and Nair, B. U. (2008) 'Synthesis of iron oxide nanoparticles of narrow size distribution on polysaccharide templates.' *Bulletin of Materials Science*, 31(1), Feb, pp. 93-96.

Ninham, B. W. (1999) 'On progress in forces since the DLVO theory.' *Advances in Colloid and Interface Science*, 83(1-3), Dec 1, pp. 1-17.

Node, K., Huo, Y., Ruan, X., Yang, B., Spiecker, M., Ley, K., Zeldin, D. C. and Liao, J. K. (1999) 'Anti-inflammatory properties of cytochrome P450 epoxygenase-derived eicosanoids.' *Science*, 285(5431), 08/20, pp. 1276-1279.

Noma, A. (1983) 'ATP-regulated K+ channels in cardiac muscle.' *Nature*, 305(5930), 09/08, pp. 147-148.

Norrish, K. and Rausell-Colom, J. A. (1961) 'Low-Angle X-Ray Diffraction Studies of the Swelling of Montmorillonite and Vermiculite.' *Clays and Clay Minerals*, 10(1) pp. 123-149.

Nozawa, K., Gailhanou, H., Raison, L., Panizza, P., Ushiki, H., Sellier, E., Delville, J. P. and Delville, M. H. (2005) 'Smart Control of Monodisperse Stöber Silica Particles: Effect of Reactant Addition Rate on Growth Process.' *Langmuir*, 21(4), 2005/02/01, pp. 1516-1523.

Nurkiewicz, T. R., Porter, D. W., Barger, M., Castranova, V. and Boegehold, M. A. (2004) 'Particulate matter exposure impairs systemic microvascular endothelium-dependent dilation.' *Environ Health Perspect*, 112(13), Sep, pp. 1299-1306.

Nurkiewicz, T. R., Porter, D. W., Hubbs, A. F., Cumpston, J. L., Chen, B. T., Frazer, D. G. and Castranova, V. (2008) 'Nanoparticle inhalation augments particle-dependent systemic microvascular dysfunction.' *Part Fibre Toxicol*, 5 p. 1.

Nurkiewicz, T. R., Porter, D. W., Hubbs, A. F., Stone, S., Chen, B. T., Frazer, D. G., Boegehold, M. A. and Castranova, V. (2009) 'Pulmonary Nanoparticle Exposure Disrupts Systemic Microvascular Nitric Oxide Signaling.' *Toxicological Sciences*, 110(1), July 1, 2009, pp. 191-203.

Nurkiewicz, T. R., Porter, D. W., Barger, M., Millecchia, L., Rao, K. M., Marvar, P. J., Hubbs, A. F., Castranova, V. and Boegehold, M. A. (2006) 'Systemic microvascular dysfunction and inflammation after pulmonary particulate matter exposure.' *Environ Health Perspect*, 114(3), Mar, pp. 412-419.

Nurkiewicz, T. R., Porter, D. W., Hubbs, A. F., Stone, S., Moseley, A. M., Cumpston, J. L., Goodwill, A. G., Frisbee, S. J., Perrotta, P. L., Brock, R. W., Frisbee, J. C., Boegehold, M. A., Frazer, D. G., Chen, B. T. and Castranova, V. (2011) 'Pulmonary particulate matter and systemic microvascular dysfunction.' *Res Rep Health Eff Inst*, (164), Dec, pp. 3-48.

Oberdorster, G. (2010) 'Safety assessment for nanotechnology and nanomedicine: concepts of nanotoxicology.' *J Intern Med*, 267(1), Jan, pp. 89-105.

Oberdorster, G., Oberdorster, E. and Oberdorster, J. (2005) 'Nanotoxicology: an emerging discipline evolving from studies of ultrafine particles.' *Environ Health Perspect*, 113(7), Jul, pp. 823-839.

Ohashi, J., Sawada, A., Nakajima, S., Noda, K., Takaki, A. and Shimokawa, H. (2012) 'Mechanisms for Enhanced Endothelium-Derived Hyperpolarizing Factor-Mediated Responses in Microvessels in Mice.' *Circ J*, Mar 30,

Okado-Matsumoto, A. and Fridovich, I. (2001) 'Subcellular distribution of superoxide dismutases (SOD) in rat liver. Cu,Zn-SOD in mitochondria.' *Journal of Biological Chemistry*, 276(42), //, pp. 38388-38393.

Okamura, T. and Toda, N. (1992) '[Regulation of vascular tone by nitric oxide (NO) derived from endothelium and nerve].' *Jpn Circ J*, 56 Suppl 5 pp. 1296-1300.

Oye, G., Glomm, W. R., Vralstad, T., Volden, S., Magnusson, H., Stocker, M. and Sjoblom, J. (2006) 'Synthesis, functionalisation and characterisation of mesoporous materials and sol-gel glasses for

applications in catalysis, adsorption and photonics.' *Advances in Colloid and Interface Science*, 123, Nov 16, pp. 17-32.

Ozkor, M. A. and Quyyumi, A. A. (2011) 'Endothelium-derived hyperpolarizing factor and vascular function.' *Cardiol Res Pract*, 2011 p. 156146.

Ozkor, M. A., Murrow, J. R., Rahman, A. M., Kavtaradze, N., Lin, J., Manatunga, A. and Quyyumi, A. A. (2011) 'Endothelium-derived hyperpolarizing factor determines resting and stimulated forearm vasodilator tone in health and in disease.' *Circulation*, 123(20), May 24, pp. 2244-2253.

Pacher, P., Beckman, J. S. and Liaudet, L. (2007) 'Nitric oxide and peroxynitrite in health and disease.' *Physiol Rev*, 87(1), Jan, pp. 315-424.

Pahl, H. L. (1999) 'Activators and target genes of Rel/NF-kappaB transcription factors.' *Oncogene*, 18(49), 11/22, pp. 6853-6866.

Paltauf-Doburzynska, J., Frieden, M. and Graier, W. F. (1999) 'Mechanisms of Ca2+ store depletion in single endothelial cells in a Ca(2+)-free environment.' *Cell Calcium*, 25(5), May, pp. 345-353.

Pan, L. L., Liu, X. H., Gong, Q. H., Yang, H. B. and Zhu, Y. Z. (2012) 'Role of cystathionine gamma-lyase/hydrogen sulfide pathway in cardiovascular disease: a novel therapeutic strategy?' *Antioxid Redox Signal*, 17(1), Jul 1, pp. 106-118.

Park, E. J. and Park, K. (2009) 'Oxidative stress and pro-inflammatory responses induced by silica nanoparticles in vivo and in vitro.' *Toxicol Lett*, 184(1), Jan 10, pp. 18-25.

Parkington, H. C., Chow, J. A. M., Evans, R. G., Coleman, H. A. and Tare, M. (2002) 'Role for endothelium-derived hyperpolarizing factor in vascular tone in rat mesenteric and hindlimb circulations in vivo.' *Journal of Physiology-London*, 542(3), Aug 1, pp. 929-937.

Parton, R. G. and Simons, K. (2007) 'The multiple faces of caveolae.' *Nat Rev Mol Cell Biol*, 8(3), Mar, pp. 185-194.

Pashley, R. M. (1981) 'Dlvo and Hydration Forces between Mica Surfaces in Li+,Na+,K+,and Cs+ Electrolyte-Solutions - a Correlation of Double-Layer and Hydration Forces with Surface Cation-Exchange Properties.' *Journal of Colloid and Interface Science*, 83(2) pp. 531-546.

Pashley, R. M. and Karaman, M. E. (2005) 'Van der Waals Forces and Colloid Stability.' *In Applied Colloid and Surface Chemistry*. John Wiley & Sons, Ltd, pp. 127-151.

Pashley, R. M., McGuiggan, P. M., Ninham, B. W., Brady, J. and Evans, D. F. (1986) 'Direct measurements of surface forces between bilayers of double-chained quaternary ammonium acetate and bromide surfactants.' *The Journal of Physical Chemistry*, 90(8), 1986/04/01, pp. 1637-1642.

Passagne, I., Morille, M., Rousset, M., Pujalte, I. and L'Azou, B. (2012) 'Implication of oxidative stress in size-dependent toxicity of silica nanoparticles in kidney cells.' *Toxicology*, 299(2-3), Sep 28, pp. 112-124.

Patricio, B. F. C., Weissmuller, G. and Santos-Oliveira, R. (2011) 'Development of the 153-sm-edtmp nanoradiopharmaceutical.' *J. Labelled Compd. Radiopharm.*, 54, //, p. 558.

Payne, C., Jones, S., Chen, C. and Zhuang, X. (2007) 'Internalization and trafficking of cell surface proteoglycans and proteoglycan-binding ligands.' *Traffic*, 8 pp. 389 - 401.

Pearson, J. D., Slakey, L. L. and Gordon, J. L. (1983) 'Stimulation of prostaglandin production through purinoceptors on cultured porcine endothelial cells.' *Biochem J*, 214(1), Jul 15, pp. 273-276.

Pennycook, S. J. and Nellist, P. D. (2002) *Scanning transmission electron microscopy: imaging and analysis.* New York: Springer New York.

Phillips, E., Penate-Medina, O., Zanzonico, P. B., Carvajal, R. D., Mohan, P., Ye, Y. P., Humm, J., Gonen, M., Kalaigian, H., Schoder, H., Strauss, H. W., Larson, S. M., Wiesner, U. and Bradbury, M. S. (2014) 'Clinical translation of an ultrasmall inorganic optical-PET imaging nanoparticle probe.' *Science Translational Medicine*, 6(260), Oct 29,

Phillips, J. K., Vidovic, M. and Hill, C. E. (1996) 'alpha-adrenergic, neurokinin and muscarinic receptors in rat mesenteric artery; An mRNA study during postnatal development.' *Mechanisms of Ageing and Development*, 92(2-3), Dec 20, pp. 235-246.

Pires, J. F., Patricio, B. F. d. C., Albernaz, M. d. S., Mendonca, G. D., Coelho, B. F., Weissmuller, G., Elias, C. N. and Santos-Oliveira, R. (2012) 'Preparation of Biodegradable Poly(L-Lactide) (PLA) Nanoparticles Containing DMSA (Dimercaptosuccinic Acid) as Novel Radiopharmaceutical.' *Advanced Science Letters*, 10(1), //, pp. 143-145.

Plane, F., Pearson, T. and Garland, C. J. (1995) 'Multiple pathways underlying endothelium-dependent relaxation in the rabbit isolated femoral artery.' *Br J Pharmacol*, 115(1), May, pp. 31-38.

Pober, J. S. and Sessa, W. C. (2007) 'Evolving functions of endothelial cells in inflammation.' *Nat Rev Immunol*, 7(10), 10/, pp. 803-815.

Popp, R., Bauersachs, J., Hecker, M., Fleming, I. and Busse, R. (1996) 'A transferable, beta-naphthoflavone-inducible, hyperpolarizing factor is synthesized by native and cultured porcine coronary endothelial cells.' *J Physiol*, 497 (Pt 3), Dec 15, pp. 699-709.

Potente, M., Fisslthaler, B., Busse, R. and Fleming, I. (2003) '11,12-Epoxyeicosatrienoic acid-induced inhibition of FOXO factors promotes endothelial proliferation by down-regulating p27Kip1.' *J Biol Chem*, 278(32), 08/08, pp. 29619-29625.

Powell, R. J., Hydowski, J., Frank, O., Bhargava, J. and Sumpio, B. E. (1997) 'Endothelial Cell Effect on Smooth Muscle Cell Collagen Synthesis.' *Journal of Surgical Research*, 69(1) pp. 113-118.

Pozzi, A., Macias-Perez, I., Abair, T., Wei, S., Su, Y., Zent, R., Falck, J. R. and Capdevila, J. H. (2005) 'Characterization of 5,6- and 8,9-epoxyeicosatrienoic acids (5,6- and 8,9-EET) as potent in vivo angiogenic lipids.' *J Biol Chem*, 280(29), Jul 22, pp. 27138-27146.

Prabhu, V., Uzzaman, S., Grace, V. M. B. and Guruvayoorappan, C. (2011) 'Nanoparticles in Drug Delivery and Cancer Therapy: The Giant Rats Tail.' *Journal of Cancer Therapy*, 2, June, pp. 325-334.

Presta, A., Liu, J., Sessa, W. C. and Stuehr, D. J. (1997) 'Substrate binding and calmodulin binding to endothelial nitric oxide synthase coregulate its enzymatic activity.' *Nitric Oxide*, 1(1), Feb, pp. 74-87.

Qualmann, B., Kessels, M. M. and Kelly, R. B. (2000) 'Molecular links between endocytosis and the actin cytoskeleton.' *Journal of Cell Biology*, 150(5), Sep 4, pp. F111-F116.

Quignard, J. F., Chataigneau, T., Corriu, C., Edwards, G., Weston, A., Feletou, M. and Vanhoutte, P. M. (2002) 'Endothelium-dependent hyperpolarization to acetylcholine in carotid artery of guinea pig: role of lipoxygenase.' *J Cardiovasc Pharmacol*, 40(3), Sep, pp. 467-477.

Quilley, J. and McGiff, J. C. (2000) 'Is EDHF an epoxyeicosatrienoic acid?' *Trends Pharmacol Sci*, 21(4), Apr, pp. 121-124.

Raghu, H., Sharma-Walia, N., Veettil, M. V., Sadagopan, S. and Chandran, B. (2009) 'Kaposi's Sarcoma-Associated Herpesvirus Utilizes an Actin Polymerization-Dependent Macropinocytic Pathway To Enter Human Dermal Microvascular Endothelial and Human Umbilical Vein Endothelial Cells.' *Journal of Virology*, 83(10), May 15, pp. 4895-4911.

Rahman, I. A. and Padavettan, V. (2012) 'Synthesis of Silica Nanoparticles by Sol-Gel: Size-Dependent Properties, Surface Modification, and Applications in Silica-Polymer Nanocomposites—A Review.' *Journal of Nanomaterials*, 2012 p. 15.

Rath, G., Dessy, C. and Feron, O. (2009) 'Caveolae, caveolin and control of vascular tone: nitric oxide (NO) and endothelium derived hyperpolarizing factor (EDHF) regulation.' *J Physiol Pharmacol*, 60 Suppl 4, Oct, pp. 105-109.

Razink, J. J. and Schlotter, N. E. (2007) 'Correction to "Preparation of monodisperse silica particles: Control of size and mass fraction" by G.H. Bogush, M.A. Tracy and C.F. Zukoski IV, journal of non-crystalline solids 104 (1988) 95-106.' *Journal of Non-Crystalline Solids*, 353(30-31), Oct 1, pp. 2932-2933.

Rejman, J., Oberle, V., Zuhorn, I. S. and Hoekstra, D. (2004) 'Size-dependent internalization of particles via the pathways of clathrin-and caveolae-mediated endocytosis.' *Biochemical Journal*, 377, Jan 1, pp. 159-169.

Richards, G. R., Weston, A. H., Burnham, M. P., Feletou, M., Vanhoutte, P. M. and Edwards, G. (2001) 'Suppression of K(+)-induced hyperpolarization by phenylephrine in rat mesenteric artery: relevance to studies of endothelium-derived hyperpolarizing factor.' *Br J Pharmacol*, 134(1), Sep, pp. 1-5.

Risau, W. (1995) 'Differentiation of endothelium.' *The FASEB Journal*, 9(10), July 1, 1995, pp. 926-933.

Rivers, R. J., Hein, T. W., Zhang, C. and Kuo, L. (2001) 'Activation of barium-sensitive inward rectifier potassium channels mediates remote dilation of coronary arterioles.' *Circulation*, 104(15), Oct 9, pp. 1749-1753.

Roche, P., Al-Jowder, R., Narayanaswamy, R., Young, J. and Scully, P. (2006) 'A novel luminescent lifetime-based optrode for the detection of gaseous and dissolved oxygen utilising a mixed ormosil matrix containing ruthenium (4,7-diphenyl-1,10-phenanthroline)3Cl2 (Ru.dpp).' *Analytical and Bioanalytical Chemistry*, 386(5), 2006/11/01, pp. 1245-1257.

Rosolowsky, M. and Campbell, W. B. (1996) 'Synthesis of hydroxyeicosatetraenoic (HETEs) and epoxyeicosatrienoic acids (EETs) by cultured bovine coronary artery endothelial cells.' *Biochim Biophys Acta*, 1299(2), Jan 19, pp. 267-277.

Roy, M., Niu, C. J., Chen, Y., McVeigh, P. Z., Shuhendler, A. J., Leung, M. K., Mariampillai, A., DaCosta, R. S. and Wilson, B. C. (2012) 'Estimation of Minimum Doses for Optimized Quantum Dot Contrast-Enhanced Vascular Imaging In Vivo.' *Small*, pp. n/a-n/a.

Ryman-Rasmussen, J., Riviere, J. and Monteiro-Riviere, N. (2007) 'Surface coatings determine cytotoxicity and irritation potential of quantum dot nanoparticles in epidermal keratinocytes.' *J Invest Dermatol*, 127(1) pp. 143 - 153.

Sá, L. T. M., Pessoa, C., Meira, A. S., Da Silva, M. I. P., Missailidis, S. and Santos-Oliveira, R. (2012) 'Development of nanoaptamers using a mesoporous silica model labeled with 99mTc for cancer targeting.' *Oncology*, 82(4), //, pp. 213-217.

Saitoh, Y., Terada, N., Saitoh, S., Ohno, N., Jin, T. and Ohno, S. (2012) 'Histochemical analyses and quantum dot imaging of microvascular blood flow with pulmonary edema in living mouse lungs by "in vivo cryotechnique".' *Histochem Cell Biol*, 137(2), Feb, pp. 137-151.

Sakellariou, G. K., Pye, D., Vasilaki, A., Zibrik, L., Palomero, J., Kabayo, T., McArdle, F., Van Remmen, H., Richardson, A., Tidball, J. G., McArdle, A. and Jackson, M. J. (2011) 'Role of superoxide-nitric oxide interactions in the accelerated age-related loss of muscle mass in mice lacking Cu,Zn superoxide dismutase.' *Aging Cell*, Mar 28,

Salerno, J. C., Ghosh, D. K., Razdan, R., Helms, K. A., Brown, C. C., McMurry, J. L., Rye, E. A. and Chrestensen, C. A. (2014) 'Endothelial nitric oxide synthase is regulated by ERK phosphorylation at Ser(602).' *Bioscience Reports*, 34 pp. 535-545.

Saliez, J., Bouzin, C., Rath, G., Ghisdal, P., Desjardins, F., Rezzani, R., Rodella, L. F., Vriens, J., Nilius, B., Feron, O., Balligand, J. L. and Dessy, C. (2008) 'Role of caveolar compartmentation in endothelium-derived hyperpolarizing factor-mediated relaxation: Ca2+ signals and gap junction function are regulated by caveolin in endothelial cells.' *Circulation*, 117(8), Feb 26, pp. 1065-1074.

Sandow, S. L. and Hill, C. E. (2000) 'Incidence of Myoendothelial Gap Junctions in the Proximal and Distal Mesenteric Arteries of the Rat Is Suggestive of a Role in Endothelium-Derived Hyperpolarizing Factor–Mediated Responses.' *Circulation Research*, 86(3), February 18, 2000, pp. 341-346.

Sandow, S. L., Tare, M., Coleman, H. A., Hill, C. E. and Parkington, H. C. (2002) 'Involvement of myoendothelial gap junctions in the actions of endothelium-derived hyperpolarizing factor.' *Circulation Research*, 90(10), May 31, pp. 1108-1113.

Sato, M., Ye, L. H. and Kohama, K. (1995) 'Myosin light chain kinase from vascular smooth muscle inhibits the ATP-dependent interaction between actin and myosin by binding to actin.' *J Biochem*, 118(1), Jul, pp. 1-3.

Schubert, A. L., Schubert, W., Spray, D. C. and Lisanti, M. P. (2002) 'Connexin family members target to lipid raft domains and interact with caveolin-1.' *Biochemistry*, 41(18), May 7, pp. 5754-5764.

Schwartz, S. M. (1997) 'Smooth muscle migration in vascular development and pathogenesis.' *Transpl Immunol*, 5(4), Dec, pp. 255-260.

Scotland, R. S., Chauhan, S., Vallance, P. J. and Ahluwalia, A. (2001) 'An endothelium-derived hyperpolarizing factor-like factor moderates myogenic constriction of mesenteric resistance arteries in the absence of endothelial nitric oxide synthase-derived nitric oxide.' *Hypertension*, 38(4), Oct, pp. 833-839.

Scotland, R. S., Madhani, M., Chauhan, S., Moncada, S., Andresen, J., Nilsson, H., Hobbs, A. J. and Ahluwalia, A. (2005) 'Investigation of vascular responses in endothelial nitric oxide synthase/cyclooxygenase-1 double-knockout mice: key role for endothelium-derived hyperpolarizing factor in the regulation of blood pressure in vivo.' *Circulation*, 111(6), Feb 15, pp. 796-803.

Scott, P. A. and Bicknell, R. (1993) 'The isolation and culture of microvascular endothelium.' *J Cell Sci*, 105 (Pt 2), Jun, pp. 269-273.

Seabra, A. B., da Silva, R., de Souza, G. F. and de Oliveira, M. G. (2008) 'Antithrombogenic polynitrosated polyester/poly(methyl methacrylate) blend for the coating of blood-contacting surfaces.' *Artif Organs*, 32(4), Apr, pp. 262-267.

Segal, S. S. and Duling, B. R. (1989) 'Conduction of vasomotor responses in arterioles: a role for cell-to-cell coupling?' *Am J Physiol*, 256(3 Pt 2), Mar, pp. H838-845.

Seino, S. (1999) 'ATP-sensitive potassium channels: a model of heteromultimeric potassium channel/receptor assemblies.' *Annu Rev Physiol*, 61, /, pp. 337-362.

Seliger, C., Jurgons, R., Wiekhorst, F., Eberbeck, D., Trahms, L., Iro, H. and Alexiou, C. (2007) 'In vitro investigation of the behaviour of magnetic particles by a circulating artery model.' *Journal of Magnetism and Magnetic Materials*, 311(1), Apr, pp. 358-362.

Shahid, M. and Buys, E. S. (2013) 'Assessing Murine Resistance Artery Function Using Pressure Myography.' (76), 2013/06/07/, p. e50328.

Shapero, K., Fenaroli, F., Lynch, I., Cottell, D. C., Salvati, A. and Dawson, K. A. (2011) 'Time and space resolved uptake study of silica nanoparticles by human cells.' *Mol Biosyst*, 7(2), Feb, pp. 371-378.

Shaw, D. J. (1992) '8 - Colloid stability.' *In* Shaw, D. J. (ed.) *Introduction to Colloid and Surface Chemistry (Fourth Edition)*. Oxford: Butterworth-Heinemann, pp. 210-243.

Shi, H., He, X., Yuan, Y., Wang, K. and Liu, D. (2010) 'Nanoparticle-based biocompatible and long-life marker for lysosome labeling and tracking.' *Anal Chem*, 82(20155925) pp. 2213-2220.

Shimoda, L. A., Sham, J. S. and Sylvester, J. T. (2000) 'Altered pulmonary vasoreactivity in the chronically hypoxic lung.' *Physiol Res*, 49(5) pp. 549-560.

Shimokawa, H. (2010) 'Hydrogen peroxide as an endothelium-derived hyperpolarizing factor.' *Pflugers Arch*, 459(6), May, pp. 915-922.

Shimokawa, H. and Matoba, T. (2004) 'Hydrogen peroxide as an endothelium-derived hyperpolarizing factor.' *Pharmacol Res*, 49(6), Jun, pp. 543-549.

Shimokawa, H., Yasutake, H., Fujii, K., Owada, M. K., Nakaike, R., Fukumoto, Y., Takayanagi, T., Nagao, T., Egashira, K., Fujishima, M. and Takeshita, A. (1996) 'The importance of the hyperpolarizing mechanism increases as the vessel size decreases in endothelium-dependent relaxations in rat mesenteric circulation.' *Journal of Cardiovascular Pharmacology*, 28(5), Nov, pp. 703-711.

Shireman, P. K. and Pearce, W. H. (1996) 'Endothelial cell function: biologic and physiologic functions in health and disease.' *American Journal of Roentgenology*, 166(1), January 1, 1996, pp. 7-13.

Shukur, A., Rizvi, S. B., Whitehead, D., Seifalian, A. and Azzawi, M. (2013) 'Altered sensitivity to nitric oxide donors, induced by intravascular infusion of quantum dots, in murine mesenteric arteries.' *Nanomedicine*, 9(4), May, pp. 532-539.

Shum-Tim, D., Stock, U., Hrkach, J., Shinoka, T., Lien, J., Moses, M. A., Stamp, A., Taylor, G., Moran, A. M., Landis, W., Langer, R., Vacanti, J. P. and Mayer, J. E. (1999) 'Tissue engineering of autologous aorta using a new biodegradable polymer.' *Ann Thorac Surg*, 68(10617020) pp. 2298-2304.

Shvedova, A., Castranova, V., Kisin, E., Schwegler-Berry, D., Murray, A. and Gandelsman, V. (2003) 'Exposure to carbon nanotube material: assessment of nanotube cytotoxicity using human keratinocyte cells.' *J Toxicol Environ Health A*, 66 pp. 1909 - 1926.

Simonsen, U., Wadsworth, R. M., Buus, N. H. and Mulvany, M. J. (1999) 'In vitro simultaneous measurements of relaxation and nitric oxide concentration in rat superior mesenteric artery.' *J Physiol*, 516 (Pt 1), Apr 1, pp. 271-282.

Skovgaard, N., Gouliaev, A., Aalling, M. and Simonsen, U. (2011) 'The role of endogenous H2S in cardiovascular physiology.' *Curr Pharm Biotechnol*, 12(9), Sep, pp. 1385-1393.

Skrabalak, S. E., Chen, J., Au, L., Lu, X., Li, X. and Xia, Y. (2007) 'Gold Nanocages for Biomedical Applications.' *Adv Mater*, 19(20), Oct 17, pp. 3177-3184.

Slowing, I. I., Wu, C.-W., Vivero-Escoto, J. L. and Lin, V. S. Y. (2009) 'Mesoporous silica nanoparticles for reducing hemolytic activity towards mammalian red blood cells.' *Small*, 5(19051185) pp. 57-62.

So, S. J., Jang, I. S. and Han, C. S. (2008) 'Effect of micro/nano silica particle feeding for mice.' *J Nanosci Nanotechnol*, 8(10), Oct, pp. 5367-5371.

Sokolov, I. and Naik, S. (2008) 'Novel fluorescent silica nanoparticles: towards ultrabright silica nanoparticles.' *Small*, 4(7), Jul, pp. 934-939.

Somlyo, A. P. and Somlyo, A. V. (1994) 'Signal transduction and regulation in smooth muscle.' *Nature*, 372(7969467) pp. 231-236.

Sotnikova, R., Nedelcevova, J., Navarova, J., Nosalova, V., Drabikova, K., Szocs, K., Krenek, P., Kyselova, Z., Bezek, S., Knezl, V., Drimal, J., Broskova, Z., Kristova, V., Okruhlicova, L., Bernatova, I. and Bauer, V. (2011) 'Protection of the vascular endothelium in experimental situations.' *Interdiscip Toxicol*, 4(1), Mar, pp. 20-26.

Souris, J. S., Lee, C. H., Cheng, S. H., Chen, C. T., Yang, C. S., Ho, J. A. A., Mou, C. Y. and Lo, L. W. (2010) 'Surface charge-mediated rapid hepatobiliary excretion of mesoporous silica nanoparticles.' *Biomaterials*, 31(21), Jul, pp. 5564-5574.

Spiel, A. O., Gilbert, J. C. and Jilma, B. (2008) 'von Willebrand factor in cardiovascular disease: focus on acute coronary syndromes.' *Circulation*, 117(11), Mar 18, pp. 1449-1459.

Standen, N. B., Quayle, J. M., Davies, N. W., Brayden, J. E., Huang, Y. and Nelson, M. T. (1989) 'Hyperpolarizing vasodilators activate ATP-sensitive K+ channels in arterial smooth muscle.' *Science*, 245(4914), 07/14, pp. 177-180.

Stapleton, P. A., Minarchick, V. C., Cumpston, A. M., McKinney, W., Chen, B. T., Sager, T. M., Frazer, D. G., Mercer, R. R., Scabilloni, J., Andrew, M. E., Castranova, V. and Nurkiewicz, T. R. (2012) 'Impairment of coronary arteriolar endothelium-dependent dilation after multi-walled carbon nanotube inhalation: a time-course study.' *Int J Mol Sci*, 13(11) pp. 13781-13803.

Stark, W. J. (2011) 'Nanoparticles in Biological Systems.' *Angewandte Chemie-International Edition*, 50(6) pp. 1242-1258.

Stöber, W., Fink, A. and Bohn, E. (1968) 'Controlled growth of monodisperse silica spheres in the micron size range.' *Journal of Colloid and Interface Science*, 26(1), 1//, pp. 62-69.

Stuehr, D., Pou, S. and Rosen, G. M. (2001) 'Oxygen Reduction by Nitric-oxide Synthases.' *Journal of Biological Chemistry*, 276(18), //, pp. 14533-14536.

Suh, J. S., Lee, J. Y., Choi, Y. S., Yu, F., Yang, V., Lee, S. J., Chung, C. P. and Park, Y. J. (2009) 'Efficient labeling of mesenchymal stem cells using cell permeable magnetic nanoparticles.' *Biochem Biophys Res Commun*, 379(3), Feb 13, pp. 669-675.

Sun, L. and Chow, L. C. (2008) 'Preparation and properties of nano-sized calcium fluoride for dental applications.' *Dent Mater*, 24(1), Jan, pp. 111-116.

Suzuki, M., Li, R. A., Miki, T., Uemura, H., Sakamoto, N., Ohmoto-Sekine, Y., Tamagawa, M., Ogura, T., Seino, S., Marban, E. and Nakaya, H. (2001) 'Functional roles of cardiac and vascular ATP-sensitive potassium channels clarified by Kir6.2-knockout mice.' *Circ Res*, 88(6), 03/30, pp. 570-577.

Tanaka, N. (2014) *Scanning transmission electron microscopy of nanomaterials : basics of imaging and analysis.* Hackensack, NJ: Imperial College Press.

Taylor, H. J., Chaytor, A. T., Evans, W. H. and Griffith, T. M. (1998) 'Inhibition of the gap junctional component of endothelium-dependent relaxations in rabbit iliac artery by 18-alpha glycyrrhetinic acid.' *British Journal of Pharmacology*, 125(1), Sep, pp. 1-3.

Tenzer, S., Docter, D., Rosfa, S., Wlodarski, A., Kuharev, J., Rekik, A., Knauer, S. K., Bantz, C., Nawroth, T., Bier, C., Sirirattanapan, J., Mann, W., Treuel, L., Zellner, R., Maskos, M., Schild, H. and Stauber, R. H. (2011) 'Nanoparticle Size Is a Critical Physicochemical Determinant of the Human Blood Plasma Corona: A Comprehensive Quantitative Proteomic Analysis.' *Acs Nano*, 5(9), Sep, pp. 7155-7167.

Thomassen, L. C. J., Aerts, A., Rabolli, V., Lison, D., Gonzalez, L., Kirsch-Volders, M., Napierska, D., Hoet, P. H., Kirschhock, C. E. A. and Martens, J. A. (2010) 'Synthesis and characterization of stable

monodisperse silica nanoparticle sols for in vitro cytotoxicity testing.' *Langmuir*, 26(19697952) pp. 328-335.

Tortora, G. J. a. G., S. R. (2003) 'The Cardiovascular System: Blood Vessels and Haemodynamics.' *In Principles of Anatomy & Physiology*. John Wiley & Sons Australia, Limited, pp. 697-701.

Tosun, Z. and McFetridge, P. S. (2010) 'A composite SWNT-collagen matrix: characterization and preliminary assessment as a conductive peripheral nerve regeneration matrix.' *J Neural Eng*, 7(6), Dec, p. 066002.

Trandafir, C. C. and Kaufman, S. (2007) 'Vasoconstrictor activity of arginine vasopressin in rat small mesenteric arteries after hindlimb suspension.' *Faseb Journal*, 21(6), Apr, pp. A950-A950.

Tsagkogeorgas, F., Ochsenkuhn-Petropoulou, M., Niessner, R. and Knopp, D. (2006) 'Encapsulation of biomolecules for bioanalytical purposes: Preparation of diclofenac antibody-doped nanometer-sized silica particles by reverse micelle and sol-gel processing.' *Analytica Chimica Acta*, 573, Jul 28, pp. 133-137.

Tsai, C.-P., Hung, Y., Chou, Y.-H., Huang, D.-M., Hsiao, J.-K., Chang, C., Chen, Y.-C. and Mou, C.-Y. (2008) 'High-contrast paramagnetic fluorescent mesoporous silica nanorods as a multifunctional cell-imaging probe.' *Small*, 4(2), 02/, pp. 186-191.

Tumur, Z., Shimizu, H., Enomoto, A., Miyazaki, H. and Niwa, T. (2010) 'Indoxyl sulfate upregulates expression of ICAM-1 and MCP-1 by oxidative stress-induced NF-kappaB activation.' *Am J Nephrol*, 31(5), /, pp. 435-441.

Turci, F., Ghibaudi, E., Colonna, M., Boscolo, B., Fenoglio, I. and Fubini, B. (2010) 'An Integrated Approach to the Study of the Interaction between Proteins and Nanoparticles.' *Langmuir*, 26(11), Jun 1, pp. 8336-8346.

Uddin, M. R., Muthalif, M. M., Karzoun, N. A., Benter, I. F. and Malik, K. U. (1998) 'Cytochrome P-450 Metabolites Mediate Norepinephrine-Induced Mitogenic Signaling.' *Hypertension*, 31(1), January 1, 1998, pp. 242-247.

Urakami-Harasawa, L., Shimokawa, H., Nakashima, M., Egashira, K. and Takeshita, A. (1997) 'Importance of endothelium-derived hyperpolarizing factor in human arteries.' *J Clin Invest*, 100(11), Dec 1, pp. 2793-2799.

Vaca, L. and Kunze, D. L. (1995) 'IP3-activated Ca2+ channels in the plasma membrane of cultured vascular endothelial cells.' *Am J Physiol*, 269(3 Pt 1), Sep, pp. C733-738.

Van Camp, J. R., Yian, C. and Lupinetti, F. M. (1994) 'Regulation of pulmonary vascular resistance by endogenous and exogenous nitric oxide.' *Ann Thorac Surg*, 58(4), Oct, pp. 1025-1029; discussion 1029-1030.

van der Staay, F. J., Fanelli, R. J., Blokland, A. and Schmidt, B. H. (1999) 'Behavioral effects of apamin, a selective inhibitor of the SK(Ca)-channel, in mice and rats.' *Neurosci Biobehav Rev*, 23(8), Dec, pp. 1087-1110.

van Schooneveld, M. M., Vucic, E., Koole, R., Zhou, Y., Stocks, J., Cormode, D. P., Tang, C. Y., Gordon, R. E., Nicolay, K., Meijerink, A., Fayad, Z. A. and Mulder, W. J. M. (2008) 'Improved biocompatibility

and pharmacokinetics of silica nanoparticles by means of a lipid coating: A multimodality investigation.' *Nano Letters*, 8(8), Aug, pp. 2517-2525.

VanRollins, M., Kaduce, T. L., Fang, X., Knapp, H. R. and Spector, A. A. (1996) 'Arachidonic Acid Diols Produced by Cytochrome P-450 Monooxygenases Are Incorporated into Phospholipids of Vascular Endothelial Cells.' *Journal of Biological Chemistry*, 271(24), June 14, 1996, pp. 14001-14009.

Vasquez, R. J., Howell, B., Yvon, A. M. C., Wadsworth, P. and Cassimeris, L. (1997) 'Nanomolar concentrations of nocodazole alter microtubule dynamic instability in vivo and in vitro.' *Molecular Biology of the Cell*, 8(6), Jun, pp. 973-985.

Vercauteren, D., Vandenbroucke, R. E., Jones, A. T., Rejman, J., Demeester, J., De Smedt, S. C., Sanders, N. N. and Braeckmans, K. (2010) 'The Use of Inhibitors to Study Endocytic Pathways of Gene Carriers: Optimization and Pitfalls.' *Molecular Therapy*, 18(3), Mar, pp. 561-569.

Verwey, E., W., J. and Overbeek, J. T. G. (1948) *Theory of the stability of lyophobic colloids.* Amsterdam: Elsevier.

Vesterdal, L. K., Mikkelsen, L., Folkmann, J. K., Sheykhzade, M., Cao, Y., Roursgaard, M., Loft, S. and Møller, P. (2012) 'Carbon black nanoparticles and vascular dysfunction in cultured endothelial cells and artery segments.' *Toxicology Letters*, 214(1), 10/2/, pp. 19-26.

Vicent, D., Ilany, J., Kondo, T., Naruse, K., Fisher, S. J., Kisanuki, Y. Y., Bursell, S., Yanagisawa, M., King, G. L. and Kahn, C. R. (2003) 'The role of endothelial insulin signaling in the regulation of vascular tone and insulin resistance.' *J Clin Invest*, 111(9), May, pp. 1373-1380.

Villa, L. M., Salas, E., Darley-Usmar, V. M., Radomski, M. W. and Moncada, S. (1994) 'Peroxynitrite induces both vasodilatation and impaired vascular relaxation in the isolated perfused rat heart.' *Proc Natl Acad Sci U S A*, 91(26), 12/20, pp. 12383-12387.

Villanueva, A., Canete, M., Roca, A. G., Calero, M., Veintemillas-Verdaguer, S., Serna, C. J., Morales Mdel, P. and Miranda, R. (2009) 'The influence of surface functionalization on the enhanced internalization of magnetic nanoparticles in cancer cells.' *Nanotechnology*, 20(11), Mar 18, p. 115103.

Vivero-Escoto, J. L., Slowing, II, Trewyn, B. G. and Lin, V. S. (2010) 'Mesoporous silica nanoparticles for intracellular controlled drug delivery.' *Small*, 6(18), Sep 20, pp. 1952-1967.

Wagner, D. D. and Frenette, P. S. (2008) 'The vessel wall and its interactions.' *Blood*, 111(11), Jun 1, pp. 5271-5281.

Waldron, G. J. and Garland, C. J. (1994) 'Effect of potassium channel blockers on L-NAME insensitive relaxations in rat small mesenteric artery.' *Canadian J. Physiol. Pharmacol.* , 72(S1) p. 115.

Wang, K. M., He, X. X., Yang, X. H. and Shi, H. (2013) 'Functionalized Silica Nanoparticles: A Platform for Fluorescence Imaging at the Cell and Small Animal Levels.' *Accounts of Chemical Research*, 46(7), Jul 16, pp. 1367-1376.

Wang, L. H., Rothberg, K. G. and Anderson, R. G. W. (1993) 'Mis-Assembly of Clathrin Lattices on Endosomes Reveals a Regulatory Switch for Coated Pit Formation.' *Journal of Cell Biology*, 123(5), Dec, pp. 1107-1117.

Wang, R. (2009) 'Hydrogen sulfide: a new EDRF.' *Kidney Int*, 76(7), 06/17/online, pp. 700-704.

Wang, X., Lau, F., Li, L., Yoshikawa, A. and van Breemen, C. (1995) 'Acetylcholine-sensitive intracellular Ca2+ store in fresh endothelial cells and evidence for ryanodine receptors.' *Circ Res*, 77(1), Jul, pp. 37-42.

Wang, X., Schroder, H. C., Wiens, M., Schlossmacher, U. and Muller, W. E. (2012) 'Biosilica: Molecular Biology, Biochemistry and Function in Demosponges as well as its Applied Aspects for Tissue Engineering.' *Adv Mar Biol*, 62 pp. 231-271.

Warheit, D. B., Laurence, B. R., Reed, K. L., Roach, D. H., Reynolds, G. A. M. and Webb, T. R. (2004) 'Comparative Pulmonary Toxicity Assessment of Single-wall Carbon Nanotubes in Rats.' *Toxicological Sciences*, 77(1), January 1, 2004, pp. 117-125.

Weintraub, N. L., Fang, X., Kaduce, T. L., VanRollins, M., Chatterjee, P. and Spector, A. A. (1997) 'Potentiation of endothelium-dependent relaxation by epoxyeicosatrienoic acids.' *Circ Res*, 81(2), 08/, pp. 258-267.

Welsh, D. G. and Segal, S. S. (2000) 'Role of EDHF in conduction of vasodilation along hamster cheek pouch arterioles in vivo.' *Am J Physiol Heart Circ Physiol*, 278(6), Jun, pp. H1832-1839.

White, R. and Hiley, C. R. (1997) 'A comparison of EDHF-mediated and anandamide-induced relaxations in the rat isolated mesenteric artery.' *Br J Pharmacol*, 122(8), Dec, pp. 1573-1584.

Whittemore, S. (1999) *The Circulatory System (Human Body: How it Works).* New York: Chelsea House.

Widstrom, R. L., Norris, A. W. and Spector, A. A. (2001) 'Binding of cytochrome P450 monooxygenase and lipoxygenase pathway products by heart fatty acid-binding protein.' *Biochemistry*, 40(4), 01/30, pp. 1070-1076.

Wiecha, J., Munz, B., Wu, Y., Noll, T., Tillmanns, H. and Waldecker, B. (1998) 'Blockade of Ca2+-activated K+ channels inhibits proliferation of human endothelial cells induced by basic fibroblast growth factor.' *J Vasc Res*, 35(5), /, pp. 363-371.

Wiesenthal, A., Hunter, L., Wang, S., Wickliffe, J. and Wilkerson, M. (2011) 'Nanoparticles: small and mighty.' *Int J Dermatol*, 50(3), Mar, pp. 247-254.

Wolfram Kuhlmann, C. R., Wiebke Lüdders, D., Schaefer, C. A., Kerstin Most, A., Backenköhler, U., Neumann, T., Tillmanns, H. and Erdogan, A. (2004) 'Lysophosphatidylcholine-induced modulation of Ca2+-activated K+channels contributes to ROS-dependent proliferation of cultured human endothelial cells.' *Journal of Molecular and Cellular Cardiology*, 36(5), 5//, pp. 675-682.

Wu, H., Huo, Q., Varnum, S., Wang, J., Liu, G., Nie, Z., Liu, J. and Lin, Y. (2008) 'Dye-doped silica nanoparticle labels/protein microarray for detection of protein biomarkers.' *Analyst*, 133(11), Nov, pp. 1550-1555.

Wu, J., Dong, H., Cai, Z. and Yu, Y. (1997) 'Stable expression of human cytochrome CYP2B6 and CYP1A1 in Chinese hamster CHL cells: their use in micronucleus assays.' *Chin Med Sci J*, 12(3), Sep, pp. 148-155.

Wulff, H., Miller, M. J., Hansel, W., Grissmer, S., Cahalan, M. D. and Chandy, K. G. (2000) 'Design of a potent and selective inhibitor of the intermediate-conductance Ca2+-activated K+ channel, IKCa1: a potential immunosuppressant.' *Proc Natl Acad Sci U S A*, 97(14), Jul 5, pp. 8151-8156.

Xu, B., Xia, M., Deng, Y., Hu, C. and Xu, Z. (2004) '[Nanotechnology & nanoparticles and their advances of investigation and application in the fields of biomedicine].' *Sheng Wu Yi Xue Gong Cheng Xue Za Zhi*, 21(2), Apr, pp. 333-336.

Yacobi, N. R., Phuleria, H. C., Demaio, L., Liang, C. H., Peng, C. A., Sioutas, C., Borok, Z., Kim, K. J. and Crandall, E. D. (2007) 'Nanoparticle effects on rat alveolar epithelial cell monolayer barrier properties.' *Toxicol In Vitro*, 21(8), Dec, pp. 1373-1381.

Yamada, M., Isomoto, S., Matsumoto, S., Kondo, C., Shindo, T., Horio, Y. and Kurachi, Y. (1997) 'Sulphonylurea receptor 2B and Kir6.1 form a sulphonylurea-sensitive but ATP-insensitive K+ channel.' *J Physiol*, 499 (Pt 3), 03/15, pp. 715-720.

Yamamoto, K., Ikeda, U., Okada, K., Saito, T. and Shimada, K. (1997) 'Arginine vasopressin inhibits nitric oxide synthesis in cytokine-stimulated vascular smooth muscle cells.' *Hypertens Res*, 20(3), Sep, pp. 209-216.

Yamamoto, R., Wada, A., Asada, Y., Yuhi, T., Yanagita, T., Niina, H. and Sumiyoshi, A. (1994) 'Functional relation between nitric oxide and noradrenaline for the modulation of vascular tone in rat mesenteric vasculature.' *Naunyn Schmiedebergs Arch Pharmacol*, 349(4), Apr, pp. 362-366.

Yamashita, K., Yoshioka, Y., Higashisaka, K., Mimura, K., Morishita, Y., Nozaki, M., Yoshida, T., Ogura, T., Nabeshi, H., Nagano, K., Abe, Y., Kamada, H., Monobe, Y., Imazawa, T., Aoshima, H., Shishido, K., Kawai, Y., Mayumi, T., Tsunoda, S., Itoh, N., Yoshikawa, T., Yanagihara, I., Saito, S. and Tsutsumi, Y. (2011) 'Silica and titanium dioxide nanoparticles cause pregnancy complications in mice.' *Nature Nanotechnology*, 6(5), May, pp. 321-328.

Yamashita, T., Kawashima, S., Ozaki, M., Namiki, M., Satomi-Kobayashi, S., Seno, T., Matsuda, Y., Inoue, N., Hirata, K., Akita, H., Umetani, K., Tanaka, E., Mori, H. and Yokoyama, M. (2001) 'Role of endogenous nitric oxide generation in the regulation of vascular tone and reactivity in small vessels as investigated in transgenic mice using synchrotron radiation microangiography.' *Nitric Oxide*, 5(5) pp. 494-503.

Yan, Q., Liu, Q., Zweier, J. L. and Liu, X. (2007) 'Potency of authentic nitric oxide in inducing aortic relaxation.' *Pharmacological Research*, 55(4), 4//, pp. 329-334.

Yiu, H. H. P., McBain, S. C., Lethbridge, Z. A. D., Lees, M. R. and Dobson, J. (2010) 'Preparation and characterization of polyethylenimine-coated Fe3O4-MCM-48 nanocomposite particles as a novel agent for magnet-assisted transfection.' *Journal of Biomedical Materials Research Part A*, 92a(1), Jan, pp. 386-392.

Yu, T., Hubbard, D., Ray, A. and Ghandehari, H. (2012) 'In vivo biodistribution and pharmacokinetics of silica nanoparticles as a function of geometry, porosity and surface characteristics.' *J Control Release*, 163(1), Oct 10, pp. 46-54.

Yu, T., Greish, K., McGill, L. D., Ray, A. and Ghandehari, H. (2012) 'Influence of Geometry, Porosity, and Surface Characteristics of Silica Nanoparticles on Acute Toxicity: Their Vasculature Effect and Tolerance Threshold.' *Acs Nano*, 6(3), Mar, pp. 2289-2301.

Zhang, D. X., Borbouse, L., Gebremedhin, D., Mendoza, S. A., Zinkevich, N. S., Li, R. and Gutterman, D. D. (2012) 'H2O2-induced dilation in human coronary arterioles: role of protein kinase G dimerization and large-conductance Ca2+-activated K+ channel activation.' *Circ Res*, 110(3), Feb 3, pp. 471-480.

Zhang, J. H., Zhan, P., Wang, Z. L., Zhang, W. Y. and Ming, N. B. (2003) 'Preparation of monodisperse silica particles with controllable size and shape.' *Journal of Materials Research*, 18(3), Mar, pp. 649-653.

Zhang, L. W. and Monteiro-Riviere, N. A. (2009) 'Mechanisms of quantum dot nanoparticle cellular uptake.' *Toxicol Sci*, 110(1), Jul, pp. 138-155.

Zhang, Q. J., McMillin, S. L., Tanner, J. M., Palionyte, M., Abel, E. D. and Symons, J. D. (2009) 'Endothelial nitric oxide synthase phosphorylation in treadmill-running mice: role of vascular signalling kinases.' *J Physiol*, 587(Pt 15), Aug 1, pp. 3911-3920.

Zhang, Y. Y., Hu, L., Yu, D. H. and Gao, C. Y. (2010) 'Influence of silica particle internalization on adhesion and migration of human dermal fibroblasts.' *Biomaterials*, 31(32), Nov, pp. 8465-8474.

Zhao, L., Wang, Y., Ma, X. and Deng, X. (2013) 'Oxidative stress impairs IKCa- and SKCa-mediated vasodilatation in mesenteric arteries from diabetic rats.' *Nan fang yi ke da xue xue bao = Journal of Southern Medical University*, 33(7), Jul, pp. 939-944.

Zhao, Y. N., Sun, X. X., Zhang, G. N., Trewyn, B. G., Slowing, I. I. and Lin, V. S. Y. (2011) 'Interaction of Mesoporous Silica Nanoparticles with Human Red Blood Cell Membranes: Size and Surface Effects.' *Acs Nano*, 5(2), Feb, pp. 1366-1375.

Zhou, H., Wu, X., Wei, J., Lu, X., Zhang, S., Shi, J. and Liu, C. (2011) 'Stimulated osteoblastic proliferation by mesoporous silica xerogel with high specific surface area.' *J Mater Sci Mater Med*, 22(3), Mar, pp. 731-739.

Zhou, H., Nakamura, T., Matsumoto, N., Hisatsune, C., Mizutani, A., Iesaki, T., Daida, H. and Mikoshiba, K. (2008) 'Predominant role of type 1 IP3 receptor in aortic vascular muscle contraction.' *Biochem Biophys Res Commun*, 369(1), Apr 25, pp. 213-219.

Appendix 1. Conference Presentations

Shukur, A., Whitehead, D. and Azzawi, M. 'The Influence of Silica Nanoparticles on Small Mesenteric Vessel Function and Contractility.'
Poster presented at the Research Day conference – hosted by MMU, John Dalton Building, Manchester, held on the 20th April 2012.

Shukur, A., Whitehead, D. and Azzawi, M. 'The Influence of Silica Nanoparticles on Small Mesenteric Vessel Function and Contractility.'
Poster presented at the Manchester Life Sciences PhD Conference – hosted by the Faculty of Life Sciences, University of Manchester, The Manchester Place, Manchester, held on the 11th May 2012.

Shukur, A., Rizvi, S. B., Whitehead, D., Seifalian, A. and Azzawi, M. 13) 'The influence of Quantum dots on Small Mesenteric Vessel Function and Contractility.'
Poster presented at joint meeting of the BMS and the Microcirculatory Society – hosted by Oxford University, Keble College, Oxford, held on the 4th – 6th July 2012.

Shukur, A., Whitehead, D. and Azzawi, M. 'Infused Silica Nanoparticles Compromise Small Arterial Function, *Ex vivo*.'
Poster presented at the International Cell Tracking Symposium (Nanoparticle-based Technologies for Cell Tracking) – hosted by the Department of Chemistry, University of Liverpool, Liverpool, held on the 1st – 2nd July 2013.

Shukur, A., Whitehead, D. and Azzawi, M. 'Infused Silica Nanoparticles Compromise Small Arterial Function, *Ex vivo*.'
Poster presented at the Northern Vascular Biology Forum (NVBF) – hosted by the University of Sheffield, North Campus Conference Centre, Sheffield, held on the 9th December 2013.

Shukur, A., Whitehead, D. and Azzawi, M. 'Infused Silica Nanoparticles Compromise Small Arterial Function, *Ex vivo*.'

Poster presented at the NVBF – hosted by MMU, Geoffrey Manton Building, Rasamond Street West, Off Oxford Road, Manchester, M15 6LL, held on the 8th December 2014.

Shukur, A., Whitehead, D., Wilkinson, F., Weston, R. Alexander, Y. and Azzawi, M. 'Infused Silica Nanoparticles Compromise Small Arterial Function.'

Poster presented at the British Atherosclerosis Society (BAS)/British Society of Cardiovascular Research (BSCR) Joint Spring Meeting 2015 with the British Cardiovascular Society (BCS); New frontiers in Cardiovascular Science – hosted by The Education Hall, Manchester Central Conference Centre, Windmill Street, Manchester, M2 3GX, held on the 8-9th June 2015.

Shukur, A., Whitehead, D., Wilkinson, F., Weston, R. Alexander, Y. and Azzawi, M. 'Rapid Uptake of Silica Nanoparticles Attenuates Vasodilator Responses in Small Mesenteric Arteries.'

Oral Presentation conducted for the Young Scientist Lecture competition at the 10th NANOSMAT Conference – hosted by the University of Manchester, held on the 13-16th September 2015. Also was a member of the organising team.

Shukur, A., Whitehead, D. and Azzawi, M. Silica Nanoparticles Attenuate EDHF Pathway Dependent Vasodilator Responses in Small Mesenteric Arteries, *ex vivo*.'

Poster Presentation conducted for the 3rd International Conference on Nanotechnology in Medicine (NANOMED) – hosted by NANOSMAT, Manchester Conference Centre, Sackville Street, Manchester, M1 3BB, held on the 23-25th November 2015. Also was a member of the organising team.

Appendix 2. Publications

Peer-reviewed Scientific Journals.

Shukur, A., Rizvi, S. B., Whitehead, D., Seifalian, A. and Azzawi, M. (2013) 'Altered sensitivity to nitric oxide donors, induced by intravascular infusion of quantum dots, in murine mesenteric arteries.' *Nanomedicine*, 9(4), May, pp. 532-539.

Shukur, A., Whitehead, D., Seifalian, A. M., Alexander, Y., Wilkinson, F. and Azzawi, M. (2015) 'Infused Silica Nanoparticles Compromise Vascular Function in Small Mesenteric Arteries.' *Heart*, 101, Jun, pp. A98-A98.

Shukur, A., Whitehead, D., and Azzawi, M. (2015) ''Rapid Uptake of Silica Nanoparticles Attenuates Vasodilator Responses in Small Mesenteric Arteries.' In submission.

Appendix 3. Calculations used for working out the number of nanoparticles per mL

$$V=(4/3)\pi r^3 \quad [1]$$

Equation 1: Calculates the volume of a sphere, where v is the volume of sphere, π is 3.14 and r is the radius of the particle in cm. This equation was used to calculate the number of particles per mL.

$$m=V\times D \quad [2]$$

Equation 2: Calculates the mass of a nanoparticles sphere, where M is mass of a particles sphere, v is volume of a sphere and d is the density of silica, which is 1.9.

$$N=m/V \quad [3]$$

Equation 3: Calculates the number of particles within a given solution, where V is the volume of a sphere at a given diameter; m is the mass of dry NP product in 1 mL of SiNPs suspension.

For example, the volume of sphere for the 98 nm sized A3 SiNPs was calculated as follows: 4/3 x π x (half of nanoparticle size (49 nm) x 10^{-7})^3 x 1.9 (silica density)

To calculate NP/mL:

$$\frac{\text{Dry mass } (0.0044 \text{ g})}{\text{Volume of sphere } (9.36 \text{ x } 10^{-16})}$$

Thus = 4.70 x 10^{12}

C1xV1 = C2xV2

4.70 x 10^{12} x V1 = 5.32 x 10^{11} x 1 mL

Hence, the initial volume to take from the A3 SiNP suspension is 0.11 mL or 111 µL to achieve a final dosage of = 5.32 x 10^{11} NP/mL.

Appendix 4. The Hydrodynamic Diameter and Zeta Potential Outputs for SiNPs

DA3 SiNPs in Ethanol

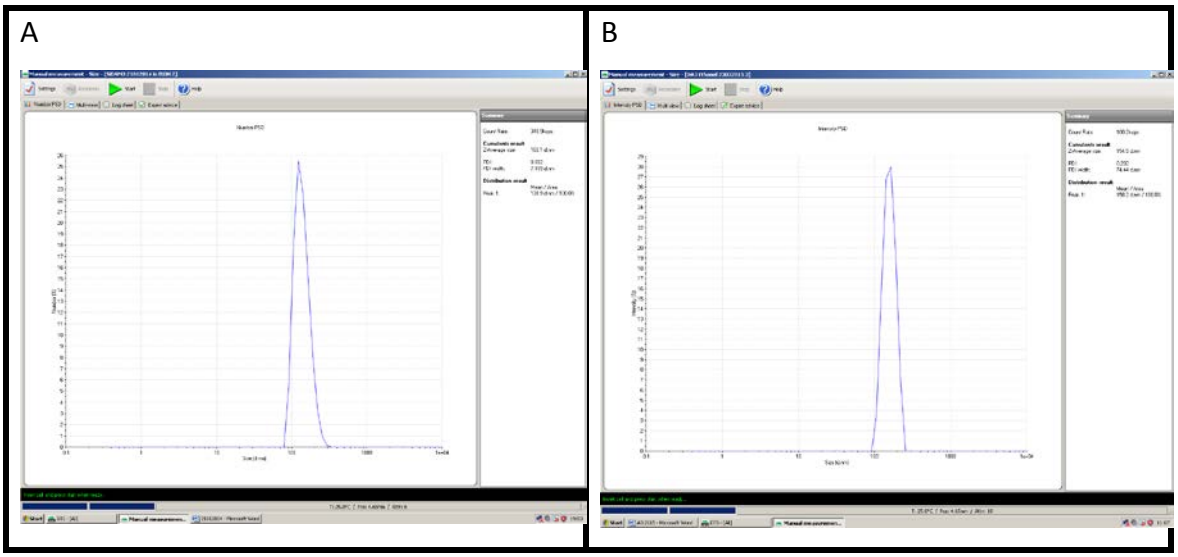

Hydrodynamic diameter graph of DA3 SiNPs sample in ethanol over time, where A) month one and B) month fifteen.

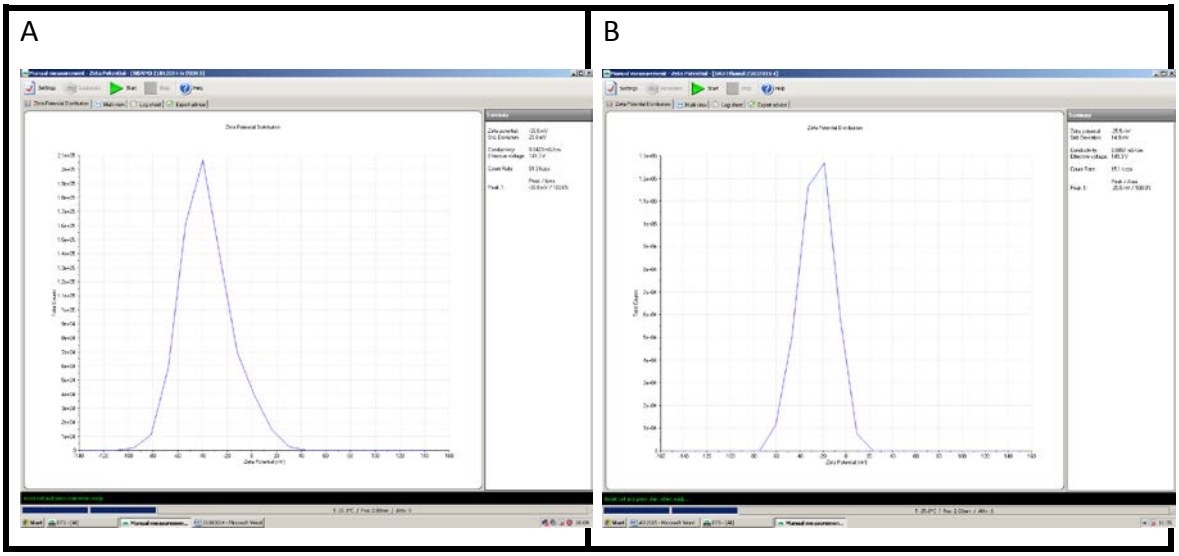

Zeta potential graph of sample DA3 SiNPs sample in ethanol over time, where A) month one and B) month fifteen.

A3 SiNPs in Water

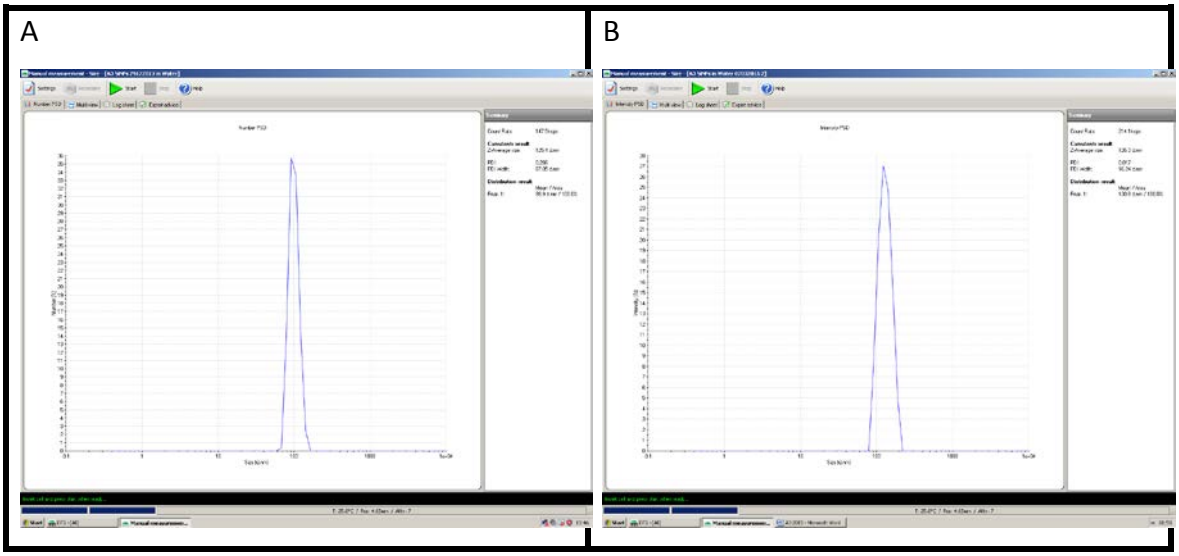

Hydrodynamic diameter graph of sample A3 SiNPs sample in water over time, where A) month one and B) month fifteen.

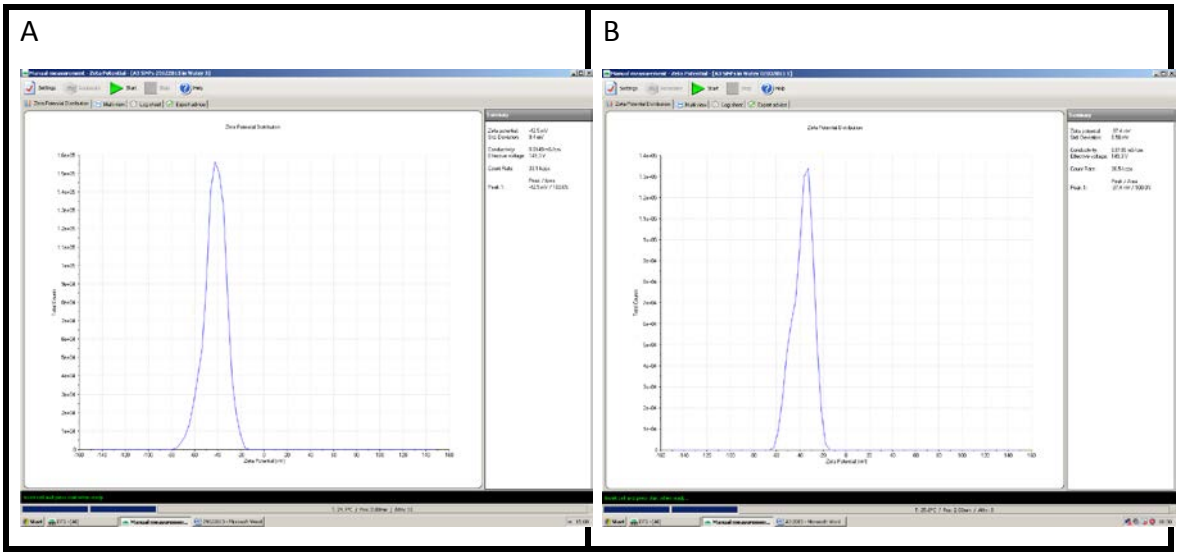

Zeta potential graph of sample A3 SiNPs sample in water over time, where A) month one and B) month fifteen.

A3 SiNPs in PSS

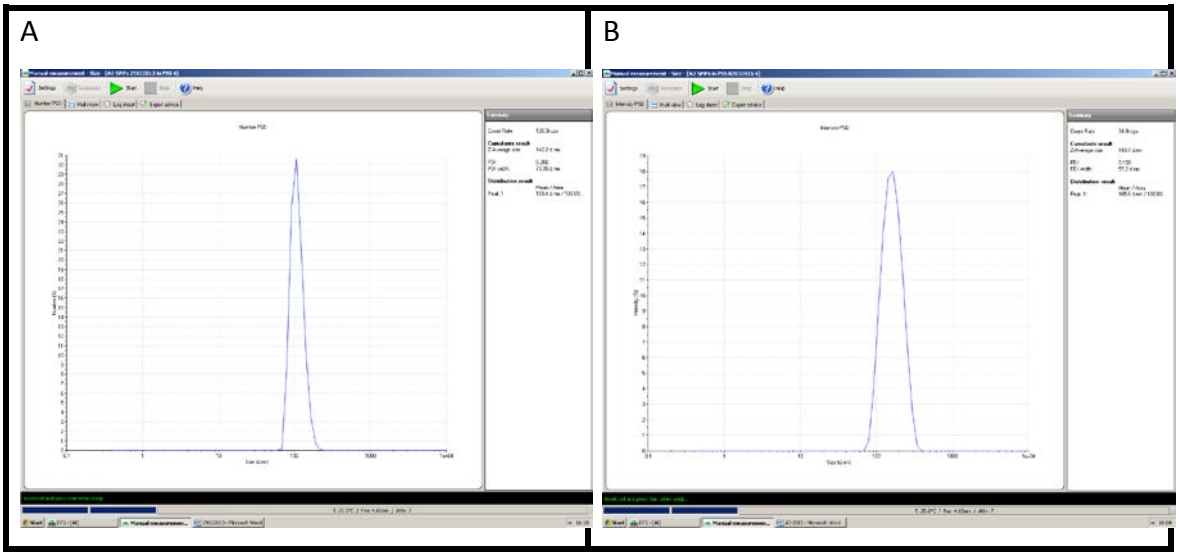

Hydrodynamic diameter graph of sample A3 SiNPs sample in PSS over time, where A) month one and B) month fifteen.

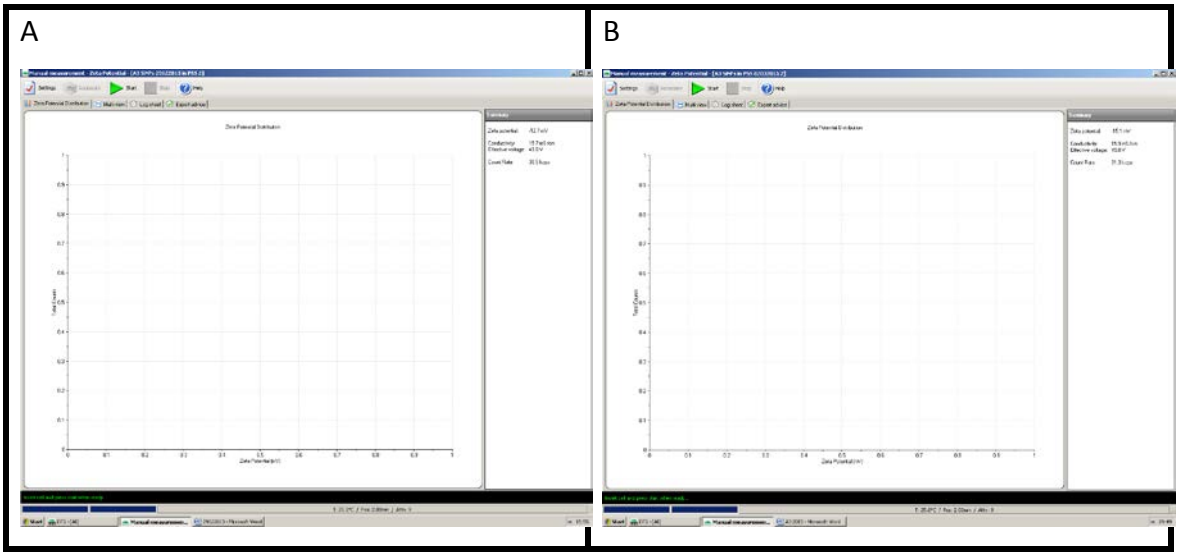

Zeta potential graph of sample A3 SiNPs sample in PSS over time, where A) month one and B) month fifteen.

Appendix 5. Preparation of Solutions and chemicals

General equations for Molar calculations

Volume = Mass (g) x Density

Number of Moles = [Mass (g)/molecular weight (g/mol)]/Volume (V)

Concentration (C) (Molar; mol/L) = Moles/V

TEM sample fixation and preservation

The fixative for TEM was prepared by dissolving 4.28 g of sodium (Na) Cacodylate in 80 mL of dH_2O. The mixture was then made to 100 mL with dH_2O, stirred and adjusted to the desired *pH* with 0.1 M of HCl added in a drop-wise fashion to allow the sample to reach *pH* of 7.4. 100 µL of the gluteraldyde solution was added to 900 µL of the above mixture to make the fixative. The wash buffer for TEM was prepared by dissolving 4.28 g of Na Cacodylate and 0.025 calcium chloride (Ca_2Cl) dihydrate in 80 mL of dH_2O. The mixture was then made to 100 mL with dH_2O, stirred and adjusted to the desired *pH*. 0.1 M of HCl was used in a drop-wise fashion to allow the sample to reach *pH* of 7.4.

TRAM-34 Preparation

TRAM-34 (molecular weight 344.84 g/mol; soluble at 2 mg/mL of DMSO) was prepared by dissolving 5 mg in DMSO, followed by water to give a final concentration of 5 mM.

Appendix 6. Preparation of the Protein Standard Dilutions

7 x 0.5 mL Eppendorf tubes were prepared and labelled from 1 to 9 for the protein standard plot as in Figure 1. The protein standard concentration was 2 mg/mL Bovine calf albumin. The dilutions in each Eppendorf tube was prepared as shown in Table 1.

Table 1. The dilutions used to make the protein standard plot.

Eppendorf Tube	Dilutions (mg/mL)	µL of Albumin Standard	µL of Lysis Buffer
1	2	40	0
2	1.6	32	8
3	1.2	24	16
4	0.8	16	24
5	0.4	8	32
6	0.2	4	36
7	0	0	40

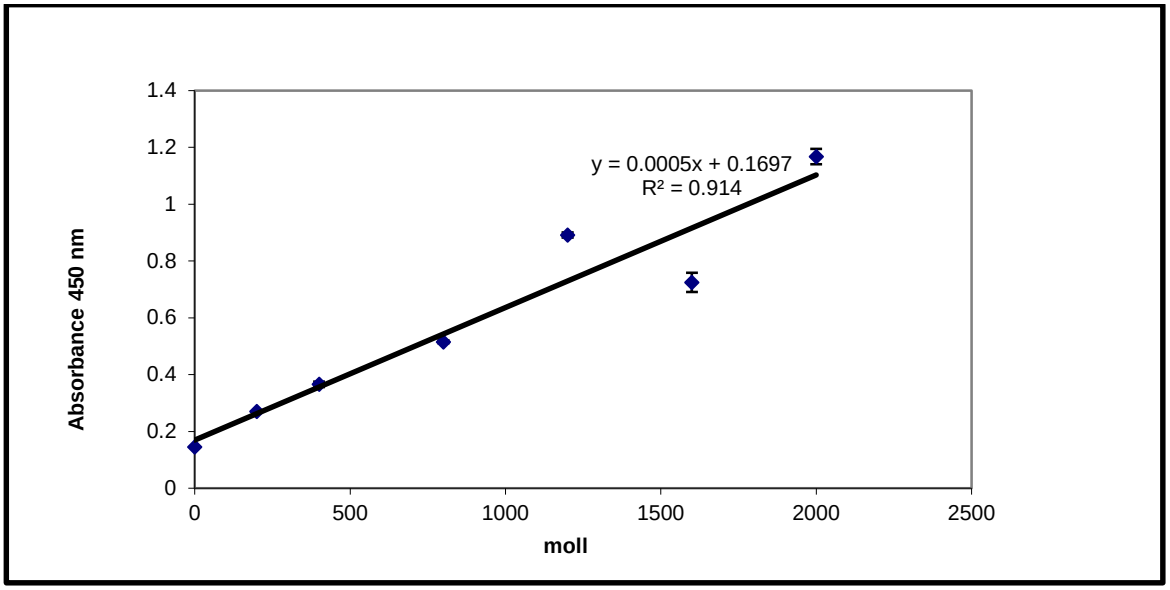

Figure 1. The standard linear regression blot used to create the line equation for the protein estimation study.

Appendix 7. The Characterisation of HCMECs Growth

HCMECs Culture

Passage 2 adult human-derived cardiac microvascular endothelial cells (HCMECs) were purchased from PromoCell (Heidelberg, Germany). The HCMECs were cultured in T-25 flasks (Iwaki, Japan), or on 6-well plates at a seeding density of 10,000 to 20,000 cells/cm^2 as per our instruction manual and maintained in a growth medium at 37°C in 5% CO_2 in a humidified incubator. The medium was replaced initially after 16-24 hours when the cells were initially obtained then every 3-4 days. HCMECs were cultured in cell type-specific endothelial cell growth medium MV for microvascular endothelial cells (PromoCell; Heidelberg, Germany) supplemented with foetal calf serum (2%), epidermal growth factor (EGF) 10 ng/mL, heparin 90 µg/mL, and hydrocortisone 1 µg/mL. Cells were subcultured every 10-14 days (at ~70% confluence). Experiments can be conducted at passage 4-8, at which time cells demonstrated good growth rates without obvious loss of phenotype.

HCMECs Growth

Healthy-looking HCMECs were observed as round with a characteristic oval-shape and a centralised nucleus in contract to unhealthy cells, which contained long processes, which are trying to communicate and reach other cells (Figure 1).

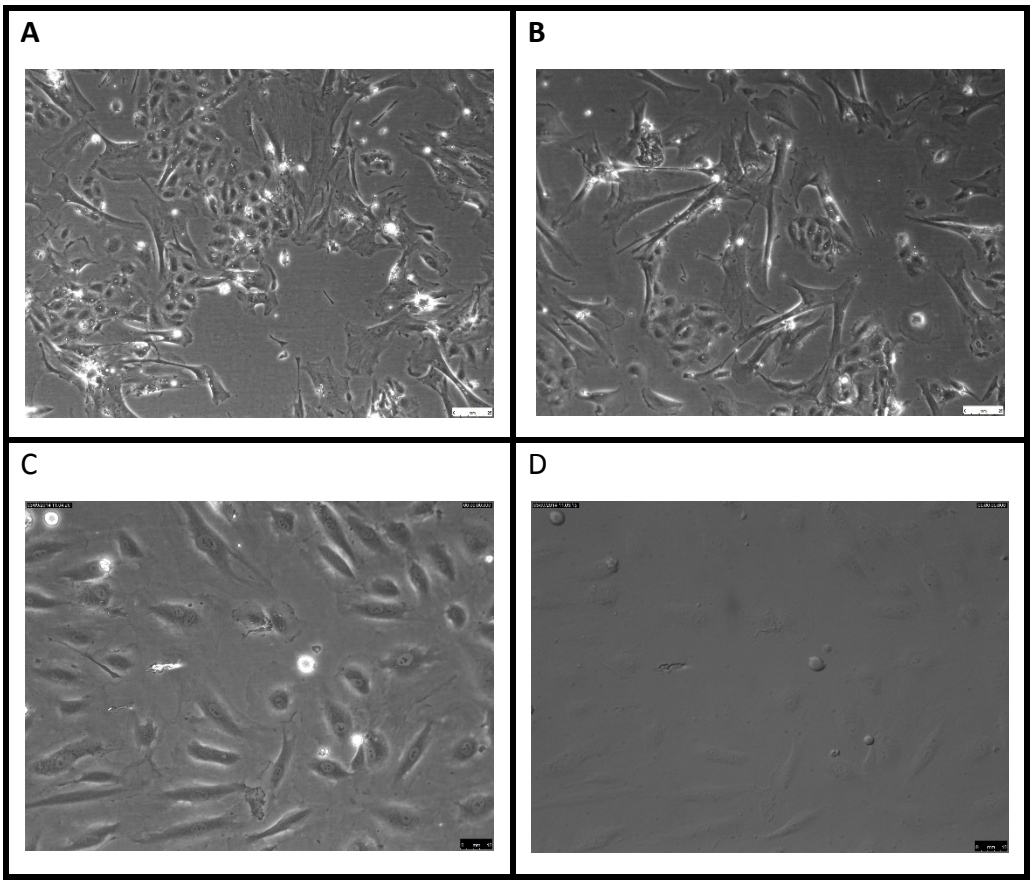

Figure 1. Passage 2 HCMECs after 13 days of culture reaching 75-80% confluence. Images were obtained using the x10 (A and B) and x20 (C and D) objectives respectively of the Leica CTR000 microscope (Microsystems, UK).